fifty years

Unesco reports
in marine science 67

Deep-sea depositional systems of the Western Mediterranean and mud volcanism on the Mediterranean Ridge

Initial results of geological and geophysical investigations during the Fourth UNESCO-ESF "Training-through-Research" Cruise of R/V *Gelendzhik* (June-July 1994)

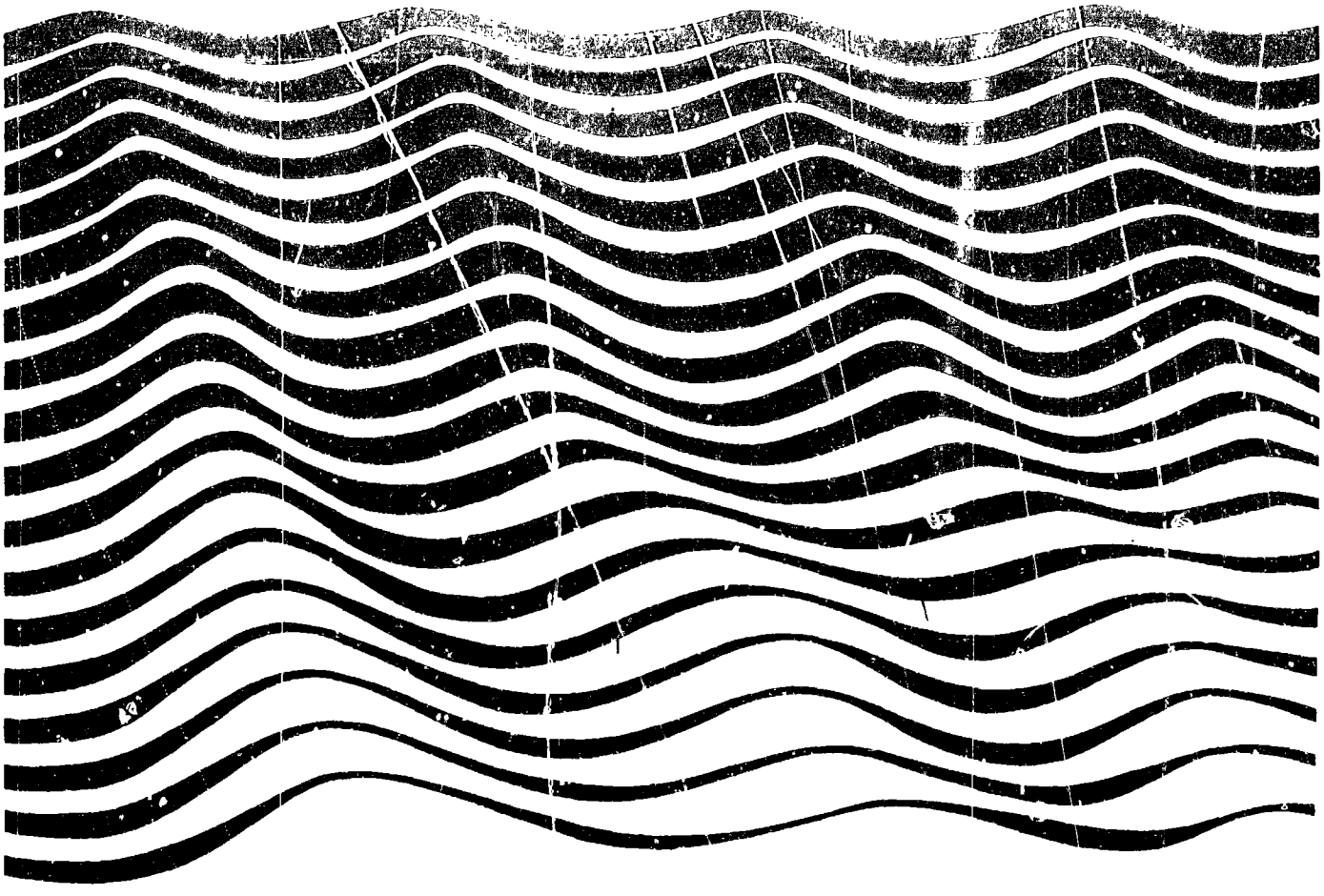

UNESCO 1995

UNESCO REPORTS IN MARINE SCIENCE

Out of stock titles are listed on the back cover

No		Year
4	Syllabus for training marine technicians. Report of an IOC/UNESCO workshop held in Miami, Florida, 22-26 May 1978 (E, F, R, S)	1979
5	Marine science syllabus for secondary schools. Report of an IOC workshop held at United World College of the Atlantic, United Kingdom, 5-9 June 1978 (Ar, E, F, R, S)	1979
6	Organization of marine biological reference collections in the Mediterranean Arab countries. Expert meeting held in Tunis, 20-23 September 1978 (Ar, E, F)	1979
8	The mangrove ecosystem: Human uses and management implications. Report of a UNESCO regional seminar held in Dacca, Bangladesh, December 1978 (E)	1979
9	The mangrove ecosystem: scientific aspects and human impact. Report of the seminar organized by UNESCO at Cali, Colombia 27 November - 1 December 1978 (E, S)	1979
10	Development of marine science and technology in Africa. Working Group of Experts sponsored by ECA and UNESCO, Addis Ababa, 5-9 May 1980 (E, F)	1980
20	Quantitative analysis and simulation of Mediterranean coastal ecosystems: The Gulf of Naples, a case study. Report of a workshop on ecosystem modelling, Ischia, Naples, Italy, 28 March to 10 April 1981. Organized by UNESCO and the Stazione Zoologica, Naples (E)	1983
21	Comparing coral reef survey methods. A regional UNESCO/UNEP workshop, Phuket Marine Biological Centre, Thailand, December 1982 (E)	1983
22	Guidelines for marine biological reference collections. Prepared in response to a recommendation by a meeting of experts from the Mediterranean Arab countries (Ar, E, F)	1983
23	Coral reefs, seagrass beds and mangroves: their interaction in the coastal zones of the Caribbean. Report of a workshop held at West Indies Laboratory, St Croix, U.S. Virgin Islands, May 1982 (E)	1983
24	Coastal ecosystems of Latin America and the Caribbean. Its objectives, priorities and activities of UNESCO's COMAR project for the Latin America and Caribbean region, Caracas, Venezuela, 15-19 November 1982 (E, S)	1983
25	Ocean engineering teaching at the university level. Recommended guidelines from the UNESCO/IOC/ECOR workshop on advanced university curricula in ocean engineering and related fields, Paris, October 1982 (Ar, Ch, E, F, R, S)	1983
26	Global survey and analysis of post graduate curricula in ocean engineering (E)	1983
28	Oceanographic modelling of the Kuwait Action Plan (KAP) Region. Report of symposium/workshop, University of Petroleum and Minerals, Dhahran, Kingdom of Saudi Arabia 15-18 October 1983 (E)	1983
29	Eutrophication in coastal marine areas and lagoons: a case study of 'Lac de Tunis'. Report prepared by Dr M. Kelly and Dr M. Naguib (F)	1983
30	Physical oceanography of the Eastern Mediterranean: an overview and research plan. Report of a workshop held in Erice, La Spezia (Italy), September 1983 (E)	1984
31	MABAHISS/John Murray 50th anniversary: Marine science of the North West Indian Ocean and adjacent waters. Report of a symposium on the occasion of the 50th anniversary of the MABAHISS/John Murray Expedition (1933/34), University of Alexandria, Egypt, 3 to 7 September 1983 (E)	1985
32	L'estuaire et la mangrove du Sine Saloum. Resultats d'un Atelier régional UNESCO/COMAR, tenu à Dakar (Senégal) du 28 février au 5 mars 1983 (F)	1985
33	Coral Taxonomy. Results and recommendations of a regional UNESCO (COMAR)/UNEP workshop with advanced training, Phuket Marine Biological Centre, Thailand, 10-26 February 1984 (E)	1985
34	Bibliography on coastal lagoons and salt marshes along the Southern Mediterranean coast (Algeria, Egypt, Libya, Morocco, Tunisia) (Ar, F, E)	1985
35	Physical oceanography of the Eastern Mediterranean (POEM). A Research Programme. Reports of the Organizing Committee Meeting, Paris, August 1984, and the Scientific Workshop, Lucerne, October 1984 (E)	1985
36	Méthodologie d'etude des lagunes côtieres. Résultats d'un atelier régional réuni à Abidjan du 6 au 11 mai 1985 (F)	1986
37	Principles of Geological Mapping of Marine Sediments (with special reference to the African continental margin) (E, R)	1986
39	Development of marine sciences in Arab Universities. Meeting of experts held at the Marine Science Station, Aqaba, Jordan, 1-5 December 1985 (Ar, E, F)	1986
40	Human induced damage to coral reefs. Results of a regional UNESCO (COMAR) workshop with advanced training, Diponegoro University, Jepara and National Institute of Oceanology, Jakarta, Indonesia, May 1985 (E)	1986
41	Caribbean coastal marine productivity. Results of a Planning Workshop at Discovery Bay Marine Laboratory, University of the West Indies, Jamaica, November 1985 (E)	1986
42	The application of digital remote sensing techniques in coral reef, oceanographic and estuarine studies. Report on a regional UNESCO COMAR/GBRMPA Workshop, Townsville, Australia, August 1986 (E)	1986
43	Quaternary coastal geology of West Africa and South America. Papers prepared for the INQUA/SEQUA Symposium in Dakar, April 1986 (E)	1987
44	Physical oceanography of the Western Mediterranean (POEM): Initial Results. UNESCO/IOC/First POEM Scientific Workshop, Erice, Turkey, 16-20 June 1986 (E)	1987
45	Marine science teaching and training at first degree (undergraduate) level. Recommended guidelines from a UNESCO/IOC workshop on university curricula, Paris, November 1986 (Ar, Ch, E, F, R, S)	1987
46	Comparison between Atlantic and Pacific tropical marine coastal ecosystems: community structure, ecological processes, and productivity. Results and scientific papers of a UNESCO/COMAR workshop, University of the South Pacific, Suva, Fiji, 24-29 March 1986 (E)	1987
48	Coastal marine ecosystems of Africa. Objectives and strategy of the COMARAF Regional Project (E)	1988
49	Eutrophication in the Mediterranean sea: receiving capacity and monitoring of long term effects. Report and proceedings of a Scientific Workshop, Bologna, Italy, 2 to 6 March 1987. Sponsored by UNESCO, FAO, UNEP, Regione Emilia Romagna and University of Bologna (E)	1988
50	Marine Geology of the West African shelf zone (E, R)	1988
51	Physical oceanography of the Eastern Mediterranean (POEM). Programme for 1988/89 (E)	1988
52	Year 2000 challenges for marine science training and education worldwide (Ar, Ch, E, F, R, S)	1988
53	Physical oceanography of the Eastern Mediterranean (POEM). The intercalibrated POEM data set and the emerging picture of the circulation, POEM Scientific Workshop, Trieste, Italy, 31 May - 4 June 1988 (E)	1990
54	Relative sea-level change: a critical evaluation. UNESCO (COMAR) Working Group on Mean Sea Level Rise and its Influence on the Coastal Zone (E)	1990
55	Physical oceanography of the Eastern Mediterranean (POEM). The new phenomenology of the Eastern Mediterranean. POEM Scientific Workshop, Cambridge, Massachusetts, USA, 29 May - 2 June 1989 (E)	1991

Cont'd on inside of back cover

Unesco reports
in marine science 67

Deep-sea depositional systems of the Western Mediterranean and mud volcanism on the Mediterranean Ridge

Initial results of geological and geophysical investigations during the Fourth UNESCO-ESF "Training-through-Research" Cruise of R/V *Gelendzhik* (June-July 1994)

Editors: A. F. Limonov
N. H. Kenyon
M. K. Ivanov
J. M. Woodside

UNESCO 1995

ISSN 0253-0112

Published in 1995
by the United Nations Educational,
Scientific and Cultural Organization,
7, place de Fontenoy, 75352 Paris 07 SP
Printed in UNESCO's workshops

PREFACE

UNESCO Reports in Marine Science are designed to serve specific programme needs and to report on developments in projects conducted in the context of UNESCO's marine science-related activities.

Designed to serve as a complement to the *UNESCO Technical Papers in Marine Science*, the systematic distribution of *Reports* **is restricted to libraries** of oceanographic institutions and governmental authorities, and documentation centres. Individual requests from specialists will, however, be examined by the Marine Information Centre and dealt with on a selective basis.

Requests for specific titles or additions to the mailing list should be addressed to:

Marine Information Centre
UNESCO
1 rue Miollis
75732 Paris Cedex 15
France

ABSTRACT

The 4th UNESCO-ESF Training-through-Research Cruise of the R/V *Gelendzhik* (1 June-16 July 1994) was principally dedicated to the study of sediments transport processes in the Western Mediterranean Sea. Secondary topics of the Cruise were related to some tectonic and seismic stratigraphic problems in the Tyrrhenian Sea, and to the continued study of mud volcanism on the Mediterranean Ridge.

The methods used were conventional echosounding, 6-channel seismic profiling, swath reflectivity surveying with long-range (OKEAN) and deep-tow (MAK-1) sidescan sonars, and bottom sampling with gravity, box, and Kasten corers.

The results of the cruise include the discovery of six possible new mud volcanoes, both exposed and buried; the determination that the Stromboli Canyon is currently very active, transporting chiefly volcaniclastic sediments to the deep Marsili Basin; the recording, on detailed sonographs, of extensive mass wasting processes in the Corso-Ligurian Basin; and the detection of much erosion and sediment redeposition, in the form of unusual bedforms, in the West-Central-Algero-Provencal Basin.

RÉSUMÉ

La 4e campagne UNESCO-ESF de formation par la recherche à bord du N/O *Gelendzhik* (1er juin - 16 juillet 1995) avait pour principal objet l'étude des processus de transport sédimentaire en Méditerranée occidentale. Elle visait secondairement des phénomènes de tectonique et de stratigraphie sismique de la mer Tyrrhénienne ainsi que la poursuite de l'observation des volcans de boue de la Ride méditerranéenne.

Les méthodes suivantes ont été utilisées : échosondage classique, profils sismiques à six canaux, mesure de la réflexivité du couloir ouvert par sonar à longue portée (OKEAN) et par sonar latéral remorqué en profondeur; échantillonage du fond de la mer par carottiers en gravité, en caissons et sonars Kasten.

La campagne a permis de découvrir l'existence probable de six nouveaux volcans de boue, affleurants ou recouverts; la certitude de l'intense activité du canyon du Stromboli, qui charrie vers le bassin profond de Marsili des sédiments essentiellement volcano-clastiques; l'enregistrement par sonographies détaillées de vastes phénomènes d'érosion en masse dans le bassin corso-ligure et enfin la découverte d'une forte activité d'érosion et de redéposition de sédiments formant d'étranges reliefs sur la partie ouest-centre du bassin algéro-provençal.

RESUMEN

La 4ª campaña "Formación a través de la Investigación" (UNESCO-ESF) del B/O *Gelendzhik* (1 de junio - 16 de julio 1994) estuvo dedicada principalmente al estudio de los procesos de transporte de sedimentos en el Mar Mediterráneo occidental. Tópicos secundarios durante la campaña estuvieron relacionados a algunos problemas de tectónica y estratigrafía sísmica en el Mar Tirreno, y a la continuación del estudio sobre el volcanismo de fango en la Dorsal del Mediterráneo.

Los métodos utilizados fueron: ecosondeo tradicional, perfilamiento sísmico de 6 canales, medida de reflectividad del área cubierta por sonar de barrido de alta resolución (OKEAN) y por sonar lateral de remolque en profundidad (MAK-1), y toma de muestras de bentos con muestreadores de gravedad, de caja y Kasten.

Los resultados de la campaña incluyen el descubrimiento de seis volcanes de fango probablemente nuevos, tanto expuestos como recubiertos; la confirmación que el Cañón del Strómboli es actualmente muy activo, transportando principalmente sedimentos de origen volcanoclástico hacia la cuenca profunda de Marsili; el registro en sonogramas detallados de vastos fenómenos de erosión en masa en la Cuenca de Córcega-Liguria; y la detección de un fuerte proceso de erosión y re-deposición de sedimentos, formando capas inusuales, en el sector centro-occidental de la Cuenca Algero-Provenzal.

РЕЗЮМЕ

Четвертый рейс НИС "Геленджик" по программе "Обучение через исследования" (ЮНЕСКО-Европейский научный фонд) проходил с 1 июня по 16 июля 1994 г. и был в основном посвящен изучению процессов переноса осадочных масс в Западном Средиземноморье. Дополнительные цели рейса сводились к решению некоторых тектонических и сейсмостратиграфических проблем в Тирренском море, а также продолжению изучения явлений грязевого вулканизма на Средиземноморском хребте.

Методы изучения включали эхолотирование, 6-канальное сейсмическое профилирование, съемку локатором бокового обзора ОКЕАН и глубоководной буксируемой акустической системой МАК-1, а также отбор донных отложений с помощью ударной трубки, коробчатого пробоотборника и пробоотборника Кастенлота.

Результаты рейса, в частности, включают: обнаружение шести новых грязевых вулканов, как обнажающихся на дне моря, так и погребенных. Каньон Стромболи, как выяснилось, является в настоящее время очень активным: по нему происходит перенос преимущественно вулканокластических осадков в глубоководный бассейн Марсили. В западной части Тирренского моря были обнаружены неожиданные свидетельства тектоники сжатия. На сонограммах высокого разрешения в Корса-Лигурийской впадине зарегистрированы следы обширного переноса осадков, а в Алжиро-Прованскальской впадине многочисленные свидетельства эрозии и переотложения осадков выявлены в виде необычных форм донного рельефа.

مستخلص

نظمت اليونسكو والصندوق الأوروبي للعلوم رحلة بحرية للتدريب من خلال البحث على ظهر سفينة البحوث جلندزيك (١ يونيو - ١٦ يوليو ١٩٩٤) وكانت الرحلة مكرسة أساسا لدراسة عمليات انتقال الرسوبيات في غرب البحر المتوسط. وشملت الموضوعات الثانوية للرحلة بعض المسائل التكتونية والسيزمية في البحر التيرنيان والدراسة المستمرة لطمي البراكين على المرتفعات المغمورة بالبحر المتوسط.

شملت الطرق المستعملة تسجيل العمق بطريقة صدى الصوت التقليدية، وعمل بروفيل سيزمي ومسح للانعكاس بجهاز OKEAN طويل المدى.

تضم نتائج الرحلة اكتشاف ستة مواقع محتملة لبراكين طينية جديدة مكشوفة ومدفونة، التأكد من أن أخدود سترومبلي البحري نشيط حاليا، وأنه ينقل بصفة أساسية الرسوبيات البركانية الى حوض مارسيليا العميق، والتسجيل التفصيلي لعمليات الفقد الكبير للمادة في حوض كورسو - ليجريان، والكشف عن مزيد من النحر وإعادة ترسب الرسوبيات في الحوض الجزائري المركزي الغربي.

文　　摘

格连茨克调查船(R/V Gelendzhik)于1994年6月1日至7月6日进行的第四次联合国教科文组织--欧洲科学基金会(UNESCO--ESF)发起的“实习培训于研究”航次调查主要致力于地中海西部沉积物搬运过程的研究。该航次的次要课题涉及蒂勒尼安海(Tyrrhenian Sea)的一些构造和地震地层学以及对地中海海脊上的泥火山进行连续性研究等问题。

调查中使用的方法包括常规的回声探测和六频道地震剖面，用远距离(OKEAN)和深拖(MAK-1)旁测声纳进行带状反射性调查，以及用重力、箱式和盒式取样管进行底质取样。

航次结果包括：发现了六个可能的新的泥火山，有裸露的，也有深埋的，确定了斯特隆博利峡谷(Stromboli Canyon)目前仍十分活跃，并将火山的沉积物搬运到马斯利海盆(Marsili Basin)的深部；在声谱仪上详细记录了在科索--利古里亚海盆(Corso Ligurian Basin)出现的大面积物质坡移过程，并在中西部阿尔者罗--普罗汶卡尔海盆(West-Central-Algero-Provencal Basin)发现了大范围侵蚀和沉积物再沉降所造成的不寻常的海底形态。

ACKNOWLEDGEMENTS

On behalf of the cruise participants, we, the editors of this report, wish to express our appreciation to all organizations and persons involved in the preparation and execution of the cruise. Special thanks are given to UNESCO (M. Steyaert, A. Suzyumov, and D. Troost) and the European Science Foundation (P. Colyer) for their important financial support, constant encouragement and assistance.

Valuable financial support to the programme also came from the Russian Committee on Geology (I.F. Glumov) and the Ministry of Science and Technical Policy (B.G. Saltykov, Z.A. Yakobashvili, A.M. Novikov, V.I. Imerekov and V.N. Jivago); the ship and equipment, which are so central to the programme, were provided by the Central Marine Geological/Geophysical Expedition and NIPIokeangeofizika (Gelendzhik). We are very grateful for this essential contribution to the success of the programme.

We thank the Netherlands Geoscience Foundation (GOA) for their continuing financial support, as well as logistical support and financial management; the personal contributions of J. Stel, E. Bringmann, and C. van Bergen Henegow are much appreciated. The Netherlands Science Foundation (NWO) also contributed to the programme through a project to promote Russian-Dutch Cooperation in Marine Geology and Geophysics (Project 713-185).

Further financial and organizational support for the cruise came from national funding institutions and universities in Italy, U.K. and Spain. The efforts of R. Kidd in this regard are especially appreciated. The authorities of Turkey lent support to the cruise by granting free passage through the Strait of Bosporus and free port call in Istanbul. M. Ergün's (Piri Reis Foundation, Izmir, Turkey) work in bringing this about is gratefully noted. An excellent geological excursion to the Lagonegro Basin under the guidance of geologists from the Institute of Marine Geology (GEOMARE-SUD, Napoli), as part of a workshop which they hosted during a mid-cruise port stop in Napoli, contributed greatly to the scientific programme. We thank E. Marsella, M. Sacchi, B. D'Argenio, and their colleagues for organizing this.

Once again the International Hydrographic Bureau provided free harbour space and hospitality during a port stop in Monaco. We thank the directors of IHB and Rear Admiral Christian Andreasen in particular for their beneficial assistance.

For their help during the preparation and execution of the cruise we also thank F. Briand (C.I.E.S.M., Monaco), D. Travine (IOC of UNESCO), V.T. Trofimov (Moscow State University, Russia), and P.B. Rozov (Chief Staff Scientist, Yuzhmorgeologiya, Gelendzhik, Russia). We thank and congratulate M. Marani (Institute of Marine Geology, Bologna, Italy), who did a great job before and during the expedition as coordinator of the TTR-4 cruise.

Some figures for this cruise report (seismic and MAK-1 images) were prepared by students of Moscow State University (E. Akent'eva, P. Shashkin, and R. Almendinger), and most of the core logs were compiled by R. Lucchi of the University of Wales (Cardiff, UK); we are indebted to them for their assistance.

CONTENTS

INTRODUCTION

A.F. Limonov and J.M. Woodside

The Fourth UNESCO-ESF Training-through-Research Cruise (TTR-4) of the R/V *Gelendzhik* occurred from 1 June to 16 July 1994 in the Central and Western Mediterranean Basin. The main aim of the cruise was to investigate the sediments transport processes in different tectonic and morphological settings.

Large turbidite systems contribute much clastic sediment to deep-water basins. They are rather easy to study by conventional methods (such as high resolution seismics, subbottom profiling, sidescan sonar observations, and so on) due to their well-known seafloor and subbottom expressions. Hence, most research of depositional systems has focused on large deep-sea fans, such as the Mississippi Fan, the Amazon Fan, and the Rhone Fan. However, greater deep-water clastic deposition is provided in all likehood by the sum total of numerous relatively small depositional systems contributing sediments from many small separate drainage areas. These sedimentary systems usually have straight channels and large canyon gradients. Levees are poorly developed or are absent. Currently, we know too little about the sedimentary and hydrodynamic processes operating in these systems. Thus it is important to study this neglected type of depositional systems, examples of which are present in the southern Tyrrhenian Sea and the Corso-Ligurian Basin.

The second important task of the Cruise was to continue the investigations of the lower Valencia Channel area, which were started within the Training-through-Research Programme in 1992 (Limonov et al., 1993). High energy bedforms were mapped by the OKEAN long-range sidescan sonar, and by one higher resolution line using the deep-towed MAK-1 system. This 30 kHz sidescan sonar showed features believed to be sand or gravel waves, erosional scarps, and an unusual bedform that may be a regular pattern of erosional scours. On the Fourth Cruise, it was intended to study this and more southeastern distal areas in more detail in search of sandy deposits from flows passing along the Valencia Channel into the Balearic Basin.

One of the secondary goals of the Cruise was to run several well-placed seismic and OKEAN lines across the eastern Sardinian margin both to tie previous seismic lines with ODP drill holes and to obtain at least one long line across the entire rifted margin.

Finally, we planned to conduct a short study in the Cobblestone area in the western part of the Mediterranean Ridge in order to check some highly reflective patches observed on the GLORIA mosaic (Kenyon et al., 1982). We expected that these features could be mud volcanoes in analogy to the mud volcanoes discovered in and around the Olimpi/Prometheus 2 area during the Third Training-through-Research Cruise (Limonov et al., 1994).

The Cruise was subdivided into three legs. The first leg was mainly devoted to training of students and to testing of the equipment. However, we managed to carry out underway investigations on the western section of the Mediterranean Ridge during the transit to the Tyrrhenian Sea. The work in this area was continued during the transit back to Novorossiysk.

The second leg was concentrated in the Tyrrhenian Sea (Marsili Basin, Palermo-Cape S.Vito offshore area, and area east of Sardinia); and the third leg was scheduled for investigations in the Algero-Provencal Basin (Corso-Ligurian Basin and distal Rhone Fan and Valencia Channel area).

During the port call at Napoli between the second and third legs, a two-day Workshop with a presentation and discussion of newly obtained data was held at the Institute of Marine Geology (GEOMARE-SUD) and a geological excursion to the Lagonegro Basin in the southern Apennines was organized by the geologists of this institute.

About 35 lectures, seminars, and presentations of new data were given aboard the ship during the cruise by both teachers and students. Eighty three teachers, students, and technicians from 17 universities and scientific organizations of 7 countries participating in the cruise are listed below.

Table 1. List by country of participants in the 4th UNESCO-ESF Training-through-Research (TTR-4) Cruise.

First leg (3-9 June, completed on 12-13 July 1994): Cobblestone area, western Mediterranean Ridge
Second leg (10-19 June): Tyrrhenian Sea
Third leg (22 June-9 July): Algero-Provencal Basin

	Legs
The Netherlands	
J.M. Woodside* (Free University, Amsterdam)	2 3
J. van Hinte (Free University)	3
S. Troelstra (Free University)	1
E. Bringmann (GOA, the Hague)	1
G. Buijs (Free University)	1 2
P. Verweij (Free University)	2
A. Oosting (Free University)	3
J. van der Hoef (Free University)	3
E. Felser (Free University)	3
O. Duizendstra (Free University)	1 2
G. de Vries (Free University)	1 2
H. de Haas (NIOZ, Texel)	3
J. de Koning (Techical University of Delft)	3

United Kingdom

R.B. Kidd* (University of Wales, Cardiff)		2	
S.J. Wakefield (University of Wales)		2	
N.H. Kenyon (Institute of Oceanographic Sciences, Godalming)			3
B. Cronin (University of Wales)			3
J. Millington (University of Leicester)			3
M. Gee (University of Wales)			
J. Herniman (University of Wales)		2	
A. Jones (University of Wales)		2	
J. Clark (University of Leicester)			3
R. Rendle (University of Wales)			3
S. Morris (University of Wales)			3

Italy

M. Marani* (Institute of Marine Geology, Bologna)	1	2	
D. Penitenti (Institute of Marine Geology)	1		
C. Savelli (Institute of Marine Geology)		2	
F. Gamberi (University of Bologna)	1	2	
C. Romagnoli (University of Bologna)		2	
R. Lucchi (present address: University of Wales)		2	3
M. de Lauro (GEOMARE-SUD, Napoli)		2	
M. Sacchi (GEOMARE-SUD)			3
F. Budillon (GEOMARE-SUD)			3
L. Ferraro (GEOMARE-SUD)		2	
A. Sulli (University of Palermo)		2	
M. Lucido (University of Palermo)		2	
M. Agate (University of Palermo)			3
S. Infuso (University of Palermo)			3

Spain

F. Perez* (Institute of Marine Sciences, Barcelona)			3
F. Martinez Ruiz (University of Granada)	1		
J. Soto Hermoso (University of Granada)		2	
C. Viseras Alarcon (University of Granada)		2	
J. de la Linde Rubio (University of Granada)			3
J. Rey (University of Jaén)			3

Chile

J. Diaz (University of Valparaiso)	1	2	

Saudi Arabia

S. Mutwally (independant participant)	1

Russia

M. Ivanov* (Moscow State University)	1 2 3
P. Rozov (Yuzhmorgeologiya)	1 2 3
V. Tsyganenkov (Yuzhmorgeologiya)	1 2 3
A. Pavlov (Yuzhmorgeologiya)	1 2 3
G. Potapov (Yuzhmorgeologiya)	1 2 3
B. Rubtsov (Yuzhmorgeologiya)	1 2 3
A. Matveenko (Yuzhmorgeologiya)	1 2 3
A. Gusel'nikov (Yuzhmorgeologiya)	1 2 3
V. Fomenko (Yuzhmorgeologiya)	1 2 3
V. Podshuveit (Yuzhmorgeologiya)	1 2 3
V. Boldyrev (Yuzhmorgeologiya)	1 2 3
A. Shanin (Yuzhmorgeologiya)	1 2 3
A. Ovcharov (Yuzhmorgeologiya)	1 2 3
V Pryadilov (Yuzhmorgeologiya)	1 2 3
V. Vasil'ev (Yuzhmorgeologiya)	1 2 3
A. Koshman (Yuzhmorgeologiya)	1 2 3
P. Lygin (Yuzhmorgeologiya)	1 2 3
D. Shilyaev (Yuzhmorgeologiya)	1 2 3
A. Limonov (Moscov State University)	1 2 3
V. Gainanov (Moscow State University)	1 2 3
A. Volgin (Moscow State University)	1 2 3
D. Ivanov (Moscow State University)	1 2 3
I. Korotkov (Moscow State University)	1 2 3
G. Akhmanov (Moscow State University)	1 2 3
E. Ivanova (Moscow State University)	1 2 3
A. Lototskaya (Moscow State University)	1 2 3
E. Kozlova (Moscow State University)	1 2 3
E. Terent'eva (Moscow State University)	1 2 3
E. Shelavina (Moscow State University)	1 2 3
P. Shashkin (Moscow State University)	1 2 3
D. Vladov (Moscow State University)	1 2 3
T. Rodionova (Moscow State University)	1 2 3
A. Akhmetzhanov (Moscow State University)	1 2 3
E. Nezlina (Moscow State University)	1 2 3
K. Svinarenko (Moscow State University)	1 2 3
K. Kunin (Moscow State University)	1 2 3
A. Shishkin (Moscow State University)	1 2 3

*National coordinator.

I. STUDY AREA 1 (WESTERN MEDITERRANEAN RIDGE)

1. GENERAL SETTING

A.F. Limonov

The Mediterranean Ridge, and in particular mud volcanism in that area, was investigated during the 3rd Training-through-Research Cruise (1993) and we refer to Limonov et al. (1994) for a comprehensive description of the general tectonic setting of the Mediterranean Ridge. Here follows a brief description of the principal features of the Mediterranean Ridge stretching through the Central and Eastern Mediterranean Sea in the form of a giant arc convex toward Africa.

The Mediterranean Ridge is considered to be an accretionary complex with ongoing rapid deformation originating from the convergence of Africa and Eurasia. This convergence has led to collision between Cirenaica and Crete. The Ridge consists of highly faulted and folded strata from the Tethyan basin and African margin. Because the central and eastern parts of the Ridge are affected by strong tectonic transpression, its inner structure is supposed to be dominated by imbricate thrusts that have a morphological expression on the seafloor. Two deformation fronts, outer and inner, were recognized on both sides of the Ridge (Belderson et al., 1970, 1978; Finetti, 1982), the inner one being characterized possibly by backthrusts (Cita and Camerlenghi, 1992).

The age and composition of the sediments that make up the Ridge are still poorly known. It is supposed that the sequence of the outer part of the Ridge comprises about 200 m of Plio-Quaternary hemipelagic and turbiditic sediments, over 1 km of the Messinian evaporites, and a few kilometres of pre-Messinian Tertiary and probably Cretaceous rocks with unknown lithologies (Kastens, 1991). However, toward the Ridge crest, the Messinian gradually reduces in thickness and is probably missing in many places on the crest and inner side of the Ridge (Hirschleber et al., 1994; Limonov et al., 1994).

The seafloor topography of the Mediterranean Ridge is characterized in general by small-scale relief consisting of depressions and ridges, 50-100 m in amplitude and 0.5-2 km in wavelength. This has been attributed to a variety of origins including karst-like forms related to dissolution of outcroping Messinian evaporites (Belderson et al., 1978; Kastens and Spiess, 1984). However, the majority of small scale features are due to tectonic disturbance (Kenyon et al., 1982) as demonstrated by the TTR-3 Cruise, although dissolution features are present as well (Limonov et al., 1994).

The first mud diapir (Cobblestone, or Prometheus dome) on the western Mediterranean Ridge was discovered in 1978 during the American R/V *Melville* cruise and was sampled from the R/V *Eastward* (Cita et al., 1989). The following cruises principally organized by Italian geologists revealed a number of mud domes grouped into areas called Pan di Zucchero, Prometheus 2 and Olimpi.

Seismic and sidescan sonar surveys during the TTR-3 Cruise inside and around the Olimpi and Prometheus 2 areas led to discovery of about twenty new mud domes, amongst which nine structures were checked by coring. Most of them are mud volcanoes rather than subsurface mud diapirs (Limonov et al., 1994). The comparison of the coordinates on the formerly known and newly discovered mud domes with those of highly reflective patches mapped by the GLORIA long-range sidescan sonar (Kenyon et al., 1982) has demonstrated their complete coincidence. Thus, it turns out that many of those patches, interpreted by Belderson et al. (1978) and Kenyon et al. (1982) as karst-like forms above salt diapirs, are in reality mostly mud domes.

Normally the feeder channel of the Mediterranean Ridge mud volcanoes is not seen on seismic sections. This could be explained by its possible irregular form, by detachment of the volcano/diapiric body from the source formations, or by the difficulty in recognizing such structures in seismic sections which have limited penetration and many diffractions from the complex deformation of strata. The possible mechanism for the mud volcanism and diapirism of the Mediterranean Ridge could be strong lateral compression leading to stacking of sedimentary strata with different lithologies and densities which are in contact along thrust planes. Less dense plastic sediments, especially if fluid- and gas-saturated, overlain by denser rocks, are able to move upward along differently dipping faults due to buoyancy and overpressuring. The process is similar to salt diapirism. Moreover, the lateral compression transmitted across the entire accretionary complex (Davis et al., 1983) is capable of squeezing the plastic members upward to the seafloor, creating the mud domes.

The goal of the investigation in Area 1 during the TTR-4 Cruise was to check a number of small strongly backscattering patches seen on the GLORIA data from the western Mediterranean Ridge. These patches are linearly arranged along a possible thrust (backthrust?) trace, and one of them represents the Prometheus mud dome, which has the oldest (Middle Cretaceous) rocks in the mud breccia (Cita et al., 1981). The planned investigations included sidescan sonar and seismic surveys for clarification of forms and locations of the assumed mud volcanoes, as well as bottom sampling for the confirmation of their existence.

2. SEISMIC PROFILING

A.F. Limonov

Seismic line PS-128 was the only profile made in Area 1 (Fig. 1). It crosses the Hellenic Trench and the northeastern slope and crest of the Mediterranean Ridge in an ENE-WSW direction and runs across the OKEAN coverage. This seismic record, as well as all of the following records, was processed on board. The processing was based on the filtering of the signal, a normal move-out correction, stacking of the traces and recovery of true amplitudes.

Generally, no correlatable reflectors were recorded along the line. The Hellenic Trench was traced from the beginning of the line to time mark 01:00. It is defined by gently-hilly morphology with a relief of about 200 m. The thickness of the inferred Plio-Quaternary sediments is about 150-200 ms. Below this, a rather flat layer, about 100 ms thick, is seen in some places (23:20-23:30, 23:40-23:55, and 00:35-01:00) at different levels. The layer is delineated by strong reflectors from the top and bottom. This may be the Messinian evaporites because the seismic signature is quite typical of them.

The seismic pattern changes within the Mediterranean Ridge. The upper 0.6-0.7 s of the seismic section is layered, but the seismic reflection configurations are chaotic. The maximum penetration is approximately 1 s. Separate short reflectors are curved and are cut by frequent faults, mostly dipping westward. Some of them are evidently thrusts, judging by their expression in the seafloor morphology (Fig. 2).

A steep and high (150 m) cliff is present near time mark 04:15. On the OKEAN images along lines 128 and 130 it was interpreted also as the edge of thrust sheet dipping westward (see Section I.3.a). The thickness of the Plio-Quaternary sediments remains unknown from this record, and no seismic pattern typical of the Messinian evaporites is observed.

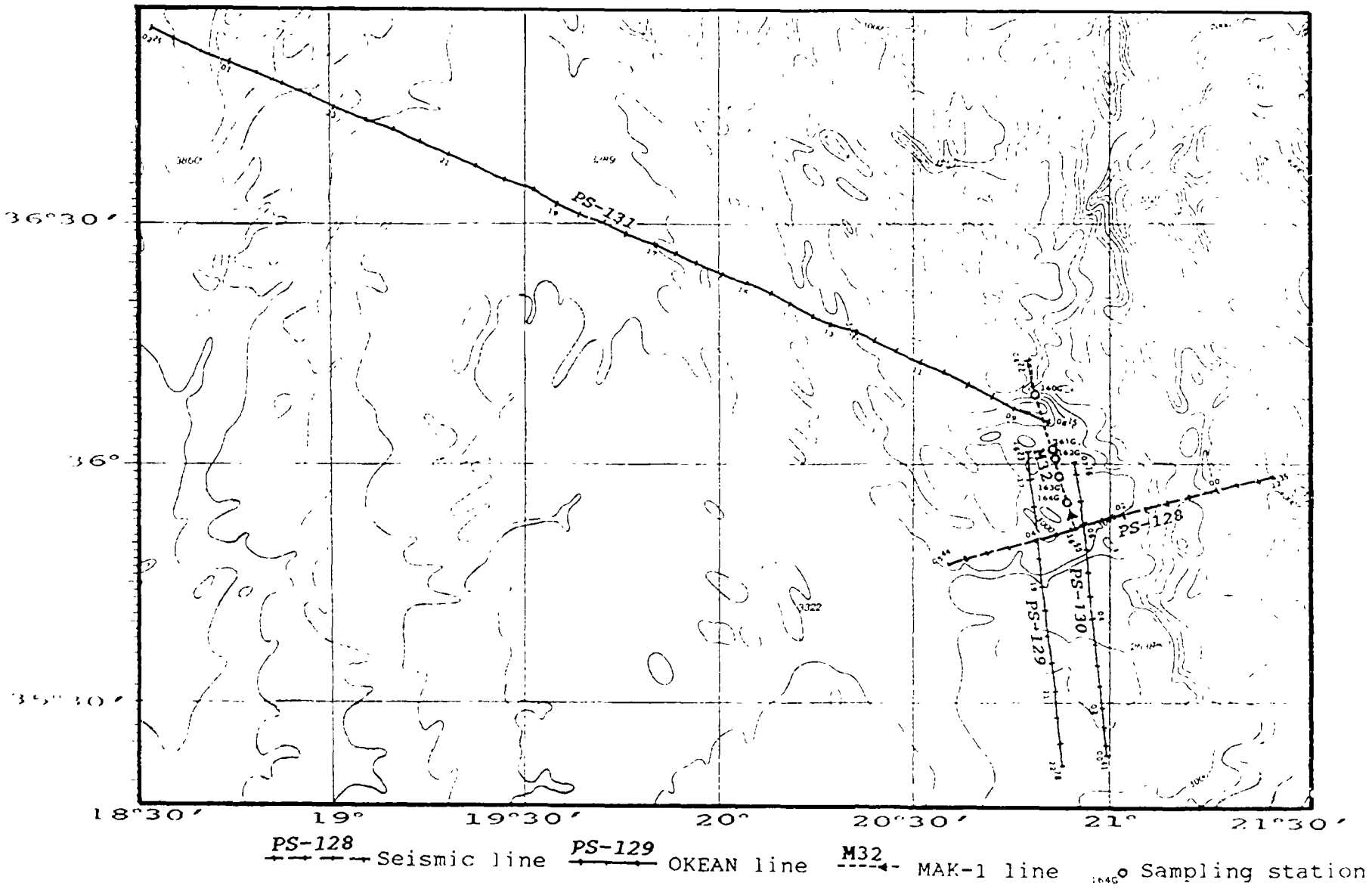

Fig. 1. Location map for Area 1. In this and all following figures the bathymetry is after IOC-UNESCO (1981)

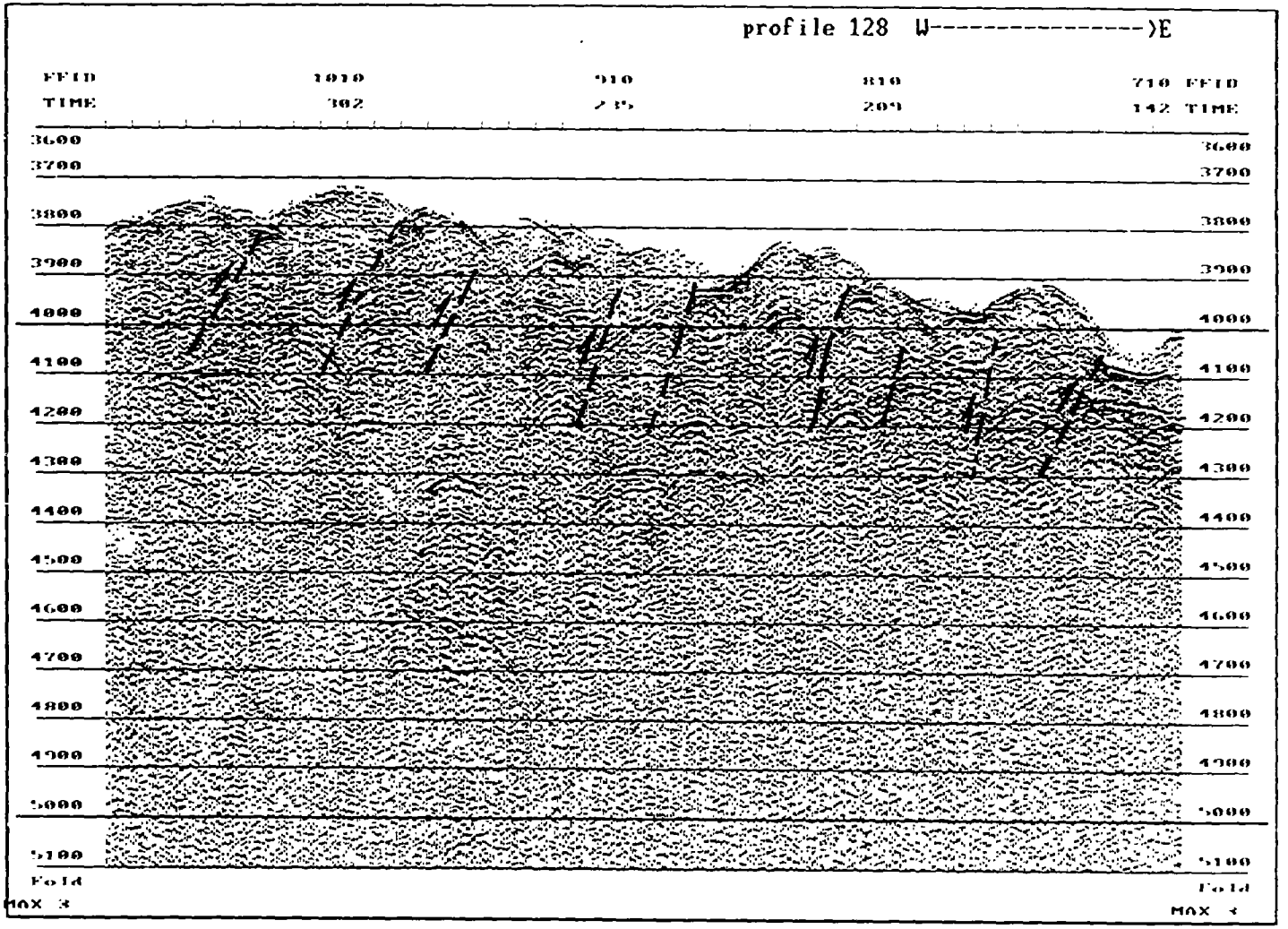

Fig. 2. Fragment of seismic section across the western Mediterranean Ridge showing possible thrusts (arrows). Seismic line PS-128

3. SIDESCAN SONAR SURVEY

a. OKEAN DATA

A.F. Limonov

Two OKEAN lines (129 and 130) were run in Area 1 in a NNW-SSE direction in order to provide overlapping of the swath coverage (about 15 km), and an additional line, 131, runs from Area 1 toward Area 2 (Fig. 1). A mosaic has been made from lines 129 and 130. The insonified area is situated on the crest of the ridge, at an average waterdepth slightly shallower than 3000 m. Two principal classes of features, linear and isometric, are seen on the sonographs.

Linear features

The main linear feature was recorded mostly on the right side of line 129 between the start of the line and time mark 21:00. This is generally highly reflective, although the rate of backscatter varies along its strike. The configuration of this feature is extremely sinuous, and sometimes it bends at right angles. Its general trend is NNW 320°, but south of time mark 19:30 it splits into two branches. The first of these bends sharply eastwards and begins to be traced on the left side of the sonograph. On the parallel line, 130, this feature was not recorded. The second branch generally follows the line 129 orientation and gradually loses its reflectivity southwards, completely disappearing south of time mark 21:00. The width of this linear feature is also variable and changes from a few hundreds of metres to about one kilometre. Some isometric dark patches on the sonograph seem to represent local widenings of this feature. A similar but poorly expressed feature appears north of time mark 04:00 on line 130. It is characterized by lower sinuosity and lower backscatter level. Its general trend is parallel to the line.

The features described, particularly those along line 129, represent rather steep cliffs on the seafloor and are interpreted to be the outcropping edges of thrust sheets dipping westwards which have probably originated quite recently. The surface of these assumed thrust sheets is remarkable for its small-scale irregularities (folds and faults?) generally elongated parallel to the local trend of the Mediterranean Ridge. Sometimes the outcropping edges demonstrate a step-like pattern and near the start of line 129, the edge is broken into small blocks.

Isometric highly reflective patches

Six high backscattering patches (dark tones on the OKEAN display, light on the GLORIA display) were recorded along the first two lines we made and are also seen on the GLORIA mosaic (Kenyon et al., 1982). Five of the patches, including that related to the Prometheus mud dome, are connected with a NNW-SSE trending lineaments which were described above.

Two dark patches (16:25 and 18:45 on line 129 or 05:10 on line 130) are thought to represent high and steep outcrops of the thrust sheet edge. The first of these patches is S-shaped and narrow, whereas the second one, with its lower reflectivity, is likely to be a wider and more gentle scarp, which may be smoothed partially by a hemipelagic blanket. Alternatively, this patch could be also an accumulation of mud breccia squeezed out from below the thrust sheet. The Prometheus mud dome is only seen in profile on the unprocessed sonograph because it was crossed through the centre. Another more probable mud dome was also crossed exactly through the centre on line 129 (20:05). It has a diameter of about 3 km, a regular rounded form, and it is clearly rimmed. On the corresponding unprocessed sonograph, the feature demonstrates a symmetrical cone rising above the seafloor. This feature is undoubtedly related to the thrust sheet.

A small dark patch is poorly seen on the left side of sonograph 129 (21:30) and is difficult to interpret. The last southernmost dark patch was recorded on the same side, further along the line (22:00). It has elliptic outlines, an obscure border and is characterized by a moderate level of backscatter. It could be a mud dome with a rather thick blanket of hemipelagic sediments.

In addition to the dark patches already shown on the GLORIA mosaic, there are some new isometric highly reflective features (Fig. 3). All of theses are interpreted as probable mud domes. One was recorded on the right side of line 129 (17:10) near the foothill of the thrust scarp. It has an irregular border, moderate backscatter, and a diameter of about 1.5 km. Two well-expressed dark patches are seen on the left sides of both sonographs (16:35 and 17:30 on line 129 and 07:25 and 06:30 on line 130). Their plan views are somewhat angular, and the reflectivity is very high. Their diameter is between 2.5 and 3 km. Their appearance is typical of mud volcanoes investigated during the TTR-3 Cruise.

On the right side of sonograph 130, at the very end of the line (07:20), a rather enigmatic structure was found. It is slightly elongated across the sonograph, has moderate backscatter and a length of about 7 km. Its western edge represents a big bulge in the seafloor topography seen on the corresponding unprocessed sonograph. This could be a mud volcano or two mud volcanoes with overlapping mud flows.

The sonograph recorded along line 131 shows different structural and morphological patterns. At the very beginning of the line, on the right side, a moderately reflecting and rather flat bathymetric high is seen. Its visible western edge has rounded outlines and probably a step-like form in cross-section, which may be also the edge of a thrust sheet. The rest of this sonograph has a uniform pattern with discontinuous and sinuous linear features, usually 4-7 km long, trending along the Mediterranean Ridge. They are interpreted as tectonic relief (young folds and faults) created by strong compressional stress. Some dissolution features are not excluded either, but they can not be distinguished against the general background of small-scale relief.

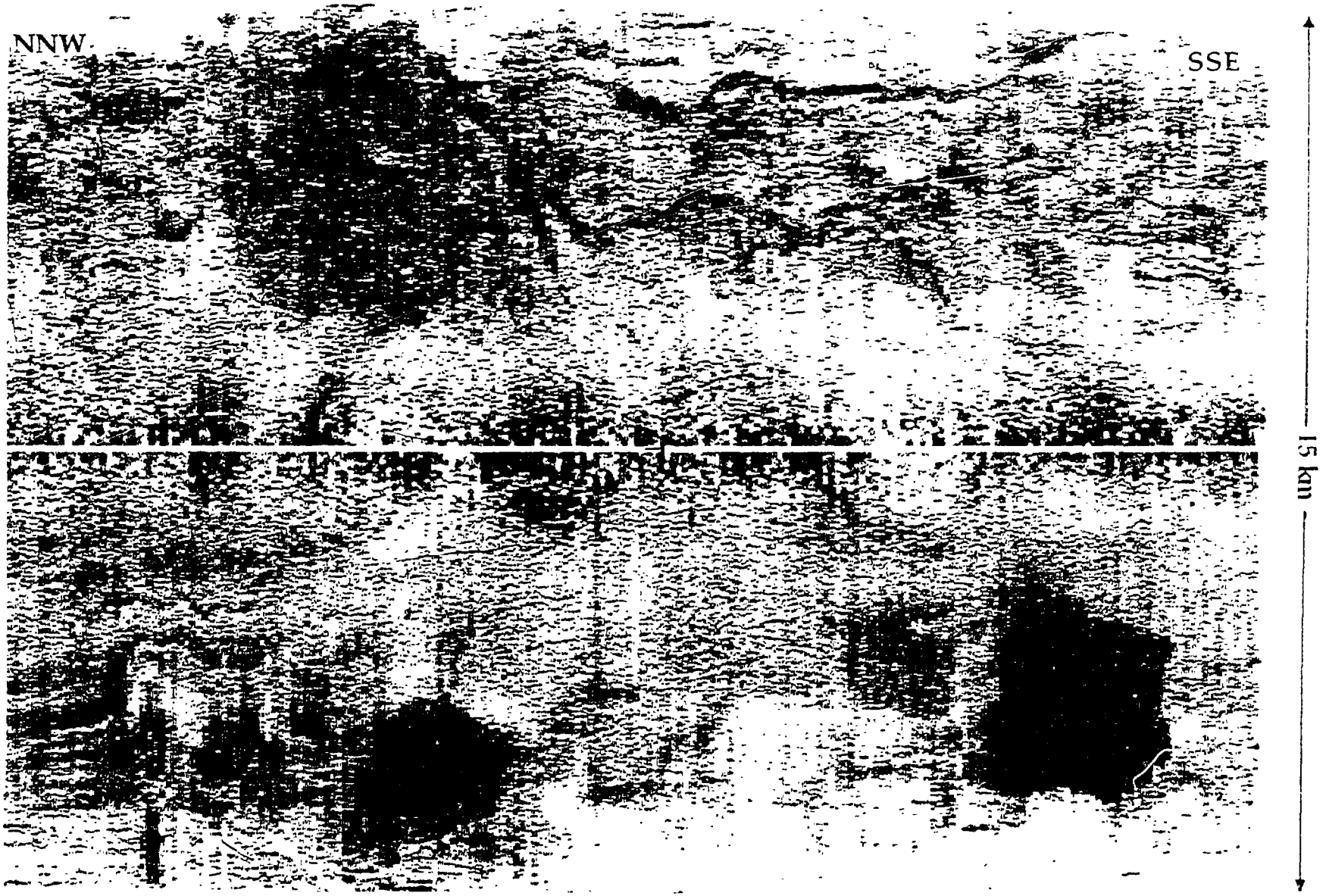

Fig. 3. Isometric highly reflective patches (assumed mud volcanoes) on the OKFAN sonograph (line 130). It is seen that most of them are related to fault traces

b. MAK-1 DATA

A.F. Limonov and M.K. Ivanov

MAK line 32 was made during the transit back to Novorossiysk from Monaco. It lies parallel to and between OKEAN lines 129 and 130 (Fig. 1). The line position was chosen on the basis of the OKEAN sonographs in order to cross at least two assumed mud volcanoes seen on the sonographs as two high reflective circular patches. The line starts between the northern portions of the OKEAN lines and continues further northwards, out of the area covered by the OKEAN swath.

The image recorded along this line is one of the most interesting and complicated of all those obtained during the cruise. It crosses the area of typical "cobblestone" topography (Hersey, 1965) and several mud volcanoes and possible clay diapir, which was not recorded on the OKEAN sonograph because of its small size.

The line starts in a region of rather smooth seafloor (as far as time mark 18:40), with a visible relief under 70 m. The seafloor features are aligned parallel to the general Mediterranean Ridge trend. They have a length of 500-700 m and en-echelon arrangement. They sometimes display a high level of backscatter on the portside of the swath (west scan) and mostly acoustic shadows on the starboard of the swath (east scan). Acoustic penetration on the profile is limited to about 30 m, and generally no continuous reflectors are recorded below the seafloor. These features could be the edges of the thrust sheets emplaced to the east or outcrops of the westwards dipping beds of sedimentary rocks.

The next prominent feature recorded between time marks 18:40 and 19:55 is a typical mud volcano (Fig. 4). It has a quite regular conical shape in cross-section, with a relative height of about 130 m and a diameter of more than 2 km. The volcano is imaged as a highly reflective area with radiating mud flows spreading from the crater down its slopes in all directions. The crater is very small (less than 100 m in diameter) and is very clearly delineated. The mud flows have a more prominent relief on the western slope of the volcano, and possibly belong to the most recent generation. No subbottom reflections are recorded on the profile. The volcano was checked by gravity corer, and the mud breccia was recovered below a 25 cm layer of the Holocene sediments. The sampling site is situated on the flank of the mud volcano, approximately 400 m from the crater. After the sampling, the volcano was named Novorossiysk after the hometown of A. Matveenko (the chief of the MAK-1 team). It is interesting to note that a submarine telephone cable is recorded on the sonograph, laid down exactly across the crater.

Between time marks 18:15 and 18:30, there is a rounded feature covered by layered sediments at least 30 m thick (Fig. 5). This feature has a diameter comparable with the Novorossiysk mud volcano and a well-expressed rimmed

structure. The northern portion of the rim is complicated by a probable diapiric structure, about 200 m in diameter and 50 m in height. This was interpreted to be a buried extinct mud volcano through which a younger mud diapir protrudes. Coring was attempted, but because of strong wind and ship's drift, we failed to hit the target, and the core was taken about 110 m north of the diapir's summit, near its foothills. The core contained a complex, principally hemipelagic sequence with numerous coloured geochemical fronts (see Fig. 9).

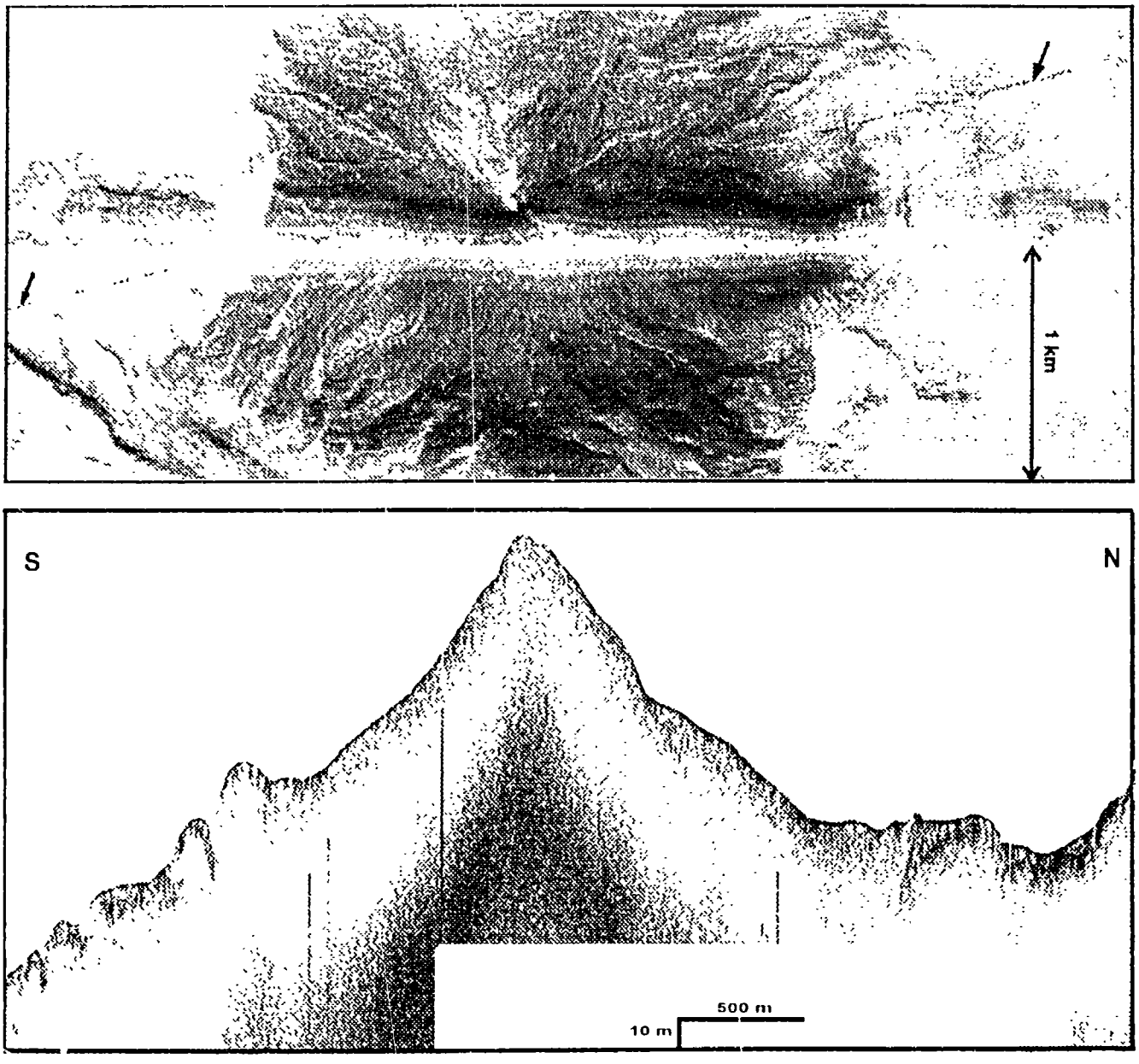

Fig. 4. The Novorossiysk mud volcano in the Cobblestone area. Arrows indicate a submarine telephone cable laid down exactly across the crater

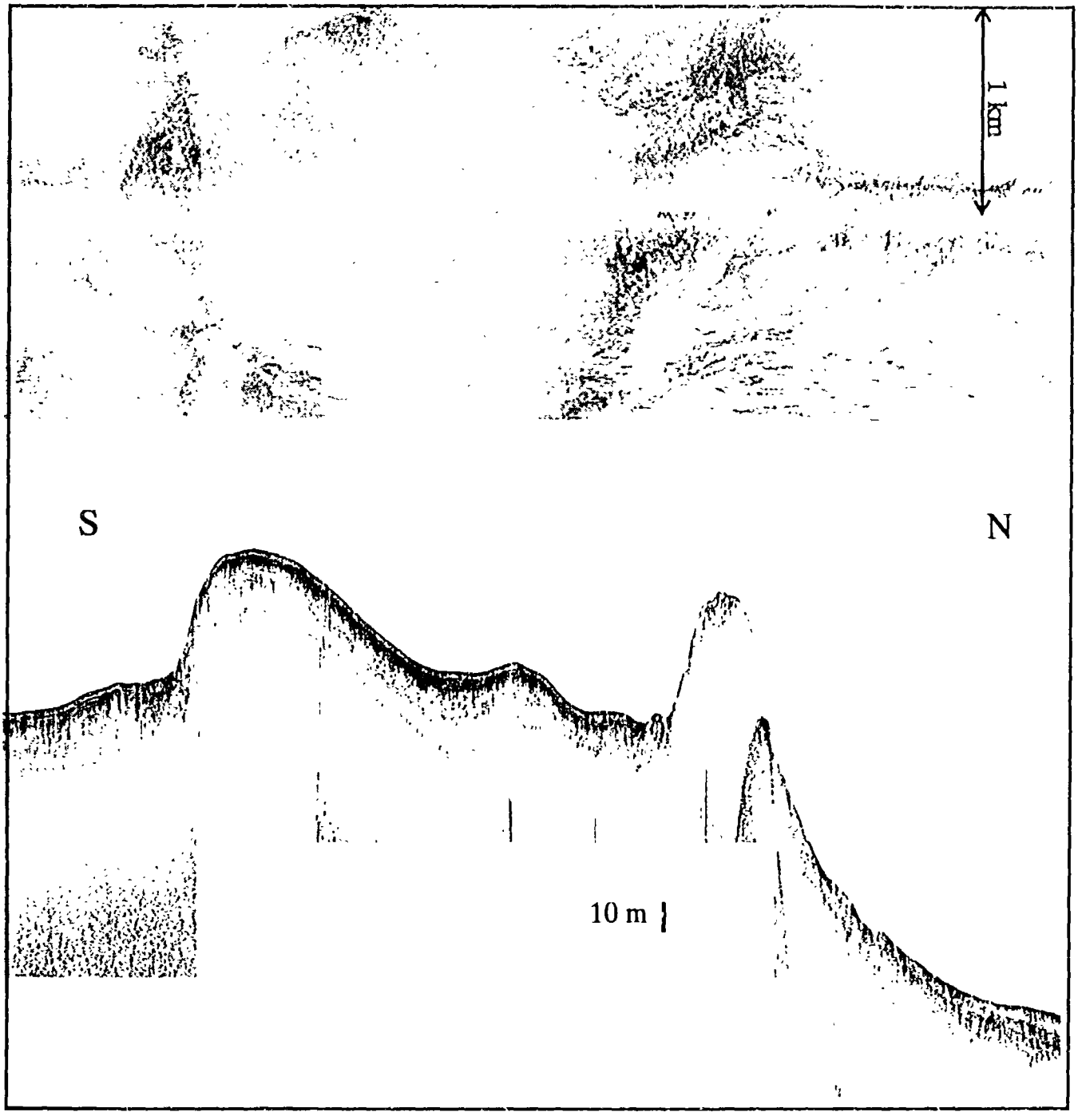

Fig. 5. Buried mud volcano in the Cobblestone area. Probable mud diapir protrudes the northern portion of the mud volcano rim. MAK-1 line 32

The next mud volcano is situated further north between time marks 21:50 and 22:35. It was crossed on its western flank, and the observed relief is no more than 50 m. However, another echosounder record showed that it has a height of about 100 m. Its diameter is approximately the same as that of the Novorossiysk mud volcano. Judging from the backscatter pattern, one may conclude that the western flank of the volcano is wider and gentler than the eastern one. The well-displayed crater is more than 200 m across. Mud flows spread mostly south- and westwards. The western flank of the volcano has a prominent patchy acoustic pattern which is evidence for the uneven surface of the mud flow. A large uplifted block is observed near the northwestern foothills, and some rounded depressions are situated to the WSW of the crater. All of these are thought to be the parasitic craters with their own mud flows. Cores obtained from this mud volcano contained mud breccia below a 20 cm cover of Holocene sediments, including the Marker Bed (see Fig. 9). The volcano was named Aros (abbreviation from Archipo-Osipovka, the hometown of V. Tsyganenkov, chief of the seismic team).

In the north, the Aros mud volcano borders on a similar structure, rising 160 m above the level of Aros (Fig. 6). The coring near the centre of this structure (sampling station 161) showed probable mud breccia at the bottom of the 3.89 m long core of hemipelagic sediments. This probable mud breccia has an unusual appearance and consists of stiff light grey clayey matter. The only semi-consolidated carbonate clast was found in this clay, but it was destroyed during washing. Such a composition of the eruptive products of this mud volcano may be the reason why it has a quite low level of backscatter on the MAK-1 sonograph. The mud volcano may be active because structures resembling pockmarks are observed near its southern and north-northwestern margins.

An elevated plateau with dissected relief is seen between time marks 23:15 and 00:40. The relief is about 100 m and is seen as frequent alternation of isometric highs and lows aligned across the scan. They form a typical "cobblestone" topography. These features could be folds although they may be related to the exposure and dissolution of the Messinian evaporites since no subbottom reflectors were recorded on the profile, thus testifying to a homogeneous composition of the shallow deposits. On some slopes, there are small fan-like features expanding from narrow gullies. These are either locally transported sediments or mud flows coming from the west.

A circular structure recorded between time marks 00:40 and 01:18 has a visible diameter of about 3 km and a well-defined rim approximately 40 m high. Inside the rim there is a depression ponded with sediments, at least 30 m thick, which are pinching out from the centre of the structure towards the rim. Two probable mud flows, distinguished by their higher reflectivity, spread from the depression centre in the northwestern and southern directions (Fig. 7). This structure was interpreted as an extinct mud volcano.

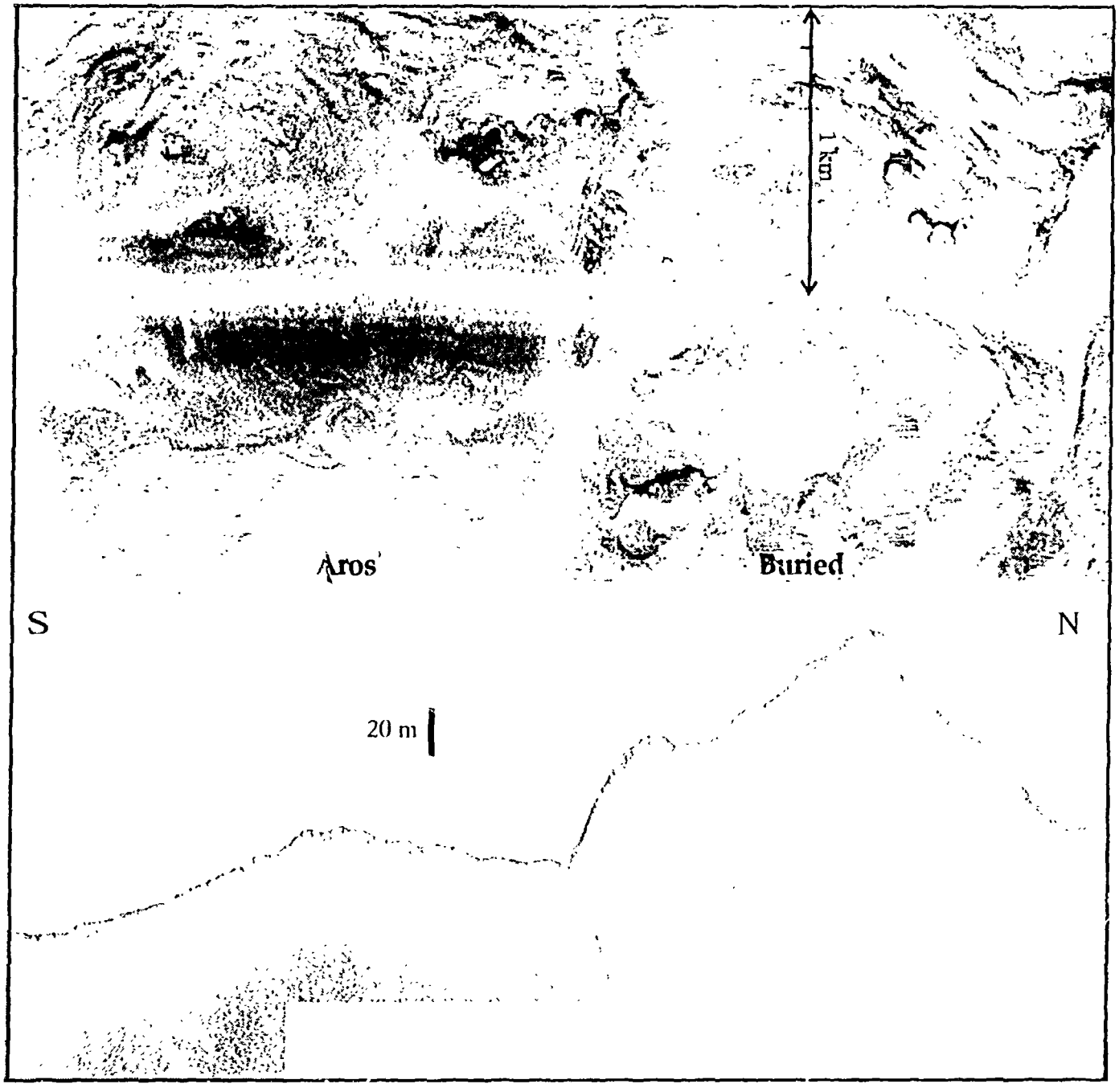

Fig. 6. The Aros mud volcano and a possible buried mud volcano in the Cobblestone area. MAK-1 line 32.

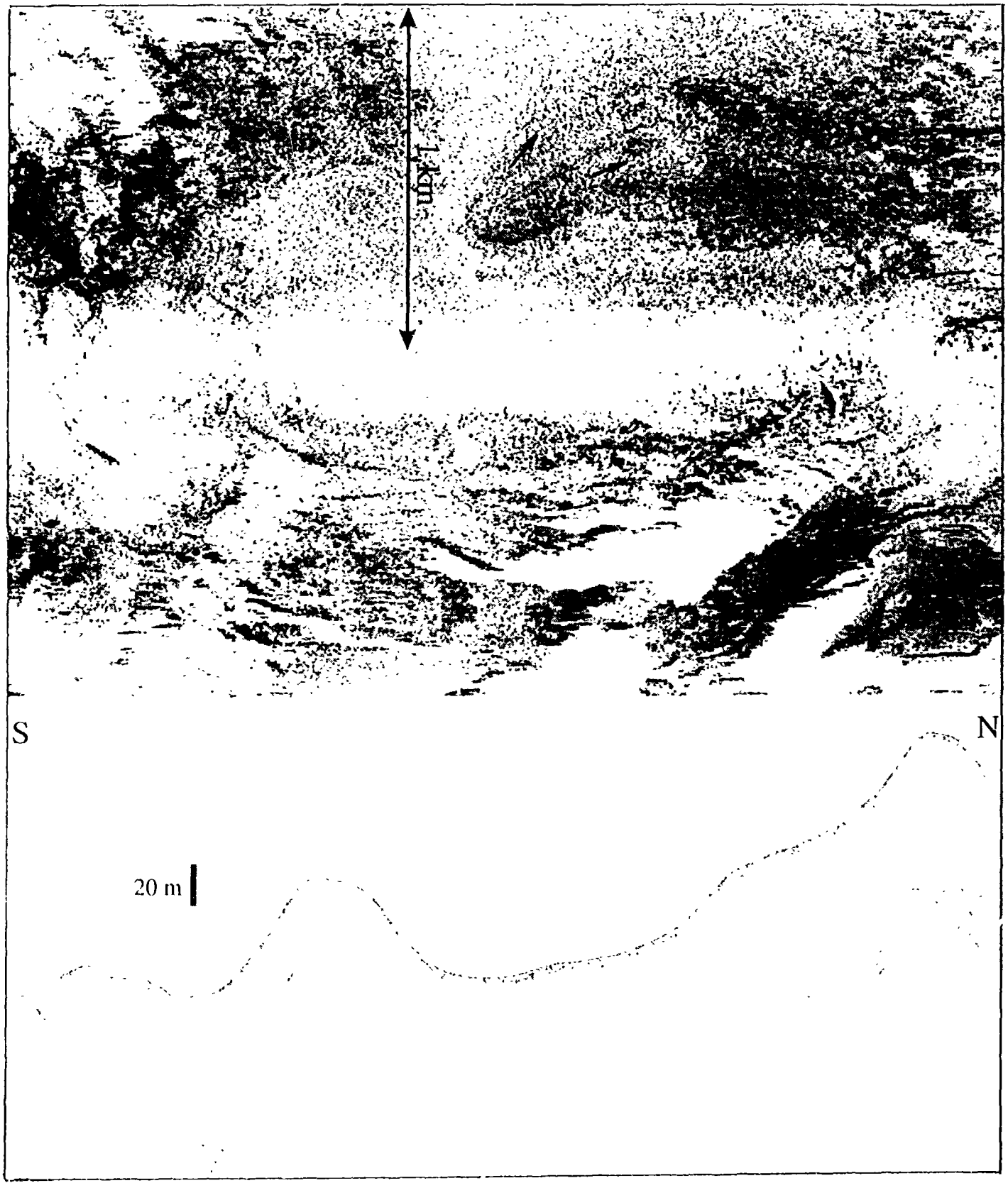

Fig. 7. Extinct mud volcano with probable mud flows (arrows) buried by sediments in the Cobblestone area. MAK-1 line 32

A large fault scarp is seen between 01:20 and the end of the MAK line. The scarp is convex to the west and probably represents the northern continuation of the same thrust zone which has already been described. On the oblique crossing near time mark 03:40 the height of the scarp is about 60 m (Fig. 7) and it bends round the 2.5 km wide circular structure, which has a moderately high backscattering level and an unusually textured surface.

While the surrounding seafloor has rather sharp relief with alternating strong acoustic echoes and shadows, the circular structure shows smooth relief with gentle small-scale undulations. The structure itself is not displayed in the seafloor topography and is situated on the northwards facing slope. No subbottom reflectors were recorded on the profile. Some features similar to craters are observed near the edge of the starboard scan. It was supposed that the structure could be a mud volcano, and, indeed, the core taken from it had mud breccia under a 5 cm layer of Holocene sediments.

4. BOTTOM SAMPLING

G.G. Akhmanov

Seven cores were recovered on Leg 1 of the TTR-4 Cruise. Cores 119G and 120B were taken for educational purposes from an isolated high within the Hellenic Trench System and the rest of the cores were obtained from the western part of the Mediterranean Ridge, in the area of mud diapirs called the Cobblestone area (Table 2; Figs. 1, 8, and 9).

The total recovery is 16.79 m. The longest core (161G) is 389 cm long, whereas the shortest one (120B) have a length of 31 cm. Before sampling in the Cobblestone area, the OKEAN and MAK-1 surveys were carried out and sampling sites were chosen on the basis of the acoustic images. We attempted to take cores from the newly discovered mud volcanoes, both exposed and buried, and from the assumed mud diapir on the margin of a buried mud volcano. In the latter case (sampling station 163), we failed to hit the small structure because of the strong ship's drift, and the core was taken at site just to the north. The gravity corer did not reach the mud breccia on the assumed buried mud volcano (sampling site 161) because of a large thickness of overlying hemipelagic sediments. The onboard investigations included splitting the cores, photographing them and making a detailed lithologic description.

Cores from mud volcanoes

Three cores contain the characteristic mud breccia below a veneer of yellowish-brown marl, rich in forams and pteropods. The mud breccia consists of centimetric to millimetric, subrounded to angular clasts of clays, mudstones, marlstones, and fine-grained sandstones supported by a silty-clay matrix. Additionally, the mud breccia from core 164G includes a 8 cm thick oxidated layer of olive colour. Core 162G was recovered from the crater of the Aros mud volcano, and its mud breccia is notable for abundant large pebbles of mudstone (up to 2.5 cm in size) and marlstone (up to 5 cm) in the lower part of the sequence.

Cores 160G and 164G were taken on slopes of the unnamed (the northernmost) and the Novorossiysk mud volcanoes respectively. They have a gently sloping contact between the mud breccia and the overlying marl. Many subrounded mudstone clasts (up to 1 cm in size), as well as an angular pebble, 5 cm in size, of fine-grained sandstone were observed in the mud breccia from core 164G (Novorossiysk mud volcano). The middle part of the sequence in core 160G shows the younger mud breccia containing the inclusion of the older mud breccia, 24 cm in size. This fragment of the older mud breccia consists of silty-mud matrix with rocks clasts, up to 5 cm in size. It is divided into two parts: the lower one is represented by grey mud breccia that grades into the upper interval represented by olive oxidated mud breccia with observed thickness of 15 cm. The inclusion is more consolidated than the host mud breccia and has sharp contacts with it.

Table 2

Summary of sampling data on Leg 1 of the TTR-4 Cruise

Core no	Latitude Longitude	Date GMT	Corr. depth(m)	Cable length (m)	No of sections	Recovery (cm)	Lithology	Setting
[illegible]G	36°04.7'N 21°57.9'E	05.06 14:27	2686	2850	6 + CC	334.5	marls sapropel S-1,5 & 6 tephra Y-5	Small ridge in the Hellenic Trench
120B	36°04.9'N 21°57.7'E	05 06 16:00	2640	2860	1	31	pteropod ooze marl marker bed	Small ridge in the Hellenic Trench
160G	36°08.9'N 20°48.6'E	12.07 08:36	2736	2888	2 + CC	140	marl mud breccia	Cobblestone area, MAK line 32
161G	36°02.0'N 20°50.6'E	12:07 10:07	2744	2880	7 + CC	389	marls sapropel S-4 & 5	Cobblestone area, MAK line 32
162G	36°00.8'N 20°51.3'E	12.07 11:09	2815	2960	3 + CC	217	marl marked bed mud breccia	Cobblestone area, MAK line 32
163G	35°58.6'N 20°51.9'E	12.07 12:12	2765	2992	6 + CC	372.5	marls tephra Y-5 sapropel S-4,6 & 7	Cobblestone area, MAK line 32
164G	35°55.3'N 20°53.0'E	12.07 13:30	2766	2990	3 + CC	195	marl mud breccia	Cobblestone area, MAK line 32

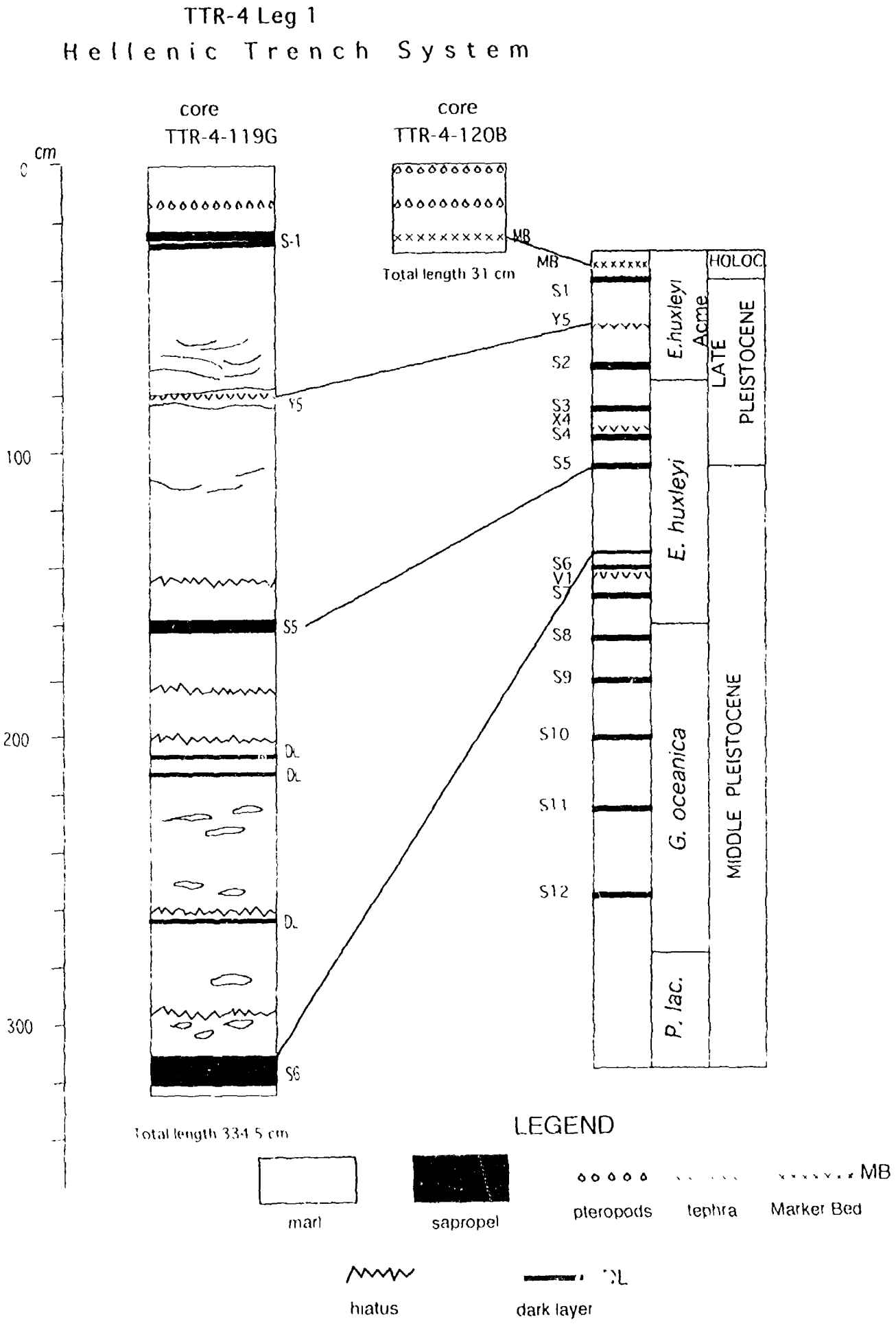

Fig. 8. Cores recovered on Leg 1 in the Hellenic Trench System

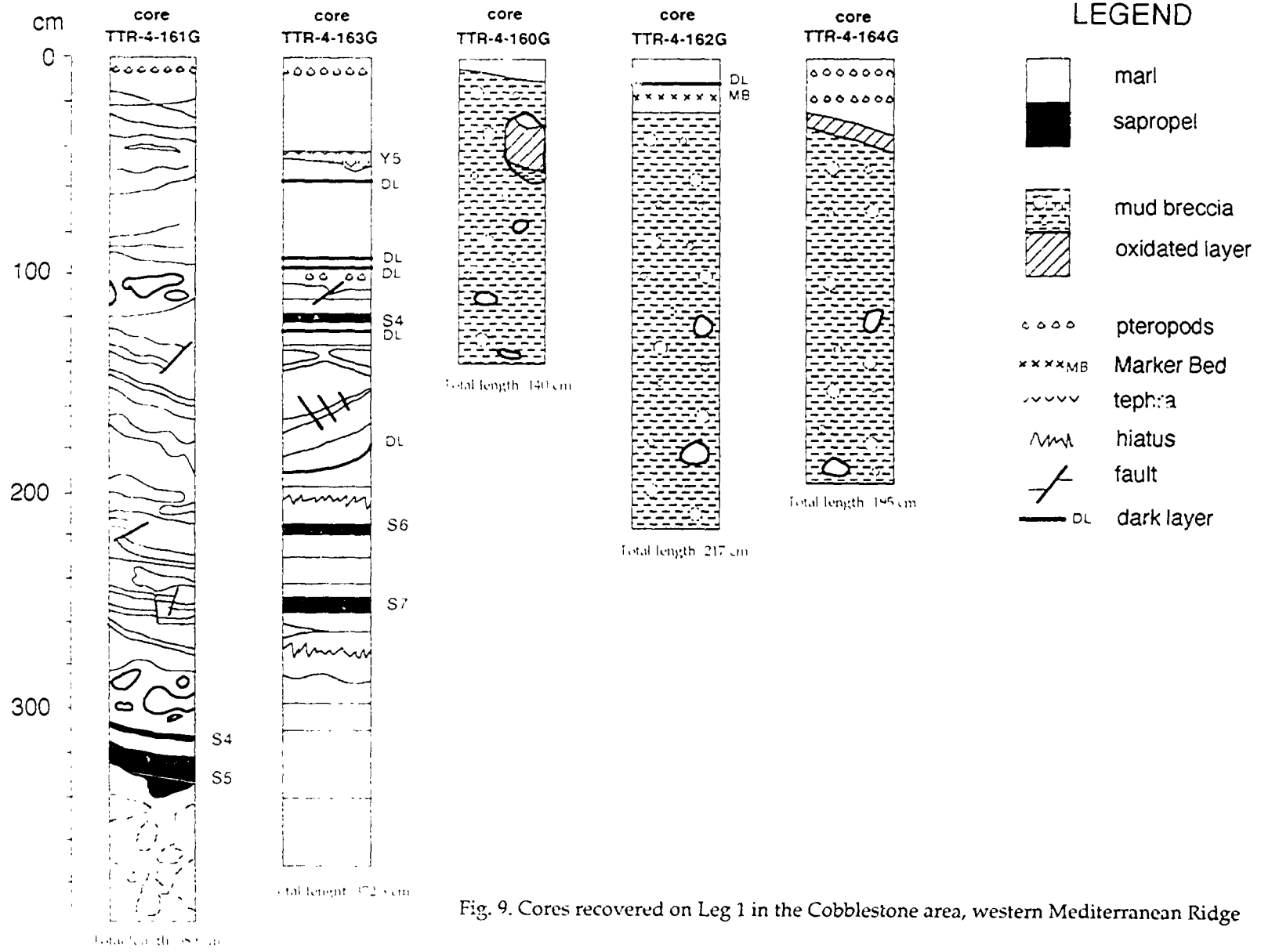

Fig. 9. Cores recovered on Leg 1 in the Cobblestone area, western Mediterranean Ridge

In addition to several large-sized clasts of fine-grained sandstones, some hundred small clasts were described for the lower interval of core 160G. A relatively poor consolidation of the clasts and high content of sand in the matrix were also noted for the mud breccia from core 160G during the onboard examination. The preliminary study demonstrates the similarity of the mud breccia from the Aros and Novorossiysk mud volcanoes and its difference from the mud breccia from the unnamed mud volcano (core 160G).

Pelagic cores

Pelagic sequences of Middle Pleistocene to Holocene age were recovered at four sampling stations. The shortest core 120B (31 cm) contains only the upper part of the continuous Holocene sequence. It is represented by yellowish-brown marl with several interlayers rich in pteropods. The Marker Bed (a peculiar layer, dated by ca. 3.5 ka, consisting of Mn micronodules) is also present at the core bottom (29-30 cm). Three other pelagic cores are significantly longer, but none of these contains a continuous sequence.

Several hiatuses and slump intervals were recorded in these cores. Sapropel S-1 of Holocene age is documented only in core 119G, while tephra Y-5 (ca. 40 ka) is present in cores 163G and 119B. Sapropel S-4 (ca. 100 ka) was found only in cores 161G and 163G. Sapropel S-5 (approximately 125 ka) is rather thick in core 119G, whereas it is included in the slump interval in core 161G and is missing in core 163G. Very thick sapropel S-6 (185 ka) is observed at the base of core 119G, but it is thinner in the middle part of the sequence of core 163G and is absent in core 161G. Sapropel S-7 (ca. 200 ka) is present only in core 163G, where it is thick and strongly bioturbated.

It is necessary to note that the lower and middle sections of core 161G from the slope of the assumed buried mud volcano contain subrounded clasts of marl and clay which may belong either to gravity flow deposits or to old mud breccia transformed by diagenesis. Numerous microfaults, slump structures and hiatuses are observed in all cores with the exception of core 120B. These features may imply high tectonic activity and slope instability in the study regions during the Pleistocene.

5. CONCLUSIONS

A.F. Limonov and M.K. Ivanov

1. The assumption that mud diapirism is a common phenomenon for the Mediterranean Ridge (Limonov et al., in press) was strongly supported by the findings of this cruise. Within the seafloor strip about 40 km long and 2 km wide, 6 new mud volcanoes were recorded and 3 (possibly 4, taking into consideration core 161G) of them were checked by coring. From the GLORIA mosaic (Kenyon et al., 1982), one can conclude that many tens of mud volcanoes may still be discovered on the Ridge crest.

2. Extinct buried mud volcanoes have never been found before in this region. There were probably several stages of the mud volcanism, and some mud volcanoes stopped their eruptions at approximately the same time because they are buried by marine sediments with approximately the same thickness. Their further activity could be expressed as fluid and gas seeps accompanied by pockmarks (Fig. 5).

3. Also confirmed was the idea that the mud volcanoes are closely linked with fault systems. Faults (more likely thrust faults), trending in accordance with the general trend of the Ridge, are clearly seen on both the MAK-1 and OKEAN sonographs, and some mud volcanoes are "perched" on these lineaments or are situated at the immediate vicinity to them.

4. The variable age and composition of the mud breccia, recovered from this close spaced group of mud volcanoes, supports the supposition that their age and composition are dependant on the depth of penetration of the faults and the degree of their mutual communication (Limonov et al., in press). The tectonic overburden can create excess pore pressure in the deep-seated plastic formations, and the lateral tectonic stress enhances their extrusion to the seafloor.

II. STUDY AREA 2 (TYRRHENIAN SEA)

1. GENERAL SETTING

F. Gamberi, M. Marani, R.B. Kidd, J.M. Woodside, M. De Lauro, L. Ferraro, M. Lucido, A. Sulli, M. Agate, F. Budillon, S. Infuso, and M. Sacchi

The collisional and back arc settings of the small ocean basins of the Mediterranean Sea were characterised by Stanley (1972) as "natural sedimentation laboratories" for earth scientists interested in the processes that deposited the marine clastic sequences that make up much of the sedimentary record in mountain belts on land. He argued that these small ocean basins with their turbidity current-deposited sediment fills were much more likely analogues for the classic outcropping turbidite sequences described and interpreted on land (Mutti, 1977; Ricci Lucchi and Valmori, 1980; etc) than open ocean abyssal plain and continental rise deposits of the Atlantic, Indian, and Pacific Oceans (Bouma et al., 1985a; Kidd et al., 1985; Kidd et al., 1987; Piper et al., 1995; etc). Certainly, the Mediterranean Basin sequences have a higher potential for preservation in the rock record because of their geodynamic setting and because their scale is much more consistent with the "flysch" basins envisaged by Alpine and other land geologists.

Despite the interest in and subsequent marine geological investigations of the Mediterranean basins over the past 15 years, many of the advances in understanding turbidity current and other gravitational processes have been made by marine geologists studying open marine continental margins and deep sea fans like the Amazon, Mississippi and Indus (Damuth and Embley, 1981; Damuth et al., 1995; Bouma et al., 1985b; Droz and Bellaiche, 1985b; Kenyon et al., 1995). The marine geological advances have been driven by the combined use of sidescan sonar systems, high resolution seismic profiling, and core sampling. Until the initiation of the TREDMAR "Training-through-Research" programme, there had been relatively little effort applied to studying basin-filling processes with these systems in the Mediterranean. Each year since 1991, the annual expedition of this UNESCO/ESF sponsored programme brings together a group of European universities and institutions with Moscow State University to carry out investigations using the research vessel *Gelendzhik*, which is equipped with the state-of-the-art Russian sidescan systems OKEAN and MAK-1 and a high resolution 6-channel seismic profiling system.

Only two large submarine fans are evident in the Mediterranean, the Nile and the Rhone, whereas there are hundreds of simple canyon-fed, short and comparatively straight channel systems with relatively steep gradients. The approach of mapping with two scales of sidescan, together with seismics and sampling, has been comprehensively applied in the study of the Madiera Abyssal Plain and Saharan Continental Rise (Masson et al., 1992; Weaver et al., 1995), which are partly fed with volcaniclastic sediments from the Canary and Madiera Islands. In that area the importance of large-scale mass wasting processes (slides and debris flows) has been recognised, as well as the role of topography in deflecting turbidity current flows (McCave and Jones, 1988; Rothwell et al., 1992).

In the southern Tyrrhenian Sea we wished to study similar systems in a more restricted setting.

The Tyrrhenian Sea is a deep basin enclosed between the Italian Peninsula and the islands of Corsica, Sardinia, and Sicily (Fig. 10). It is a back arc basin originating in Miocene time in a region previously occupied by the suture between the Alpine and the Apenninic chains. This collisional belt came into existence from Oligocene time due to the counterclockwise rotation of the Corsica-Sardinia block (Alvarez et al., 1974). During this process, the subduction of the African north-dipping plate beneath the Corsica-Sardinia microplate occurred. As a consequence, in the region overlying the descending African slab, the Tyrrhenian back arc basin started to form, resulting in the collapse of the previous orogenic edifice (Malinverno and Ryan, 1986). Deep-focused earthquakes (Gasparini et al., 1982) and an active emerged volcanic arc in the southern Tyrrhenian area indicate that this subduction process is still active but, according to Savelli and Gasparotto (1994), may be at a senile stage.

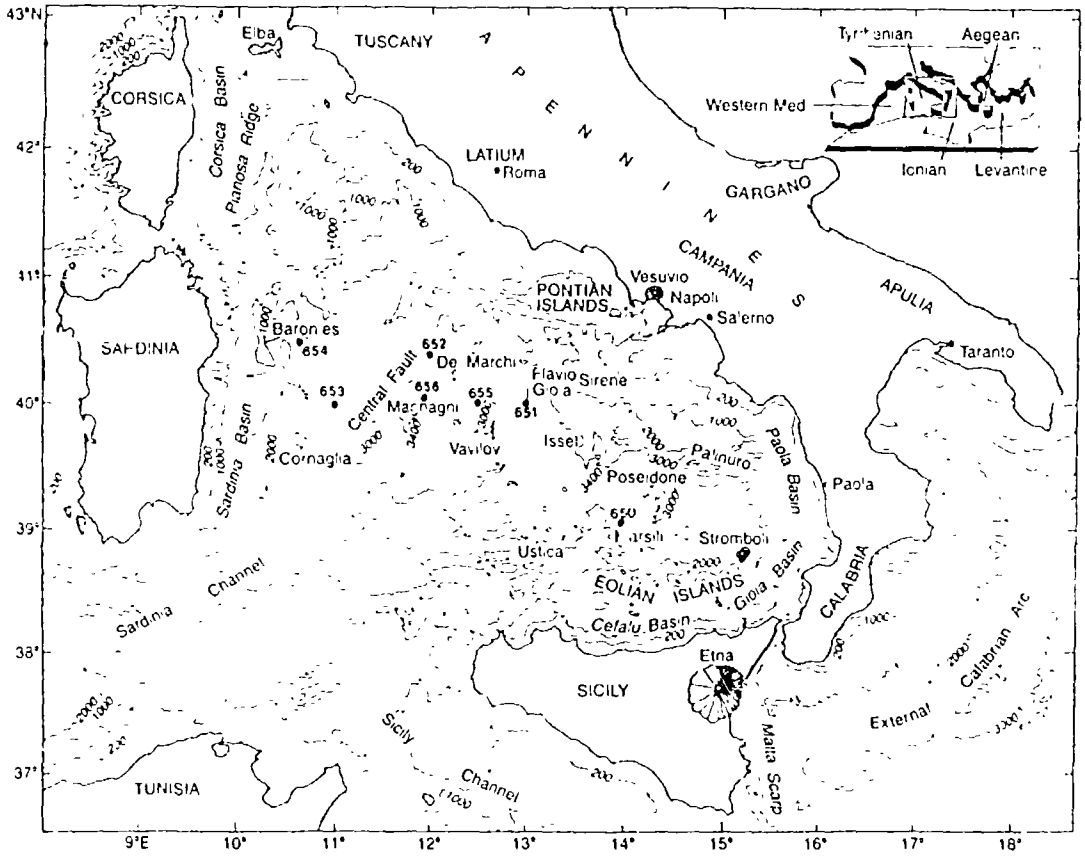

Fig. 10. General setting of the Tyrrhenian Sea (after Kastens et al., 1987).

The extensional tectonics, which led to the opening of the Tyrrhenian back arc basin, took place in a complex way; in general, however, the migration of tectonic (Sartori, 1990) and magmatic activity (Savelli, in press) toward the east is recognized. The western Tyrrhenian side was in fact the first region affected by

extensional movements. Here, from the Tortonian time, a series of tilted blocks bounded by east-dipping extensional faults originated (Kastens et al., 1988). The resulting structural setting closely resembles that of a rifted margin. The tectonic features of the eastern side of the Tyrrhenian Sea are, on the contrary, very different from those described above. Here, a series of confined slope basins are present (Fabbri et al.,1981; Canu and Trincardi, 1989; Argnani and Trincardi, 1988). Capri, Paola, Gioia and Cefalu Basins (Fig. 10) are the most important of these. They are usually filled with turbiditic deposits intercalating with frequent chaotic sedimentary bodies formed by gravitational mass movement (Canu and Trincardi, 1989).

The deep-water central area, reaching a depth of more than 3500 m, separates the western and the eastern Tyrrhenian margins. A north-south trending sill divides this deep bathyal plain into two small oceanic basins: Vavilov to the west and Marsili to the east. The differentiation of these two basinal regions is also evidenced by geophysical data. The crustal thickness is less than 10 km in the Vavilov and Marsili Basins, while it increases up to 15 km in the north-south trending lineament in between them (Steinmetz et al., 1983). In addition, two highs of Bouguer gravity anomaly (over 250 mGal; Rehault et al., 1987) and of heat flow (more than 250 mW/m^{-2}; Della Vedova et al.,1984) are centred on the Vavilov and Marsili Basins. All these geophysical data are in agreement with two areas floored by oceanic crust. The data obtained by the drilling of 655 (western rim of the Vavilov Basin), 651 (axis of the Vavilov Basin), and 650 (western rim of the Marsili Basin) ODP sites during Leg 107 (Kastens et al., 1988) (Fig. 10) confirmed this view. These drillings actually reached basaltic oceanic rocks below a variable thickness of sediments.

The data collected during ODP Leg 107 (Kastens et al., 1988) have also shown that the Vavilov and Marsili Basins are characterized by a different geological history. In the Vavilov Basin, the formation of the oceanic crust began in the Late Miocene (Tortonian) about 9 Ma ago, whereas in the Marsili Basin, the onset of the spreading process took place only about 2 Ma ago (the latest Pliocene). Three morphologically and structurally different areas in the Tyrrhenian Sea were studied during TTR-4 Leg 2 and they are described successively in chronological order of investigation.

a. MARSILI BASIN (AREA 2a)

The Marsili Basin is the most recent expression of the back arc spreading that has created the Tyrrhenian Sea since Late Tortonian time, 9 Ma (Rehault et al., 1987; Kastens and Mascle, 1990). The volcanic expression of the islands and seamounts reflects the steeply subducting slab that is present parallel to the Calabrian Arc (Peterschmitt, 1956; Gasparini et al., 1982). The oldest sediments, overlying the basaltic crust, have been dated with biostratigraphic and paleomagnetic data to 1.67-1.87 Ma (Kastens et al., 1988). Their benthic foraminifera content and the very high vesicularity of the basalts directly below them suggest a deposition at a water depth of 1000 to 2000 m, showing that, 2.0 Ma ago, the Marsili Basin was not deeper than 2000 m (cf current water depth of more than 3500 m, implying a very fast subsidence rate, c.700 m/Ma, since then).

A number of volcanic islands and seamounts surround the Marsili Basin. To the south and to the east, the basin is bounded by the Aeolian Volcanic Arc (Beccaluva et al., 1985). The Aeolian Island Arc is a complex of seventeen volcanoes forming a chain of islands and seamounts from Garibaldi Seamount in the west to Stromboli in the east. To the north the basin is delimitated by the E-W trending Palinuro Seamount (Colantoni et al., 1981). The extension of the basin to the west is limited by a structural sill. This series of highs, which encloses the Marsili Basin, is cut, between Stromboli Island and the Lametini Seamount, by the submarine Stromboli Canyon (Selli and Fabbri, 1971). In the central area of the basin, a large active volcanic edifice, Marsili Seamount, rises from a bathyal plain at to a depth of 482 m (Savelli, 1992). It has an elevation of about 3000 m over the surrounding seafloor. It is elongated in a N10°E direction and is flanked on both sides by two small highs with the same direction.

Seismic profiling demonstrated that the basin retains a fill of stratified sediments that is generally less than 600 m thick, and ODP drilling at Site 650 in the basin east of Marsili showed that this fill was largely of turbidity current deposits resting on a tholeitic basalt basement (Kastens et al., 1988). Canyon systems feed sediment to the Marsili basin on all but the western side and the slopes of Marsili Seamount are a further possible source. The easternmost part of the basin is represented by an embayment in the 2500 m isobath that is fed by the Stromboli Canyon system and its tributaries. The canyon system appears to drain both the Calabrian and Sicilian borderland basins and the slopes of the Aeolian chain (Morelli, 1970).

Investigations in the eastern Marsili Basin (Fig. 11) were devoted to a study of basin filling processes north of the Aeolian Islands. This leg was aimed at addressing a perceived over emphasis on deep-sea fan processes and to further investigate volcaniclastic processes with the long-range and deep-towed sidescan systems.

Stromboli Canyon

It is mainly via the Stromboli Canyon that turbidity currents and other mass gravitational flows reach the deep Marsili Basin. Here, they are ponded behind the Marsili Volcano and are deposited in alternating sequences with pelagic muds. The head of the Stromboli Canyon begins at around 1100 m water depth in the Gioia Basin between Lipari and the Sicily margin and continues northeastwards as a deep incision fed by a number of tributaries to a depth of 2200 m east of Stromboli. It then swings westward through the embayment between Stromboli Island and Lametini Seamount and reaches the Marsili bathyal plain at around 3200 m, an overall length of about 120 km. On the eastern side, the main tributaries are the Mesima Canyon and particularly the Angitola Canyon. The latter runs with an east-west strike in the southern side of the Paola Basin and reaches the Stromboli Canyon just south of its bend. On the western side, is another tributary that drains the area between Panarea and Stromboli Islands.

Gabbianelli et al. (1993) have described three zones of the Canyon system

based upon bathymetric and 3.5 kHz acoustic profiling and sampling. The upper zone covers a 50 km length between the 1100 m and 2100 m isobaths. Here the Canyon has a V-shaped cross profile, a width of between 250 m and 1 km and a gradient of more than 1°. The intermediate zone lies between 2100 and 2650 m and is 40 km in length. Here the Canyon turns westwards through the embayment described above and is up to 4 km wide with a gradient of 0.6 to 0.8°. Between 2650 m and 3000 m, the Canyon is restricted again, to between 300 m and 1 km over a length of 20 km. The gradient is approximately 1 degree. The R/V *Gelendzhik* concentrated its surveys in the intermediate zone embayment and out onto the eastern Marsili Basin.

b. PALERMO - CAPE S. VITO OFFSHORE AREA (AREA 2b)

This area of northwestern Sicily lies off the coast between Cape S.Vito and the Palermo Mountains and runs north as far as the Drepano Seamount - Anchise Seamount and Ustica Island (Fig. 19). The shelf break is situated at an average depth of 140-150 m. The continental slope is very irregular and steep, testifying to the recent formation of the Northern Sicilian margin. The slope is characterized by narrow, north-south trending incisions, particularly in Gulfs of Castellamare and Palermo. On the continental slope there are several basins alternating with structural highs. These are, from west to east, the Trapani Basin, Scuso Bank, the Erice Basin, the S. Vito High, the Castellamare Basin, the Palermo High, and the Palermo Basin.

This area is a part of the Sicilian segment of the Apenninic-Maghrebide Chain that is derived from deformation of carbonate platform and basinal domains which formed the northern continental margin of the African Plate from the Triassic to the Tertiary period (Catalano and D'Argenio, 1982). From northwest to southeast the area is subdivided into three main sectors: (1) the Sicilian-Magrebian Chain in the northern and central parts of Sicily and its offshore prolongation, which is tectonically overlain by the Kabilian-Calabrian Units along the Drepano Thrust Front; (2) the foredeep of Caltanisetta-Gela area, deformed in the Plio-Pleistocene time, and the recent foredeep located in the Gela Basin in front of the Gela Nappe (the southernmost front of the Chain) (Catalano et al., 1993); and (3) the foreland in the Hyblean Mountains and Sicily Channel.

Since the Early Miocene, following the collision between the African and European Plates, and particularly with the anticlockwise rotation of the Corsica-Sardinia block, this region has been characterized by the formation of a fold and thrust belt with an east and southeast vergence. Afterwards, during the Late Miocene-Early Pliocene time, the deformations prograded toward more external domains, finally involving the foredeep, and in part the foreland area, during the Late Pliocene-Pleistocene.

The studied area represents a part of the chain formed principally by a stack of detached and thrust carbonate platform units. These units built up a very thick tectonic wedge (Catalano et al., 1993). During the Plio-Pleistocene, a general tension decreased, probably due to the Tyrrhenian Sea opening, giving rise to

west-east and NNW-SSE trending basins. Sedimentary successions, 500-1500 m thick, record the tectono-sedimentary evolution during the last 5 Ma. The study of the Plio-Pleistocene sequence, using basin analysis and sequence stratigraphy methods, allows us to recognize both the effects of alternating of extensional and compressional (or inversion) tectonics and those associated with subsidence and eustatic fluctuations of sea-level (Agate et al., 1993).

c. AREA EAST OF SARDINIA (AREA 2c)

The study area (Fig. 21) runs east-west for about 250 km between Lat. 40° 00'N and 40° 30'N. It extends from the eastern Sardinia continental margin to the Tyrrhenian bathyal plain (Vavilov Basin).

The most striking morphological feature is a relatively narrow continental shelf passing to a wide, structurally controlled continental slope, mostly corresponding to the Cornaglia Terrace. The slope is dissected by several canyons, among which the most important are the east-west trending Orosei Canyon and the north-south trending Sarrabus Canyon. The abyssal plain, which develops about 3000 m below sea level to the east of a morphostructural threshold (Central Fault), is characterized by a number of basins interspersed with structural ridges and volcanic highs.

Two main north-south trending structural domains are recognized, from west to east: (1) European foreland formed by rocks related to the Corsica-Sardinia Block, and (2) a remnant segment pertaining to the Alpine Chain (Mt. Baronie, Mt. della Rondine, Mt. Cassinis, and Marche Smt.). The superimposed extensional tectonics (late Tortonian-early Pliocene in age) created a typical passive margin with westward tilting blocks (Malinverno and Ryan, 1986; Kastens et al., 1988).

The ODP Leg 107 was important in understanding Tyrrhenian Basin evolution. It demonstrated that extensional processes become younger from NW to SE until the formation, during the late Miocene-early Pleistocene, of two relatively small basalt-floored areas (Vavilov and Marsili Basins) (Kastens et al., 1988). The transitional area between the newly formed oceanic crust and eastern Sardinia continental crust is marked by the NNE-SSW trending Central Fault, which represents a major structural element within the Tyrrhenian domain.

The focus of the research in this area is the analysis of the structure and stratigraphy of the Neogene sedimentary successions, which fill peri-Tyrrhenian basins (Fabbri et al., 1981), using sequence stratigraphy models and tools (Vail and Wornardt, 1991; Agate et al., 1993). To reconstruct the tectono-stratigraphic evolution of the western Tyrrhenian margin, a number of multichannel seismic reflection profiles have been recorded across ODP Leg 107 drilling sites; well log data have been utilized to calibrate the newly obtained and existing seismic lines.

2. SEISMIC PROFILING

a. MARSILI BASIN

A. F. Limonov, M. Marani, and F. Gamberi

Six seismic lines were run in Area 2 (Fig. 11). The first(PS-132) was oriented in a SW-NE direction and was run between the Aeolian Islands and the Calabrian coast. The main lines (PS-133, 134, and 136) are oriented in an ESE-WNW direction, covering part of the slope, the Marsili bathyal plain and the 3 km high Marsili Seamount. Lines PS-135 and 137 are short connecting ones. The total length of the seismic lines is about 520 km. The studied continental slope of the Marsili Basin is cut by the Stromboli Canyon which trends NNE in its upper reaches, changing to an western trend downslope. In general, the seismic lines follow the trends of this canyon. The nearest ODP Site 650 is situated 27 km from the termination of line 136, and the seismic stratigraphic subdivision of the recorded sections took into consideration the stratigraphic units recovered at that site (Kastens and Mascle, 1990).

Line PS-132, which follows the eastern slope of the upper Stromboli Canyon, can be subdivided structurally into three parts. Each part represents a different type of deformation and a different thickness and possesses a seismic signature of the sedimentary infill. The first part of the record (Gioia Basin) continues till time mark 08:45, where a tectonic boundary separates it from the second part.

Four seismic members are defined within the sedimentary succession (Fig. 12). The lowermost recorded reflector, the top of the acoustic basement, is probably related to the top of the Calabrian units (Fabbri et al., 1981). This is the first seismic member. It is disturbed by faults and folds, and its top seems to be an erosional surface. Above, there is a semi-transparent seismic member (the second one), about 250 ms thick, which is also controlled by faults and folds. This member possibly represents the initial stage of rifting in the Marsili Basin (Early-mid Pliocene).

The overlying third seismic member rests unconformably on the previous one and consists of an alternation (both laterally and vertically) of transparent and stratified seismic units. The transparent units could represent slump deposits or, more generally, mass movement deposits due to gravitational instability during the subsidence episode in the Marsili Basin (end of Pliocene-early Pleistocene?). The transparent unit at the top of this member has a thickness of up to 100 ms and it can be traced for a long distance, also across the whole second portion of the line. The emplacement of this acoustically transparent body seems to have taken place after the folding and faulting, which is clearly seen at time mark 08:40-08:45.

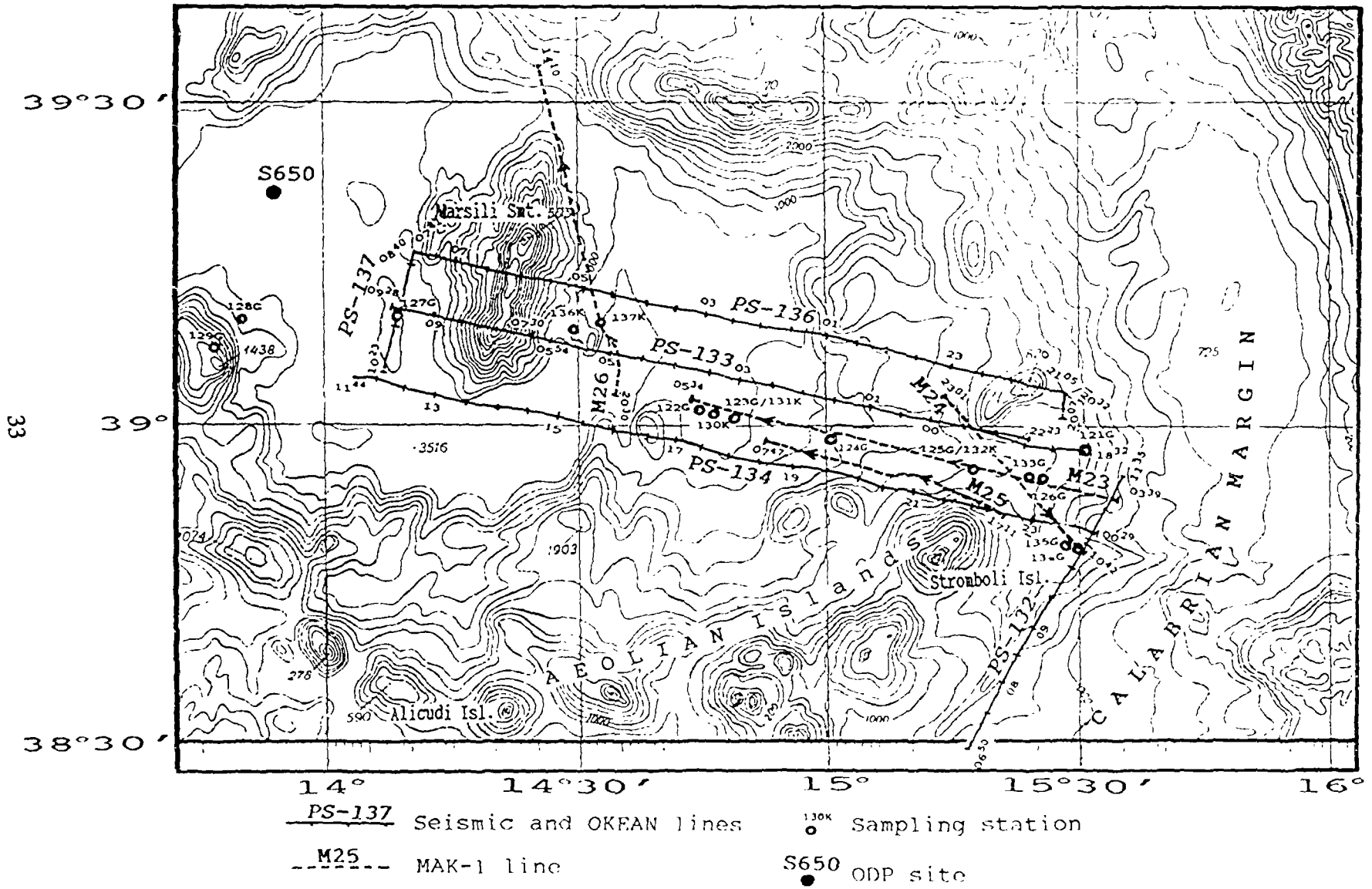

Fig. 11. Location map for the Marsili Basin area

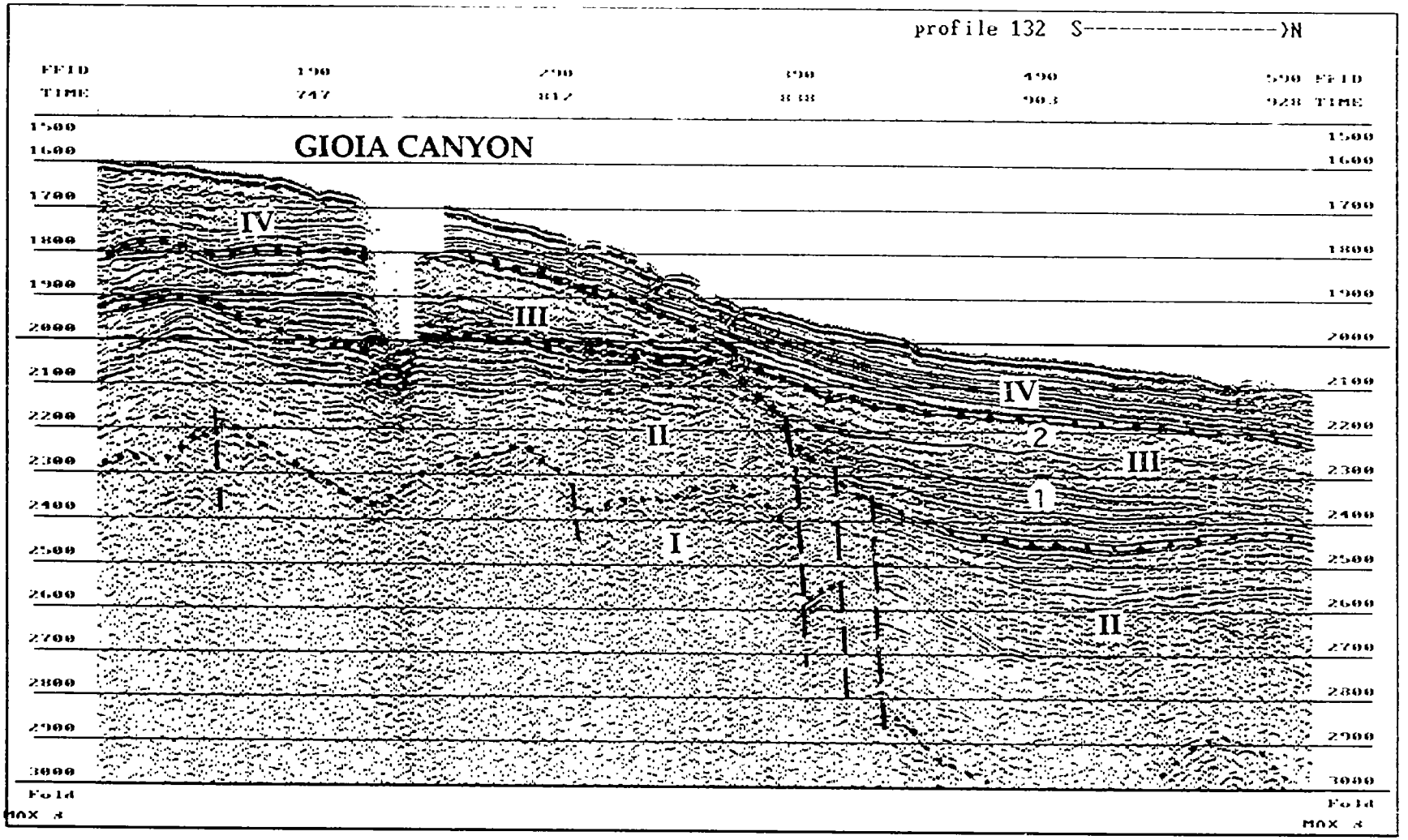

Fig. 12. Principal seismic members in the Marsili Basin area. I - Calabrian Units; II - Early-mid Pliocene, initial stage of rifting; III - end of Pliocene-early Pleistocene (?), fast subsidence episode (1 and 2 - two seismic units of seismic member III); IV - mid Pleistocene-Recent, recent stage of the basin evolution. Seismic profile PS-132

The upper fourth seismic member (mid Pleistocene-Recent) shows a lateral gradation from a semi-transparent seismic signature (slump deposits?) to a well-layered sequence basinwards (turbidites and hemipelagic sediments). It also occurs unconformably on the underlying member, and its surface is cut by several small incisions representing tributary channels of the main Stromboli Canyon. The third and fourth seismic members are also downcut by the fault-controlled Gioia Canyon near time mark 07:50.

The central portion of the recorded section is separated from the previous one by a series of large extensional, north-dipping faults, with a total throw of about 500 ms (Fig. 12). They do not influence the thickness of the second seismic member and therefore originated after its accumulation (before early Pleistocene?). The thickness of the third seismic member in the central portion increases to about 500 ms. In addition to the slump unit described above, there is an underlying one that is separated from it by a highly reflective unconformable surface (Fig. 12). The thickness of the uppermost seismic unit remains almost constant, about 150 ms. It shows a downlap pattern above the slump unit and is composed of continuous plane-parallel reflectors.

The boundary between the central and final portions of the seismic record is represented by the Angitola Canyon, which cuts through the whole sedimentary section. The more gentle northern flank of this canyon is controlled by a series of south-dipping faults, which downthrow the basement with a total offset of 800 ms (10:00-10:15). The steep southern slope of the canyon is probably delineated by a single fault.

The final portion of the record represents the Paola Basin. The acoustic basement (Calabrian units) occurs in the Paola Basin at a shallower depth and demonstrates a similar seismic facies as was previously described. Above this, the second seismic member can be distinguished, with a rather constant thickness of about 100 ms. The third seismic member begins with thick acoustically transparent sediments which pass upwards into a more acoustically layered member. The third member maintains a rather constant thickness along the line, of about 300 ms. Both second and third members are cut by an extensional fault with a 100 ms offset at the very end of the line. Some other small faults are also observed along this portion of the record. The third member is separated from the upper one by its unconformity with an onlap pattern, which was produced by an episode of fast subsidence of the basin axis. The average thickness of the upper member is about 150 ms. The member is characterized by middle amplitude plane-parallel and continuous reflectors and is affected by very young deformation near 10:30 that is well-expressed in the bottom relief (Fig. 13).

The Paola Basin seems to experience the ongoing subsidence uncompensated by sedimentation, which is evidenced by the approximately constant thickness of the upper seismic member. Due to this rejuvenated subsidence the flanks of the Paola Basin show ample folds that affect the full sedimentary sequence and connect the basin axis with the delimiting highs.

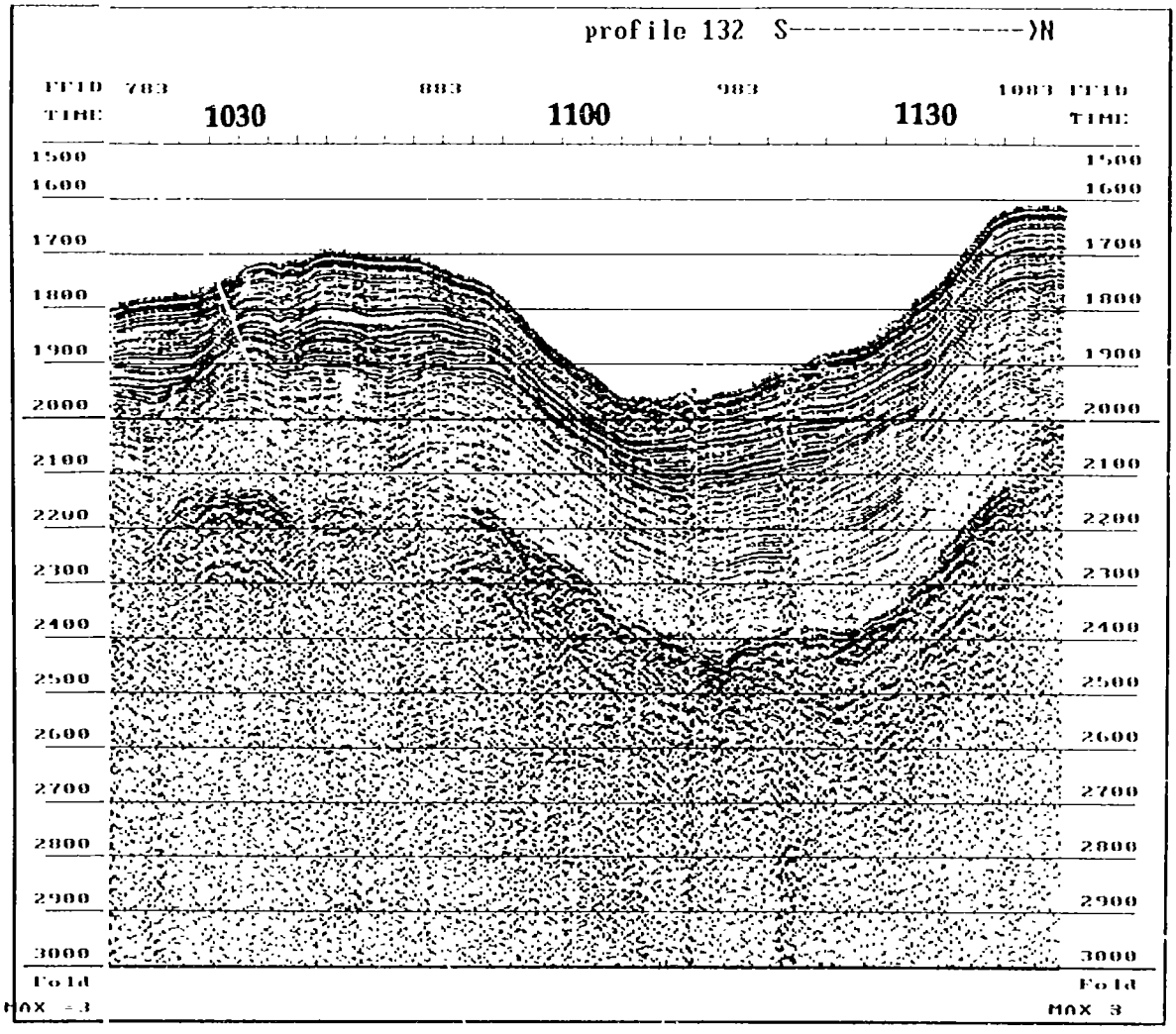

Fig. 13. Young tectonic deformation in the Paola Basin. Seismic profile PS-132

The second line, PS-133, runs parallel to the north bank of the Stromboli Canyon and partially along its thalweg, crossing the south slope of the Marsili Seamount. The previously described seismic stratigraphic members can also be identified in this portion of line PS-133. The acoustic basement (Calabrian stratigraphic units) is cut by extensional faults and dips westwards from a depth of 650 ms below the seafloor at the beginning of the line to 1000 ms at 19:40, where the southern extension of the Lametini volcanic(?) Seamount protrudes. Three sedimentary members, separated by unconformities, overlie the basement in this portion of the seismic section. Only the upper part of the second sedimentary member shows a slight basinward thickening, whereas the third one has clearly seen downslope diverging reflectors, testifying to the fast Pleistocene subsidence of the basin and probably to its less extensive margin.

The uppermost member, 200 ms thick, has downlap and onlap patterns at its base. Its topmost part shows evidence of sediment gravitational instability (Fig. 14), which is also confirmed by MAK-1 survey (see Section II.3.b). Small erosional incisions, seen at 19:20 and 19:50, are downcut into slump sediments. The interrelation between the basement and the Lametini Seamount is not clear, but west of the Lametini Seamount/Stromboli Volcano, the acoustic basement has different characteristics and could be represented by volcanic rocks.

The part of the seismic line between the Lametini Seamount and 23:30 is characterized by a shallow depth of the volcanic basement covered by a sedimentary layer up to 300 ms thick. The top of the basement is represented by high-amplitude reflectors, and is probably cut by faults with small offsets. The basement gradually shallows along the line and subcrops at a depth of a few tens of metres near time mark 22:35. The sedimentary cover consists, here, of two members, semi-transparent below and well-layered above, which probably represent normal marine and interfingering normal marine and volcaniclastic sediments. The assumed age of this sequence is Plio-Pleistocene, and it probably reflects the oldest volcanic activity in this area.

Between time marks 23:35 and 00:40, there is a generally flat-topped topographic high rising 220 m above the neighbouring seafloor. The inner structure of this high drastically differs from the surroundings. It is characterized by discontinuous, strong, curved and rare reflectors in the lower part of the seismic section (from 200 to 900 ms below the seafloor) and by well-stratified seismic member in the upper part (Fig. 15). This feature resembles an exotic block bordered by décollement surfaces and may be a large slump block resulting from mass movement down the continental slope.

From this exotic block to the end of the line, the seismic pattern changes. The acoustic basement occurs at a depth of up to 650 ms below the seafloor and has a highly reflective, gently undulating surface. Possible outcrops of the basement on the seafloor are seen near time marks 01:15 and 02:10. The basement is strongly offset by a near-vertical extensional fault or faults with a 200 ms throw at time mark 02:30. A similar fault but with a smaller, 300 ms, throw is present at 01:25 time mark. We suppose that the larger fault delimits, to the west, the area of oceanic type crust drilled during ODP Leg 107 (Kastens and Mascle, 1990) (Fig. 16). The basement to the east of this fault has a similar seismic facies, that is indicative of a probable volcanic origin, but its nature is hard to determine definitely.

On the block delimited by the two faults, both of which show an eastward tilting. The seismic character of the sedimentary cover is seen as a series of discontinuous weak reflectors which can be traced 250 ms below the seafloor. The sedimentary cover in the area underlain by oceanic crust can be clearly divided into two acoustic members which are separated by a strong unconformity, the lower member showing gentle undulations indicative of tectonic activity, while the upper member shows a sequence with plane-parallel reflectors, which belong

to the final basin fill (Fig. 17). The thicknesses of the members are 400 ms and 200 ms respectively. The tectonic activity affecting the lower member may be indicative of the strong Pliocene-Early Pleistocene subsidence of the Marsili Basin, and the unconformity is probably correlated to the upper one described for the beginning of the seismic line. The basal part of the lower member is semi-transparent in some places but grades into layered seismic pattern further along the line. The semi-transparent record may represent volcaniclastic material or rather homogeneous nannofossil oozes recovered in Site 650. The layered sequence is probably due to intercalating volcaniclastic and hemipelagic sediments. The base of the upper member onlaps the gentle undulating unconformable surface. It is well-stratified, the reflectors being discontinuous and with a high amplitude.

A narrow submarine rise, more than 250 m high, which is related to the eastern slope of the Marsili Seamount was crossed by the profile near time 05:20. The slopes of this rise have a complex morphology. A probably analogous volcanic feature, but buried by Pleistocene sediments about 150 ms thick, was recorded at time mark 04:15. Between time marks 07:50 and 08:40 the line crosses the Marsili Seamount. The interrelation between the oceanic crust of the Marsili Basin and the volcanic body is not evident, but one may suppose that the oceanic basement goes beneath the seamount. The sedimentary cover eastwards of the Marsili Seamount bears resemblance to that described for the area underlain by oceanic crust.

Seismic line PS-134 runs parallel to line PS-133 in an opposite direction, crossing the foothills of the Marsili Seamount, the southern part of the Marsili Basin, the foot of Stromboli Volcano, and terminating at the Calabrian margin. The main characteristics of the acoustic basement along this line are similar to those described for line PS-133; that is, a change from the probable Calabrian units dowslope to the volcanic basement west of the Stromboli Volcano, although there are some differences in the members overlying the basement.

Within the Calabrian margin, the same seismic members, with similar thicknesses as on line PS-133, can be identified. This part of the margin has a step-like form due to the presence of a large extensional fault with a 500 ms offset and westward dip. This fault is also seen in the previous line.

The Stromboli Canyon shows very strong evidence for erosion on only one side (Fig. 18). Because of this the canyon has an asymmetric cross-section with a very steep eastern flank and outcropping sedimentary sequences equivalent to those already described. The western flank is more gentle and is represented by the foot of Stromboli volcano. This asymmetry is probably due to the different resistance to erosion of sedimentary and volcanic rocks.

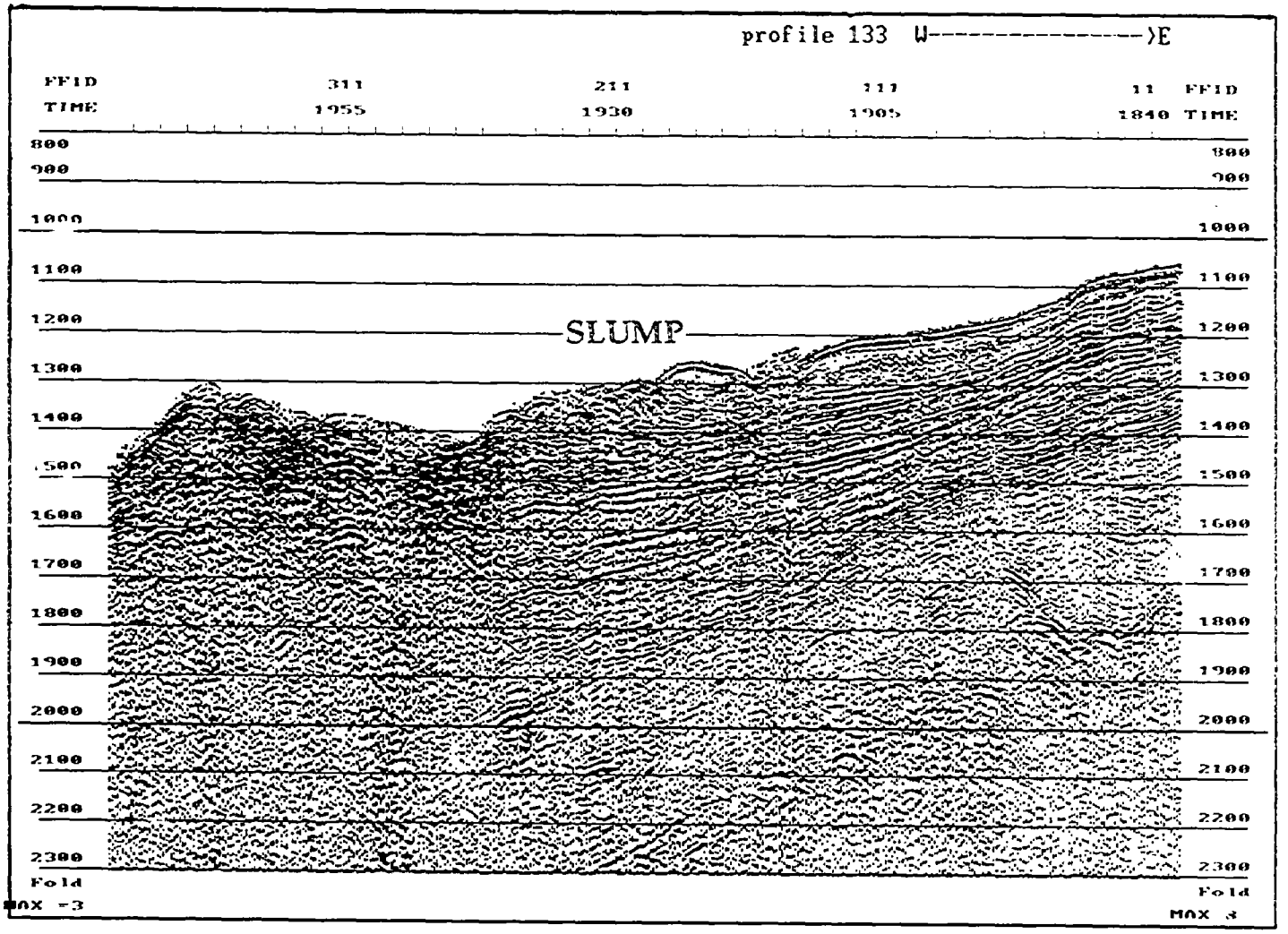

Fig. 14. Example of sediment instability on the western Calabrian slope. Seismic profile PS-133

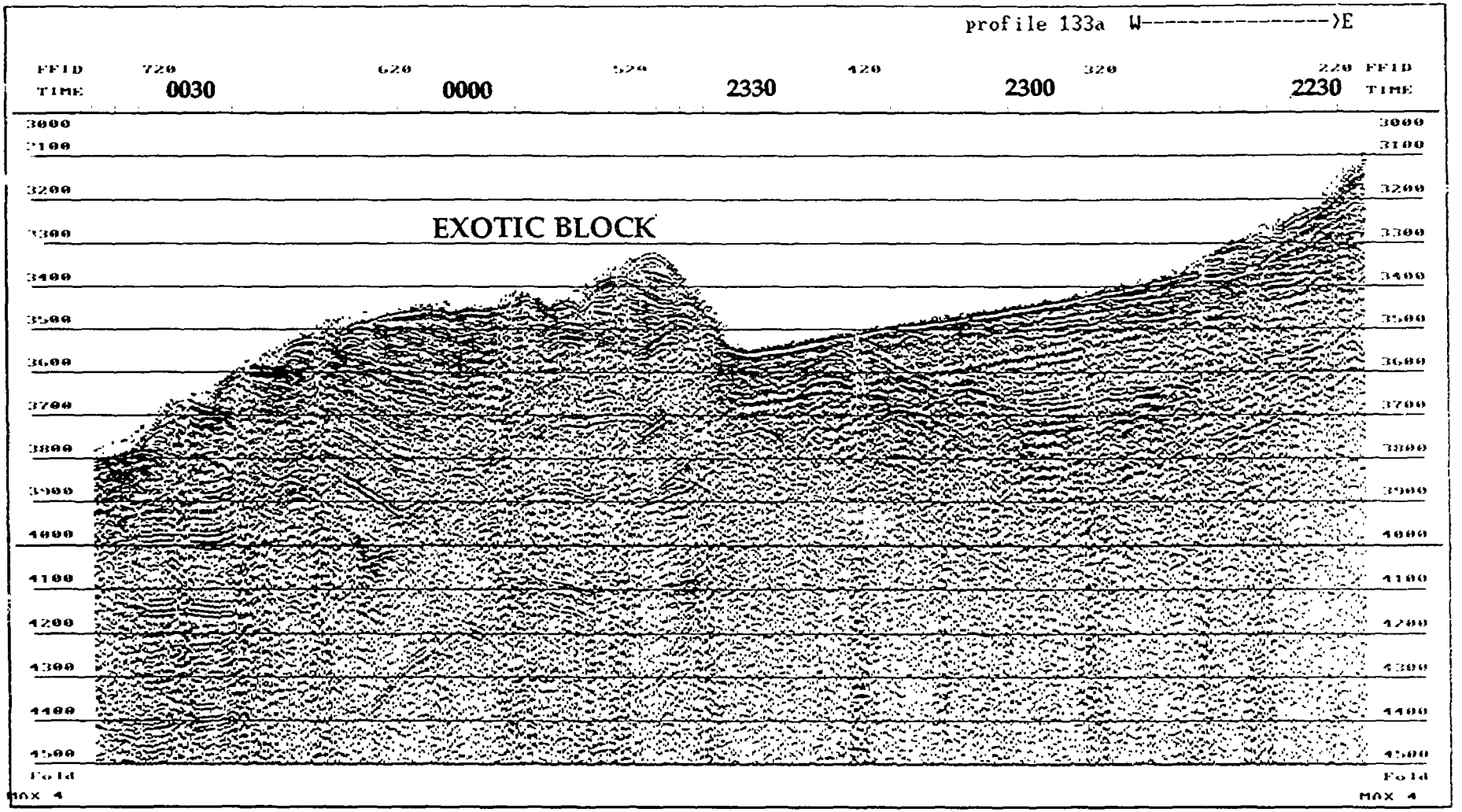

Fig. 15. Possible exotic (slump) block on the Calabrian margin. Seismic profile PS-133

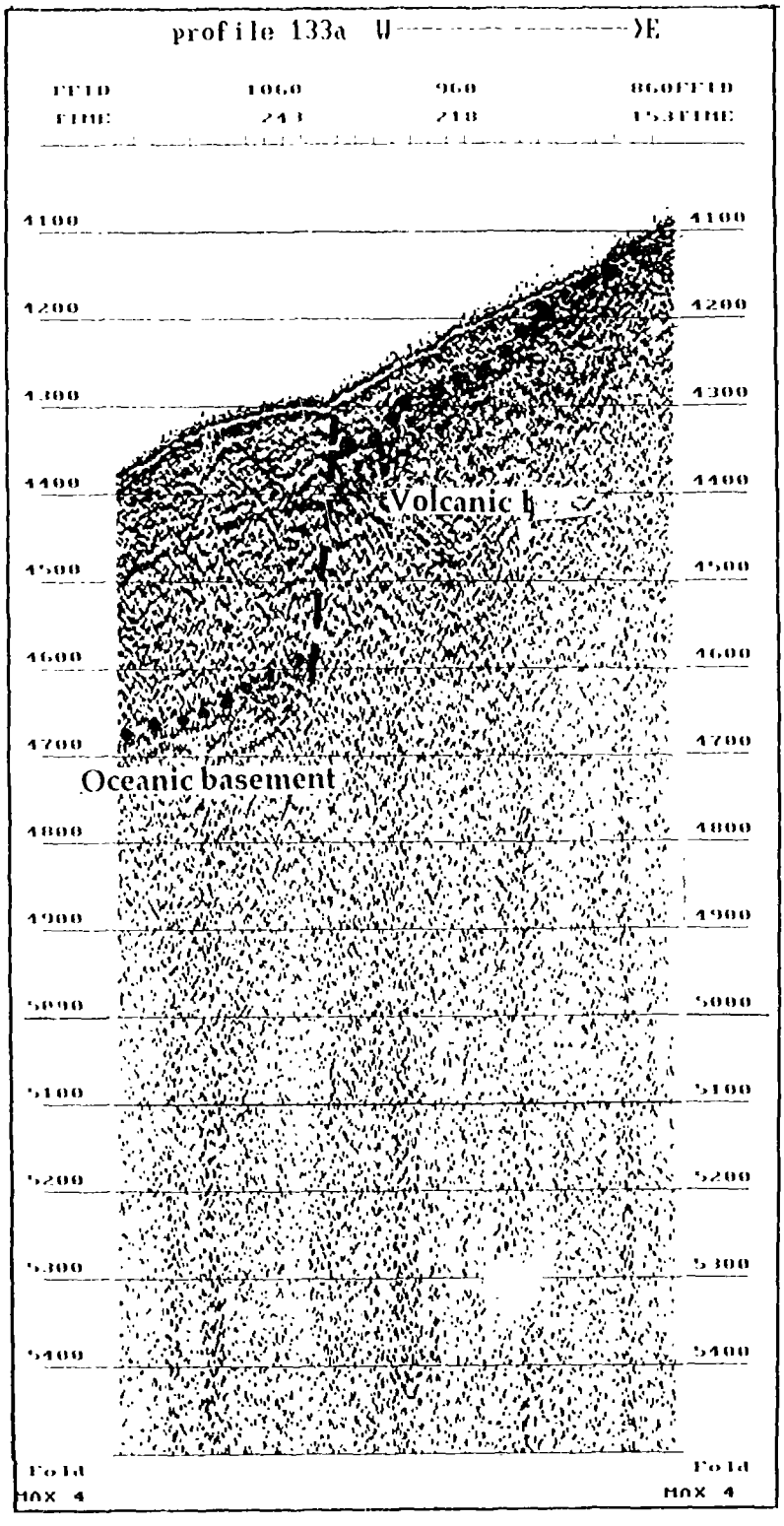

Fig. 16. Large fault in the east Marsili Basin probably delimiting the areas with oceanic (in the west) and volcanic (in the east) basements. Seismic profile PS-133

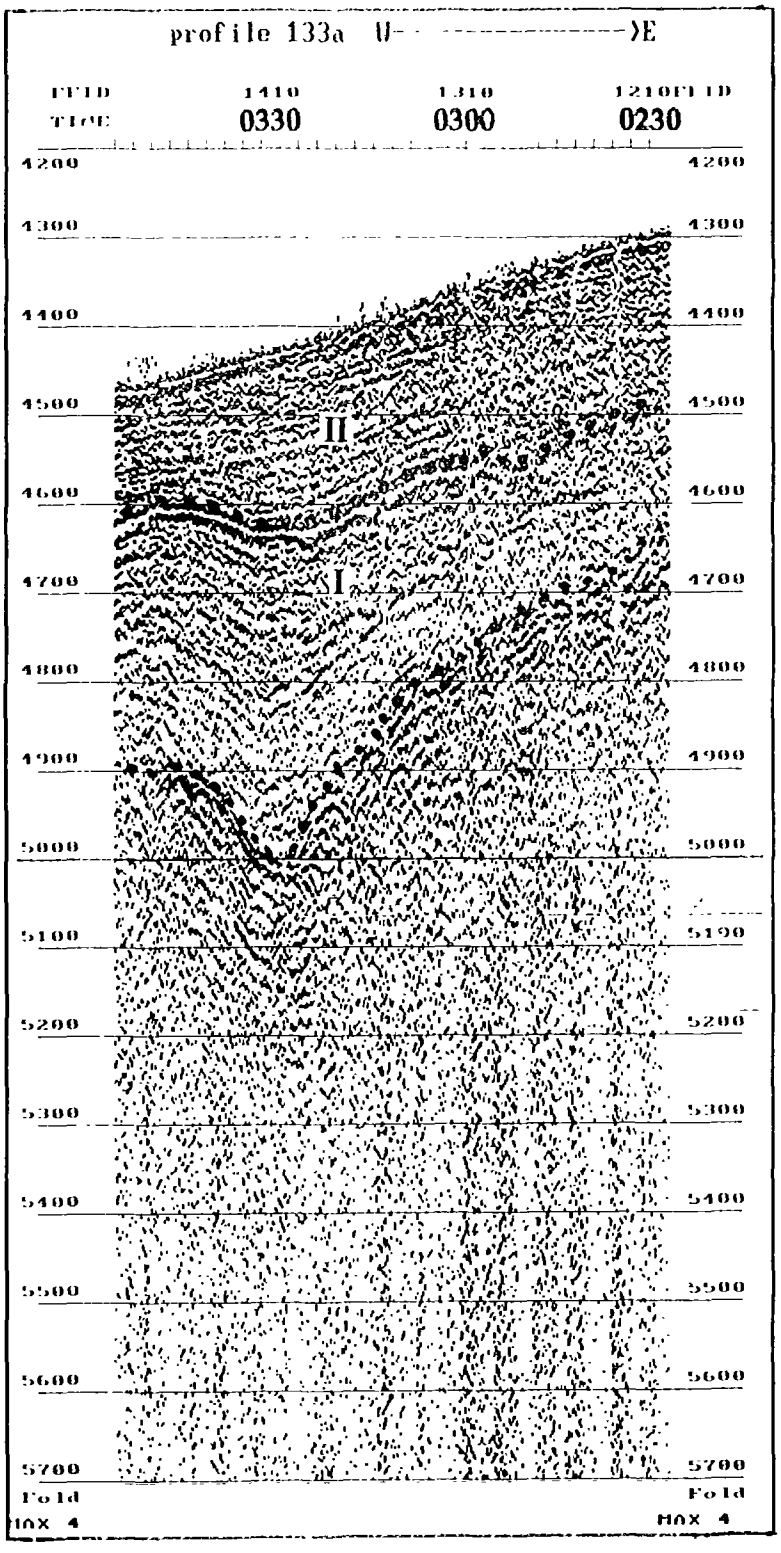

Fig. 17. Two seismic members overlying the oceanic basement in the deep Marsili Basin. The lower one, reflecting a fast basin subsidence in the Pliocene-early Pleistocene time, is separated by a strong unconformity from the upper one, which belongs to the final basin fill. Seismic profile PS-133

The volcanic basement beyond Stromboli towards the Marsili Basin occurs at a shallow depth and is covered by a maximum 100 ms of sediments. It is also possibly cut by normal extensional faults forming gentle steps in the seafloor topography. A positive topographic feature positioned at the margin of the basin (16:30) shows a 300 ms thick inclined layer of sediments on its eastern flank. It is difficult to interpret but considering its location near the mouth of a flat-bottomed canyon (IOC-UNESCO, 1981), it could be a large slump block. In the west, close to this assumed slump block, there are also two smaller positive features which, in contrast to the slump block, have much stronger backscatter on the OKEAN record and are interpreted as representing volcanic edifices.

The Marsili Basin shows about 500 ms of the Upper Pliocene-Pleistocene sediments with a rather uniform seismic pattern above the oceanic basement. Generally, this pattern is very similar to that described for this basin on line PS-133. The basement has several positive structures, some of which have bathymetric relief and are probably volcanic in origin.

The general structure along the northernmost line PS-136 resembles that recorded along line PS-133. Only those features that are different will be discussed. The first of them is the Lametini Volcano, crossed near its summit and rising about 1200 m above the surrounding seafloor. Another feature is a graben-like structure adjoining the Marsili Seamount (03:45-04:35) with a throw of about 250 ms and clearly affecting the seafloor topography. The unconformity described within the Marsili Basin-fill sequence is well shown by this structure, which probably has the same age and seems to be related to the basin-wide extensional regime.

From the above description the following conclusions can be drawn. The study area is subdivided into three parts underlain by different types of acoustic basement, which are from east to west: Calabrian units, volcanic basement and oceanic basement. The overlaying stratigraphic sequence consists in general of three stratigraphic members that reflect different stages of the Marsili Basin evolution. They are separated by well-expressed unconformities. The lower one may have a Lower-mid Pliocene age; it is spread mainly within the Calabrian domain and could represent the initial stage of rifting in the Marsili Basin. Normally this member is cut by extensional faults and deformed in accordance with the undulations of the acoustic basement. The middle member (Upper Pliocene-Lower Pleistocene?) shows an onlap character and was probably accumulated during the phase of fast subsidence of the Marsili Basin. Its characteristic feature is a broad development of slump bodies. Normally this member increases in thickness basinwards. The uppermost member reflects the recent stage of development of the study area. It is probably made up of alternating volcaniclastic and hemipelagic sediments (Kastens and Mascle, 1990).

Mass movement process plays an important role in the formation of the basinal infill. Numerous indications of sediment wasting are seen on the seismic sections in the form of acoustically transparent layers or separate slump bodies.

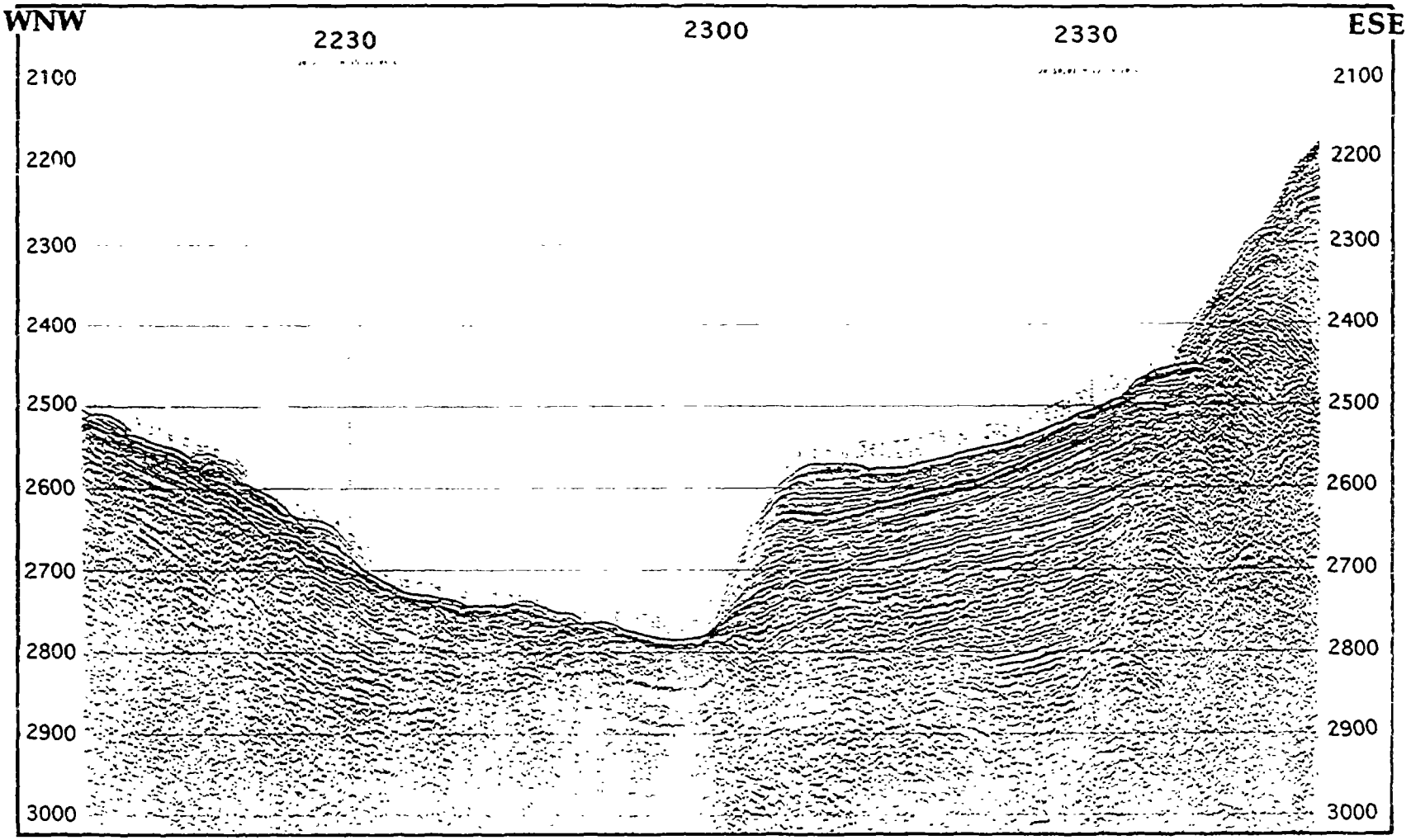

Fig. 18. Stromboli Canyon showing evidence for erosion on its eastern flank. Seismic profile PS 134

b. PALERMO-CAPE S.VITO OFFSHORE AREA

M. De Lauro, L. Ferraro, M. Lucido, and A. Sulli

Ap[proximately 250 km of 6-channel seismic profiles with air-gun source were made in this area (Fig. 19). West-east trending line PS-138 extends for 80 km from the Palermo Basin to the Castellamare Basin. In this profile, we have distinguished a pre-Pliocene substrate represented by characteristic seismic facies formed by high amplitude and low continuity reflectors interpreted as a Miocene clastic succession. Below this, the seismic facies is transparent, and it is not possible to distinguish the top of the carbonates which outcrop onland. The top of these strongly deformed by faults and folds successions is frequently represented by an erosional surface. The Plio-Pleistocene succession, with a maximum thickness of 1000 m in the Castellamare Basin and a minimum of about 100 m on the Palermo High, can be divided into two seismic members. The lower part shows a transparent seismic signature with reflectors parallel to the underlying pre-Messinian succession, whereas the upper is characterized by medium amplitude and good continuity reflectors. The Plio-Pleistocene is dislocated by normal faults in some places, the main ones being responsible for formation of the two basins.

Lines PS-139 and PS-140 trending SSE-NNW and NW-SE, respectively, extend for 90 km from the Castellamare Basin to the Drepano Seamount. In these sections the pre-Messinian succession includes the thin Miocene clastic deposits, while in some sectors the high reflectivity of the pre-Pliocene substrate is interpreted as being linked to carbonate rocks. The Plio-Pleistocene succession is not more than 300 m in thickness and is absent in some localities. The structural setting of the pre-Messinian carbonate and clastic units shows the typical geometries of this sector of the fold chain.

West-east trending line PS-141 runs for 78 km from the Castellamare Basin to the Solunto High. In this profile it is possible to recognize a characteristic alignment of morphological highs and lows (Fig. 20). They correspond to structural highs and basins, which were mainly formed following the Plio-Pleistocene extensional tectonics after placement of the fold chain. The Miocene succession is characterized by high amplitude and low continuity reflectors, with evidence of deformation and erosion. The Plio-Pleistocene deposits, 0 to 300 m thick, are noticeable for being a very transparent seismic facies that becomes chaotic in its uppermost part. Mass wasting is present in this portion of the seismic section, particularly near the steep slopes, which link structural highs and lows. In the eastern part of the section, inside the Palermo Basin, the bottom morphology shows that the sediment supply could come from the uppermost continental slope.

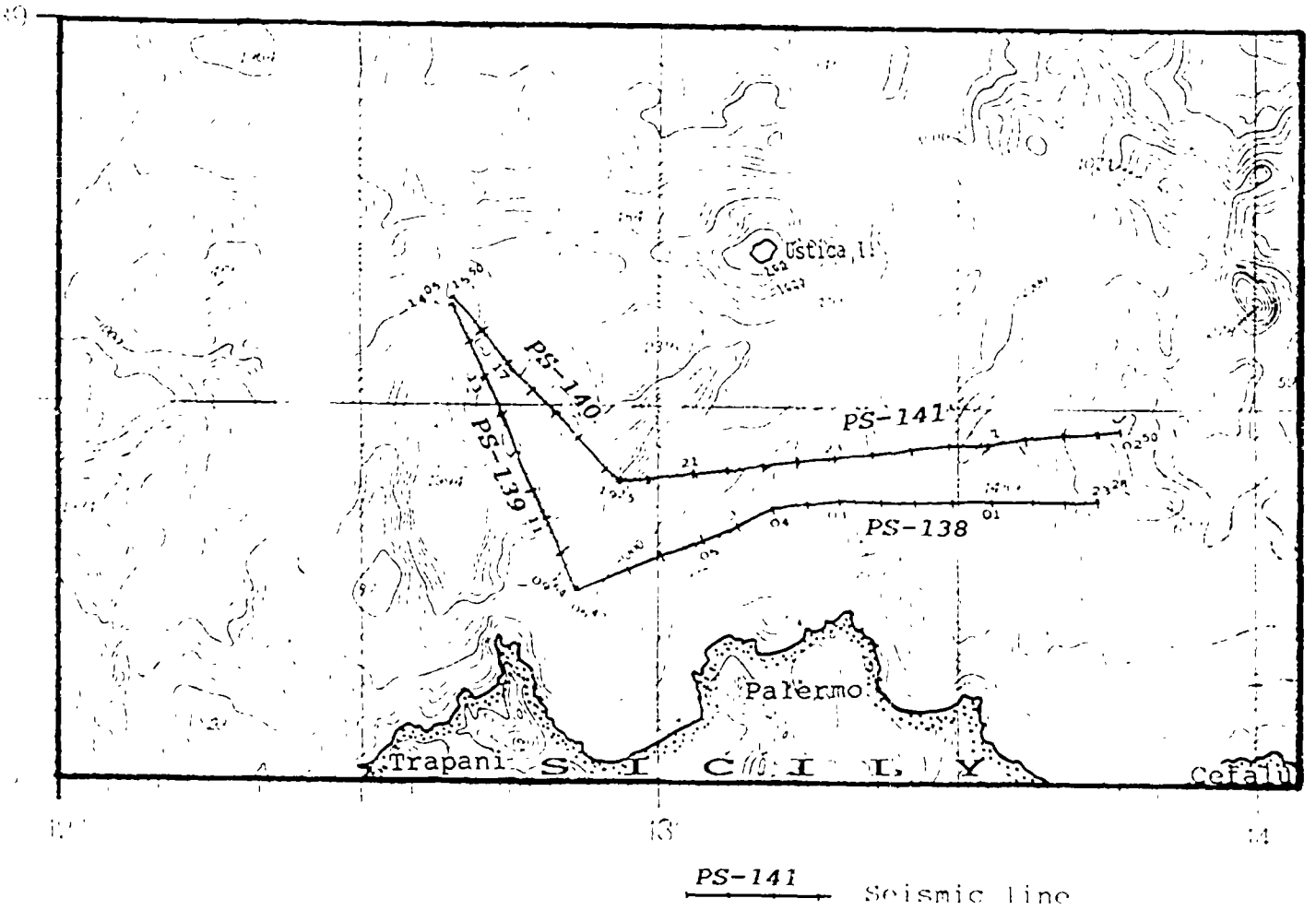

Fig. 19. Location map for Palermo-Cape S.Vito offshore area

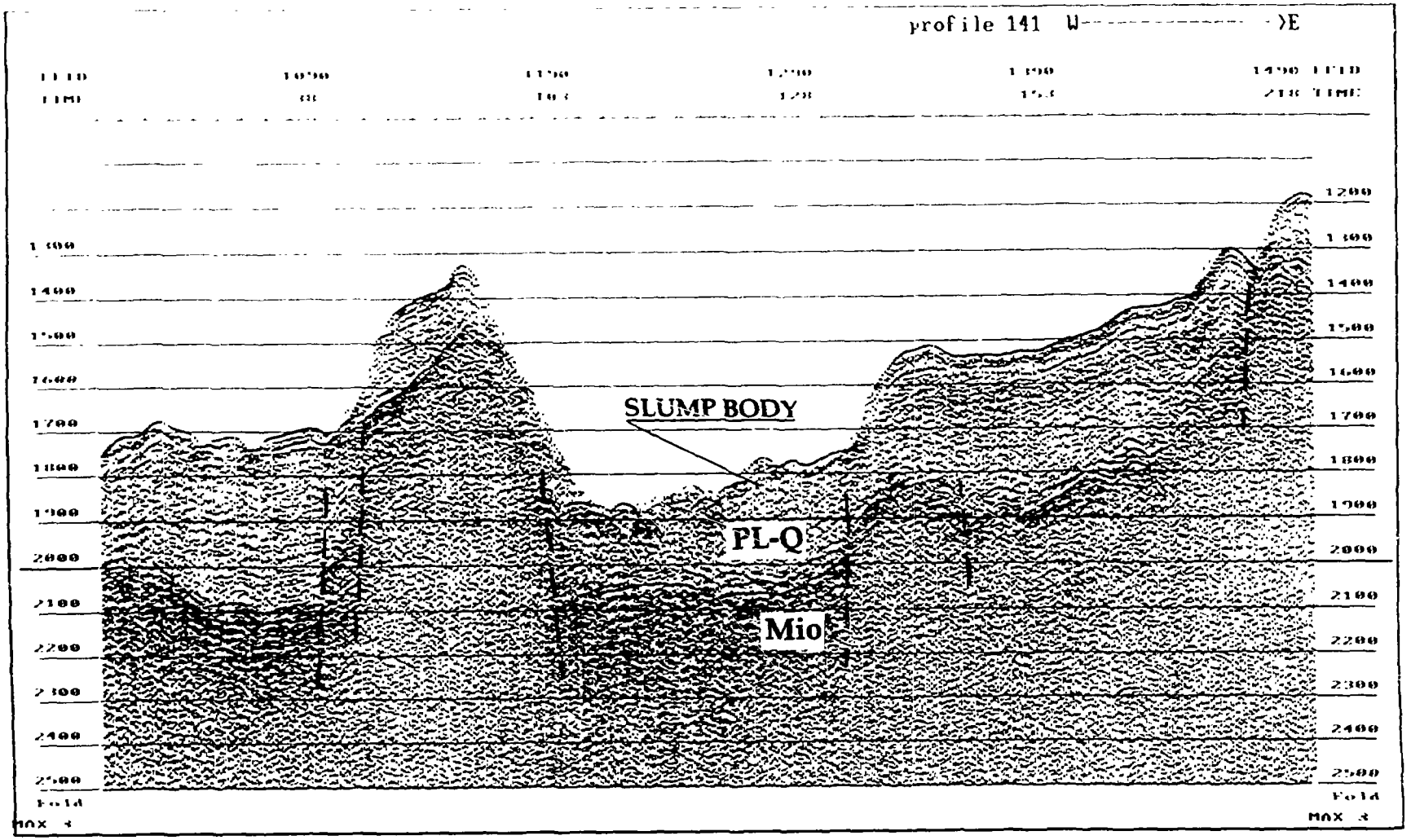

Fig. 20. Structural highs and basins on seismic profile PS-141. Mio - Miocene, Pl-Q - Plio Quaternary. Note a semi-transparent slump body in the upper section between 01:05 and 01:25

c. AREA EAST OF SARDINIA

M. Agate, F. Budillon, S. Infuso, and M. Sacchi

About 430 km of 6-channel seismic profiles with air-gun source have been recorded in the area (Fig. 21). Line PS-142 is the northernmost section, 74 km long and oriented WSW-ENE. It starts northwest of De Marchi Seamount near ODP site 652, crossing the Central Fault and the Cornaglia Terrace as far as ODP site 653. From east to west there are a number of westward-tilting fault blocks comprising synrift deposits, followed by a post-rift sequence which is subdivided into two main seismic units (Fig. 22). The lower unit, partially involved in the growth faulting, is characterized by low amplitude and lateral discontinuity of reflections (transparent seismic facies). The upper unit is characterized by predominantly high amplitude and lateral continuity of reflections. Site 652 allows us to calibrate the succession into: synrift deposits (500 m down well), Messinian(?)-early Pliocene in age, consisting of gypsiferous and terrigenous sediments and showing, on the seismic section, a very continuous reflector with high amplitude is associated with a pebble layer at about 4.9 s (Fig. 22); and a post-rift sequence (about 180 m down well), Plio-Pleistocene in age, represented by calcareous biogenic sediments.

In the central part of the seismic line, we have recognized a fault system, trending NNE-SSW, already known as the Central Fault. Westwards it is more difficult to distinguish structures below the seismic facies associated with the Messinian which shows discontinuous, high amplitude seismic reflections and is affected by tectonic deformation. The overlying Plio-Pleistocene sequence, about 220 m from the core at site 653, consists of nannofossils and foraminiferal oozes. Its thickness is relatively reduced with respect to the same sequence east of the Central Fault.

Line PS-144, crossing the Cornaglia Terrace and the abyssal plain, connects ODP Leg 107 sites 656, 655, and 651 (Fig. 21). The west-east section, about 120 km long, shows a characteristic alignment of morphological highs (mostly represented by basalts east of De Marchi Ridge) and fault-bounded basins filled with up to 1000 m of sediment. As in the previous line, a significant difference in thickness of the Plio-Pleistocene sequence is observed on both sides of the Central Fault. East of the Ancona Ridge, a well-developed channel, showing both depositional and erosional features, is recognized (Fig. 23).

Line PS-145 is the longest across the Sardinian margin and offers a complete section from the upper continental slope to the bathyal plain. It starts NE of the Vavilov Seamount, running roughly east-west across the Gortani and Ancona Ridges and a number of minor interspaced basins. These basins are often bounded by listric normal faults, sometimes with growth of bedding and are filled with a thick sedimentary succession, up to 800 ms. They also show an alternation of a transparent seismic facies and a facies with plane-parallel, high amplitude, laterally continuous reflections.

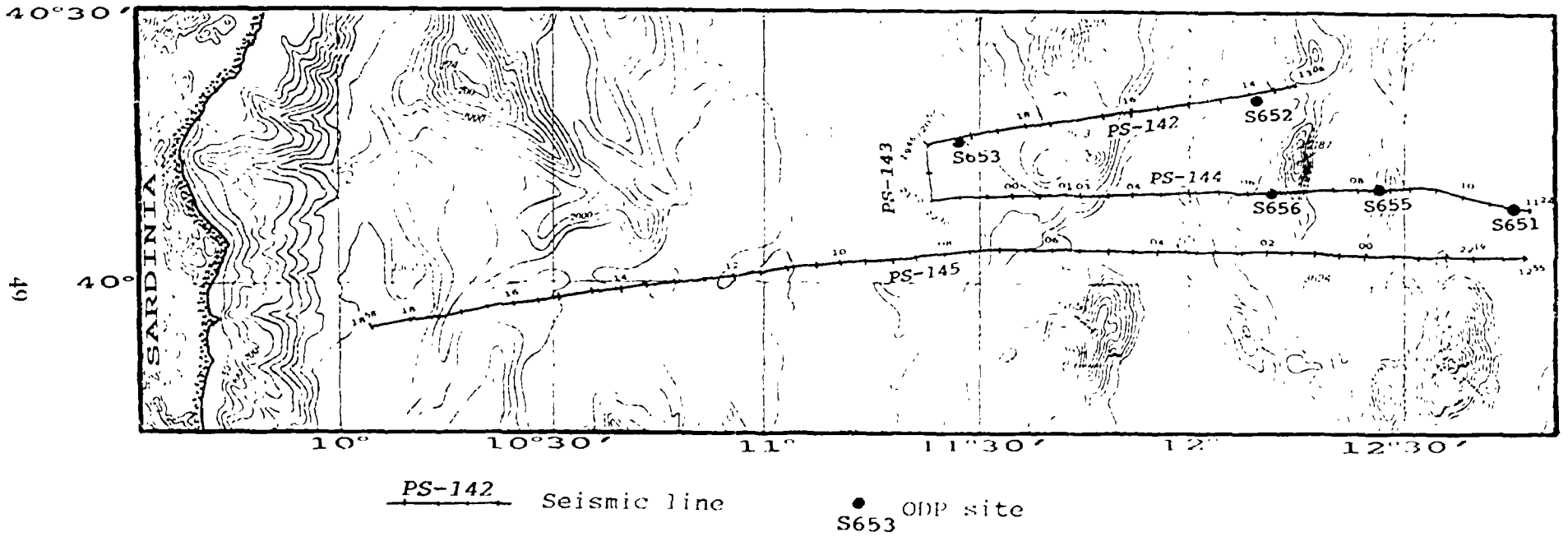

Fig. 21. Location map for the area east of Sardinia

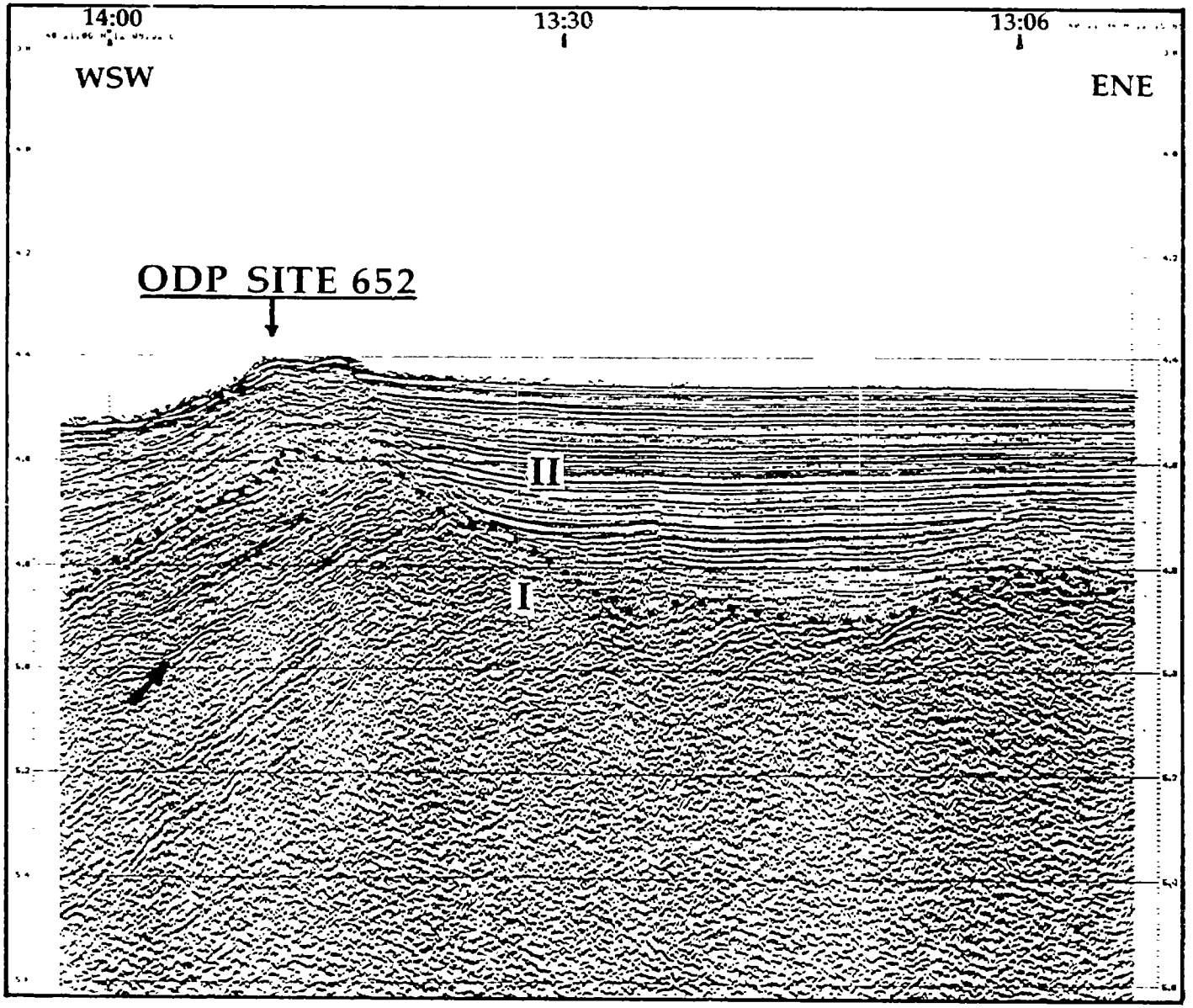

Fig. 22. Principal seismic members in the area east of Sardinia. I -Messinian-early Pliocene, synrift deposits; II - Plio-Pleistocene, post-rift sediments. Arrow indicates a pebble layer at about 4.9 s (TWTT). Seismic profile PS-142

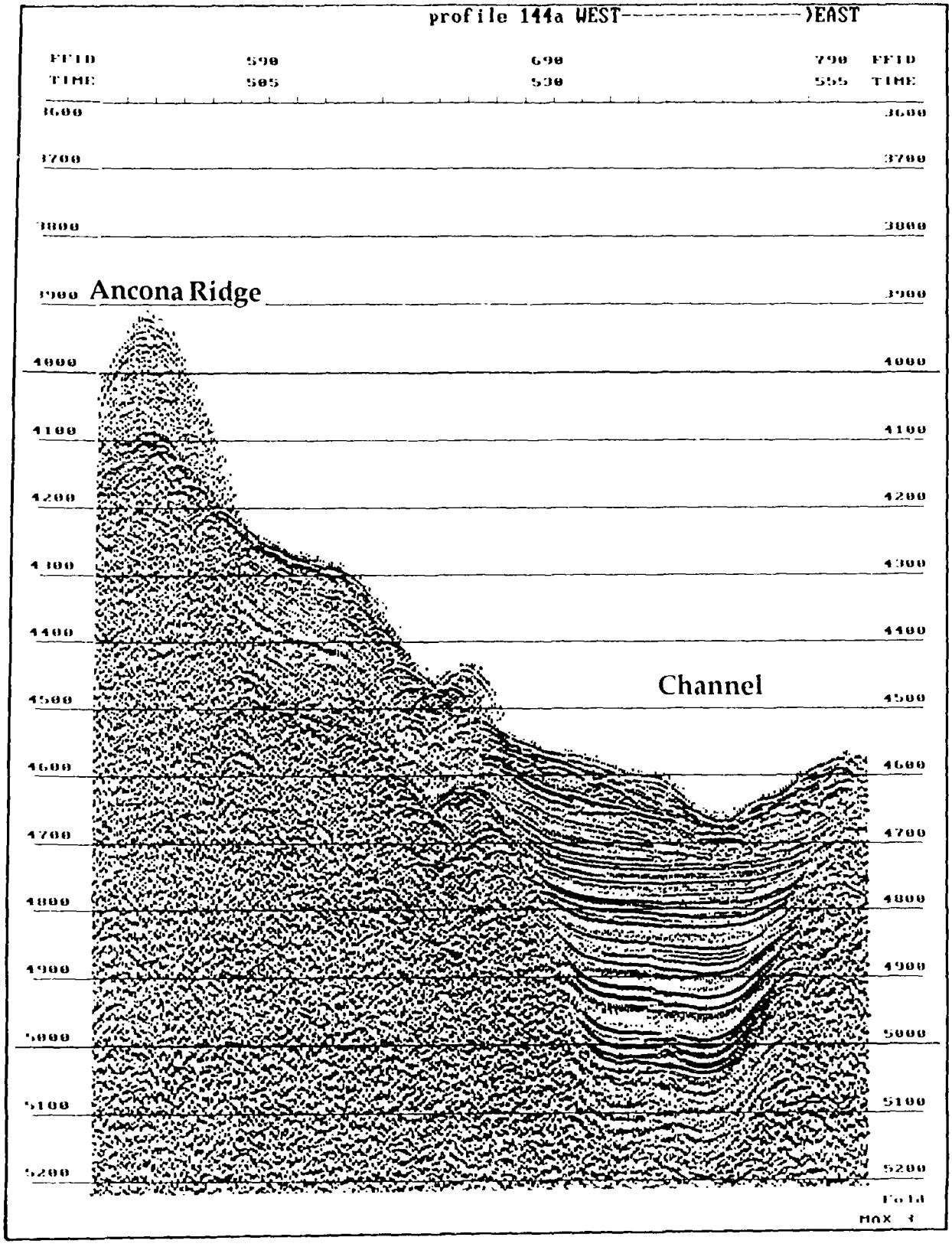

Fig. 23. A well-developed channel with depositional and erosional features east of the Ancona Ridge. Seismic profile PS-144

Although the eastern Sardinian margin has always been considered as a typical passive margin with fault block systems arranged in a half-graben pattern, we have recognized evidence of compressional deformation west of the Central Fault: reverse faults and inverted basins (Fig. 24). Our initial hypothesis is that the latter structures, which occur only in this area, are due to a transpressive component along north-south trending faults.

Interesting morphological features, clearly visible along this seismic line, are a number of erosional channels, about 100 m deep and a few kilometres wide (Fig. 24). These erosional features belong to the sinuous Sardinia Valley, which comes from the Sardinian margin.

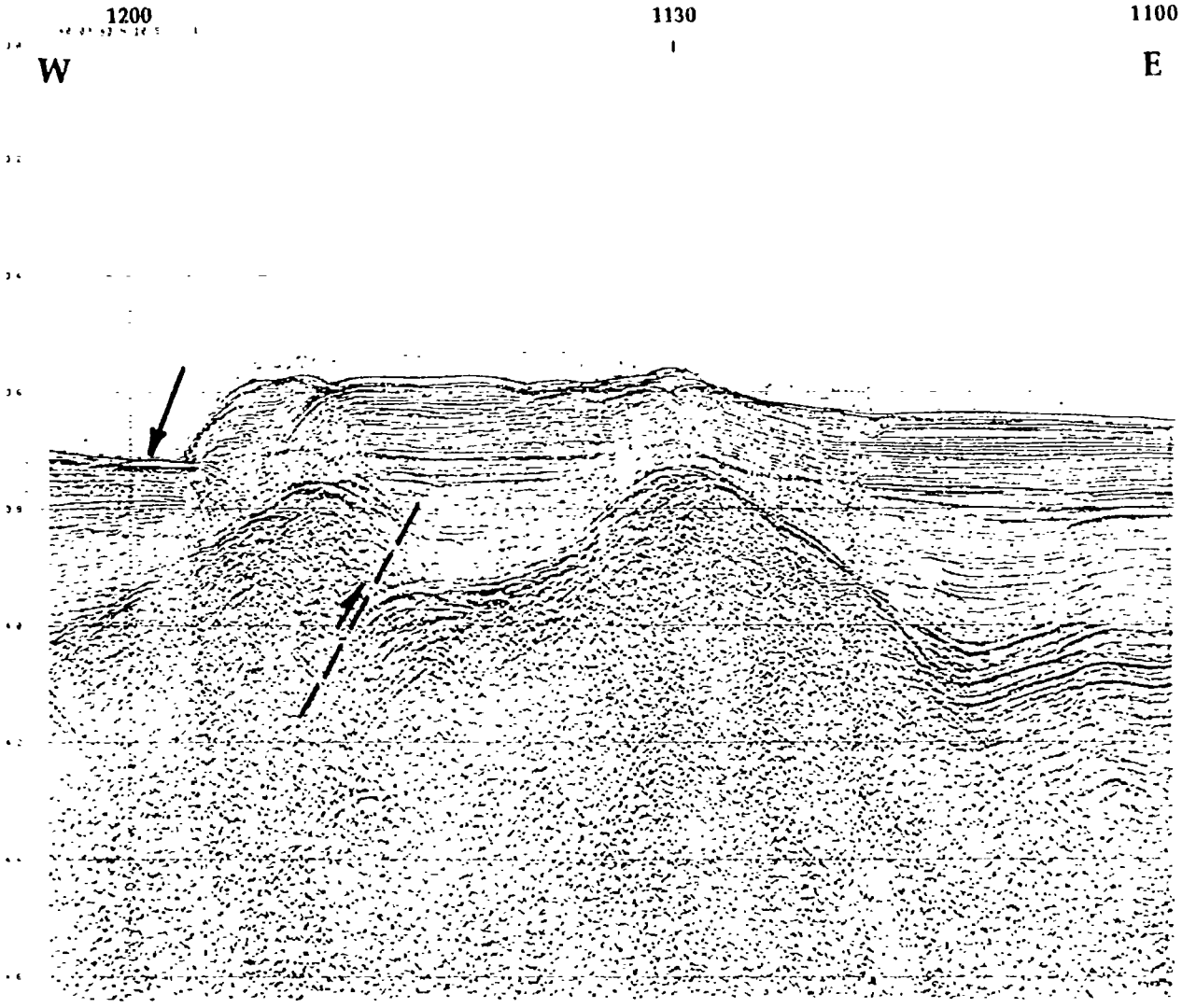

Fig. 24. Evidence for compressional deformation in the form of reverse faults and an inverted basin west of the Central Fault in the Tyrrhenian Sea. The erosional incision (arrow) is due to the Sardinia Valley. Seismic profile PS-145.

3. SIDESCAN SONAR SURVEY

a. OKEAN DATA

Marsili Basin

J.M. Woodside

OKEAN long-range sidescan images were made along seismic lines PS-132 to and including PS-137 in the Marsili Basin region (Fig. 11). The intention was to build up a mosaic of seafloor images, which would serve as a guide to further work with MAK deep-towed sidescan and subbottom profiling, as well as to sampling locations. Some GLORIA sidescan sonographs had previously been made in the basin (Belderson et al., 1974) but were not available and did not provide complete coverage in the desired location. The targets of research were the Stromboli Canyon system and the ultimate resting place of sediment, which travelled through that system, and the Marsili Seamount.

The area covered by the survey can be divided into several provinces. A small eastern province takes in the continental slope of Calabria where incised canyons, fault scarps, and mass downslope sediment movement are observed. The Stromboli Canyon at the base of the slope is a structurally and tectonically controlled conduit actively transporting sediment westward into the Marsili Basin across several north-south oriented steps created by volcanic ridges. Stromboli Volcano and several associated smaller volcanoes shed considerable debris into the central part of the area; and in the southern part of the basin this sediment is draped over the volcanic relief and is ponded in front of the ridges. This central province is characterized on the OKEAN records by patches of high amplitude backscatter from outcropping volcanic rocks and from debris from slides and slumps. The Marsili Basin is relatively devoid of backscatter signal except for echo returns from roughly north-south oriented ridges probably related to the Marsili volcanism. Marsili Seamount is the principal feature in the west of the study area.

Line PS-132

The line starts east of the island of Volcano and runs a few kilometres to the east of and parallel to the upper reaches of the Stromboli Canyon. Stromboli Canyon can be seen to the west of the ship's track on the outer part of the sidescan record. It turns eastward at time mark 07:00 but resumes a roughly north-northeastward trend again shortly after, at a point where a northwest trending tributary can be seen joining the channel. The tributary is remarkably straight and may be fault-controlled. From the confluence of the two channels, the Stromboli Canyon appears to widen and deepen. Several small tributaries, intersecting the canyon from the east, may cause some channel flank erosion which may be responsible for part of the widening.

Just before the 08:00 time mark, the Gioia Canyon merges with the Stromboli Canyon from the east (Fig. 25). Gioia Canyon is very straight and narrow and is almost certainly fault-controlled, judging by the accompanying seismic reflection profile. The Stromboli Canyon widens again downstream from the entry of the Gioia Canyon but the channel within it lies in a restricted portion of the canyon. Restriction of the canyon and its widening is here accomplished by large scale slumping of material from the margin of the canyon. One large slump at 08:00 is particularly well-imaged on the western margin of the canyon, and more slumping is seen on the same side at a westward bend in the canyon shortly afterwards. From here, the canyon takes a more northerly direction. Small channels are observed feeding the Stromboli Canyon from the west, down the slopes of the volcanic ridge on which the volcanoes of Panarea and Stromboli are situated. Some mass wasting and a slump scar between 09:20 and 09:40 are seen on the eastern (Calabrian) continental slope.

The Angitola Canyon enters the Stromboli Canyon west of the OKEAN line at time mark 09:45. It crosses the entire sidescan image from east to west. Fault control of the Angitola Canyon is inferred from the seismic profile as well as from the steep and straight southern wall of the canyon morphology. The north side of the canyon is much less steep and is stepped at places. Upslope to the east, the canyon floor widens, and the margins of the canyon have a scalloped appearance as a result of large slumps. The course of the upper canyon from the northeast is observed to mimic the meanders of the channel around the slumped material. Downslope to the west, the canyon narrows slightly. The slope region north of Angitola Canyon is best characterized as a series of large slides and slumps with associated slump scars upslope and debris flows downslope.

Line PS-133

Line PS-133 is the middle of three lines which cross the Marsili Basin from the Calabrian margin to the basin west of Marsili Seamount. The other two lines are PS-134 to the south and PS-136 to the north. Together the three lines provide a broad continuous image of the southern two thirds of the basin. At the eastern end of line PS-133 there are two slump scars (e.g. at time marks 17:30 and 18:10) on the southern side of the scan and what may be debris flows between 18:50 and 19:00 on the right side of the scan (originating from the basin slope to the northeast).

Stromboli Canyon appears on the port side between 19:20 and 20:30 as a triangular, high backscattering (black on our image) area. It is oriented roughly perpendicular to the ship's track but is not actually crossed because it turns abruptly westward before the crossing. A large slump is observed entering the canyon at the bend (at about 19:30). The western half of the channel has low to intermediate reflectivity in contrast to the eastern half, and the western margin is observed as a scarp cutting across the port scan from the outer edge at 19:30 to

the middle at 20:00. Some slumping into the canyon from the south is observed along the southern margin of the canyon between 20:00 and 20:30. This section of the canyon was also observed in greater detail on MAK lines 23 and 24, and should be analyzed in that context.

The reason for the abrupt change in course of Stromboli Canyon is the presence of a seafloor volcano to the north. This is the southernmost termination of two small volcanoes called the Lametini Seamounts. The volcano appears on the starboard scan between 19:50 and 20:25 (and repeated between 22:45 and 23:25 because of a loop in the line to restart the seismic profile without losing coverage) as a conical structure with a crater on the top. On the repeat crossing of the south flank of the volcano, two small slump scars are visible on the eastern flank; and they are probably associated with mass downslope movement from the northeast. Another slump scar is seen to the west of the volcano between time marks 23:45 and 00:20 on the starboard scan (Fig. 26). The slumps are clearly directed southward into the Stromboli Canyon (see also discussion of seismic profile PS-133).

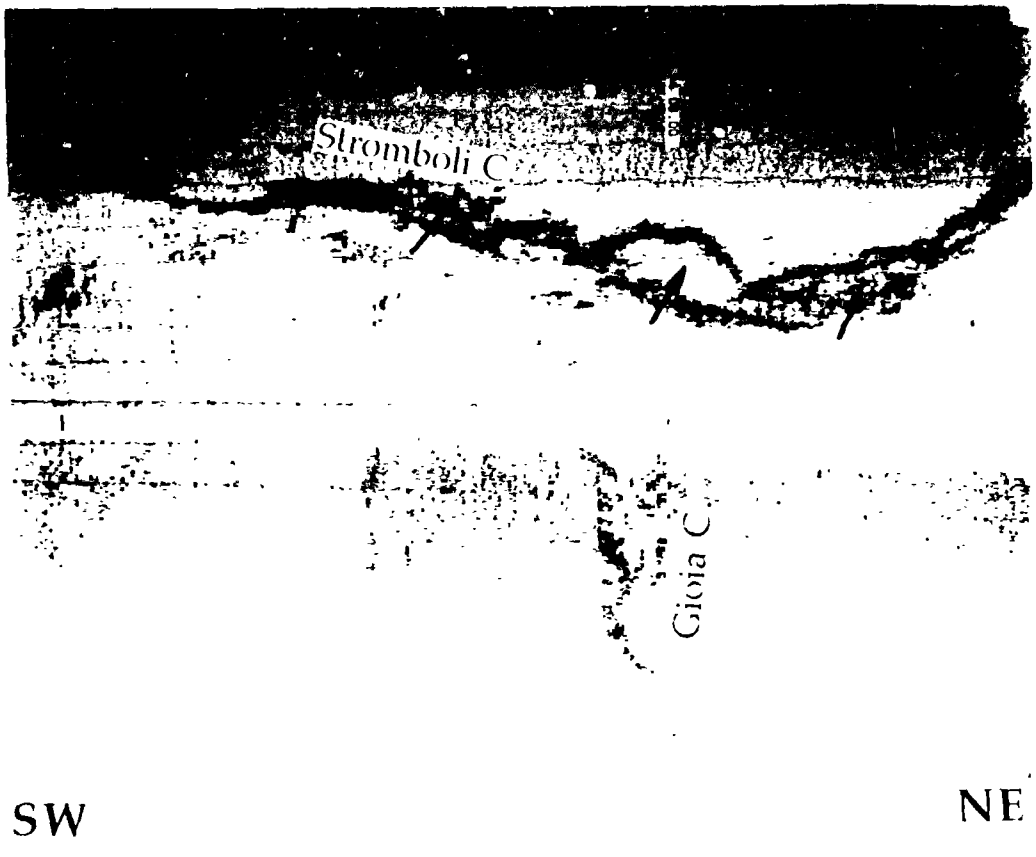

Fig. 25. The OKEAN sonograph (unprocessed) showing the Gioia Canyon merging with the Stromboli Canyon. Note extensive slumping on the Stromboli Canyon slopes (arrows). The swath range is 15 km. Line 132

Outcropping volcanic rocks are inferred between 00:50 and 02:00. They appear as highly reflective patches up to 3 to 4 km across, which together form an area of about 7 km in diameter. Seismic basement is seen to approach or breach the seafloor in the accompanying seismic profile; and rounded lava flows, inferred to include lava tubes and pillows, are observed as highly reflective globular masses on MAK line 23, which crosses the patch seen in this OKEAN image. Putting OKEAN line PS-134 together with this line, and noting the structures observed in detail on MAK line 23, this area of volcanism appears as a circular complex about 12 km in diameter, with a rim and central region suggestive of a volcanic crater with circular centre of volcanism slightly displaced to the northwest quadrant of the crater (Fig. 27). This structure is interpreted as the remains of seafloor volcano, which is now being buried slowly with sediment primarily from the Aeolian Islands to the south but with the most prominent topographic features still exposed through the ponded sediments. This former volcano has also acted like a dam to sediments from the east and marks the edge of the Stromboli subbasin of the Marsili Basin. To the west the seafloor deepens more than it does over a similar distance on the side of the structural blockage.

Northeast of the partially buried volcanic crater are more outcrops of volcanic rocks (between time marks 01:30 and 03:00 on the starboard scan). These outcrops coincide with the increasing seafloor gradient down towards the Marsili basin floor to the west. This suggests that the previously described extinct volcano is situated on a volcanic ridge which crosses the basin in a north-south direction. Seismic basement is also seen to be shallow between time marks 01:30 and 02:30. The exposure of basement in this area may result from erosion from the Stromboli Canyon system which must enter the Marsili Basin in this area.

The volcanic ridge or sill to the west is crossed by a number of roughly north-south oriented ridges and faults. Unfortunately, the roughly north-south orientation of the line is not ideal for imaging these features with sidescan sonar. Furthermore, they should also be analyzed in conjunction with the seismic profiles and the adjacent lines (PS-134 and PS-136). These structures appear as highly reflective and fairly continuous lineations on the sidescan record at time marks 04:30, 05:15, 06:00, and 06:45. A small volcanic hill was crossed on the lineation at 06:00. At least one scarp seen on the seismic profile at 06:30 is not seen on the OKEAN record suggesting that it is either non-volcanic or well-buried, although the east facing scarp must have been a relatively recently active fault. Highly reflective seafloor on the starboard scan between 05:30 and 06:00 may be correlated with the highly reflective seafloor observed in MAK line 26 and interpreted as turbidity flows of coarse volcanic detritus from the basin margins.

Marsili Seamount is crossed to the south of its peak between time marks 07:00 and 09:00. This elongated volcanic complex is also oriented in a NNE to SSW direction. In the sidescan image it appears to taper to the south. The lavas, which build up the southeastern flank, are observed as globular clusters of flows

with strong point reflectors against a background of low to intermediate backscatter. The volcano may be draped in sediment, as large sections of the slope are represented by a more uniform area of intermediate backscatter. The eastern side of a long linear hill, parallel to the western flank of the seamount, is observed at 09:10 on the northern scan and at 09:30 on the southern scan.

Line PS-134

This line runs from west to east parallel to PS-133 and about 14 km to the south of it. It should be analyzed with PS-133 especially for the central portion of the basin; however, it also provides information about the southern margin of the basin. Thus, the southern tip of Marsili Seamount is observed on the north scan (between 13:20 and 14:30), dipping beneath the basin sediments; but sediment transport from the southern continental slope and rise is also imaged.

A volcanic ridge extends northward across the southern scan of the image at 15:45 but does not continue on the northern scan. It may deep northward beneath the basin sediments in continuity with the ridge observed on line PS-133 at 06:00. At the southern margin of the basin the ridge acts as a partial sediment trap and deflects sediments travelling downslope from the south towards the centre of the basin.

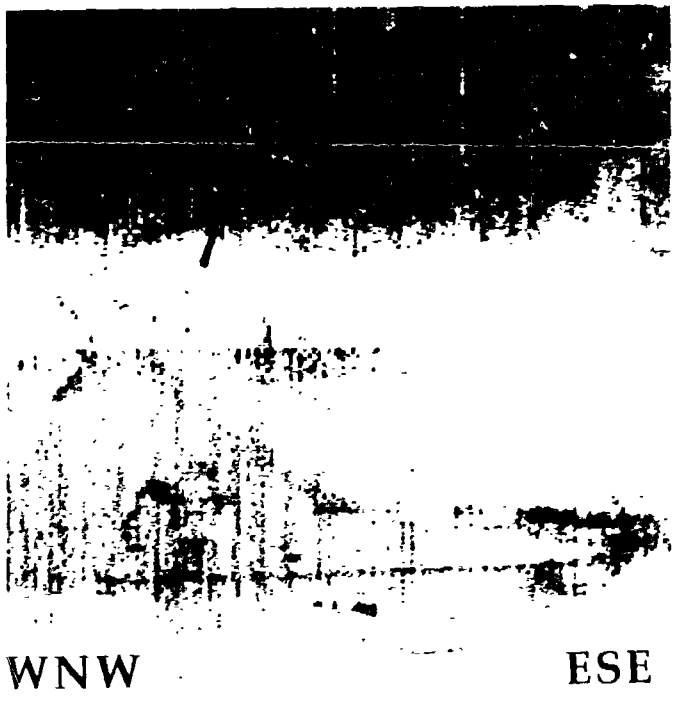

Fig. 26. The OKEAN sonograph showing a slump scar (arrow), which was left by a large slump block observed on seismic profile PS-133 (see Fig. 15). The swath range is 15 km. Line 133

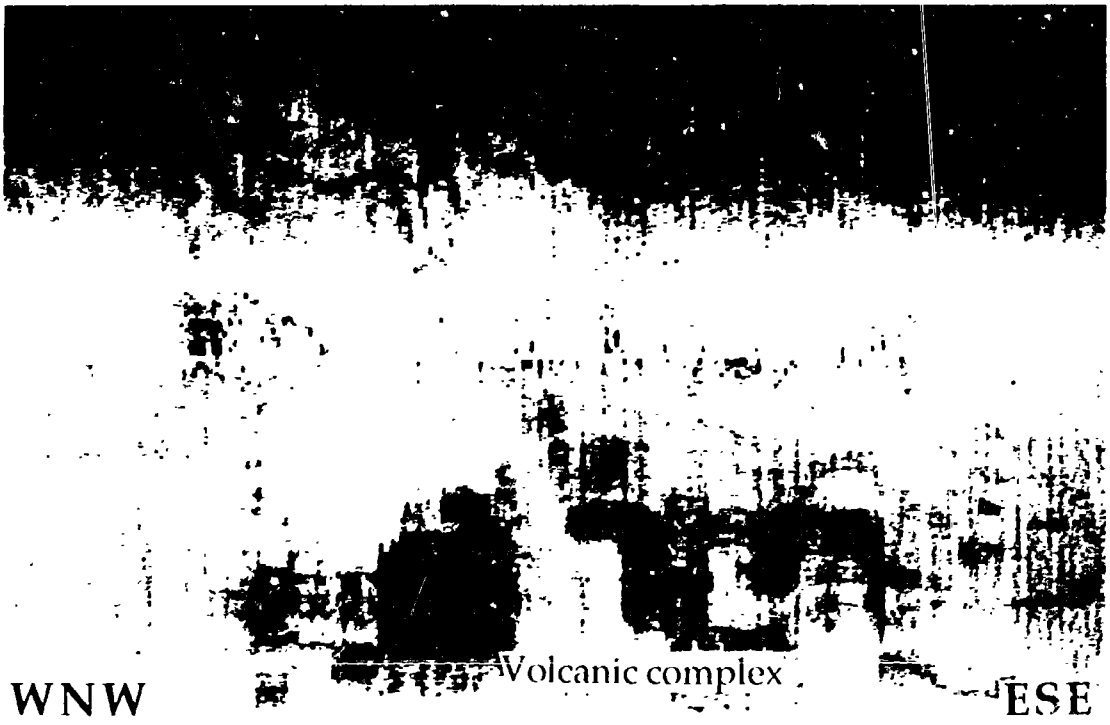

Fig. 27. Outcropping volcanic rocks observed on the OKEAN sonograph. Together with seismic section PS-134 and MAK-1 sonograph 23 one can map a circular volcanic complex about 12 km in diameter. The swath range is 15 km. Line 133

A large slump seen on the accompanying seismic line between 16:20 and 17:20 shows up as patchy, low to intermediate backscatter on a very low backscatter background, in contrast to the strong backscatter from the volcanic relief elsewhere in the basin. This is the only major feature until the beginning of the volcanic zone at about 18:40, which is seen also on line PS-133 to the north.

The patches of high amplitude backscatter between 18:30 and 20:00 are interpreted as exposed lava flows in an area of gradual coverage by volcanic sands and gravels, derived from the south and southeast. The patches form the southern arcuate edge of the volcanic complex described on line PS-133. There is slightly more draping of sediment over the volcanics here compared to PS-133 because of the greater proximity to the source of sediment to the southeast.

To the south of the inferred volcanic crater stand two small seafloor volcanoes at the base of the continental slope. This suggests that the volcanism in the central part of the basin is part of a north-south trending zone of volcanism or a volcanic ridge. The volcanoes are not well-imaged by the OKEAN but the edge of the base of the volcanoes shows up as a strong rugged echo between about 19:00 and 20:30. There appears to be material eroded from the volcanic pedestal, and several small slump scars are visible between time marks 19:45 and 20:00 on the northern slope of the eastern of the two volcanoes.

Stromboli Volcano and debris eroded from it dominate the sidescan image between the two volcanoes just described and the Stromboli Canyon at 22:45 (Fig.

28). The platform on which Stromboli sits is outlined to the south between time marks 21:20 and 23:00. Medium to high backscatter from the flank of the volcano is textured to show downslope movement of debris, which makes up the slope and eventually ends up below the slope on the gentle rise to the north. The talus exhibits streaks radiating from the outline of the island from this downslope movement. One particularly obvious strip of high backscatter from the northwest side of Stromboli (roughly between time marks 21:10 and 21:20) may represent the active canyon which follows the scar created by a slide associated with a caldera collapse event. The speckled appearance of the sidescan image to the north of the volcano may arise from volcanic blocks and smaller debris carried down the canyon, which have been deposited on the seafloor and then draped with thin hemipelagic sediments. Small canyons are visible also on the northeast flank of Stromboli.

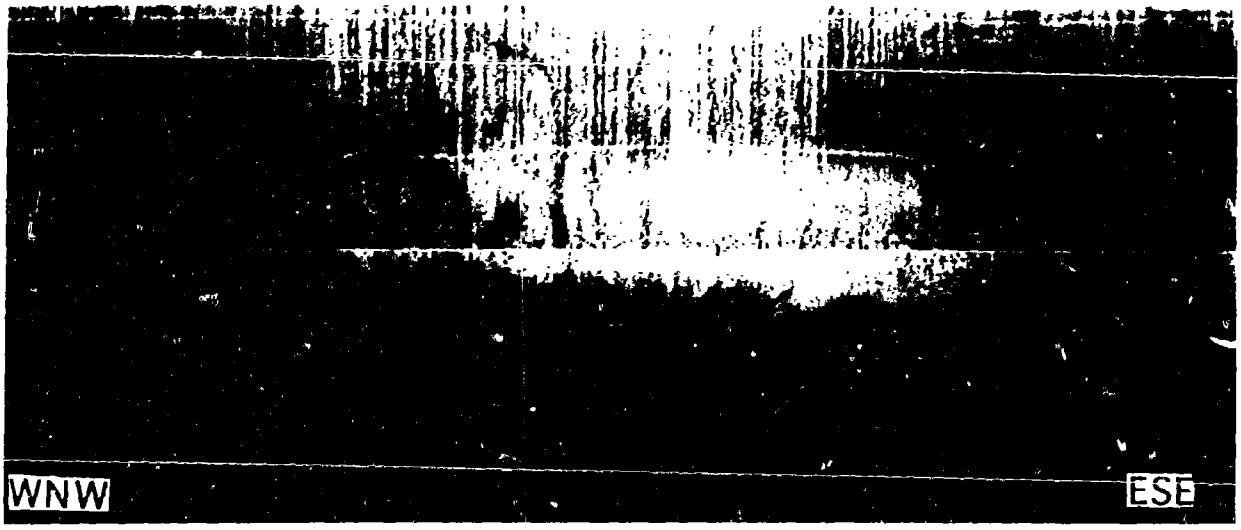

Fig. 28. Stromboli Volcano and flows of debris eroded from its slopes. Stromboli Canyon is seen east of the volcano. The swath range is 15 km. OKEAN sonograph 134.

Stromboli Canyon follows a rather straight south-north course to the east of Stromboli (at time mark 22:45). It appears to be incised through the lower flank of Stromboli in a very narrow valley that opens out to the north. The canyon floor northward is visible as a very high backscatter region, which fans out northward and curves slightly west of north. The eastern edge of the canyon exhibits a highly reflective scarp, especially on the northern scan, where it bifurcates as if there was a small terrace along the eastern margin of the canyon. The scarp itself is not aligned with the canyon to the south; thus, the present course of the canyon through the lower flank of Stromboli may represent a westward shift in the canyon axis, or it could mean that the canyon has scoured eastwards along the escarpment, where the canyon expands at the base of Stromboli and is joined by the Angitola Canyon from the east.

It appears likely that the escarpment along the east side of the Stromboli Canyon is controlled by a north-south fault which can be traced southward through what look like several elongate depressions on the southern scan of the sidescan image. Another scarp (at 23:45) lies parallel to the eastern margin of the canyon and may therefore be controlled by a parallel fault. It appears that sediment has slid over the edge of the scarp to the south of the line.

Lines PS-135 and PS-136

PS-135 is a short 40 minute line segment run on the approach to the start of line PS-136. It is on the Calabrian slope east of Lametini Seamounts and north of line PS-133. There are a few small patches of high backscatter in a surrounding area of low backscatter, which could represent debris carried down the slope from the northeast.

Line PS-136 lies parallel to line PS-133, about 6 to 7 km to the north. With lines PS-133 and PS-134, it provides continuous coverage of the southern two thirds of the eastern part of Marsili Basin. Consequently, it should be examined with the other two lines because it crosses the same provinces within the basin. Because the line crosses almost directly over the northeastern peak of the Lametini Seamounts, there is little to see of the seamount in the sidescan image. The southeastern peak of the two volcanoes is not observed either, except for some speckled areas of higher backscatter, which may be caused by debris on the flank. The OKEAN image suffers from noise along most of the line, making it difficult to detect clearly some of the features observed on the other lines. Slumps and slides from the northern margin of the subbasin are seen as large areas of intermediate backscatter along the northern scan between time marks 23:30 and 01:30. The upslope scarps, making the origin of the slides, are visible within this section of the record.

A volcanic ridge observed in the seismic records at about 01:00 marks the edge of a bathymetric slope, which increases the depth of the seafloor about 600 m or so to the west. The slope is seen vaguely on the sidescan image, especially to the north, but the crossing is at too high an angle for good resolution by the OKEAN. To the south, however, there appears to be outcropping volcanic rock previously described for line PS-133. Outcrop of a volcanic ridge further to the west may have occurred near time mark 03:05.

A small step in the seafloor provides a long linear north-south lineation on the sidescan record at 04:45. This feature may represent a small eastward thrust, which has raised the seafloor to the west; however, it is associated with a volcanic hill crossed on line PS-133. This is the first of a series of parallel features associated with Marsili Seamount, which is crossed near its summit between time marks 05:00 and 07:30. On the west side of Marsili, another long linear ridge is very strongly and clearly imaged at about 07:30.

Line PS-137

This is a very short line running southwards along the west side of Marsili Seamount. Apart from one example of high backscatter from the seamount at the beginning of the line, most of the image is of the ridge, which runs parallel to the seamount along its western flank. On the ridge are seen two spots raised above the general level of the ridge and probably indicating small volcanic cones.

Area east of Sardinia

A.F. Limonov

The only OKEAN sonograph was recorded along the corresponding seismic line PS-145. Its total length is about 240 km, but the most prominent feature was observed on the second portion of the line, over a distance of about 140 km. This is the Sardinia Valley, whose sidescan image was obtained for the first time. The Valley starts on the lower Sardinian continental slope and cuts the Cornaglia Terrace at a water depth of 2000 to 3000 m. In the east, the Sardinia Valley, bending round the Magnaghi submarine volcano, opens out into the Vavilov Basin. It ponds its sediments in front of the northern segment of the Ancona Ridge.

The Valley is fed by sediments derived from eastern Sardinia via some tributaries, the largest of them being the Orosei Canyon (in the north) and the Sarrabus Valley (in the south) (Savelli and Wezel, 1979). The OKEAN line follows exactly the trend of the valley (Fig. 29). Although the average width of the Sardinia Valley is 5 km, it often goes beyond the swath range due to its sinuosity, which is about 1.2. The Valley is incised into the seafloor to an average depth of 140 m, as can be seen from the corresponding seismic section.

The head of the Sardinian Valley shows up as a fan-shaped feature. High-backscattering strips, converging eastward into a single valley, may represent narrow canyons, which are downcut into bedrock to a shallow depth. The deepest incision is observed at the confluence with the Sarrabus Valley. It is 900 m deep relatively to the west slope (along the line) and 340 m deep relatively to the east slope according to the seismic section, but this relief is poorly imaged on the sonograph.

The seafloor within the Sardinia Valley is characterized by an alternation of areas with monotonous low backscatter and areas with highly reflective patches sharply contrasting with the seafloor outside the Valley. These patches are of different size, from a few hundreds of metres to 1.5-2 km, isometric or elongated, the latter being directed either along or obliquely to the Valley trend. In the absence of MAK-1 data, they are difficult to interpret. They may be different erosive features like large scour holes or outcropping bedrocks (for linear features particularly), small blocks transported by currents, or large blocks that have slid from the Valley walls. The uniformly backscattering Valley floor represents the areas covered by soft sediments.

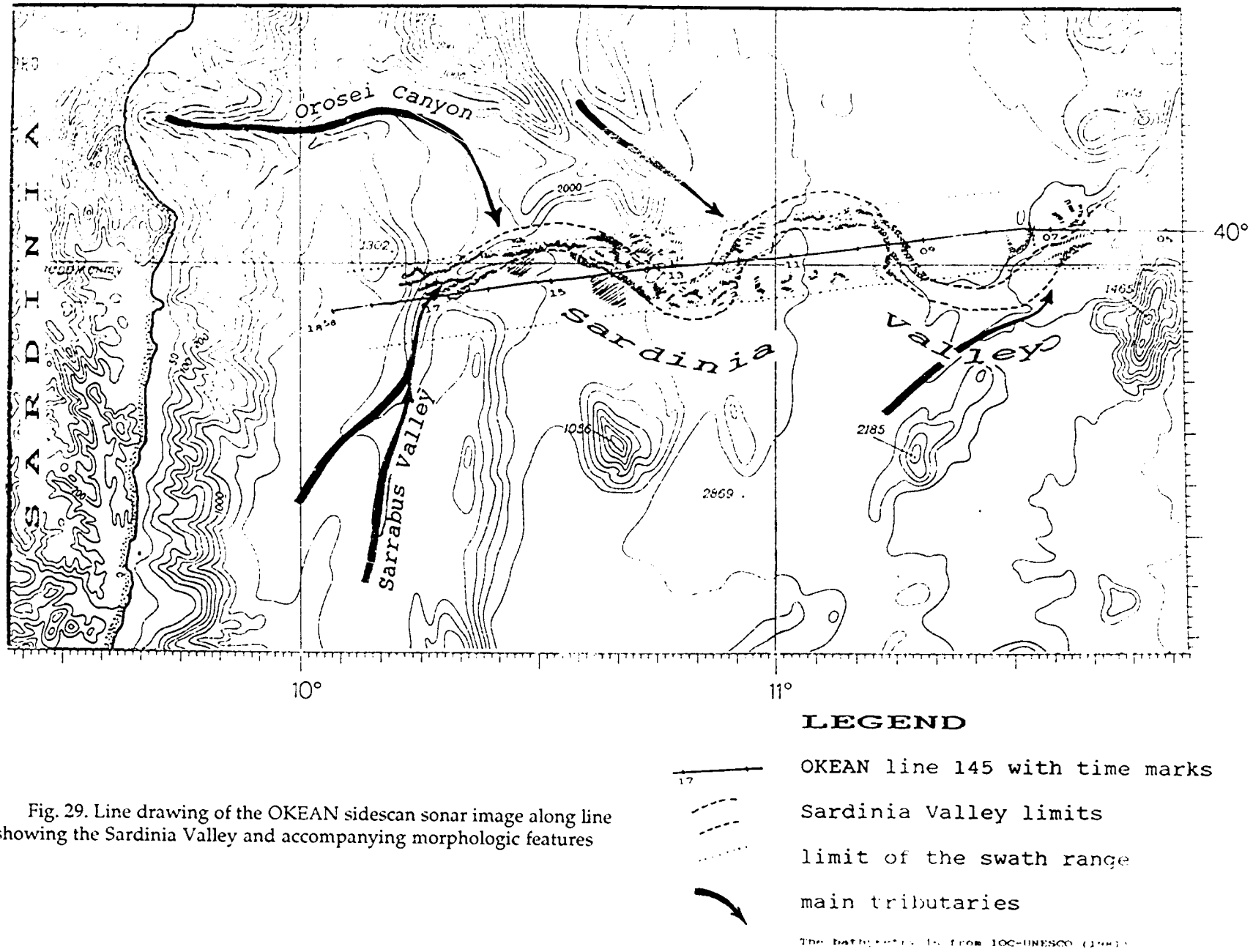

Fig. 29. Line drawing of the OKEAN sidescan sonar image along line 145 showing the Sardinia Valley and accompanying morphologic features

b. MAK-1 DATA

R.B. Kidd, J.M. Woodside, C. Romagnoli, A.V. Volgin, and C. Savelli

MAK line 23

MAK high resolution surveys (Fig. 11) were begun in the embayment represented by the sharp bend in Stromboli Canyon. MAK line 23 began at a water depth of about 1200 m on the western slope of the Canyon at 03:10 on 12 June and ran for almost 27 hours roughly WNW downslope into Marsili Basin, crossing the east-west portion of the Canyon floor between Lametini Seamount and the northern slopes of Stromboli. The slopes of these two volcanic edifices are well-imaged on the OKEAN records, and the bend in Stromboli Canyon appears even more sharp than is apparent from existing bathymetry, with a stepped 120 m scarp forming the northern angle of the bend. OKEAN sonographs display circular areas of outcropping basement around 15°E, and these were crossed by the MAK survey before the line was terminated in the deeper parts of the eastern Marsili subbasin at 3200 m.

The initial part of this line covers the Calabrian slope down to the bend in the Stromboli Canyon. This slope is characterized by gravitational slump folds, rotational slides, scars and debris flows (Fig. 30). Between 03:30 and 04:10 a northwest to southeast trending fault scarp appears to have initiated a series of slump folds that decrease in amplitude downslope from about 15 m to about 3 m. The overall slope direction is to the northwest as indicated by the course of a channel that is about 50 m wide on the port side of the swath, and by the direction of debris flows with a rough mounded surface at around 06:00. The profiler shows evidence of earlier slumping that has been draped by subsequent sedimentation. The area of debris flow is tongue-shaped in plan view and originates in a slide scar area of stepped fractures. South of the debris flow the profiler shows two slides, up to 10 m thick, stepping downslope. A north-south trending scarp is crossed at around 07:00, which appears aligned with the eastern side of the north-south sector of the Stromboli Canyon. This 75-m scarp seems to have shed a number of slump units; and below this the slope levels off, and the profiler displays a transparent wedge of debris flow that is approximately 2 km wide and is up to 15 m thick. Above and below the debris flow are stratified sediments. Core 126G apparently cored the downslope "feather edge" of this debris flow. On the eastern edge of this plateau, a slump scar is crossed, that is about 1 km from north to south and 400 m from west to east. The sediments within this amphitheatre-shaped feature are folded in their upper part and thrust on its downslope western end. Just below the slump scar there is a steeper 100 m wide section of slope with a gradient of about 6°. Beyond this is a very high backscatter zone of exposed slope that is almost concave in section and appears to be covered with very coarse sediment (gravel?).

The crossing of Stromboli Canyon is in an oblique direction and represents a true cross-sectional width of about 4 km. The depth of the canyon floor increases

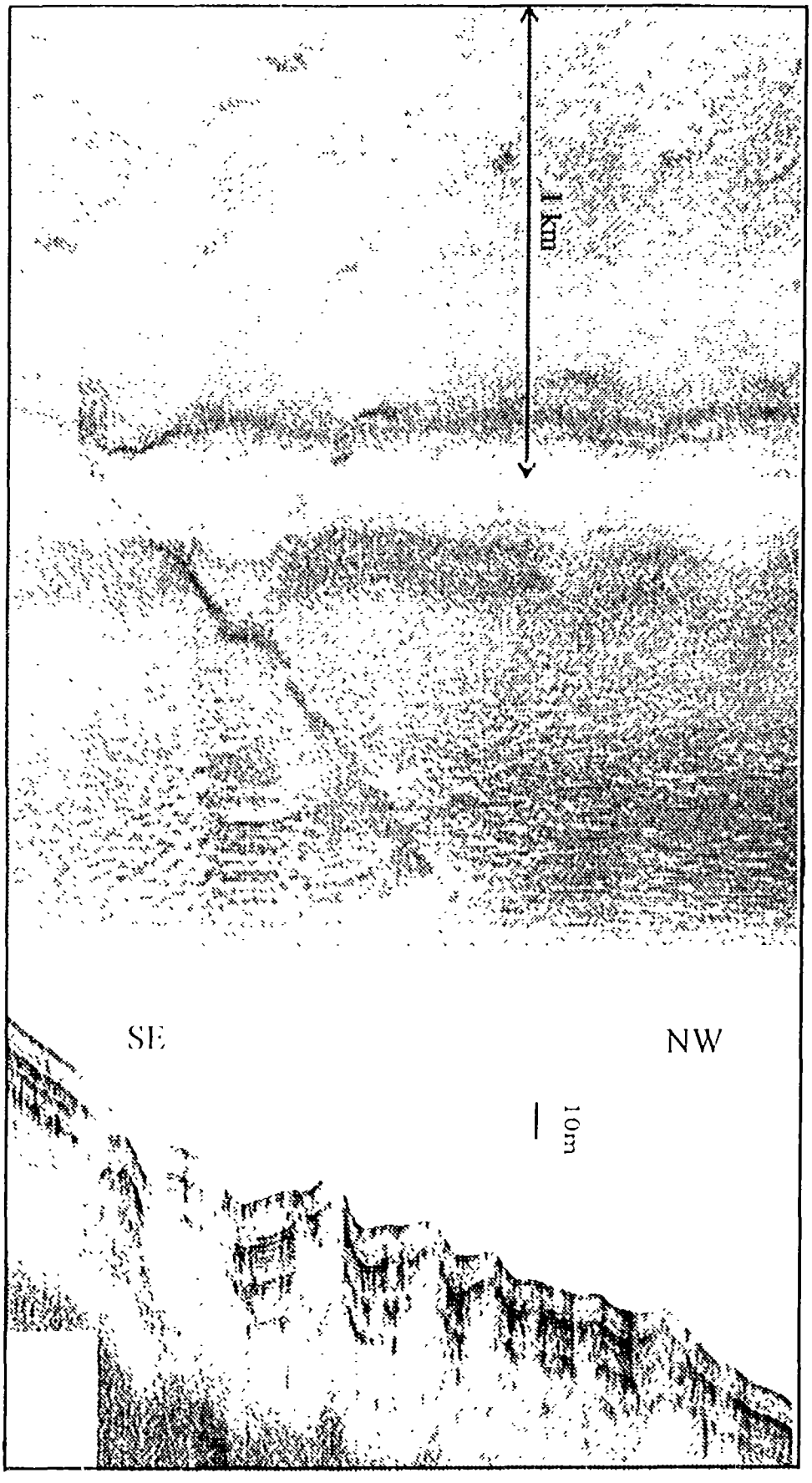

Fig. 30. Slump folds on the western Calabrian slope. MAK-1 line 23, sonograph and profile

by 90 m from east to west. The western scarp of the canyon is 60 m high. Three principal zones are observed across the canyon: high energy scouring of bedrock along the eastern margin over a distance of about 900 m (and represented by extremely high backscatter) (Fig. 31), a section of sand waves about 2400 m wide, and a lower energy zone along the western flank about 2000 m wide and represented by intermediate backscatter levels.

The sand waves in the eastern part of the canyon have wavelengths of about 100 to 200 m and amplitudes of a few metres at most. The largest waves are furthest east, but there is a transition through three zones, with the western and eastern waves at the ends of the range. The backscatter variation is highest in the central region of sediment waves, ranging from extremely high to very low. The highest backscatter in this zone is in patches that frequently are seen to align with the waves and may represent coarse gravel in the lows, or possibly outcropping basement volcanics, on the basis that there is basement exposed a few hundreds of metres to the east. The high backscatter patches are the sources of streaks of high backscatter material which lie perpendicular to the waves and extend for one to two kilometres.

The western zone of gentle relief lies between a 15-m high ridge to the east and a 90-m scarp to the southwest. It is broken by arcuate (convex down canyon) depressions, 100 to 300 m long, which look like scours. The western scarp is cut by slumps. Although the sediment appears to be thicker in this region of the canyon, mainly because there does not appear to be high reflectivity material showing through where the scours are seen, the subbottom profiler does not show any penetration of the bottom sediments throughout the canyon, except just below a western slump where there may be material from previous slumping.

To the west of the canyon lies a plateau region with very gently undulating relief with an amplitude of no more than about 5 m. The plateau dips in this crossing towards the west (although the true dip is presumably more northwest), the deepening being about 30 m over a distance of about 5 to 6 km. The subbottom profiler displays very high amplitude continuous reflectors throughout the depth of penetration of about 25 to 30 m. The presence of internal reflectors here is in contrast to the area of the canyon where no internal structure is seen, and the strength of the backscatter is almost the same (except for the previously described patches of higher backscatter). The internal reflectors are spaced very closely and are resolved on the scale of a metre or so (e.g. about 15 layers are observed on average per 10-m section, suggesting resolution of 70 cm thick layers).

The western part of the plateau region is cut by slump structures. The largest of them is seen on the subbottom profiler record as a deformed area, about 100 to 200 m wide, and a few metres below the surrounding level of the plateau. Other slumps are seen on to the north; and all the slumps seem to originate from a line which could be drawn eastwards to the canyon. It is inferred that this northwestward slumping is towards the continuation of the Stromboli Canyon just to the north of this MAK line.

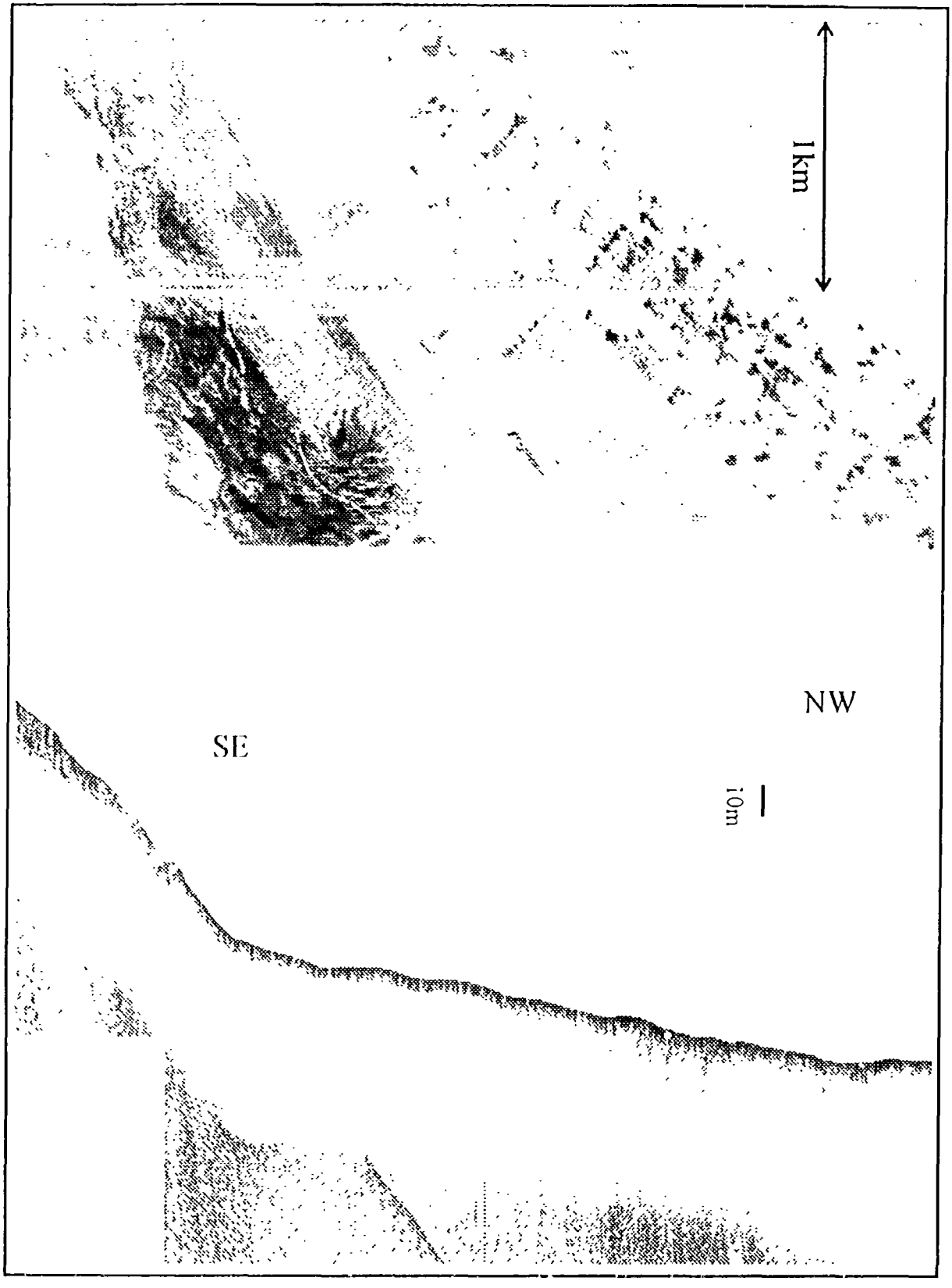

Fig. 31. High energy scouring of bedrock in the Stromboli Canyon. MAK-1 line 23, sonograph and profile

The western margin of the plateau (at about time mark 13:45) is marked by a steeper westward facing slope, about 60 m high. Below the slope is a gentler slope, between time marks 14:00 and 14:50, where the depth increases by a further 60 m. The penetration depth across the gentle slope is less, but the layering is as thin as on the plateau; the difference here is that the strata are folded and in some places display greater distortion. It may be further inferred that this slope represents the outbuilding apron of fine sediment, apparently being shed down the northern and northeastern slopes of Stromboli (see discussion of MAK line 25).

Between 14:50 and 16:00 is a region of elongated generally parallel crenulated features, lying in a roughly east-west direction and up to 1.5 km long and about 5 m high. The subbottom profiler penetrates only about 5 m of the very high amplitude continuous thinly stratified material. The relief appears to be caused by folding perpendicular to the direction of downslope flow of material from Stromboli. Thus it could be caused by slow downslope movement by the volcanic sand assumed to comprise the sediment. There may be some reworking of the material by downslope currents and turbidity currents causing a mixture of scouring and draping, which also exposes and transports underlying coarser volcanic debris over distances of no more than 200 m or so.

These reworked coarser deposits are generally found further to the northwest on the sidescan image, confirming the inference that the thickness of the overlying finer volcanic sediment from Stromboli thins in that direction. These coarser deposits are seen as small patches with extremely high backscatter. We suggest that they are eroded from underlying coarser debris from earlier debris flows down the northwest flank of Stromboli. On MAK line 25 to the south can be seen the increasingly more proximal coarser part of these deposits. Between 16:00 and 17:00 the coarser material is associated with low linear obstructions to the northward transport of finer sediment from Stromboli; but some of the sediment flows past the obstructions in broad lobes several hundred metres across. Between 15:20 and 16:05 two relatively horizontal ponds of sediment can be observed. The obstructions are seen as individual elements in a narrow east-west belt of highly reflective objects. This belt could be the front of a debris flow carrying very coarse (metre-sized rocks) material from Stromboli. In at least one case (about 210 m to the right of the track around 16:40) there is seen a large highly reflective block several metres in diameter and with enough relief to cast a sonar shadow.

Between 16:40 and 17:00 the depth increases by about 45 m to another gentle slope, which increases in depth by 100 m from time marks 17:00 to about 18:40. Within this zone is very little relief except for a 10-m deep scour at 17:25 and a moat about 5 m deep which is scoured around an outcrop of presumed volcanic lava at 18:10. Thin sedimentation is inferred again on this section from the subbottom profiler, although the penetration is only about 5 m or so and the reflectivity is extremely high. Volcanic basement may outcrop at the base of the eastern margin of the this section, at the foot of the 45-m slope. Further to the west, volcanic basement outcrops more extensively. The volcanic basement is

seen as irregular globular patches of high to extremely high backscatter, which are accompanied by shadows suggesting rounded relief. The reflective patches are about 200 m across, and the relief of the inferred volcanic outcrops is several metres. The ubiquitous volcanic sediment appears to have ponded around the volcanic hills.

Volcanic lavas outcrop between 18:40 and 18:50 with a linear west-facing scarp forming the western edge of the outcrop (Fig. 32). The scarp is about 45 m high and runs south-southwest to north-northeast across the profile. Sediments are ponded to the east of the scarp suggesting that it is a buried asymmetric ridge with the gentle eastern slope outcropping through the ponded sediments in places, as noted above. Sediment has flowed over the scarp in places and forms a deeper pond to the west, as indicated by the absences of outcropping volcanic rock. We interpret this ridge as the edge of a caldera lying in the depression to the west. This interpretation is based in part on the circular pattern displayed by the highly reflective volcanic rocks in the OKEAN profiles (see Section II.3.a).

The inferred volcanic caldera extends from 18:50 to 00:50. Volcanic rocks outcrop in the central region between 21:00 and 22:00. Shadows thrown by some of the volcanic edifices indicate that the relief is greater here, reaching up to about 10 m. Sediments are ponded around the volcanic outcrops and show indications of variable northwestward and westward flow among the projecting volcanic outcrops (e.g. scours, low sand waves with an amplitude around a metre or so and wavelength of about 40 m, and short trains of coarser material showing higher backscatter). The level of the seafloor deepens rather abruptly to the west of each area of volcanic outcrop: thus there is a deepening of the seafloor by about 120 m across the volcanic centre of the caldera. The depth increases again by almost 60 m across the volcanic outcrops between 22:45 and 23:15. At the western edge of the volcanic complex, between 00:40 and 00:50, there is a final step of about 90 m down to the west. From east to west across the caldera, the sediment layer appears to thin because the ponding is less and, as a consequence, the local relief is greater, increasing from a few metres to more than 5 m.

West of the inferred volcanic complex, the seafloor relief slopes gently westwards into the Marsili Basin. The increase in depth is around 200 m and the local relief, especially just to the west of the volcanic complex, is 10 to 15 m as far as time mark 01:50, and thereafter is only a few metres. The higher relief is caused by south-southwest to north-northeast trending sinuous to saw-toothed (in plan view) west-facing scarps over which sediment is starting to drape. Flow direction is along track, indicating that the MAK line at the west end is perpendicular to the bathymetric contours. Shadows thrown by the edges of some ridges indicate a very sharp break in the seafloor topography possibly caused by plucking and scouring of sediment on the downslope side of the ridge. At time mark 02:00, the scouring has reaching a coarser underlying sediment, which shows higher backscatter and appears to have been carried up to 200 m downslope. The west-dipping stratified rocks, which are moulded in this fashion, are inferred to represent flows of incohesive volcanic ejecta on the western flank of the volcanic

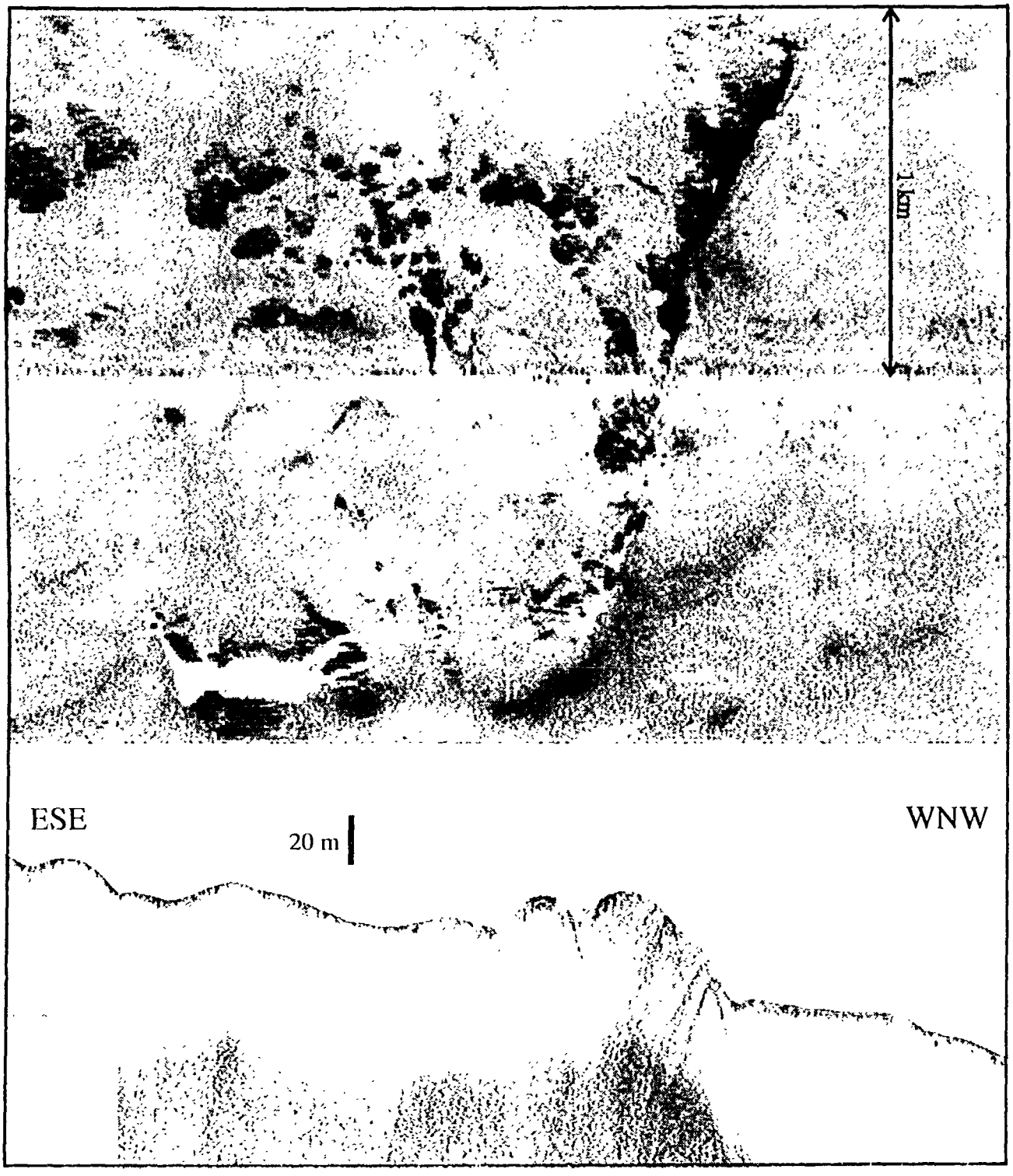

Fig. 32. Outcrop of volcanic lavas (edge of an inferred caldera) acting as a sedimentary trap. MAK-1 line 23, sonograph and profile

complex. West from 02:30 the slope is gentler and without the local relief just to the east; but locally there are small scour holes up to 20 m across, and minor flows of coarser sediment from the south.

Various flows of volcanic turbidites of different grainsize and thickness are ponded (between time marks 03:30 and 04:30) east of a volcanic ridge observed also on the seismic and OKEAN records (Fig. 33). The backscatter of these deposits varies from intermediate to high as a function of different overlapping flows. Flow direction here is roughly east to west but there are local variations: some of this material has flowed into a region previously scoured out or excavated as the result of a slump (just west of the line at 03:50). Some blocks up to a few metres across are seen near the east side of the ponded sediment.

Sediment waves with an amplitude of less than a metre and wavelengths between 20 and 60 m are observed near the end of the MAK line on a region of westward slope. The sediment waves appear like cirrus clouds (low backscatter white) on a background of higher backscattering (darker) material. Their orientation suggests current and sediment movement downslope from the southwest where the OKEAN and seismic data indicate the presence of a canyon down which sediments have slumped; but an alternate view might be that they come from the northwest as part of flows from the Stromboli Canyon system as it passes the central volcanic complex and enters the eastern Marsili Basin. Flows of presumed volcanic turbidites are observed to have come from the south and ponded in places (e.g. between time marks 04:50 to 05:10).

MAK line 24

MAK line 24 was run for about 12 hours in a southeastward direction from about 7 km west of Lametini Seamount to the eastern side of the north-south section of Stromboli Canyon near the confluence of the tributary Angitola Canyon. Lametini Seamount is prominent on the OKEAN sonographs as a conical hill with a summit crater. The MAK transitted its steep western and southern slopes. The steep scarp on the northern bend of Stromboli Canyon was crossed at roughly the same location as on the MAK line 23 providing a further view of that part of the main canyon floor.

The northwestern section of the MAK line crosses a large slump block imaged by the seismic and OKEAN systems. The slump lies between time marks 22:45 and 02:30. On the basis of the subbottom profile image, the northwestern end of this section is inferred to be relatively flat-lying thinly layered (of the order of a metre) volcanic sediment with low surface relief (less than 5 m). A large block of this is starting to slump southwards (on the southwest scan between 23:10 and 23:50). Further along the line to the southeast, the topography increases dramatically in an area composed of disjointed blocks within the larger slumped mass.

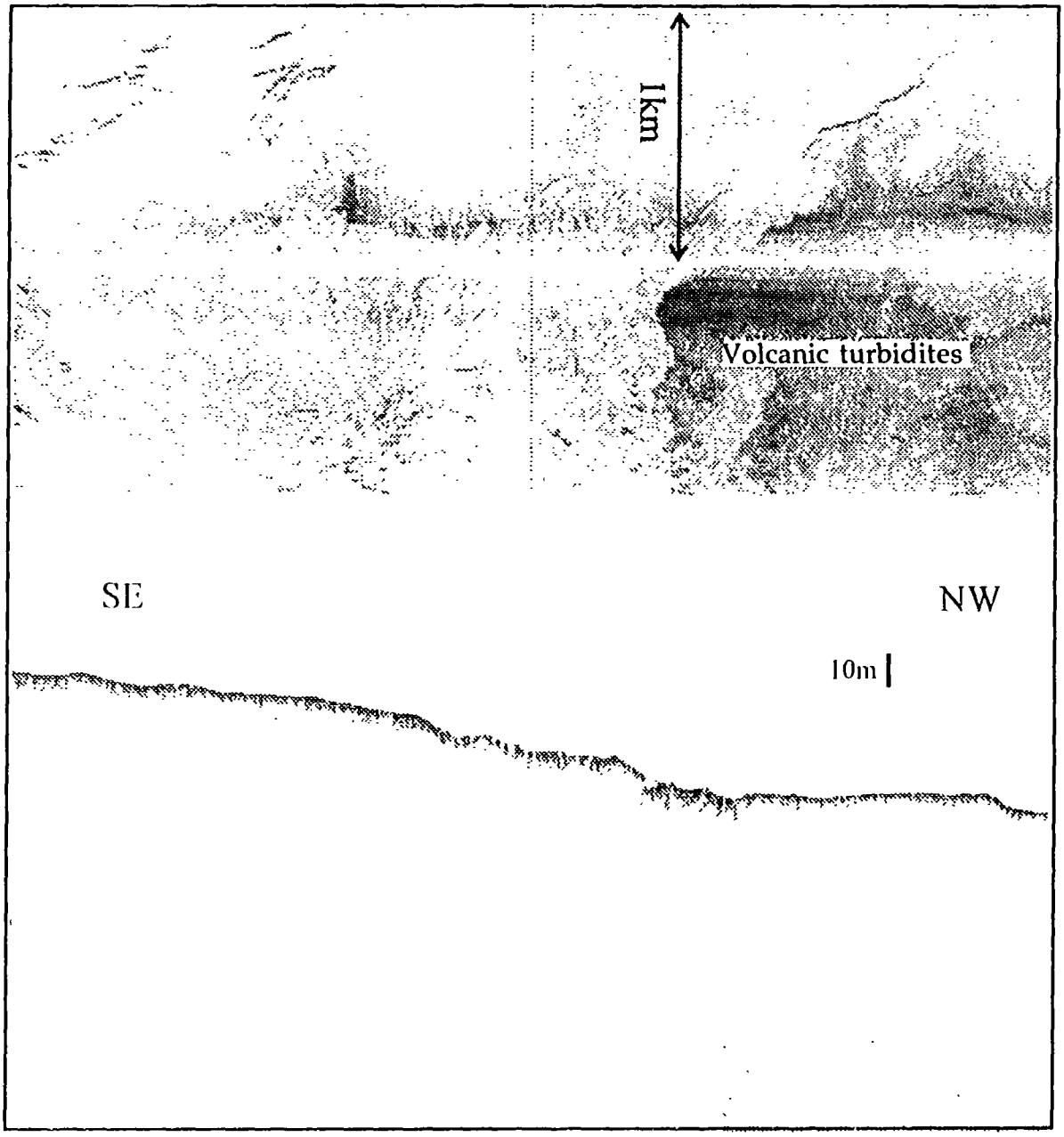

Fig. 33. Volcanic turbidites ponded in the distal segment of the Stromboli Canyon east of a volcanic ridge. MAK-1 line 23, sonograph and profile

The most disjointed mass of the aforementioned slide lies between 00:00 and the eroded edge of the mass, where it is cut by the Stromboli Canyon (at time mark 02:30). The relief reaches 70 m in this section. Blocks of sedimentary rocks with greatly differing stratal orientations are juxtaposed here. Around and across the blocks, canyons have been cut to carry sediment into the Stromboli Canyon to the south. Some of the faulting and tilting among the blocks is caused by mass movement towards the Stromboli Canyon. One canyon crossed at 00:22 is fed by a number of small tributaries along its western side; another two, crossed at 00:45 and 00:49, join about 300 m southwest of the line and continue down towards the Stromboli Canyon across some small steps, which are probably a result of small faults associated with the downslope movement of the whole mass.

The deepest canyon is crossed at 01:17. It is incised into the underlying sediment by about 70 m. Approximately 100 m to the northeast of the line is the confluence of three canyons, which carry sediment into the deep main canyon (Fig. 34). This canyon system has downslope-concave steps considered to be caused by slumping and scouring; and upslope in the two western tributaries the same origin may be attributed to similar arcuate features along the canyon axes. A poorly (newly?) developed canyon is incised about 15 m at time mark 01:50.

The line crosses the edge of the large slide block obliquely. A number of small slumps are seen along the edge, including one at 02:25, which displays a coherent tilted block of sediment. The fine pattern on part of the MAK sonograph at about time 02:40 to 02:50 shows surface sediment movements, which partly cover and smooth out the small scale slump structures.

Between 02:30 and 07:45, the bend in the Stromboli Canyon, which was described for MAK line 23, is crossed very obliquely. All the features seen on the previous line are again recorded from a slightly different angle of insonification. It is easy, however, to match up individual features which have a specific backscatter characteristic or shape. A description of the different bottom facies across the canyon can be found in the description for line 23. Additional data from line 24 includes a section of the canyon downstream from the bend at the Lametini Seamounts and a little more of the canyon upstream from the line 23 crossing.

Following the abrupt bend of the canyon through an angle of the order of about 120° the canyon broadens and simplifies in so far as there is less variability across it in the types of bed forms and sediment. The thicker sediment containing scour marks on the inside of the bend seem to terminate rather abruptly at what may be either a barely outcropping roughly east-west volcanic ridge or a linear train of coarse (gravelly?) material which gives a very high backscatter (Fig. 35). There appear to be sand waves across the entire canyon floor and some of them show signs of entraining coarse sediment (gravel?) which forms streaks of high backscatter material parallel to the inferred flow direction. The wavelength of the sand waves is roughly 100 to 150 m and the amplitudes are no more than 2 m. A small patch of smaller sediment waves with wavelengths around 20 m can be

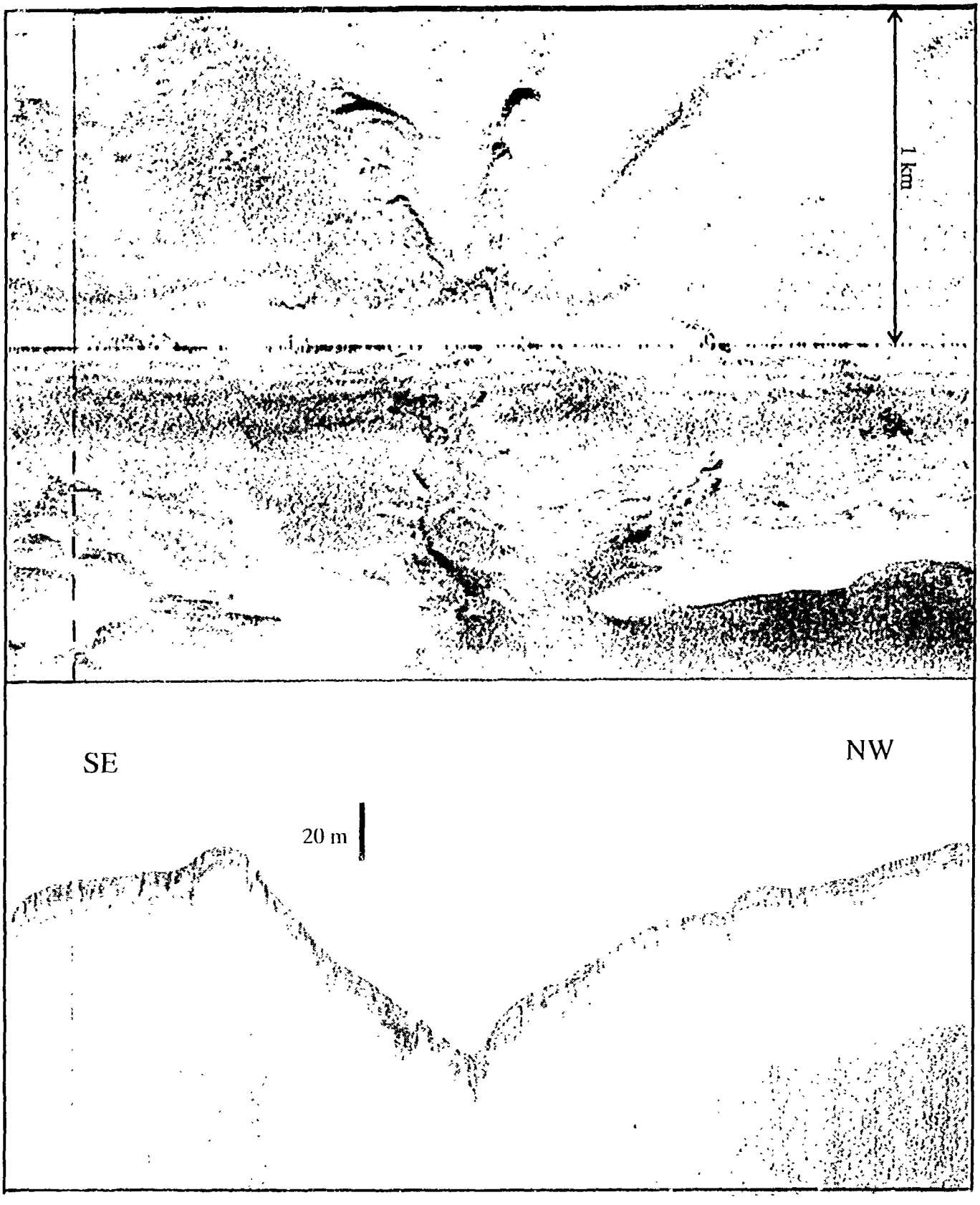

Fig. 34. One of the northern tributary systems of the Stromboli Canyon with slumping and scouring pattern. MAK-1 line 24, sonograph and profile

observed near the inside corner of the bend. Between 04:00 and 04:30 on the northeast scan (in the canyon near the outside corner of the bend), there appears to be exposed bedrock, which is presumed to be volcanic rock on the northern flank of the Lametini Seamounts. The bottom of a scoured east-west channel (about 200 to 300 m wide) incised at the base of the flank is ponded with sediment about 5 m deep. We infer that the abrupt turn in the course of the canyon is structurally controlled by the presence of this volcanic edifice. Across the bend in the canyon, the depth of the seafloor along the outside part of the canyon floor changes by about 250 m over a distance of about 20 km.

The different grazing angles of observation for lines 23 and 24 provide an opportunity to compare features which have been insonified at different angles. For example, the elongated ridge between the more actively eroding part of the channel and the thicker sediments on the inside bend (between 04:35 and 06:00 on line 24 and 09:35 and 10:20 on line 23) shows up as a more strongly backscattered lineation on line 24 than on line 23 because line 23 sees it from a steeper grazing angle. Likewise, the eastern flank of the canyon, which was crossed perpendicularly on line 23 and therefore did not show much detail perpendicular to the line, displays several terraces (possibly related to slumping) on line 24 on the lower part of the slope and some outcropping strata near the upper edge of the slope (at 07:45).

From the edge of Stromboli Canyon to the southeast, the sonograph resembles line 23 in general. A slump is observed at the top of the roughly 180-m high scarp on the east side of the canyon. Another scarp of about 120 m high at time mark 08:07 crosses the eastern slope obliquely. It is likely that it is the upper scarp of a large slide and may possibly be correlated with the upslope scarp of a slump at time mark 07:00 on line 23. If this is the case, then the scarp is a large crescent-shaped scar cutting out a section of the lower Calabrian slope perhaps as much as 15 km long and 5 km wide. This interpretation makes more sense than others, such as faulting, because there is no direct linear continuation of the scarp between the two lines and the entire block between scarps appears to have moved slightly downslope.

Between the scarp marking the edge of the slide and time mark 08:55 is a more horizontal section of seafloor, which appears to have slid downslope slightly. Slumping is observed from the lower (western) edge of this slide onto the larger slide below, and slumps or debris flows from upslope can be observed in the subbottom profile at 08:53 overlying the upslope edge of this slide to a depth of about 10 to 12 m.

Upslope from time mark 08:05, the Calabrian slope is dominated by debris flows and, near the end of the line, by slumps from the upper section of the slope and slides of thin sheets of surficial sediment. What begins as slumps may develop downslope into debris flows. The subbottom profile displays a long record of debris flows on this slope at least to the penetration depth of 60 m. In fact the entire section of debris flows may be creeping downslope. Slump scars exhibit morphological features like gullies.

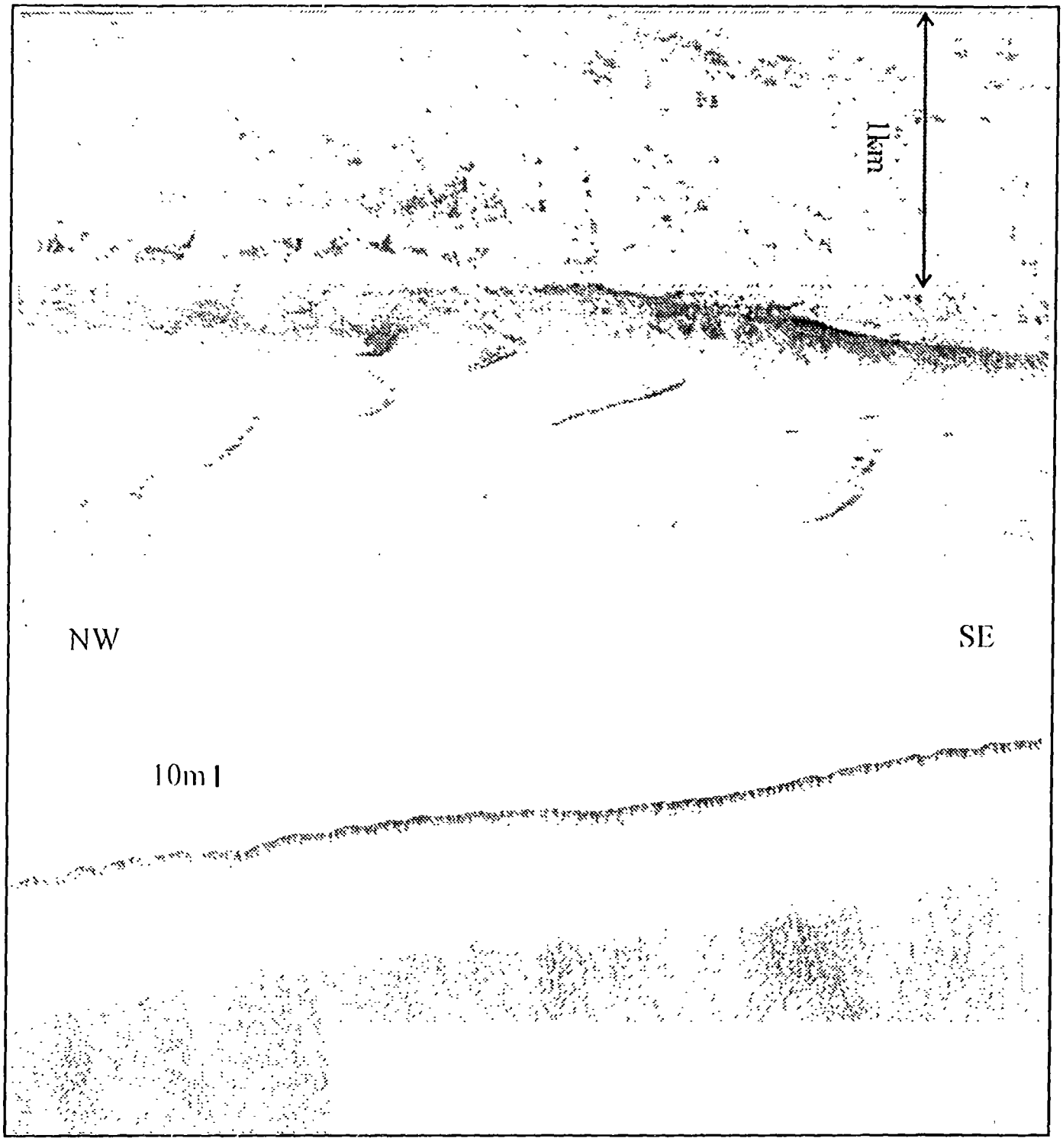

Fig. 35. Scour marks and sand waves in the bend of the Stromboli Canyon. MAK-1 line 24, sonograph and profile

MAK line 25

MAK line 25 ran for almost 15 hours from ESE to WNW from the north-south sector of Stromboli Canyon, across the northern slopes of Stromboli Volcano and on to the deepest parts of the eastern Marsili subbasin. It lies parallel to MAK line 23 to the north and was planned to study the downslope effects of a recent caldera collapse of the northwest slope of Stromboli, the Sciara del Fuoco, that had been mapped to a water depth of 2200 m by Romagnoli et al. (1993). The western end of the line was planned to cross the circular outcrop feature detected by OKEAN at 15°E and also crossed by MAK line 23 (see above).

The first section of the line, between time marks 17:05 and 20:10, crosses the northern flank of Stromboli Volcano. Thus the bathymetry rises until the point of nearest approach at about 18:35, and then deepens westward along this oblique crossing of the northwestern flank of the volcanic edifice. The entire north slope of Stromboli in this section exhibits downslope transport of sediment in almost straight channels 200 to 300 m wide (Fig. 36). Because of long linear scour marks in these sediment chutes, and boulder trains defining their margins, it is possible to discern a history of overlapping flows, which are diverted around the small scale local relief features. The local relief is about 5 m in general, but can be as much as 30 or 40 m for some ridges. The subbottom profiler displays finely stratified sediment with different types of events perhaps indicated by the different strengths and frequency characteristics of the reflectors. The reflectors can be seen to the depth at which the signal is too weak to be seen (up to 20 m), and suggest strata layered at a submetric level. The fine sediment from these chutes is carried out onto the basin floor where it accumulates as finely laminated deposits observed also on MAK line 23 to the west of the Stromboli Canyon.

The larger chute, which carries debris downslope from the area of caldera collapse on the northwest side of Stromboli, is observed between time marks 20:20 and 21:10; and the apron of coarse debris extends beyond there to perhaps 00:10, although this western edge is more difficult to define because of sediment drape. To the north, this area of debris probably continues into the section of MAK line 23 between 14:45 and about 16:45 or perhaps even 17:45 (see above). Large rounded blocks of volcanic rock are observed at the base of the slope and appear to decrease in size rapidly with distance out onto the basin floor. Some of the blocks appear to be as large as 60 m across, and there are some occurrences of blocks as large as 20 m across well out into the basin. Most of the blocks are draped in fine sediment, which probably decreases in thickness northwestward, eventually ponding behind and around volcanic outcrops. The outcrops of volcanic rock are more numerous and larger in the area towards the west; however, a number of individual volcanic hills are seen poking through the sediment cover even closer to Stromboli (e.g. at time mark 00:10), and what may be a buried volcanic ridge is seen at 22:55.

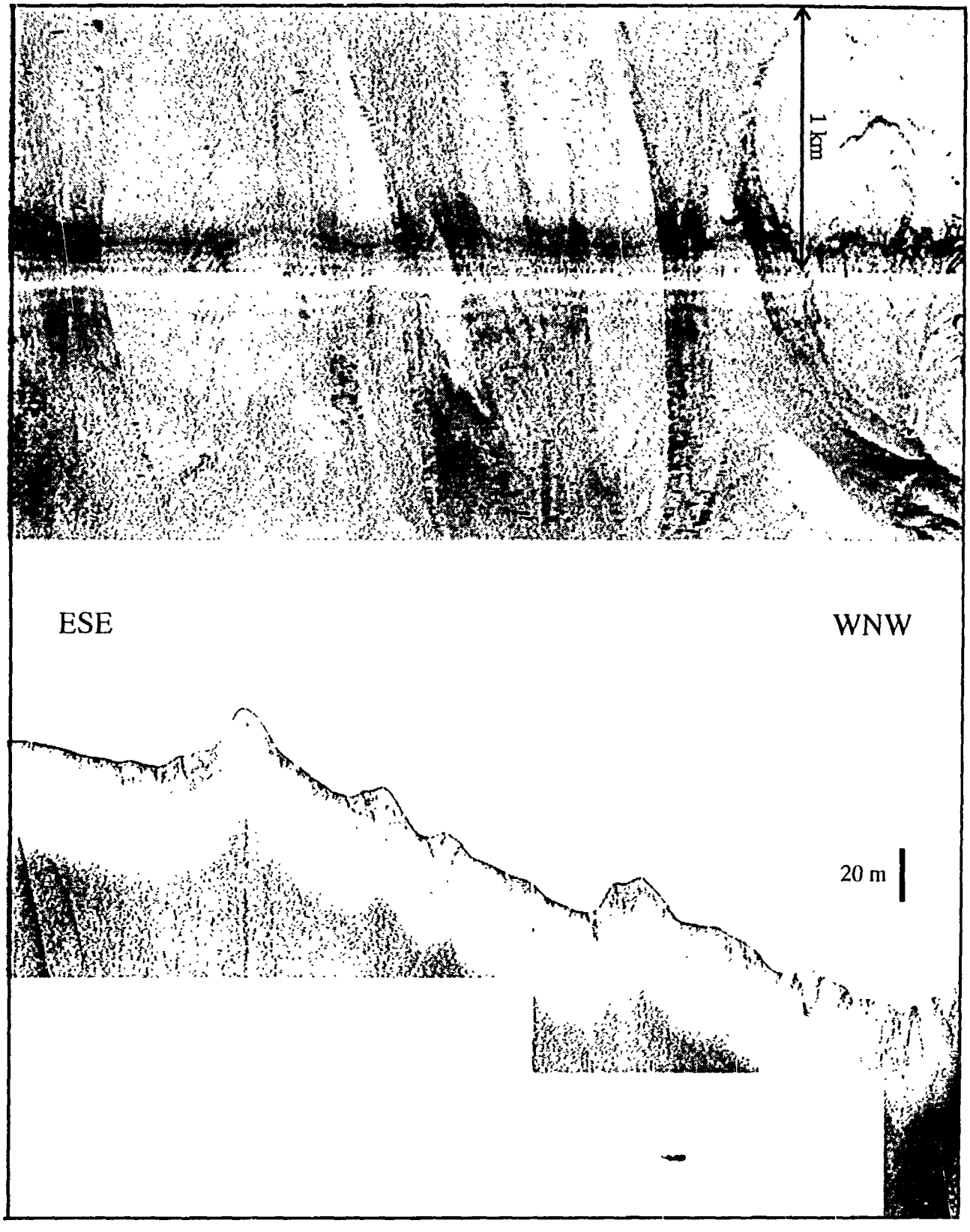

Fig. 36. Sediment transport from the northern Stromboli Volcano slope down into the Stromboli Canyon. MAK-1 line 25, sonograph

In the region between about 00:30 and 02:00, the sediment forms waves with a wavelength of about 200 m and an amplitude of around a metre. These sediment waves indicate a flow direction obliquely across the sidescan image towards the northwest. Highly reflective streaks emanating from patches of high backscatter could be coarser material (gravel trains) deposited up to several hundred metres from their sources.

In the vicinity of the outcropping volcanic rocks (between about 02:30 and 05:00) the sediment has higher backscatter in places. This could be either because the sediment is coarser, having been deposited near source, or because it is thinner, with the underlying volcanic rocks contributing to the backscatter.

Westwards of the volcanic outcrops is a section of dune-like sediment structures (Fig. 37). The sediment may be thicker here because of ponding to the south of the region of volcanic rocks to the north. These features have steep west-facing sides in comparison to the upslope eastern sides, and they have a vaguely convex downslope (westwards) shape in plan view. Relief of the sediment ridges is 10 to 30 m. In at least one location (between time marks 05:45 and 05:55), cross-bedding can be discerned in the upper sediments. The appearance on the sidescan record is of dunes, which are moving westward by deposition of sediment on the steep downslope flank. A long tongue of sediment extends westward from this area to about time mark 07:05. The line ends just where a channel cuts across the sediment lobe from the southeast. This channel has almost no relief but is a linear area of slightly higher backscatter, containing within it several arcuate scour marks, concave downslope, to the west.

MAK line 26

MAK line 26 targeted the eastern slopes of Marsili Seamount. A survey was run from the bathyal plain east of a faulted block, which rises about 200 m above the plain, onto the lower slopes on the northern tip of the main seamount. This NNW trending MAK line was extended, making a total of 18 hours, over the threshold between the eastern and western Marsili subbasins and on to the slopes mapped by OKEAN, which trend east-west from Palinuro Seamount.

The beginning of MAK line 26 (time 20:40-23:12) is characterized by a pattern of different sediment flows, which are probably the same as those observed near the end of line 23. Slump features near this pattern and the shape of the flows indicate that the direction of sediment transport is from east to west, which is in agreement with the direction of flows inferred from MAK line 23 situated 14 km toward east. Thus the whole area between the beginning of line 26 and the end of line 23 is covered by volcanic turbidites coming from the east. The few metres penetration of the subbottom profiler signal indicates these sediments may be coarse-grained. From sidescan sonar images and subbottom records further to the north, parts of these sediment flows are buried by finer material.

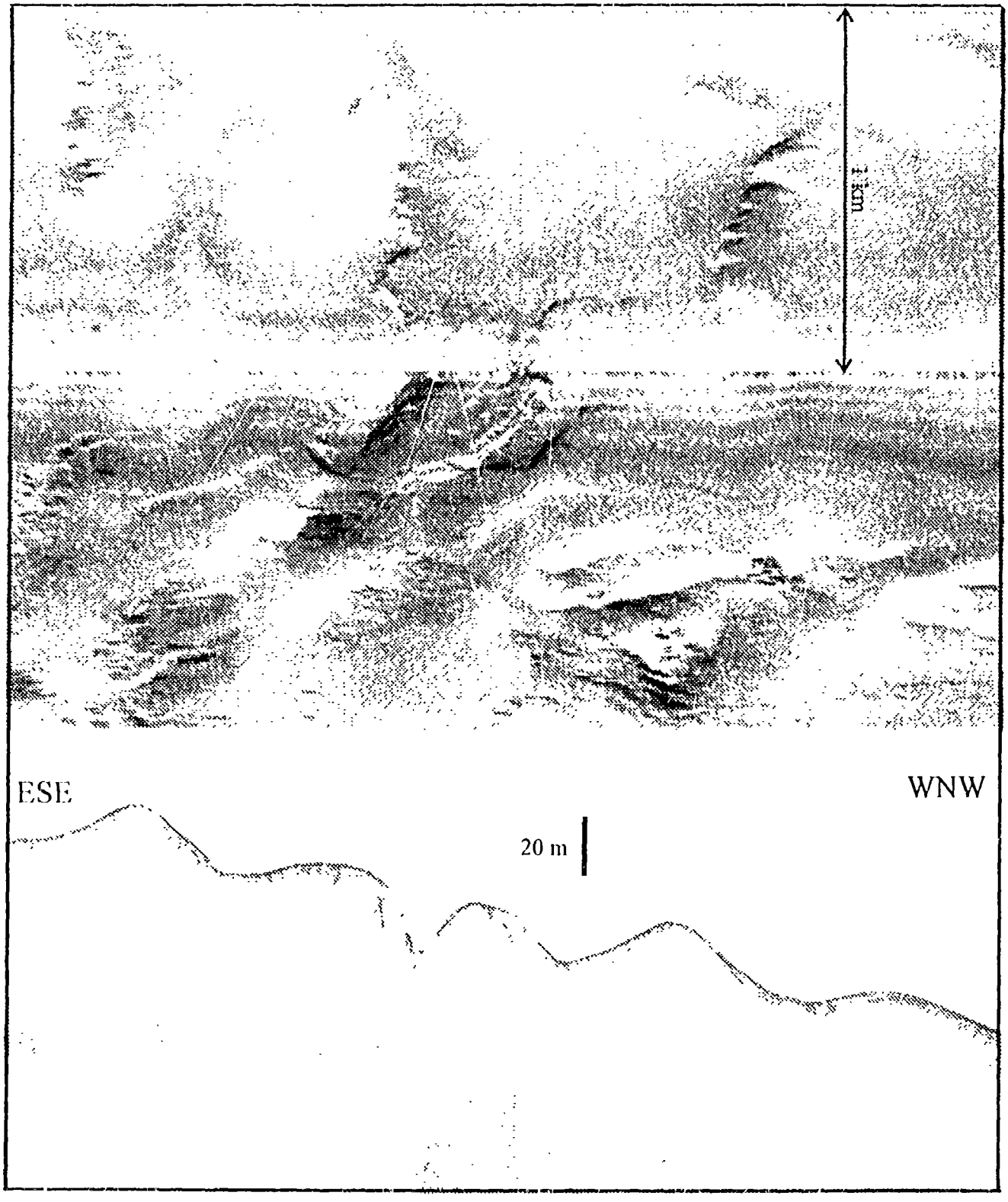

Fig. 37. Dune-like sediment ridges in the distal segment of the Stromboli Canyon. MAK-1 line 25, sonograph and profile

The relief of this area is smooth and the water depth decreases by about 25 m per 8 km along line to the north-northwest. Note that no sediment waves were observed here in comparison with the last (western) part of MAK line 23.

The section of line 26 between 23:12 and 01:18 displays a uniform, moderate backscatter intensity, and the penetration depth through the layered strata increases from 5 m in the south to about 20-m depth in the north. Thus it may be that the thickness of layered sediments slowly increases towards the seamount above a more impenetrable layer or that the facies is gradually changing in such a way that there is less attenuation of sound energy.

At time mark 01:18, the line crosses a scarp 107-m high and is oriented in a north-northeast to south-southwest direction. It appears as an elongated area of high reflectivity on the western side and as shadow on the eastern side of the sonograph due to the different direction of illumination. There is clear evidence of several slumps. One of the slumps, between time marks 01:30 and 01:52, is about 400 wide and extends about 700 m from the scarp.

The area between 01:50 and 03:05, where the relief and thickness of layered sediments is seen to increase, is characterized by a pattern similar to that of the region in front of the steep scarp. The pattern terminates against a local mound or ridge, which has a height of about 50 m and a width of about 600 m, crossed at time 03:18. To the northwest is the slope of a sediment-covered ridge about 350 m high. The ridge might be a talus cone at the base of the seamount or it might be volcanic material with a thinner drape of sediments which have moved downslope. Several parallel bands of slump structures lie along the flank in south-southwest to north-northeast direction. They form gentle steps in the flank about 600 m apart. The thicknesses of transparent-looking slump bodies vary from 15 to at least 30 m. In places, stratified sediments are observed beneath the slump bodies. Outcrops of coarse material exposed by slumping events on slopes are recorded as patches of relatively high backscatter intensity. In places, local debris flows are seen in association with the slumps. Where the slope becomes steeper to the north, the downslope movement looks more like talus shedding with fewer slumps.

Linear features with slightly different backscatter intensities than the surrounding slope are recorded on the sonograph between time marks 04:56 and 06:40 (Fig. 38). They are interpreted as surface sediment flows from west to east and spreading out in the same direction. A scour channel about 50-m deep and 1-km wide appears between time marks 05:45-06:06. The bottom of this channel is indicated by the apparent flow of coarse material (high backscatter intensity). Thin sheet-like slides of material into the channel are observed a little upslope, and a narrow (width about 70 m) linear channel, which crosses the MAK line at time 05:48, joins the larger channel just downslope. Coarse material estimated to lie at a depth of about 5 m, is exposed by slumps and moves downslope as talus as it is eroded back. The results of this process are displayed on the starboard (downslope) side of the sonograph as patches of high backscatter energy (time 05:58).

Another system of local small channels is separated from those just described by a feature with relief of about 65 m (time 06:00-06:28). It seems clear that the relief features control the local direction of slope sediment flow, as well as their dynamics. We can expect higher velocity of flow where the channel is narrower and steeper, and consequently more active erosion, scouring, and downslope sediment movement. Note that thickness of sediment layers is less in the channel than beyond it. A good example of a small channel, crossing the MAK line, occurs at 06:28 (Fig. 38). This channel is about 60 m wide and 10 m deep. Several other channels join it just above the well-defined 150-m wide slump scar at about 06:30.

The next part of the MAK line to the north (from 06:33 to 07:18) is characterized by moderate reflectivity and a layered sediment sequence with a thickness in the range from 10 m to 20 m. This is greater than on the previous part of the line. Several large sheet-like bodies appear to have slid downslope with the space around them having been filled by sediment and debris flows.

Across the northeastern rise of the seamount, the line crosses a region where outcropping lavas form a scarp made up of globular lava flows and highly reflective talus slopes (between times 07:18 and 11:00). The depth increases by 370 m from the ridge in the south to a small basin of ponded sediments at the foot of the lava flows. The sonograph and profiler show the volcanic lavas to be draped partially by more recent sediments derived in general from upslope. Different tongues of lava appear on the sidescan record with a large range of backscatter depending on the direction of illumination. The lava have flowed downslope to the east. The contact between volcanic rocks and sediments is smoother in plan view between 07:46 to 08:22 than between 08:22 to 09:02, because there is a higher influx of sediment from the south into this basin than from the west. There are several subparallel slump structures on the slope of a local depression (07:48-07:58), which is fill by sediments coming downslope.

A small basin about 2 to 3 km wide on this crossing, and lying between two large tongues of lava, was crossed in the time interval from 07:58 to 09:02. The subbottom profiler record shows a fine and well-stratified sequence of sediments with a total thickness at least 60 m. This is the greatest penetration by the subbottom profiler through layered strata obtained on this MAK line or any of the others described previously.

The basin is bounded to the northwest by outcrops of volcanic rocks with very rough relief, which may locally exceed 100 m. This part of the lava flows is characterized by lower backscatter intensity because of covering sediments. The topography of this area looks like a series of terraces created by different lava flows with ponded sediments on top. The level of backscatter across the terraces is uniformly low to intermediate except at their edges, where higher backscatter may result from outcropping lavas or from the steep slopes between terraces. The terraces are arcuate in plan view, suggesting that lava flows in a northeasterly

direction. On the profiler record, the height of each step is in the range 30-70 m and the width is about 800 m. The subbottom profiler indicates that there is a lower terrace in the sequence buried by about 20 m of sediment to the north. The lava disappears at depth on the subbottom profiler around time 11:22, and the thickness of sediment increases rapidly to over 30 m.

A region of moderate backscatter intensity characterizes an area between 11:22 and 13:05, where the morphology is a result of sediment movement through the channel north of Marsili, between the eastern and western Marsili subbasins. The features observed are narrow subparallel strips, a zone of mound-like structures, and elongated features corresponding to slumps. The linear strips lie in a northwest to southeast orientation and are locally associated with small ridges a few metres in height (especially between 11:55 and 12:?0). These strips are observed from 11:22 to 12:20 and are especially well-defined on the west part of the sonograph, appearing as alternating straight, light and dark strips, tens of metres apart and up to about 1 km long. They are also seen crossing the edge of a slump in the western part of the image. The profiler shows a finely layered sequence, about 20-25 m thick, overlain by a more transparent sequence with a variable thickness, averaging 10 m. The lower laminated sediments are eroded around time mark 12:15; and the resulting depression is filled with a structureless sequence, which may represent a debris flow or slump deposit. Folding in the lower sequence may be a result of sliding or may be caused by compression from a lava flow. Between 11:36 and 12:02 there is a transparent unit, on the profile, that is interpreted as a debris flow with a thickness of over 20 m.

The line ends on the northern flank of the channel. This flank is characterized by downslope movement of sediment into a broad channel seen on the bathymetric chart as coming in from the northeast. Several slump masses are seen on the slope between 12:20 and 13:00. In some cases the slides bring down layers of sediment, which are around 5 m thick and retain internal stratification, as shown by the subbottom profiler. Numerous small and large slump scars are visible upslope, to the west, and slide blocks are seen downslope to the east. At the base of a rather steep section of slope at 13:50 is a channel, which appears to be carrying coarser material and larger blocks.

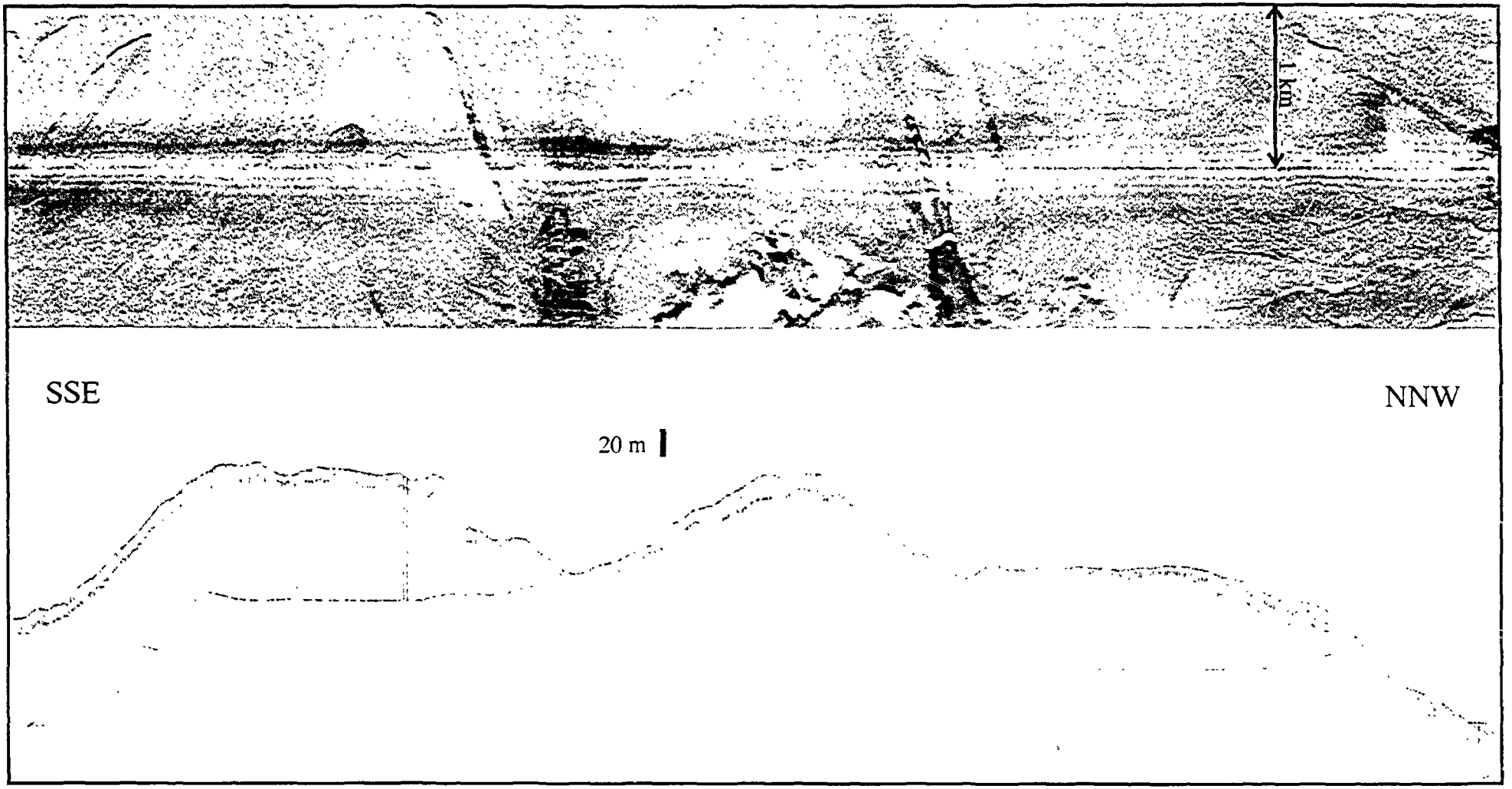

Fig. 38. Sediments flows and resultant scoured channel down the eastern slope of the Marsili Seamount. MAK-1 line 26, sonograph and profile

4. BOTTOM SAMPLING

a. GENERAL RATIONALE AND APPROACH

R.B. Kidd and R. Lucchi

The MAK and OKEAN sidescan surveys were used to select core sampling sites. We targeted areas where we hoped to calibrate the acoustic facies that we had interpreted from the sonographs. In addition to simple calibration, we selected sites in particular settings in order to understand sedimentary processes or stratigraphy, or for stratigraphic/paleoceanographic studies to look for changing conditions in the Tyrrhenian Sea through the Late Pleistocene glacial stages, trying to detect any onset of sapropelic deposition. For paleoceanographic studies, we needed cores from pelagic settings on slopes or seamount features. For studies of sedimentary processes involved in basin filling from canyons and slope areas, we needed cores in and around the major Stromboli Canyon and in Marsili Basin; also around the slopes of the Aeolian Islands and the central Marsili Seamount itself.

A special objective was to investigate the size and behaviour of turbidity currents in restricted basins, such as Marsili, and to study this we needed to core on small highs within the basin, on lower slopes around the basin, and on the outer and inner bends of the feeder Stromboli Canyon. Sometimes a chosen setting proved to be useful for pelagic stratigraphic objectives but not for studies of upslope turbidity current mechanisms, whilst sometimes the opposite proved to be true and there were thin turbidites in the section. In some cases slumping on the slopes negated either kind of study but provided groundtruth for our interpretations of slump scars from the sidescan records.

For this report we divided the coring sites into three study areas (Fig. 11):
(a) the Stromboli Canyon and the Calabrian slopes
(b) the slopes north of the Aeolian Islands
(c) the Marsili Basin and the surrounding basin floor

b. CORING OPERATIONS, TECHNIQUES, AND SUBSAMPLING

S. Wakefield, J. Herniman, A. Jones, G.G. Akhmanov, O. Duizendstra, and A.M. Akhmetzhanov

Two types of corers were utilized: a gravity corer and a modified Kasten corer. The gravity corer was 6.5 m long, 148 mm inner diameter and with a weight of about 1500 kg. Within the barrel, there was a plastic core liner, 6.1 m long and 137 mm inner diameter. Two Kasten core barrels were used, each of 15 cm x 15 cm cross section, one of 1 m length and the other of 4 m length.

Table 3 summarises the coring operations undertaken during the leg.

Table 3

Summary of coring operations on Leg 2 of the TTR-4 Cruise

Core no	Latitude Longitude	Date GMT	Corr. depth	Cable length Pull length	No of sections	Length, cm	Age	Setting
121G	38°56.7'N 15°30. 7'E	10.06 17:18	2069 m	2120 m	3+16 cm	203	*E. huxleyi* Acme	Embayment at bend in Stromboli Canyon
122G	39°00.9'N 14°44.5'E	13.06 10:20	3301 m	3412 m	-	pumice p	-	Basin plain ENE of Stromboli and NW of a small seamount. High backscatter, wavy pattern.
123G	39°00.4'N 14°48.8'E	13.06	3246 m 3330 m	3340 m	-	pumice p	-	Basin plain ca. 5 km of 122G. High backscatter, flat topography
124G	38°58.2'N 15°00.4'E	13.06 14:35	2872 m	2960 m	-	basalt p marl	*E. huxlyei* Acme	S of Stromboli Canyon and N of tributary. High backscatter, patchy pattern, blocky relief
125G	38°55.4'N 15°17.2'E	13.06 16:45	2401 m	2400 m	-	clay smear	*E. huxleyi* Acme	North of Stromboli at the S side of the canyon. Stratified sediments
126G	38°54.1'N 15°25.0'E	13.06 18:10	2210 m	2300 m 2290 m	9	510	*E. huxleyi*	Slump scar on the E flank of Stromboli Canyon bend
127G	39°10.3'N 14°08.4'E	14.06 12:29	3140 m	3240 m	6	372	*E. huxleui*	Small high WSW of Marsili Seamount on the W basin plain
128G	39°09.8'N 13°49.9'E	14.06 15.00	3332 m	3445 m	9	527.5	*E. huxleyi*	NE flank of Glauco Seamount SW of Marsili Seamount NE-dipping apron toward the basin plain
129G	39°07.2'N 13°47.1'E	14.06 16:53	2097 m	2200 m	8	491	*E. huxleyi*	W summit of Glauco Seamount
130K	39°00.6'N 14°45.9'E	16.06 10:58	3291 m	3360 m 3354 m	-	-	-	Eastern Marsili Basin plain. (C.f. 122G)
131K	39°00.4'N 14°48.8'E	16.06 12:31	3246 m	3310 m 3292 m	-	pumice p volc. s	*E. huxleyi*	Eastern Marsili Basin plain. (C.f. 123G)
132K	38°55.4'N 15°17. 3'E	16.06 16:07	2412 m	2480 m	-	lost	-	Stratified sediments S of Stromboli Canyon. (C.f. 125G)
133G	38°54.6'N 15°23.3'E	16.06 17:16	2387 m	2400 m	-	fine volc. s	-	Stromboli Canyon floor NE of Stromboli
134G	38°47.9'N 15°29.9'E	17.06 13:15	1402 m	- 1410 m	6	353.5	*E. huxleui*	SE end of MAK 24 line. Upper slope of a rounded hill E of Stromboli Canyon. Stratified sediments

Table 3. Continuation

Core no	Latitude Longitude	Date GMT	Corr. depth	Cable length Pull length	No of sections	Length, cm	Age	Setting
135G	38°48.8'N 15°29.0'E	17.06 14:22	1703 m	1720 m	8	489	*E. huxleyi* Acme	Smooth terrace on slope E of Stromboli Canyon, below a steep scarp. Stratified sediments
136K	39°09.0'N 14°29.4'E	18.06 13:35	3373 m	3470 m	-	391	*E. huxleyi*	Small high ESE of Marsili Seamount on the basin plain
137K	39°09.6'N 14°32. 6'E	18.06 16:17	3288 m	3441 m	-	138	*E. huxleyi* Acme	NE of 136K on the basin plain E of Marsili Seamount. Sloping toward NE

p=pebbles
s=sand

Gravity corers

Following the removal of the core liner from the barrel, the core was extracted by pushing the sediment up from the bottom. Sixty centimetre lengths of extruded sediment were cut and taken to the geological laboratory. Here the lengths were split vertically using a thin nylon line. The two halves of the core were separated and treated as follows:

- One half was photographed and described in detail. Smear slide samples were extracted at key horizons and analyzed on board. Further sampling for individual Moscow State University student projects was also carried out from this half of the core. When all subsampling had been completed, an entire quarter of the core was packed dry for return to Moscow State University.
- The second half of the core was used to provide an entire length of archive sample in 1 m lengths of 5 cm x 5 cm PVC trunking. These samples were stored cool on board ship before being transported in a refrigerated van to the University of Wales, Cardiff, where they will be stored in a temperature- controlled core repository. Further samples for individual projects, e.g. glass shard analysis, micropalaeontological studies, and grainsize evaluation, were also taken from this half.

Kasten sampling

Sediment was extruded from the core barrel using a procedure modified from that of Zangger and McCave (1990). The corer has an inner base plate, which can be raised to reveal the core (Fig. 39). The lid of the barrel was removed and a complete core length was revealed to be photographed and described. Two complete core lengths were taken using 1 m lengths of 5 cm x 5 cm PVC trunking, which provided archive samples for the Cardiff University core repository. Between these sections subsamples were extracted for individual projects. The base plate is raised to expose fresh core face, from which 33 cm x 15 cm slabs were taken for X-ray analysis. The remaining length of core was used for trunking samples for Moscow State University and Free University of Amsterdam. Further samples were then taken for individual projects as for the gravity corer.

c. CORES RECOVERED

R.B. Kidd, R. Lucchi, E.M. Ivanova, and A.A. Lototskaya

Nine cores were recovered on Leg 2 in 17 attempts. The lack of core recovery at 8 sites is not entirely a loss since they had been selected to calibrate acoustic facies on the MAK records, and in most some sample was obtained in the core catcher, providing indications of pumiceous sands and gravels that were unrecoverable by any of the methods that we had available to us aboard ship. The cores that were recovered are summarised in Fig. 40. They include 7 gravity and 2 Kasten cores with a range of lengths from 1.38 m to 5.27 m. All were split,

described, and photographed aboard ship. Microscope analyses were carried out for sedimentology (smear slides and sand residues) and for biostratigraphy (foraminifera and nannofossils).

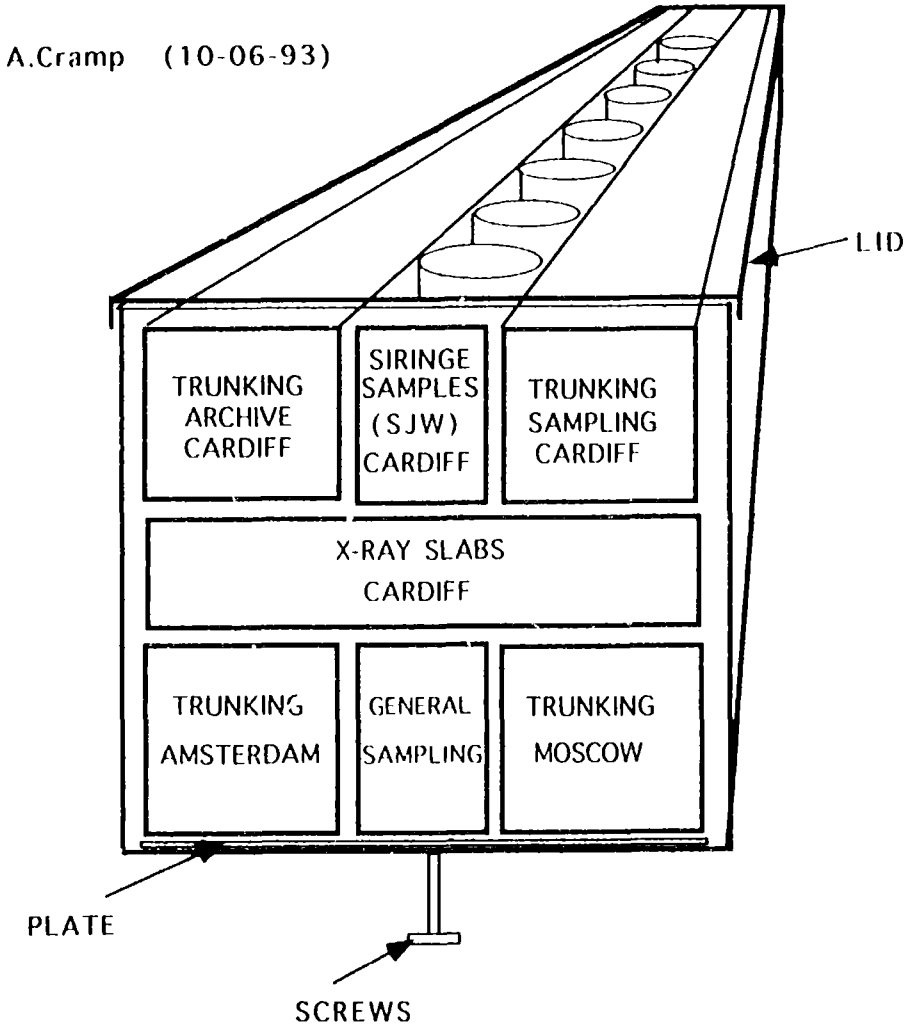

Fig. 39. Subsampling procedure from Kasten core samples

Most of the cores reach the Late Pleistocene. The oldest sediments recovered were in the largely pelagic core 128G which, at a subbottom depth of over 5 m, is around 100 ka old (see Biostratigraphy report). The individual core logs and stratigraphy are included here as Figs. 41 to 49.

TTR 4 Leg 2 Tyrrhenian Sea

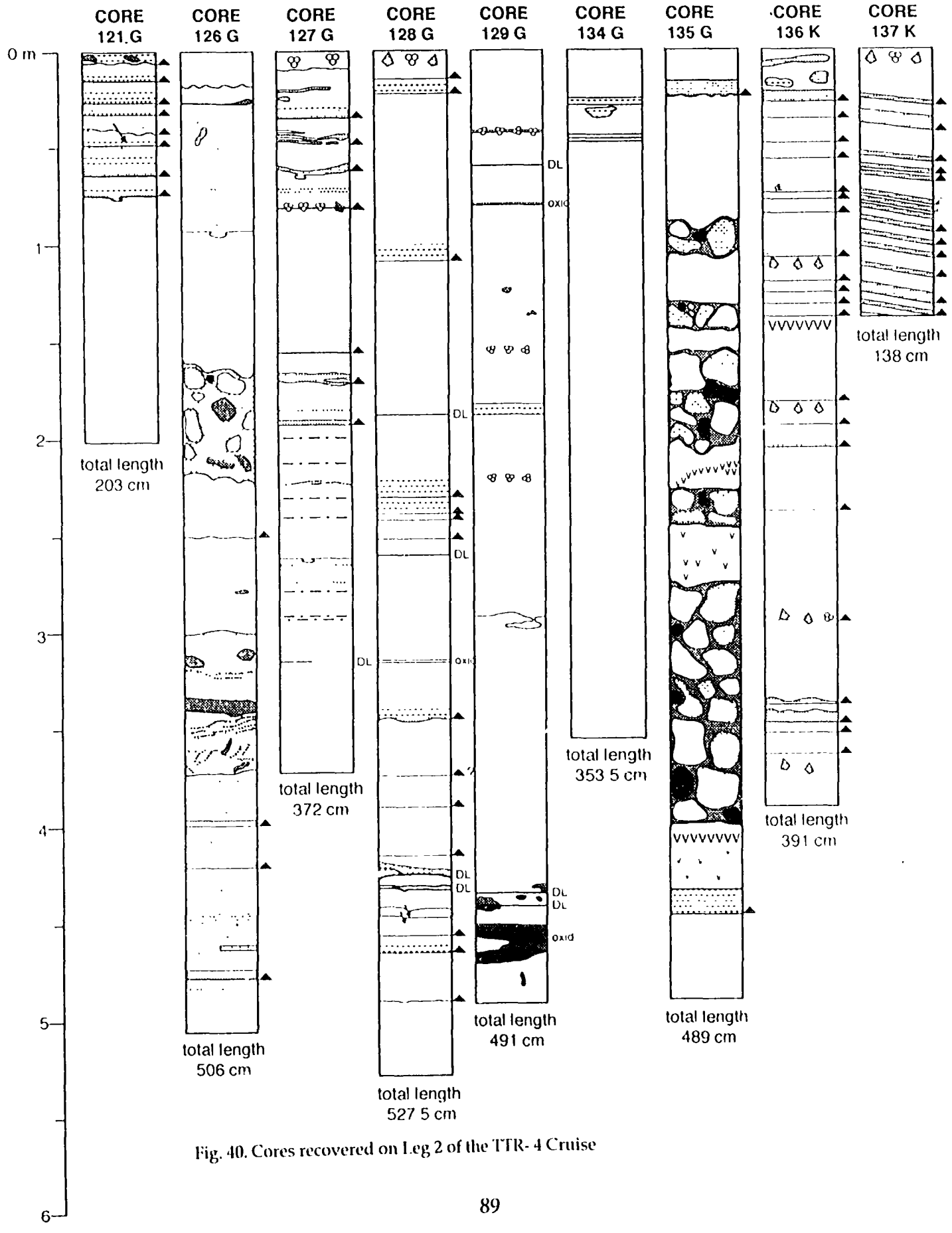

Fig. 40. Cores recovered on Leg 2 of the TTR- 4 Cruise

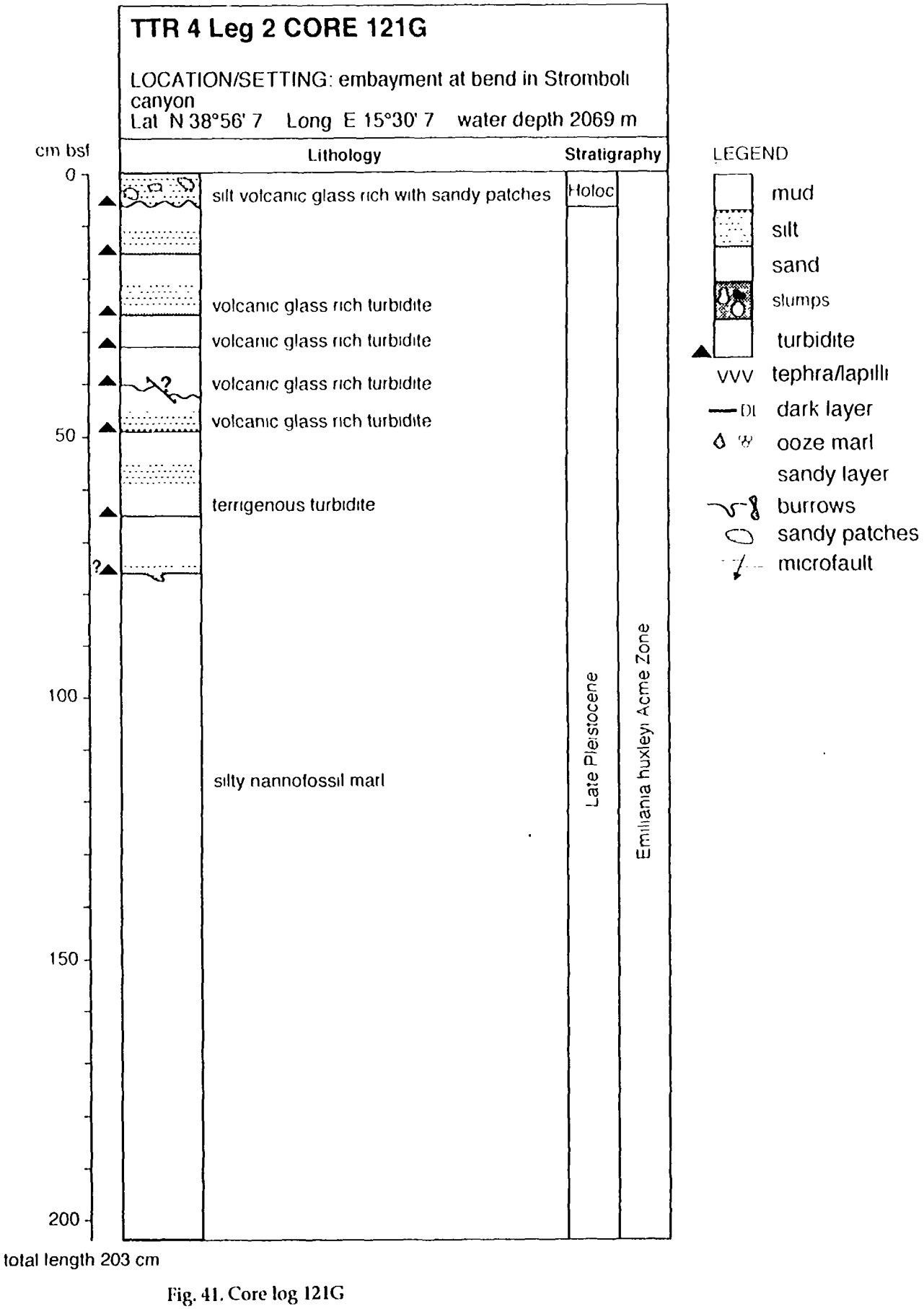

Fig. 41. Core log 121G

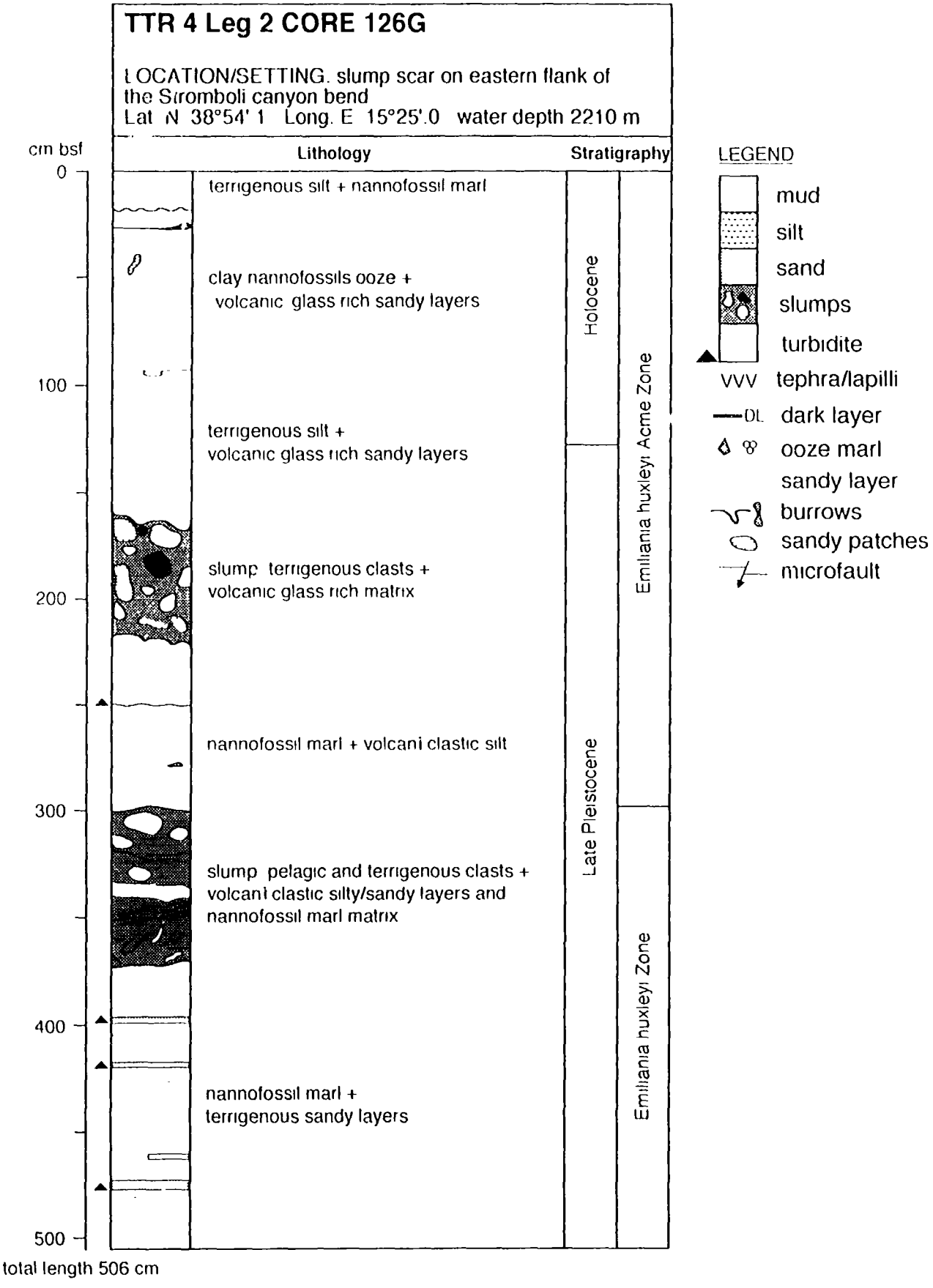

Fig. 42. Core log 126G

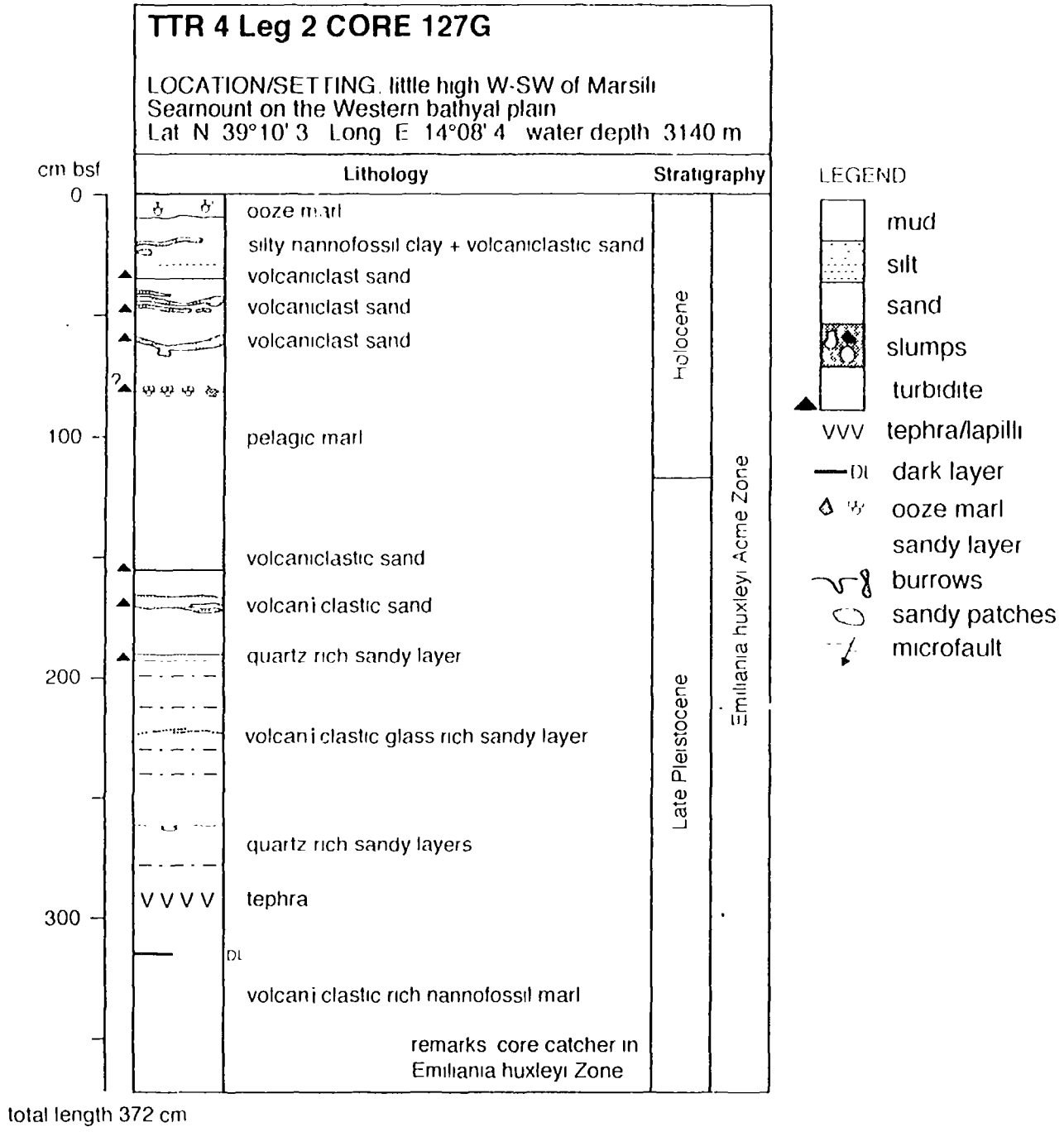

Fig. 43. Core log 127G

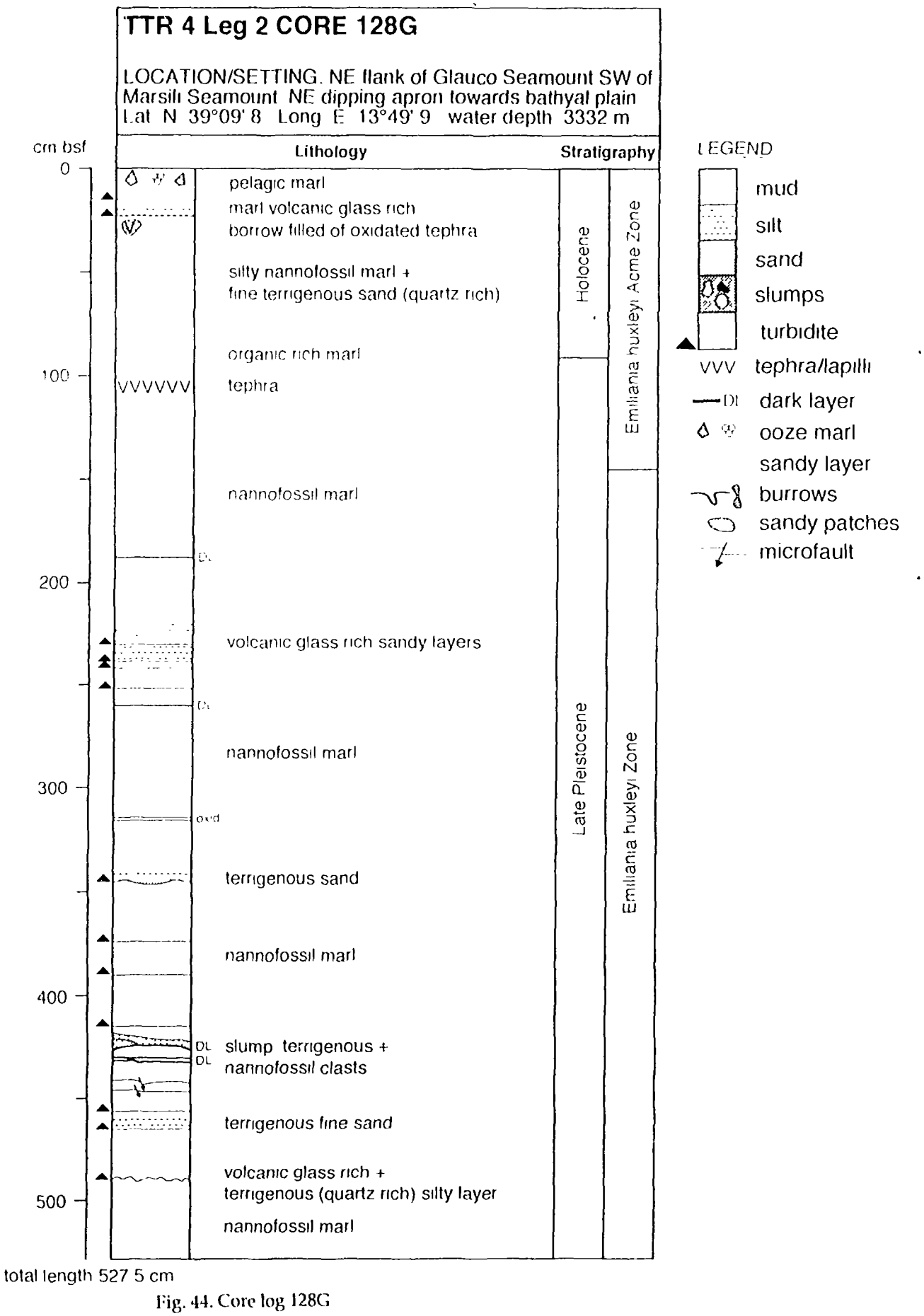

Fig. 44. Core log 128G

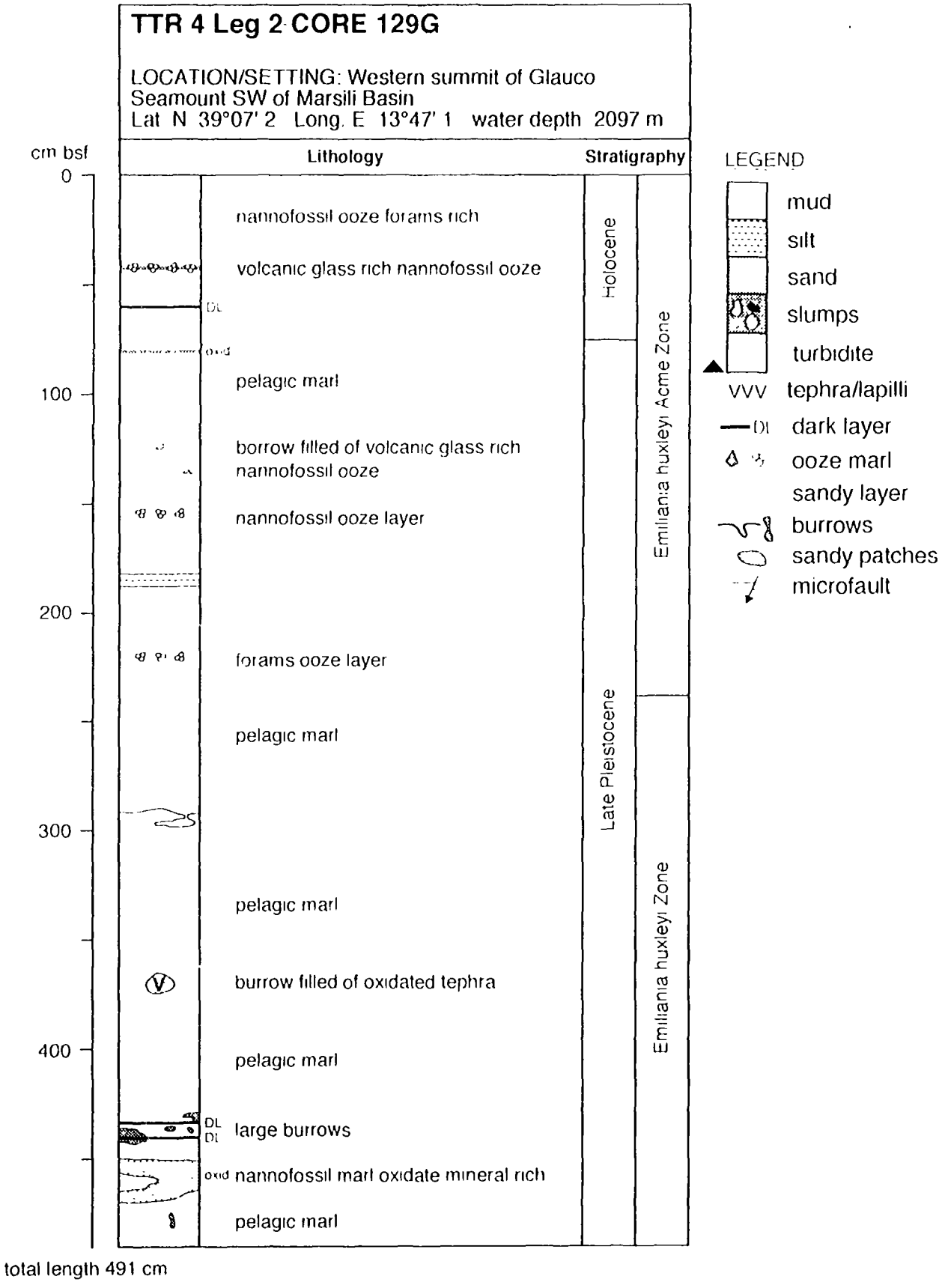

Fig. 45. Core log 129G

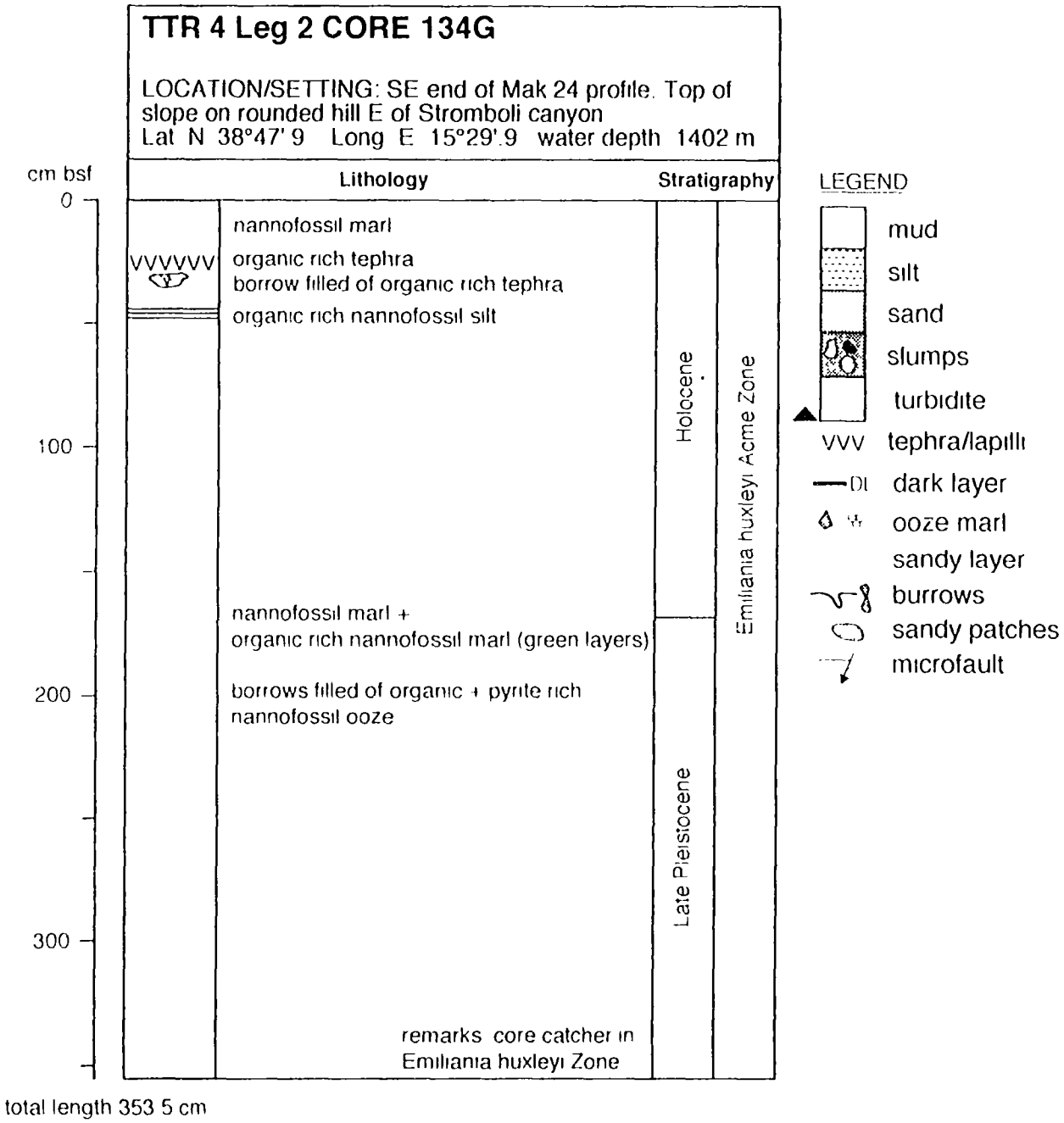

Fig. 46. Core log 134G

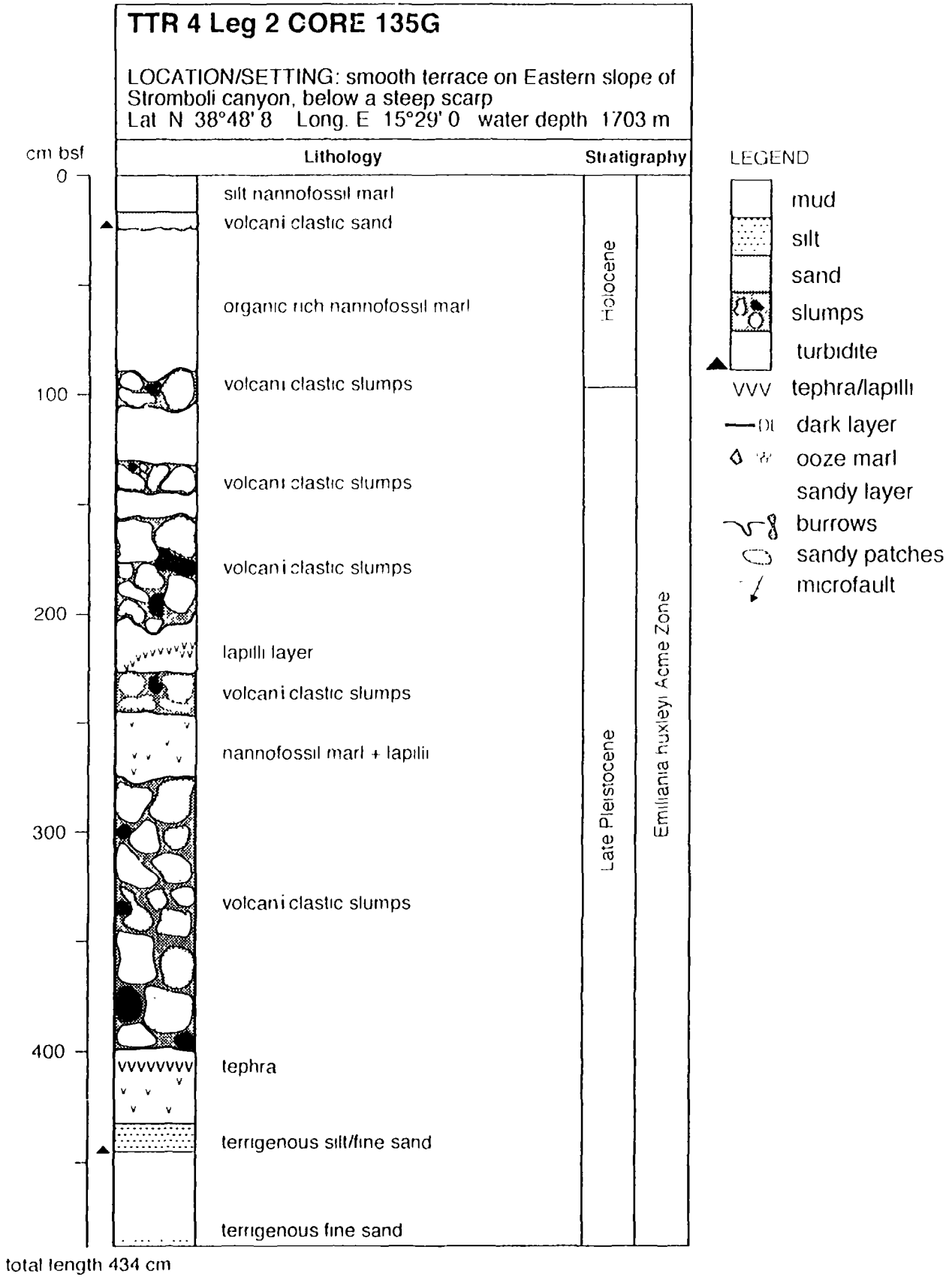

Fig. 47. Core log 135G

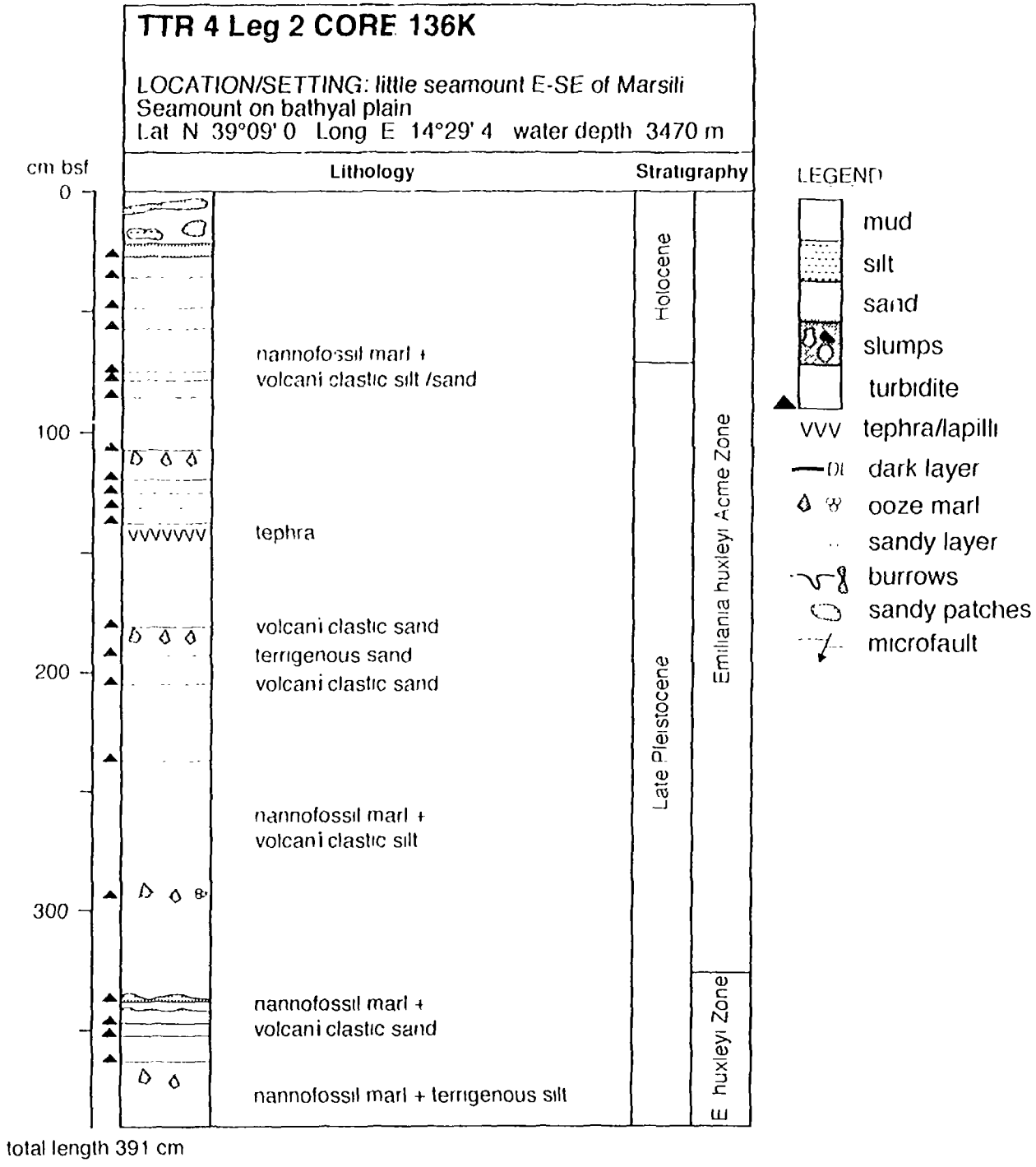

Fig. 48. Core log 136K

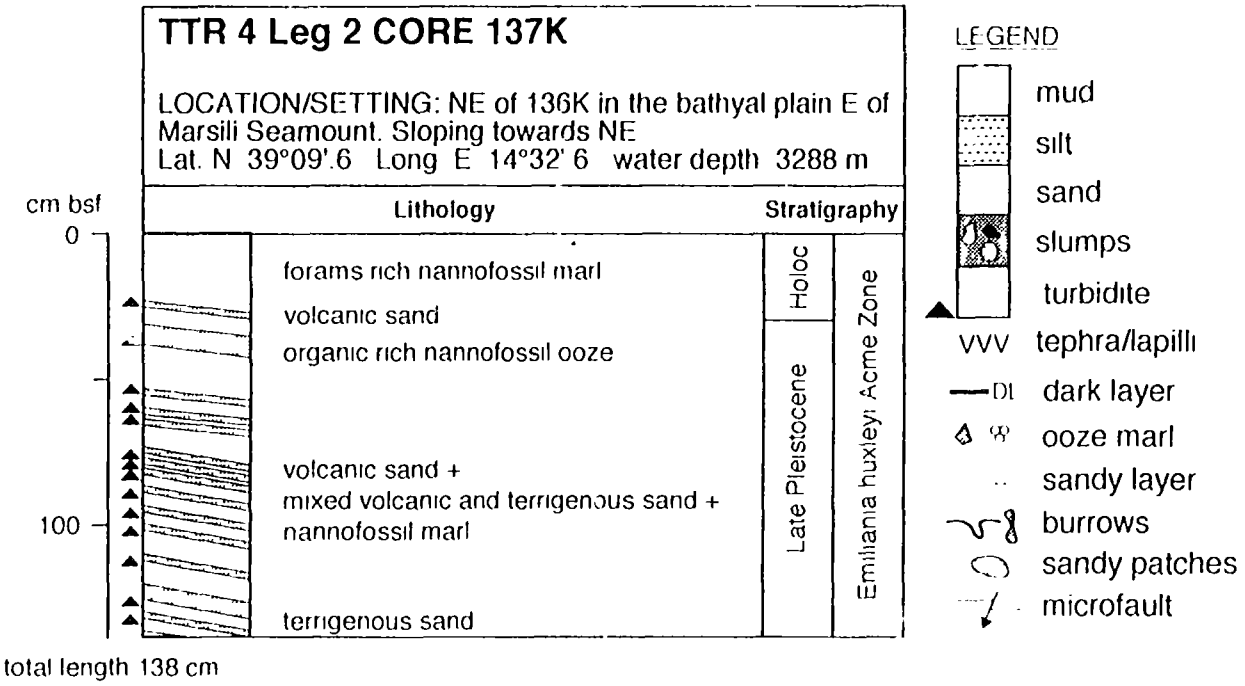

Fig. 49. Core log 137K

Stromboli Canyon and nearby slopes

In this area we took cores on the slopes to the north and west of Stromboli Canyon that have a strong signature of gravitational mass movement on the MAK records. The slope cores here (121G, 126G, 134G, and 135G) contain up to 2-m thick slumped intervals, interpreted as debris flows; thin graded beds, interpreted as turbidity current deposits (turbidites); and tephras from volcanic ashfall. The turbidites are of two types: the majority are volcaniclastic but a minority are largely terrigenous, containing minerals from metamorphic terrains. Both contain shallow-water shell debris and benthic foraminifera. We interpret these as turbidites, which have been deposited from flows that have "overbanked" from Stromboli or its tributary canyons.

We failed to recover any core from either the Stromboli Canyon floor (133G) or from the stratified area that one might consider as the Canyon's inner bend overbank area (132K). The scouring and evidence of outcrop and gravel trains in the canyon floor itself makes it unsurprising that we had no recovery there, but on the stratified inner "overbank" we suggest there is a stronger link to the Stromboli northern slope (see later).

Slopes of the Aeolian Islands

We recovered no cores along the MAK 23 line run along foot of the slope north of Stromboli Island and the Aeolian slopes to the west. In each case we suspect that very coarse pyroclastic material has made it impossible for the corers

to penetrate; indeed, most did collect small amounts of pumice fragments in the core catcher. The above-mentioned "stratified area" lies downslope from the Stromboli slope area designated as "chutes" in the MAK interpretations, and we conclude that core stations 132K and 125G were over this kind of pyroclastic talus. At the western end of this transect at station 124K we were apparently over the downslope equivalent of the Sciara del Fuoco collapse feature (Romagnoli et al., 1993: see Section II.3.b). Further west we again failed to collect core at station 123G, which is in the area that we now recognize as containing significant amounts of outcrop as a circular caldera-like feature with possibly the even more distal effects of the last Stromboli collapse draped thinly over parts of it.

Marsili Seamount and Basin

We attempted sampling in both sectors of Marsili Basin, on either side of the central seamount edifice. No core was obtained in two attempts (122G and 130K) in the southern deepest parts of the eastern sector, where sonographs show flow-like highly backscattering lobes that are presumably the downslope input from canyon systems. Two cores were obtained on fault blocks, flanking the main feature, that rise some 150 m or so above the basin plain, one in the eastern subbasin (136G and 137G) and the other in the western subbasin (127G). Both contain many thin graded units that are interpreted as turbidites that have been obviously deposited upslope of the surrounding plain. To the extreme southwest, Marsili Basin is limited by Glauco Seamount, and here we attempted to obtain our most pelagic cores. The longest record is in core 128G from the foot of the seamount slope, but this again contains a large number of thin turbidite units. Dark organic-rich layers at around 4.5 m in this and the near summit core 129G may be related to sapropelic events, but this observation must be followed up by shore-based analyses.

Biostratigraphy

Biostratigraphy of 9 cores was defined on the basis of foraminifera and calcareous nannofossil semiquantitative analyses. The Late Quaternary climatic fluctuations determined by changes in foraminifera assemblages were interrelated to the standard calcareous nannofossil zonation and used for biostratigraphic subdivision of the cores (Figs. 41 to 49). Samples for foraminifera were taken from different lithological units, washed over 63 μm sieve, dried and studied with binocular microscope (magnification x25 and x50). Calcareous nannofossils were studied in smear slides with the OLYMPUS polarizing microscope (magnification x1000).

Three main types of surface paleowater conditions were identified by the dominance of different planktonic foraminifera assemblages:

(1) Warm surface waters. The assemblage is dominated by *Globigerinoides ruber, Gs. sacculifer, Globigerinella aequelateralis,* and *Orbulina universa.*

(2) Temperate surface waters. The assemblage is dominated by *Globorotalia inflata, Gl. truncatulinoides, O. universa,* and *Globigerina bulloides.*

(3) Cool surface waters. The assemblage is dominated by *Neogloboquadrina pachyderma, Turborotalia quinqueloba, Globigerinita glutinata, G. bulloides,* and *Globorotalia scitula.*

The Holocene (last 10 ka) is presented in all of the cores. The sediments of this age contain warm water planktonic foraminifera and calcareous nannofossil assemblages with high faunal and floral diversity. *Gephyrocapsa oceanica, G. caribbeanica, Florisphaera profunda, Umbellosphaera tenuis, U. irregularis, Rabdosphaera clavigera, Umbilicosphaera sibogae,* and *Scapholithus fossilis* are typical for the Holocene calcareous nannofossil assemblage.

The lower part of the Holocene is characterized by the temperate water planktonic foraminifera assemblage and mainly by *Gl. inflata*. The transition from the Late Pleistocene to the Holocene was identified by the change from the cool water assemblage, typical of the Late Pleistocene glacial time, to the temperate one. P/B ratio (planktonic/benthic foraminifera) is normally higher in the Late Pleistocene sediments. Higher diversity of benthos reflects the shallowing of the basin during the glaciation. The Late Pleistocene calcareous nannofossil assemblage is rich in cool water species *Gephyrocapsa muellerae.*

The Holocene/Pleistocene boundary occurs in the cores at 80 to 160 cm from the top except for 121G and 137K where the uppermost part of the unit probably was washed out. Thus, the sediment accumulation rates for the Holocene in the area vary from 8 to 16 cm/ka. None of the sediments from the investigated cores extends below the *Emiliania huxleyi* Zone. Although, 5 of 9 cores bottom within the *Emiliania huxleyi* Acme Zone, the others do not reach this level. The predominance of *Emiliania huxleyi* in the whole coccolith assemblage is considered to mark the boundary between these two zones, which is dated as 70 ka for the Western Mediterranean (Rio et al., 1990).

The longest sediment record was found in core 128G. From the interpolation of foraminifera and calcareous nannofossil data, the base of the core was dated as about 100 ka. The whole residue greater than 63 μm was checked for reworked shallow-water material (benthic foraminifera, bivalves, etc.) to identify the origin of the sediments (for example, definition of turbidites and tephra layers) and the activity of the slope processes in the area.

A small amount of reworked Miocene-Pliocene calcareous nannofossils was found in all cores. Cores 126G and 135G from the Stromboli Canyon area have the largest content of the reworked species.

5. CONCLUSIONS

A.F. Limonov and R.B. Kidd

1. The Stromboli Canyon and its major tributaries are tectonically controlled features bounded over a considerable distance by normal faults related to the general extensional stress characterizing the Marsili Basin area. The second controlling factor is the presence of volcanic mountains which cause the canyon to change its course.

2. The data obtained show that mass wasting processes are currently very active in the Marsili Basin area. We found evidence for them everywhere on slopes of the basin. They vary in scale, from frequent gravitational folds on steep slopes and small slumps and debris flows on localized scarps, to large blocks, which have slid downslope for a distance of some hundreds of metres, and extensive turbidity currents acting in the canyon.

3. Downslope mass transport presumably started from the very beginning of the basin formation, and this was enhanced in periods of the increased basin subsidence. This subsidence was irregular and discontinuous. The disconformities observed in the sequence may be conditioned by both this irregular subsidence and sea-level fluctuations. The further task of the research is to distinguish the influence of tectonics from sea-level fluctuations on the basin infill architecture.

4. The alternation of rather thick seismically transparent or semitransparent units (debris flows) and stratified units (turbidites and hemipelagites) in the sequence suggests that different kinds of mass transport acted at different times during the basin evolution.

5. The bottom of the Stromboli Canyon is characterized predominantly by active erosion. Sediment deposition takes place only in sedimentary traps, such as, behind morphological highs and in the inner bends of the channel. However, this deposition is rather unstable and bears the traces of sediment reworking.

6. The expedition was an extremely successful coring exercise. We have around 35 m of well-described and archived sample material along with numerous discrete samples that will be analyzed using more sophisticated laboratory techniques at our respective institutions over the next year. Despite a relatively large number of "nil recoveries", we have successfully calibrated all of the main acoustic facies on the MAK-1 records, to provide real "ground-truthing". We have learned much already of the ability of the huge turbidity current events that scour Stromboli Canyon, as well as others in the area, to travel upslope and variously interact with topography.

7. A preliminary mineralogical study has shown that volcanic mountains of the Aeolian Arc are the principal sedimentary supply. Volcaniclastic sediments clearly dominate the transported material. Mass movements are observed on both the Stromboli and Marsili slopes on MAK-1 sonographs.

8. We have possible indications of Late Pleistocene reducing conditions in the Tyrrhenian Sea. The shore-based analyses should yield much new information to this study.

9. The reverse faults and inverted basins observed on seismic sections in the Vavilov Basin are evidence for Pleistocene compressional tectonic events. They may be related to transpression due to strike-slip movements there.

III. STUDY AREA 3 (ALGERO-PROVENCAL BASIN)

1. GENERAL SETTING

a. CORSO-LIGURIAN BASIN (AREA 3a)

N.H. Kenyon

Turbidites and related deposits, that is deposits of mass wasting and interbedded pelagic/hemipelagic material, have the greatest volume of any types of sediment in basin fills. Much of the work on modern turbidite systems has been on the very large deep-sea fans, such as, the Mississippi and Amazon Fans. These are characterized by, among other things, single shelf edge canyons, highly sinuous distributary channel-levee systems, and relatively low overall gradients. However, these are not common types of turbidite systems, and there are only two of them in the Mediterranean, the Nile and the Rhone Fans. On the other hand, there are hundreds of simple canyon-fed systems, which are characterized by short and relatively straight channels, with poor or no development of levees and by relatively steep maximum canyon axis gradients. These low-input systems are likely to have a higher proportion of sands than the large high-input systems. These lower-input types should also be the norm in ancient turbidite systems. Thus, it is important to study examples of this neglected type of turbidite systems, such as, those fed by canyons to the basin west of Corsica and Sardinia. Channelised turbidite systems are believed to have predominantly sandy deposits beyond the channel mouth. However, sandy channel mouth lobes are little studied because they are difficult to identify from profiles, being fairly flat, and because it is difficult to recover coarse clastics with conventional corers.

Provence and Corsica-Sardinia are continental blocks that rifted apart in the late Aquitanian-early Burdigalian (Burroz, 1984). The western part of the rifted basin is filled with sediments from the Rhone drainage basin. To the east, there is presently a wide trough, called the Corso-Ligurian Basin on the charts of the International Hydrographic Bureau (IOC-UNESCO, 1981), that is downslope of the distal Var turbidite system and of some other systems that come from the slope of southern France and from the Corsican margin. The trough floor slopes gently and gradually down to the south. It is characterized on unpublished surface-towed 3.5 kHz profiles, that were available to us, by discontinuous subbottom layers. Eventually the sloping discontinuous layers give way to the flat and more continuous layers of the Balearic (Algero-Provencal) Basin plain, just west of the northernmost point of Sardinia. Some authors have placed the basin plain a long way north of where we find it. The basin floor is bounded on the west by the gentle slopes of the inactive eastern Rhone Fan and bounded on the east by the steep canyoned slopes of Corsica and Sardinia.

The west Corsican canyons have been commented on for many years. They are very steep and head in close to the mountainous coast. Many of them are a submarine extension of the steep valleys seen on land, and because of this

and the resistant rocks, that they were cut into, it was proposed that they must be formed subaerially. The idea of margin flexure was proposed to account for this (Bourcart, 1959). The drying out of the basin during the Messinian could account for some of the deep erosion into hard rocks. The canyons are tributary systems, which have some development of levees, near the base of the slope and preferentially on the northern (right hand) side (Bellaiche, 1993). A GLORIA long-range sidescan sonar survey was undertaken in this area in 1983 for ELF Aquitaine Plc. This survey was used as a basis for planning our work in the Corso-Ligurian Basin. It showed that the canyon floors have a high level of acoustic backscatter, whereas the canyon walls have a relatively low level of backscatter. It also showed that the latest deposits of the basin floor onlap the Rhone Fan deposits and must therefore be a younger depocentre.

On the distal floor of the trough, there is a pattern of regular bedforms on the sonographs, similar to some that have been seen previously on the sandy lobes of the Orinoco Fan (Belderson et al., 1984) and on the Umnak turbidite system in the Bering Sea Basin (Kenyon and Millington, 1995). They have been called *braid-like bars*, but the real process that formed them, and even their composition, is unknown. Because of their relationship to areas beyond channels and because of their acoustic character we expected to find that there are deposits of coarse clastics, with a facies that is characteristic of sandy lobes. Such sediments could come from sources upslope, including canyons and the intervening slopes, but not from the Rhone Fan which has been inactive on its eastern side since the emplacement of the slide deposits, mapped as the eastern transparent facies (Droz and Bellaiche, 1985a).

b. DISTAL RHONE FAN AND VALENCIA CHANNEL (AREA 3b)

A.F. Limonov and N.H. Kenyon

The distal parts of deep-sea depositional systems, for example, channel-mouth and channel-lobe transitional zones are still poorly understood, in contrast to other elements of the systems, such as, valleys and channel-levee deposits. These distal parts generally have a very monotonous morphology when considered as a whole (Nelson and Nilson, 1974; Mutti, 1977; Nelson et al., 1978). However, modern high resolution exploration methods, including high resolution seismics and short-range deep-towed sidescans, show very complex morphological and sedimentological patterns in these elements. Normally, sandy lobes show poor subbottom penetration on profiler records. A channel-lobe transitional zone is characterized by both depositional and erosional features, but erosion usually predominates due to the action of turbidity currents probably undergoing a hydraulic jump at this place (Mutti and Normark, 1991). Traces of a hydraulic jump in the form of differently sized scours were recorded by the MAK-1 system downslope of the Rhone Neofan valley in 1992 during the TTR-2 Cruise (Limonov et al., 1993).

The upper and middle Rhone Fan has been studied in some detail and its principal features are fairly well-known (Bellaiche et al., 1981; Bellaiche et al., 1984, 1986; Droz and Bellaiche, 1985a; Alonso et al., 1991; Droz, 1991; Limonov et al., 1993; Bellaiche, 1993; and others). Like most of the large turbidite systems in the Western Mediterranean, the Rhone Cone came into existence during the Messinian sea-level fall, but the history of Messinian and Plio-Quaternary fans is not well understood. The post-Messinian Rhone Fan covers most of the Gulf of Lions rise, extending from the lower continental slope to the Balearic abyssal plain. The fan was principally fed by Alpine-derived sedimentary material carried to the sea by the Rhone River. During the Pliocene, the fan was supplied with sediments through most of the canyons along the neighbouring margin. This has led to accumulation of numerous turbiditic bodies which partially overlap each other. Since the Pleistocene, this clastic material is funnelled to the fan via the Petit-Rhone Canyon. As a result, the Quaternary megasequence of the fan shifted laterally westward, and there was a longitudinal basinward progradation of depocentres (Droz, 1991). The Quaternary megasequence consists of three main channel-levee complexes, which include several stacked turbiditic units. Numerous bodies with chaotic seismic reflection configurations on high resolution seismic records or transparent acoustic facies on the MAK-1 records, as well as gravitational folds indicate sediment instability on the continental slope (Limonov et al., 1993).

A characteristic feature of the Rhone Fan is the development of the neofan at the recent stage of evolution. The neofan is a small sedimentary body, a sandy lobe, of the newly avulsed channel on the western Rhone Fan. The feeder channel appears as a very dynamic system with ongoing downslope migration (Limonov et al., 1993). The neofan body is represented by a bedded seismic facies about 30-40 ms thick. The distal part of the Rhone Fan is still poorly studied. This area was partially covered by an OKEAN mosaic and two seismic lines during the TTR-3 Cruise. This is a region of very low relief, but with alternating bands of high and low backscatter on the OKEAN sonographs. These bands are oriented approximately along the bathymetric contours and could be either low seafloor undulations or areas with contrasting sediment composition (Limonov et al., 1993).

The Valencia Valley has also been intensively investigated, chiefly by Spanish and American scientists (Palanques and Maldonado, 1983, 1985; Maldonado et al., 1985 a, 1985 b; Alonso et al., 1991; Palanques et al., 1994, and others). The area beyond the Valencia Valley has been called the Valencia Fan. Data from the TTR-3 Cruise (Limonov et al., 1993) have shown that there is currently erosion in the region referred to as "the middle Valencia Fan" (Maldonado, 1985a, b). This means that, in reality, the deposits of coarse sediments of Valencia Fan should be situated further southeast, in an area of the Balearic Basin plain. This area has been partially investigated only recently (Palanques et al., 1994).

The area beyond the Valencia Valley is supplied with sediments through a complex system of canyons incised into the Iberian margin and also from the Rhone Fan via the neofan channel. The Valencia Valley runs from the deepest axial part of the Valencia Trough toward the Balearic Abyssal Plain for a distance of about 400 km. It also originated during the Messinian time (Palanques and Maldonado, 1983; Alonso et al., 1990). The corresponding paleo-fan is suggested to be located near the north termination of the Valencia Trough, whereas the buried Pliocene Valencia Fan is situated presumably near the northern Balearic margin (Limonov et al., 1993). The Valencia Valley is fringed by well-expressed levees, and its lower sector is interrupted by three volcanic outcrops causing the valley to branch into two, which go around opposite sides of the outcrops. The lowermost reaches of the valley are characterized by very low relief, and the valley itself is seen as an extremely shallow feature (about 10-15 m) with a width of about 7-8 km.

2. SEISMIC PROFILING

a. CORSO-LIGURIAN BASIN

A.F. Limonov and J.M. Woodside

Two seismic lines were completed in the area west of the Corsica-Sardinia block, along the eastern continental margin of the Algero-Provencal Basin. Both lines ran parallel to each other in a SSW-NNE direction, spaced at about 11 km apart in order to provide overlapping OKEAN swaths (Fig. 50). Their total length is 230 km.

The first line, PS-146, was shot close to the Corsica/Sardinia continental margin, and line PS-147 is situated seaward of it. The seismic pattern is rather similar for both lines and they will be described together on a comparative basis. Structurally, the lines cover two different domains: the Corsica-Sardinia margin domain (20:50-23:30 on line PS-146 and 20:00-02:35 on line PS-147) and the Ligurian-Provencal Basin plain domain. In terms of acoustic pattern, the recorded sections along the two lines are divided into four seismic members. These are, from bottom to top (Fig. 51): a chaotically layered member, without any coherent, continuous reflections; a member with high amplitude, usually low frequency reflectors, which are normally discontinuous and curved, sometimes forming chaotic reflection configuration; an acoustically transparent (or semitransparent) member; and the uppermost member, which has moderately strong, high frequency, parallel and continuous reflectors.

The lower member is represented probably by late post-Variscan sedimentary and magmatic rocks exposed on Corsica (Bigi et al., 1992). They can be traced within the Corsica/Sardinia margin domain for a limited distance, and probably form a large uplifted block bounded by faults on line PS-146 (22:50-23:30), which changes into structural terrace on line PS-147 (20:30-21:30).

The overlying member within the Corsica/Sardinia margin domain seems to be represented by younger deposits up to shallow-marine Messinian facies. Its maximum thickness reaches about 500-600 ms. The member is intensively deformed, particularly on line PS-146, where it is cut by numerous faults. At least four slightly unconformable units are seen in this member. The member outcrops at the confluence of Ajaccio, Valinco and Moines Canyons, where Upper Oligocene-Lower Burdigalian and Messinian deposits were recovered (Bigi et al., 1992) almost exactly at the place where line PS-146 is positioned.

The third member can be dated as Pliocene on the basis of its stratigraphic position and seismic character. It spreads through both domains and directly overlies the Messinian surface in the Ligurian-Provencal domain. The transparent appearance of this member could be explained by its rather uniform, presumably mainly marly composition. The thickness of this member averages

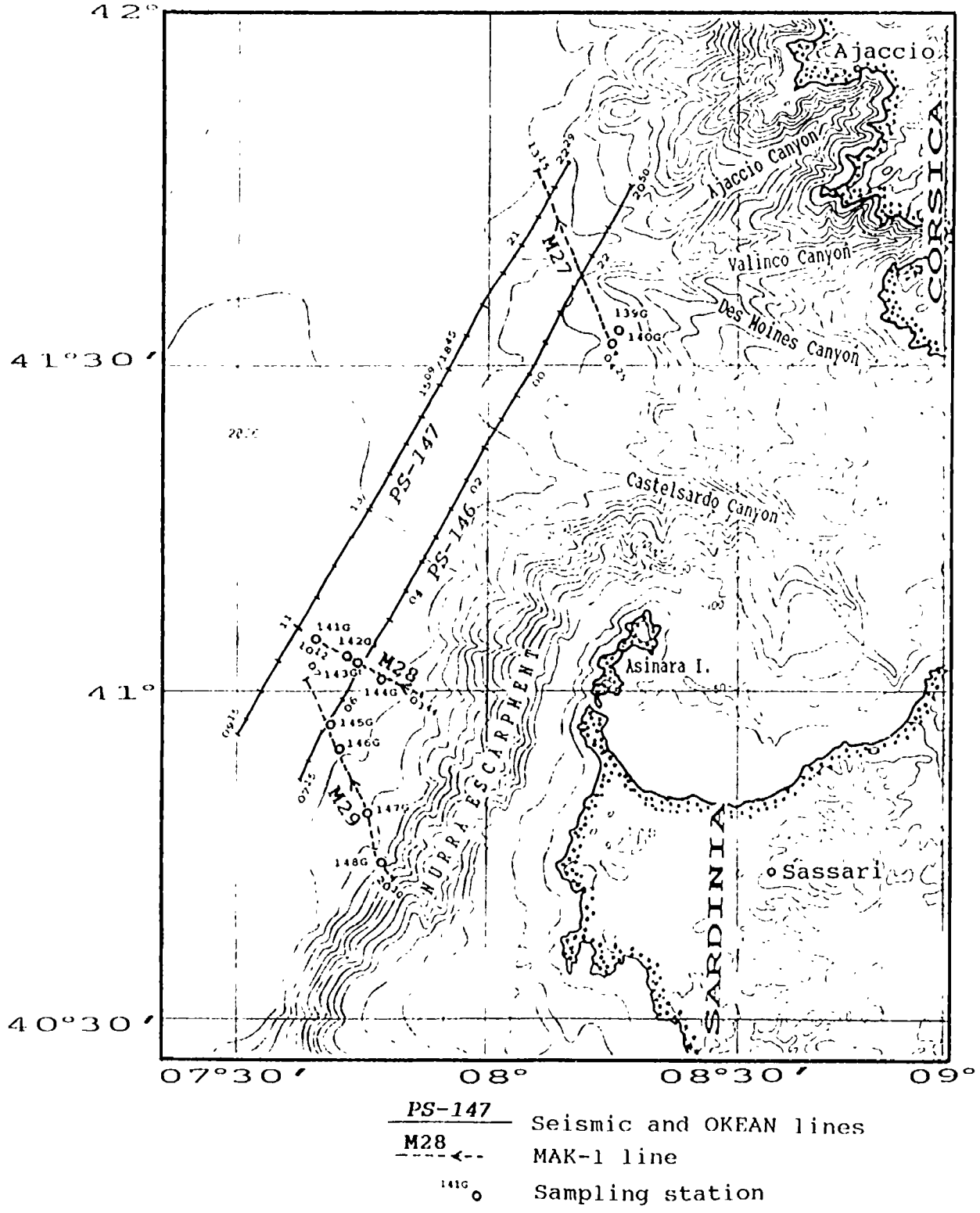

Fig. 50. Location map for Area 3a (Corso-Ligurian Basin)

about 200 ms, with a maximum of 300 ms. A strong unconformity displayed as a high amplitude reflector is seen inside this member close to the start of line 146 and the end of line PS-147 (Figs. 51 and 52). This member is exposed in the walls of the Moines Canyon, and it probably pinches out or is replaced by a chaotically layered unit on the above mentioned structural terrace on line PS-147.

The uppermost Pleistocene member generally increases in thickness toward the basin plain. It shows many examples of mass wasting processes. Their traces show up as chaotically layered or acoustically transparent lenses, especially well seen on line PS-147 (19:30, 20:10, etc). A seafloor high with a wavy surface at the very beginning of line PS-146 could also be a slump block.

The Corsica/Sardinia margin domain underwent young deformation, which could have taken place during Pliocene and later. It is worth noting that clear evidence for a compressional event is present on seismic section PS-147 at 21:30 (Fig. 51). A large high in the seafloor morphology is related to a thrust or reverse fault with about 250 ms offset. The time of this thrust emplacement seems to be correlated with the unconformity within the inferred Pliocene member because the semitransparent Pliocene unit below the unconformity pinches out on the upthrust wing of this structure. At the same time an uplifted block, bounded by normal faults, is present near 23:00 on line PS-146. This is evidently post-Pliocene deformation because the thickness of the transparent seismic member does not change across the block.

In the transitional zone between the two domains, the thickness of the Messinian probably increases quickly basinward. In the Ligurian-Provencal domain, the seismic sequence includes principally the Messinian evaporites and Plio-Quaternary sediments. The base of the Messinian is seen only at one place (04:20 on line PS-146) where the thickness of the evaporites is 700 ms. The visible Messinian sequence consists of an upper layered unit ("upper evaporites") and a chaotically layered lower unit (salt). The whole sequence is characterized by multiple and frequent diffractions related to sharp undulation of the M-Reflector (at the top of the Messinian). These undulations are caused by halokinetic deformations. The style of deformation changes basinward, from salt pillows to frequent small and narrow piercing diapirs. None of them reaches the seafloor and neither do they have any morphological expression at the seafloor. This change in the style of halokinetic deformation is probably related to the increasing thickness of the evaporites.

The overlying Plio-Quaternary sediments (third and fourth seismic members) have a thickness of about 400-500 ms. The inferred Pliocene transparent layer pinches out above the high at the base of the Messinian (04:20 on line PS-146). The Pleistocene units most likely consist of an alternation of turbidites and hemipelagic sediments. Some thin transparent lenses, which could be debris flow deposits, are present in the Pleistocene sequence on both seismic sections.

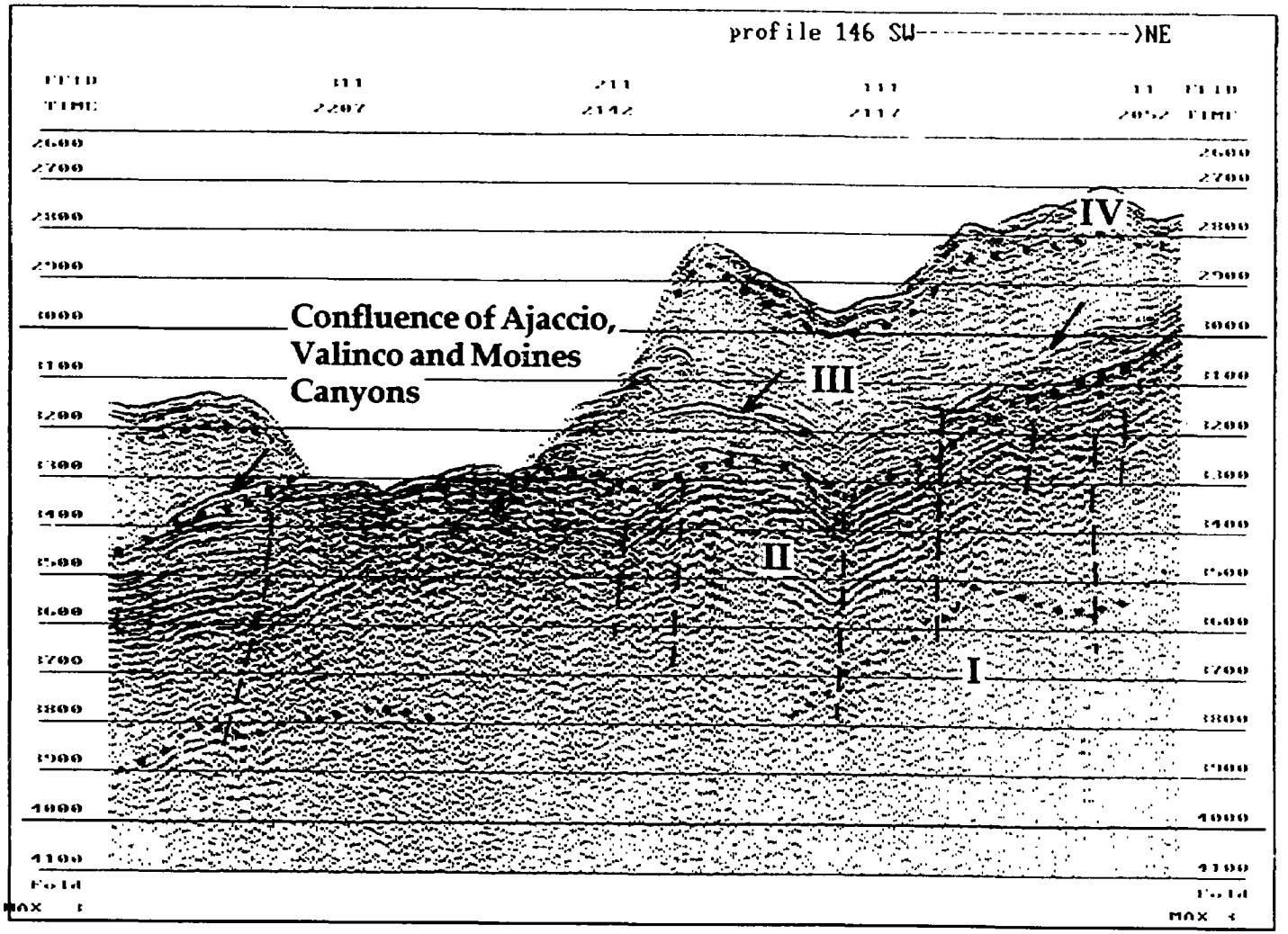

Fig. 51. Principal seismic members in the Corso-Ligurian Basin (Area 3a). Seismic line PS-146. I - late post-Variscan rocks; II - pre-Messinian Tertiary; III - Pliocene; IV - Pleistocene-Recent. A strong unconformity in the Pliocene sediments is indicated by arrows

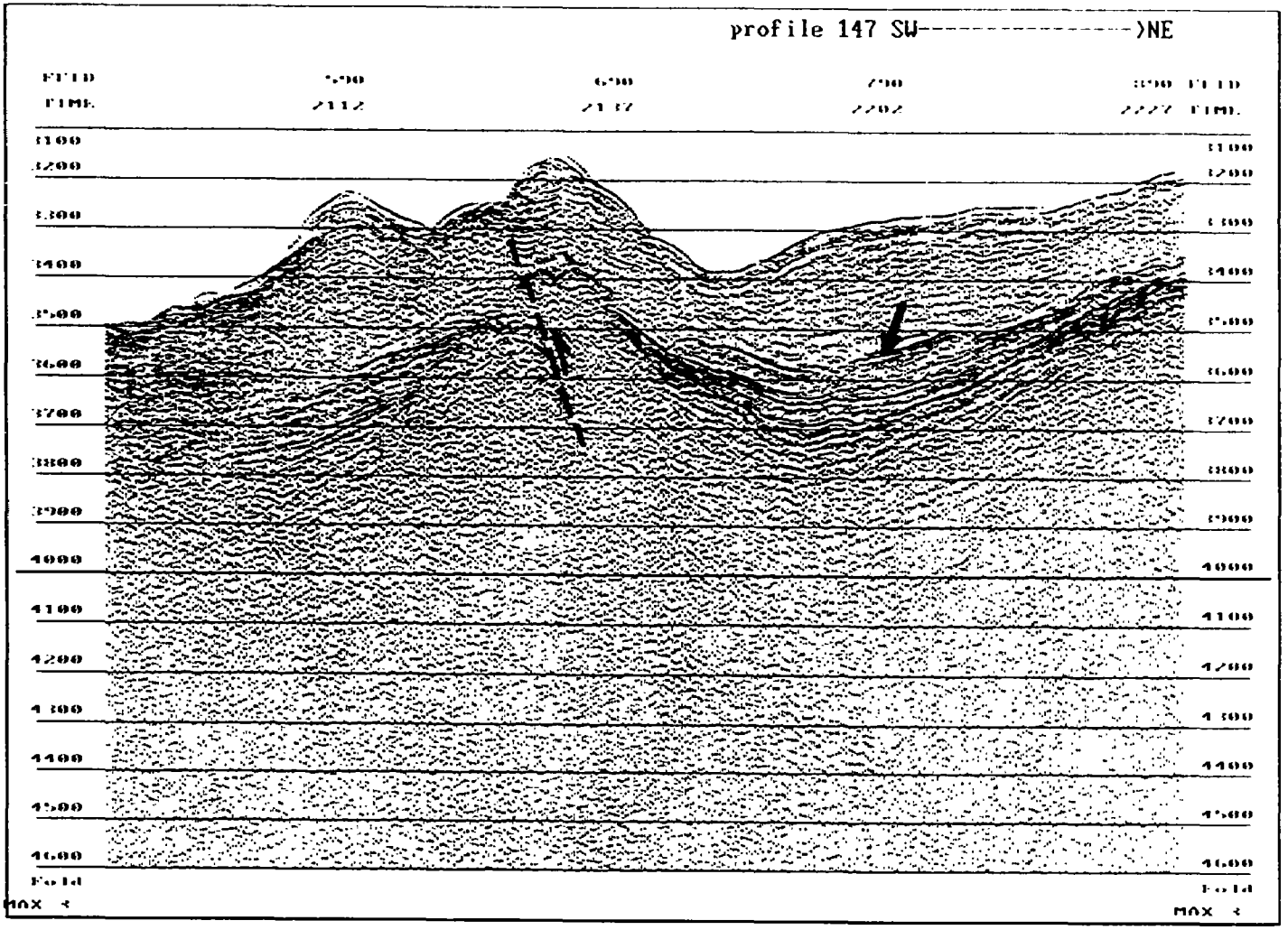

Fig 52. A strong unconformity (arrow) in the Pliocene sediments in the Corso-Ligurian Basin. The unconformity is probably evidence for short-term compressional event. Seismic line PS-147

b. DISTAL RHONE FAN AND VALENCIA CHANNEL

A.F. Limonov and E. B. Terent'eva

Six seismic lines were shot in Area 3b (Fig. 53), in the region of the assumed Valencia Fan, northeast of the Menorca Island. They are mostly aligned in a NW-SE direction (lines PS-148 to 150 and 153), and were chosen to enable the accompanying OKEAN sidescan sonar to map the expected extension of the flow paths into the Balearic Basin plain. Lines PS-151 and 152 are connecting lines to tie the DSDP drilling Site 372 with the seismic sequence observed on the sections. The total length of the lines is 535 km.

The observed sequence is divided into two seismic members represented by the Messinian evaporites and the overlying Plio-Pleistocene sediments (Fig. 54). The evaporitic member consists of two units, chaotically layered in the lower part (salt) and well-layered, with parallel strong reflectors in the upper part (upper evaporites), although sometimes the whole sequence looks acoustically transparent. The M-Reflector can be traced for rather limited distances because the top of the evaporitic sequence is highly disturbed by halokinesis. Multiple diapirs rise from the evaporitic layer to the seafloor. Some of them are reflected in the seafloor morphology as hills, a few tens of metres high and 1.5-2 km in diameter. Some diapirs are truncated at the seafloor. They have a quadrangular shape in cross-section and are flat-topped (Fig. 54). Generally, the diapirs which rise above the seafloor are grouped around the northwestern segments of the seismic lines, while the truncated diapirs are situated basinward.

The overlying Plio-Quaternary member has a similar seismic pattern to that of the Rhone Fan deposits. However, in contrast to the Rhone Fan area, the thickness of the Plio-Quaternary sediments in the study area rarely exceeds 0.8 s. Like the underlying Messinian evaporites, they also enclose two seismic units, acoustically transparent below and well-stratified above, with continuous, high amplitude reflections intercalated with acoustically semitransparent layers. This stratified unit is evidently made up of alternation of hemipelagic and turbiditic sediments, whereas the transparent Pliocene(?) unit seems to represent mostly homogeneous hemipelagic sediments. It was suggested earlier (Limonov et al., 1993) that the Pliocene Valencia Fan could be situated along the north Menorca Rise, and the observed seismic pattern confirms this assumption.

In fact, what we see on the seismic sections is not a fan *sensu stricto*, but a broad, shallow channel on the continuation of the Valencia Valley. The area is notable for a very subtle seafloor morphology. Clear evidence for active modern sedimentation can be seen only on line PS-151 (15:45-16:15), where a very gentle depositional body with positive morphology is observed. The uppermost 30-40 m of sediments display an acoustic transparency and seem to be composed of sand accumulation. Sediment accumulation evidently predominates in the surveyed area closest by the Menorca Rise (end of line PS-151 and start of line PS-152), but this is certainly not related to the Valencia sedimentary input.

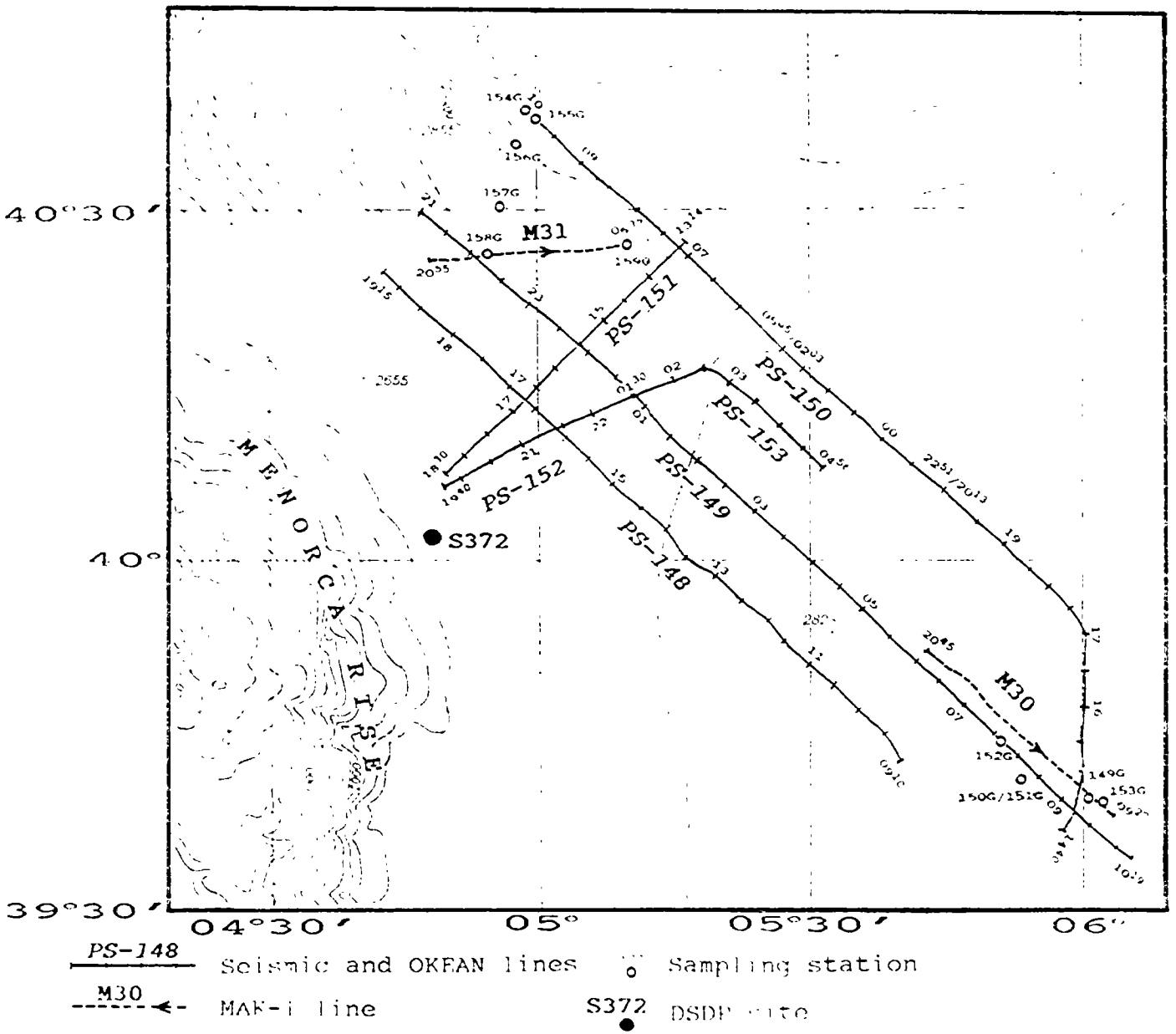

Fig. 53. Location map for Area 3b (distal Rhone Cone and Valencia Channel)

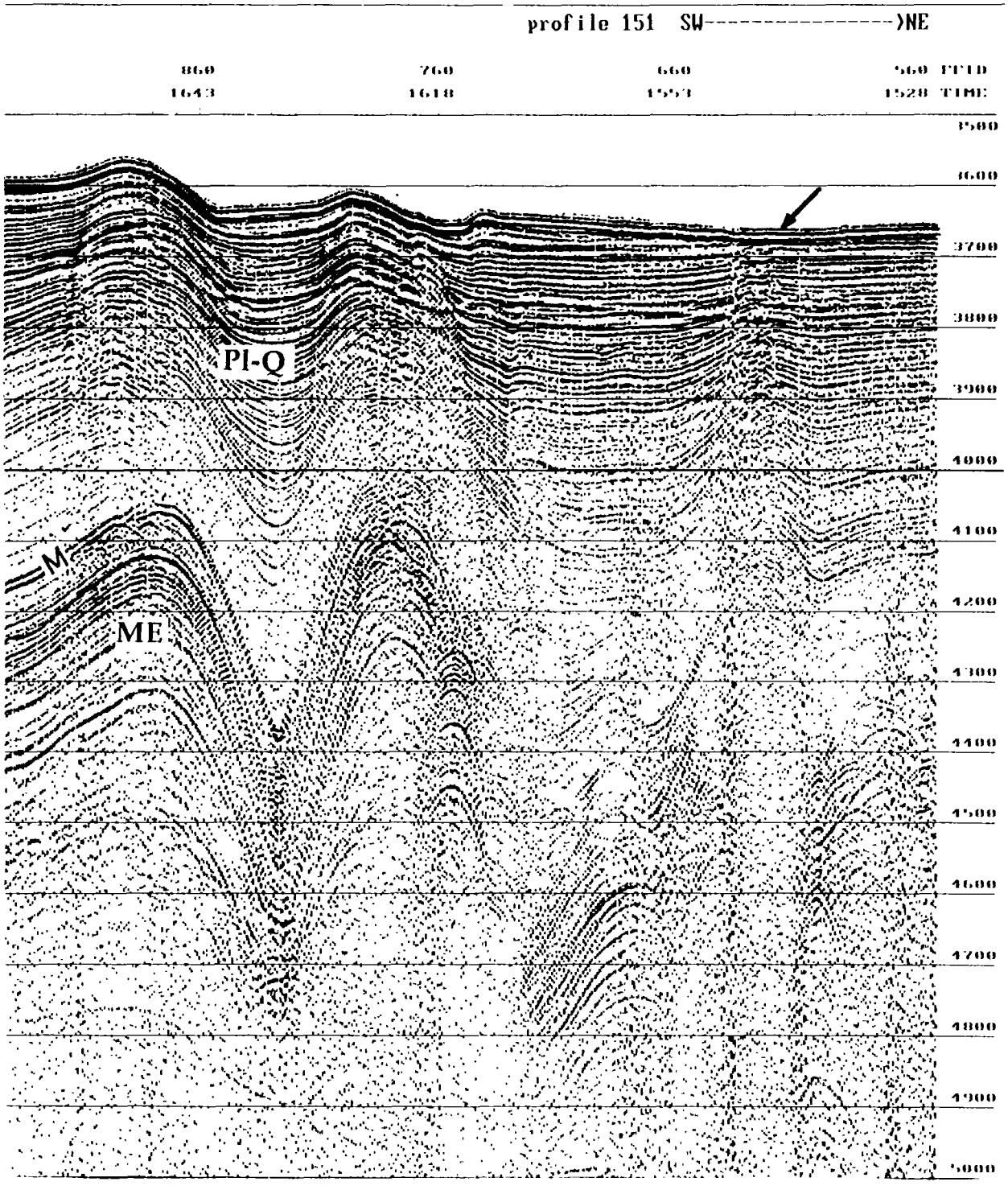

Fig. 54. Principal seismic members in the lower Valencia Channel area. ME - Messinian evaporites; Pl-Q - Plio-Quaternary; M - M-Reflector. Also shown are salt domes and diapirs displayed in the seafloor topography and one of the truncated diapirs (arrow). Seismic line PS-151

Different shapes of the salt diapirs presumably result from whether accumulation or erosion prevails within the study area. The truncated diapirs differ in their interrelation with the host sediments from the diapirs which have a seafloor expression. There is an abrupt termination of the near horizontal Plio-Quaternary sediments against the walls of the truncated diapirs, whereas the layers bend upward and frequently display an onlap pattern near the walls of the diapirs with seafloor expression. The truncation of the diapirs is probably caused by erosion that is contemporaneous with diapiric growth and compensates for it. Thus, the southern part of the study area is characterized by a very complicated pattern of lithodynamics, probably with active erosion and redeposition of sediments which is not typical of deep-sea fans. This is also confirmed by MAK-1 data from line 30, where unusual bedforms, indicative of strong current activity, cover the seafloor. The northern and central sectors are distinguished by a slight predominance of accumulation over erosion.

Summarizing, one can conclude that the sandy fan, if it exists, should be situated even further south than the study area, as a sheet sand accumulation. However, it is not excluded that the sandy fan may turn out to be a very small region because most sediments are accumulated in levees along the Valencia Valley.

3. SIDESCAN SONAR SURVEY

a. CORSO-LIGURIAN BASIN

N.H. Kenyon, J. Clark, H. de Haas, and J. Millington

OKEAN data

Two OKEAN lines were run along the expected pathway for gravity flows at the southern end of the north-south trending Corso-Ligurian Basin. They run from the lower Ajaccio Canyon which drains part of the slope west of Corsica, past an expected channel-lobe transition zone and a potential sandy lobe to the Balearic Basin plain (Fig. 50). The basin plain extends here to the northeast into the Corso-Ligurian Basin.

Higher backscatter is found on OKEAN sonograph of the floor and walls of Ajaccio Canyon and its extension onto the floor of the basin. This extension shows that the pathways of gravity flows turn to the left down the basin axis. Beyond is a zone of weak backscatter with a number of scattered spots of higher backscatter, and then a well-defined belt of longitudinal "braid-like bars". These are relatively highly backscattering, with narrow "channel-like" strips between. They are up to 10 km long and 2 km wide and are rounded at their upflow ends (Fig. 55). The belt extends across from the foot of the Sardinia slope to the foot of the Rhone Fan (this latter observation is from unpublished GLORIA data). There is another irregularly shaped area of high backscatter in a setting on the lower slope between Ajaccio and Castelsardo Canyons. It extends downslope from 1800 m to 2400 m.

A comparison between the OKEAN and the GLORIA sonographs shows that all the main features can be seen on both data sets. The OKEAN, being of a higher frequency, shows more details than the GLORIA. There is one small area at the foot of the slope that is recorded as medium strength of return on the GLORIA but is not seen on OKEAN. This may be because the 6.5 kHz GLORIA sound penetrates deeper than the 9.5 kHz sound of OKEAN, and the feature is buried at a depth that OKEAN cannot reach.

MAK-1 data

Basin floor

Two deep-tow lines (MAK 28 and MAK 29) were run across the distal part of the basin (Fig. 50). One crossed the "braid-like bars" and the other was intended to cross the boundary between the "braid-like bars" and the basin plain. From the acoustic character of the profile, the ponded basin plain does not seem to have been crossed and presumably lies further out into the basin.

The shapes of the "braid-like bars", or stringers, could be recognised from the sonographs, but they have much less contrast with the surrounding floor than is shown on the OKEAN records. One explanation for this is that the backscatter is coming from a depth that the 30 kHz sonar cannot reach. There is a very faint mottling in the area of stringers. Upslope from the stringers, there are longitudinal trains of small spots of slightly higher backscatter. These resemble the trains of blocks seen on sonographs from the distal Monterey Fan (Masson et al., 1995).

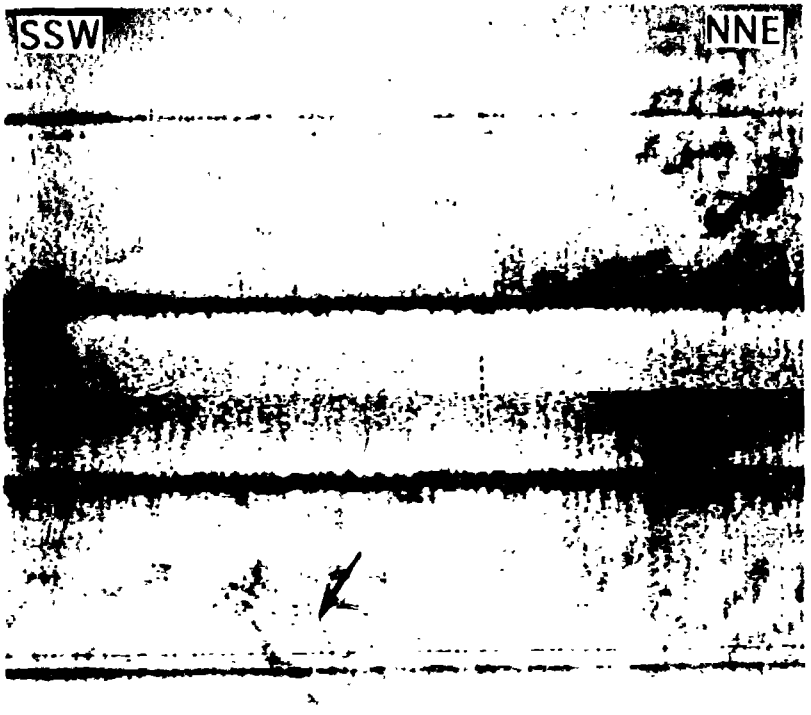

Fig. 55. "Braid-like bars" (arrow) along the western Corso-Sardinian margin. OKEAN sonograph 147 (unprocessed). The swath range is 15 km

The penetration on the 5.5 kHz profiler is about 25 m near the bars and 35 m further out into the basin. There are clearly seen repetitions of well-bedded sequences that are about 4 to 5 m thick. The strength of the reflectors increases upwards through each sequence. Some erosion of no more than 1 or 2 m is seen in places. The uppermost sequence is only about 2 to 2.5 m thick and pinches out to the east at approximately the boundary of the easternmost stringer. The acoustic facies to the east of this boundary is rather different in style, with sequences that show more erosional horizons and a more even strength of the reflective beds within each sequence.

The line across the basin floor (MAK line 29), southeast of the stringers, is featureless on the sidescan records apart from an area of mottled ground near to the foot of the Nurra Escarpment. Two cores from the mottled ground had deposits from polymictic debris flows, containing many kinds of clasts.

Towards the edge of the basin the penetration on the profile decreases and sequences pinch out. At the outer (northern) end of the line the uppermost two sequences are each about 4 m thick and well-layered. They change character gradually as they near the base of slope, thinning and losing subbottom horizons until they become one sequence and finally become 5 m thick and largely transparent. The transparent layer then pinches out abruptly at the base of slope.

Inter-canyon slope

Line 27 with the MAK-1 system was run approximately SSE-NNW and crossed the Ajaccio Canyon and the slope deposits on either side of the canyon. The line was taken to study the morphology and sedimentary processes. The Ajaccio Canyon was crossed at a depth of 2500 m, downslope from the convergence with the Valinco and Moines canyons. Another MAK line (29) crossed the foot of the steep Nurra Escarpment and the base of slope, west of Sardinia.

South of the Ajaccio Canyon, the profile shows an area of low relief (maximum of 35 m), and good penetration (up to 50 m), with largely parallel bedded deposits. On some canyon-facing gentle slopes, flow lines are observed, possibly erosive and trending downslope. An isolated strip of slightly lower backscatter with small waves trends downslope. This direction, almost perpendicular to the general slope direction, is due to a localized depression seen on the profile. The waves are arcuate (convex downslope) and show a regular wavelength of approximately 7 m. These features may be slump folds on the surface of a flow.

At the southern end of the line, highly irregular patches of very high backscatter are found in association with areas of low backscatter (Fig. 56). No discernible relief is observed on the profiles across these "Enigmatic Black Blobs" (EBBs). The EBBs can be separated into three areas, which are discussed below. The cause of the high backscatter in these areas may result from a single process or several different processes.

(1) The southernmost EBB appears as a large area with sharp sides and a very irregular outline. The backscatter level over the feature is homogeneous. Smaller, linear high-backscattering patches can be observed. This feature may have a very low positive relief and possibly be the result of the deposition of a very coarse-grained flow (debris flow/grain flow). The relief is observed as a narrow shadow on the side furthest from the transducers.

(2) The second area of EBBs shows a group of high-backscattering, sharp-bounded irregular, semi-linear features. There is an arcuate distribution of this group of EBBs. No shadows are observed.

(3) The third area is a group of linear and arcuate SE-NW trending strips of high backscatter.

All three areas appear to be associated with lenses of transparent acoustic facies observed on the profile. A small fault seen on the profile coincides with

the northernmost crossing of the EBBs. It is suggested that the EBBs may be related to the scarps and scar-fill of buried sediment failures. The transparent facies are likely to be the chaotic scar-fill and the observed fault, the scarp margin. These features are buried by 3-5 m of post-failure deposits, and hence the MAK-1 sidescan sonar is unlikely to penetrate down to record these features. However, if minor reactivation of the scar has occurred, as is suggested by the emergent fault plane, surface expressions of these features may be the cause of the arcuate distribution and group of linear EBBs. One possibility is that fluids or fluidized sediments have migrated to the surface via the described scar surfaces, disrupting the surface and subsurface sediments, producing irregular areas of high backscatter. Alternatively, the slight relief observed on the southernmost large area may indicate that these features are deposits, either coarse-grained or chaotic. Although the three identified areas of EBBs are most likely to result from the same causes, the alternative explanations for their formation offered above indicates that their origin remains unclear.

The northern overbank of the canyon is steeper and generally shows poor penetration on the seismic profiles and a streaky backscatter pattern with varied backscatter intensity (low to moderate). The foot of the slope is 3.5 km north of the canyon. The steep slope area is clearly an area of numerous sediment failures, showing small-scale scours, gullies and flow lines orientated downslope, i.e. northerly, perpendicular and away from the canyon axis. An area of uniform moderate backscatter (<1 km wide) is seen as flat-lying and shows some penetration on the corresponding seismic profile. This small area has not undergone the same level of sediment failure seen elsewhere in this region of the slope. At the foot of the overbank slope, there is another sediment pathway with flow lines indicating movement towards the northwest. The flow lines may be caused by shear bands in debris flows.

Canyon

The Ajaccio Canyon runs to the west here. It is incised into the slope deposits and has a terraced cross-sectional profile (Figs. 57 and 58). The terraces are clearly the result of mass wasting on the canyon walls, as the terrace walls are major unconformities at the seafloor. The canyon-floor area is 3.3 km wide and lies between two very steep walls that are about 100 m high. The floor of the canyon contains some very high backscatter features and corresponds to an area of hard reflection on the seismic profile.

The axial zone of the canyon floor has scours with a flute-like geometry that can be seen at various scales (the largest being 800 m wide and 40 m deep), and often showing scours within scours. Their base contains very high-backscattering, sinuous-crested bedforms which extend downslope. These bedforms show wavelength spacing of 40 m and 15 m. Outside these arcuate scours are longitudinal high backscatter scours and fields of the sinuous-crested bedforms, possibly representing the presence of coarse-grained clastics, probably gravels, and outcropping rocks.

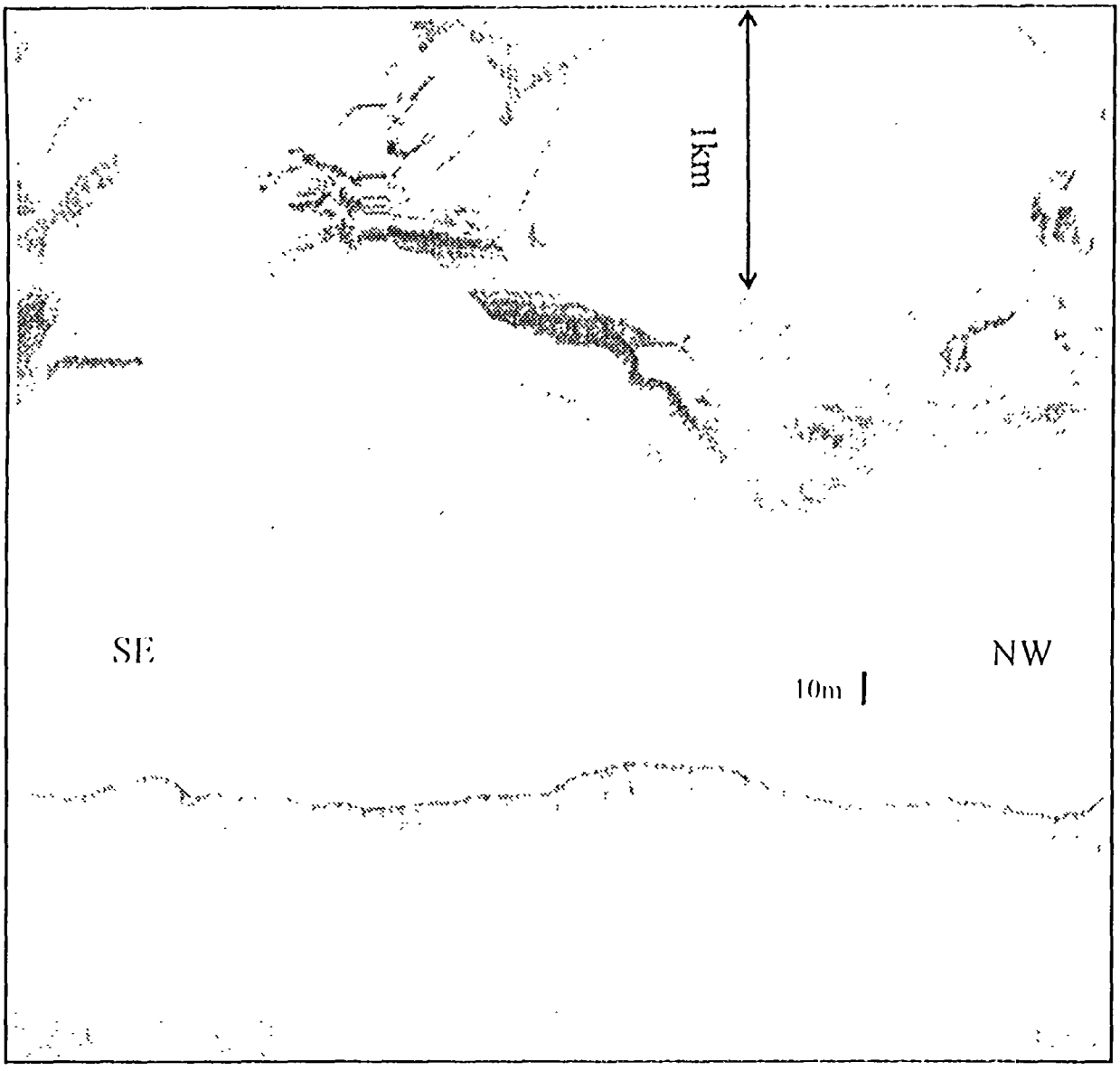

Fig. 56. "Enigmatic Black Blobs" at the southern end of MAK line 27. There is a large irregular-shaped patch at the start of the record, a group of high-backscattering, sharp-bounded irregular, semi-linear features, and a group of linear and arcuate SE-NW trending high backscatter strips. The profile shows the buried lens-shaped transparent facies, which are interpreted as scar-fill deposits

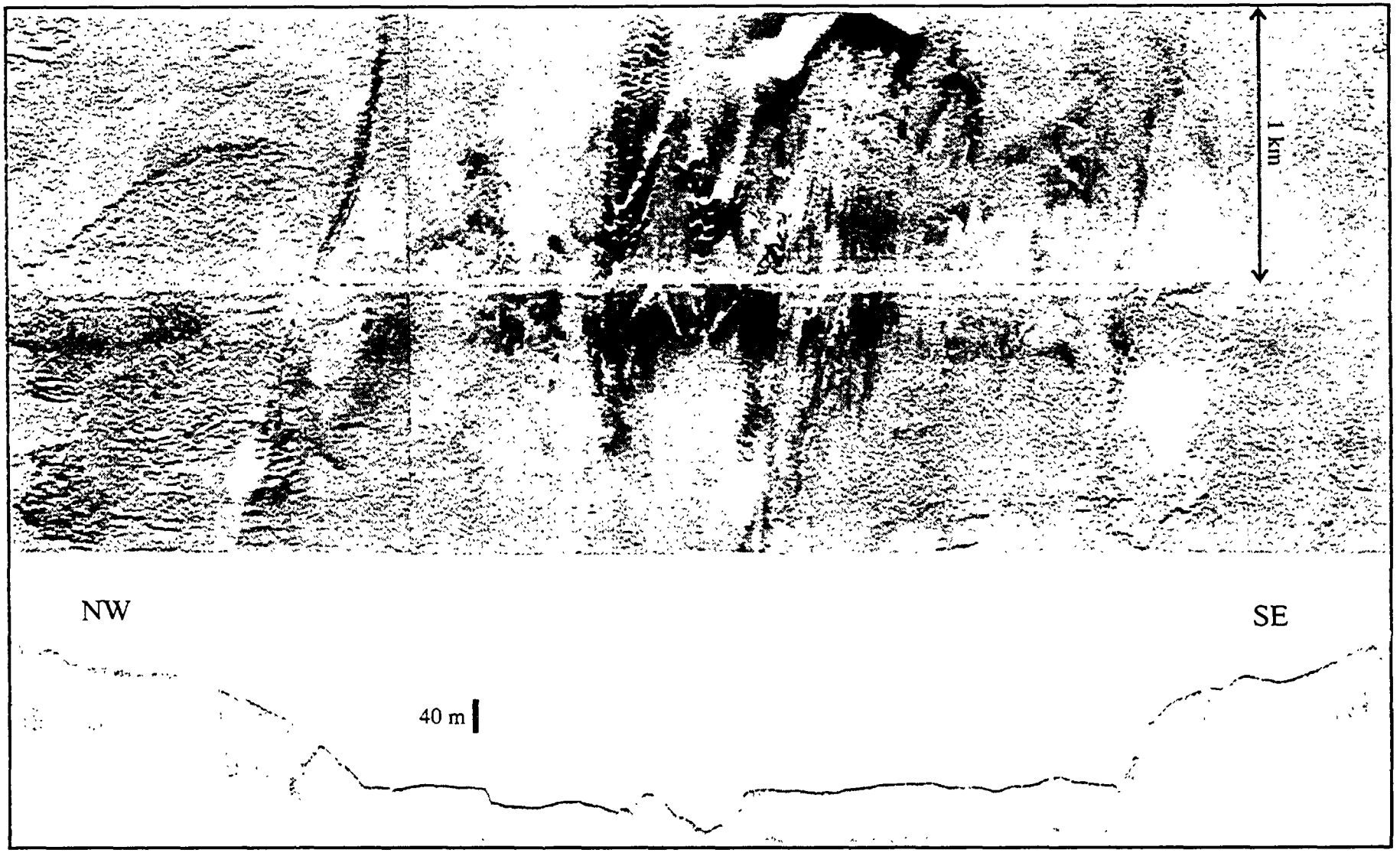

Fig. 57. The Ajaccio Canyon crossed on MAK line 27. The sonograph shows the central-canyon area, bounded by steep walls and containing large flute-like scours. Note that this area of the canyon corresponds to a hard reflection on the profile. The slopes flanking the central-canyon area show numerous sediment-failure features

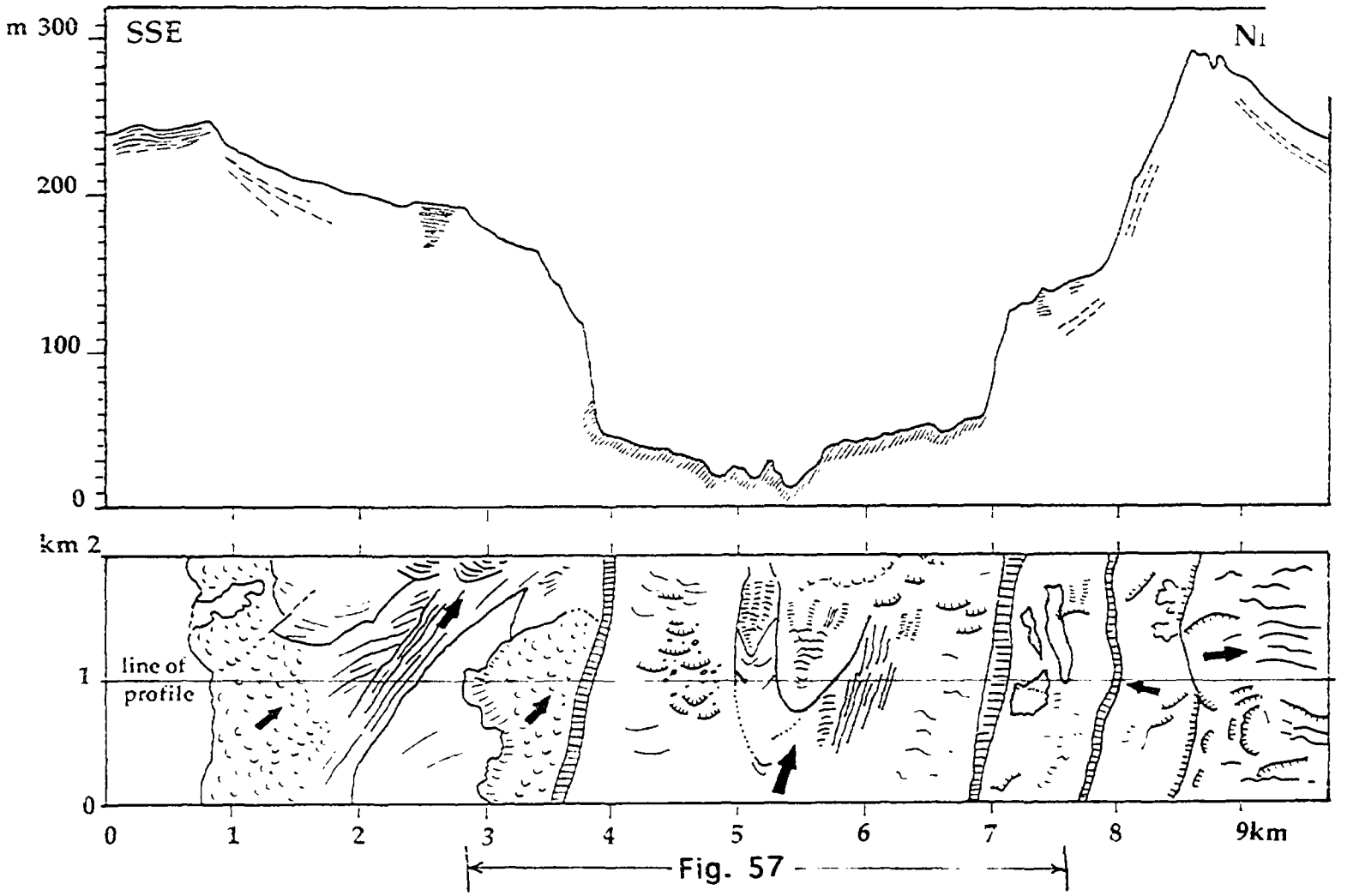

Fig. 58. Sketch interpretation of the profile and sonograph from the crossing of the Ajaccio Canyon (MAK line 27). The central part of the drowing is displayed in Fig. 57. Arrows indicate sediment flow directions within the central-canyon area, on the terraced canyon walls and on adjacent slope areas. Note the downslope trends on the northern canyon overbank. (See the legend in Fig. 59)

The floor's axial zone is flanked by gently inwardly-dipping slopes with irregular backscatter distribution, due to irregular blocks and scars. The sediment transport direction is parallel to the canyon axis.

The southern and northern terraces show numerous scarp features and mass transport directions obliquely down towards the canyon floor. Transport paths are towards the northwest on the southern margin and towards the south on the northern margin. Both margins are largely characterized by the transparent acoustic facies that is here associated with chaotic deposits. However, small raised areas of parallel-bedded reflectors can be seen as homogeneous backscatter on the sidescan record. Such areas are either parts of the slope that have not failed or large rafted blocks of sediment, which have not undergone extensive deformation. On the southern margin, a large block of sediment has moved approximately 500 m downslope. It shows tension cracks and can be fitted to the outline of the scarp upslope from it.

Mass-failure processes at the base of the Nurra Escarpment

MAK line 29 traversed from the Nurra Escarpment, on the slope of northern Sardinia and north onto the basin floor. A previous GLORIA survey revealed that this region of the Nurra Escarpment contains a series of elongate, high-backscattering features running down the steepest part of the slope from the mid-slope at about 1800 m to near the base of slope. A number of different mass-failure processes operate on this slope. Fig. 59 is a schematic interpretation of the sidescan acoustic facies of the Nurra Escarpment.

Acoustic Facies I occurs throughout the profile, and consists of moderate to low, largely featureless backscatter.

Acoustic Facies II shows generally low and moderate backscatter, with a highly scoured surface ornament. The scours have an irregular geometry and are approximately parallel to flow lines (northwest trending). The corresponding profile shows moderate to low penetration on steep slopes. Small gullies can be seen cutting into this area and trending northwest.A large shadow zone on the eastern side of the record is probably the site of the steep wall of a relatively large gully.

Acoustic Facies III occurs below this gully in an extensive area of extremely high backscatter, extending downslope (Fig. 60). A pattern of radiating sinuous-crested bedforms can be seen at the seafloor, with a wavelength increasing downslope from 300 m to 700 m. On the corresponding profile, the smaller bedforms can be seen to have amplitudes of 0.5 to 0.7 m. This facies is interpreted as a coarse-grained, probably conglomeratic, deposit as pebbles were recovered. The maximum cross-flow width of this funnel-shaped deposit is 1.6 km. The extremely high backscatter feature probably corresponds to one of the high backscatter strips seen on the GLORIA records.

Acoustic Facies IV occurs adjacent to Facies III and is an area of relatively low backscatter, with very sharp-bounded high backscatter lineations. It corresponds to a transparent facies on the profile, and to a slightly raised topography. A possible explanation for this facies is that it represents an eroded

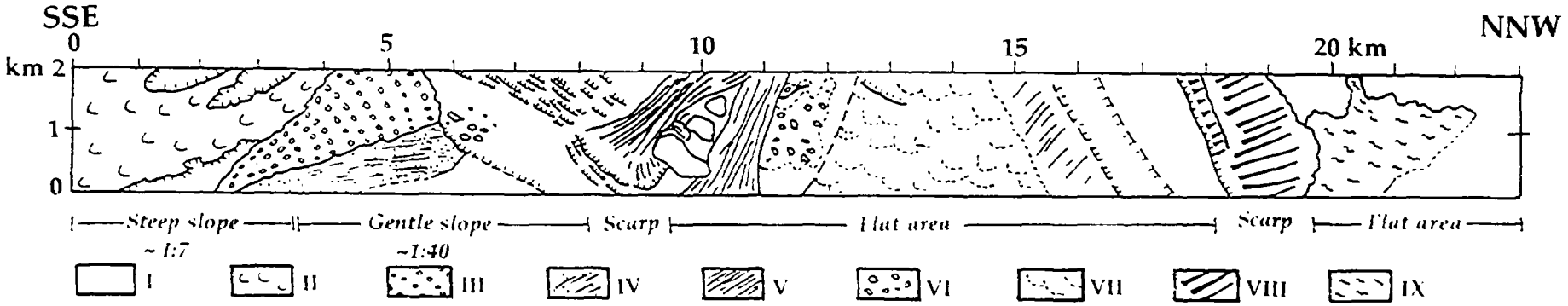

Fig. 59. Sketch interpretation of the sonograph from MAK line 29, showing the distribution of acoustic facies on the middle and lower slopes of northeast Sardinia. Individual features, such as, scarps and blocks are also shown. Acoustic facies: I - largely homogeneous backscatter (ranging from low to moderate), showing faint surface ornamentation; II - intensely scoured medium backscatter; III - very high backscatter with downslope radiating sinuous-crested wave forms; IV - low backscatter with numerous downslope orientated linear striations (high backscatter); V - varied backscatter intensity showing flow lineations. Flow lineations may be weakly or strongly seen; VI - highly varied backscatter intensity with areas of scouring and numerous scattered small blocks; VII - area of irregular distributions of varied backscatter intensity, showing downslope flow directions; VIII - medium backscatter area on scarp surface with well-defined downslope- orientated lineations (rills) and small patches of irregular high backscatter; IX - low to medium mottled backscatter variation in an area of debris flow deposition at the base of the slope

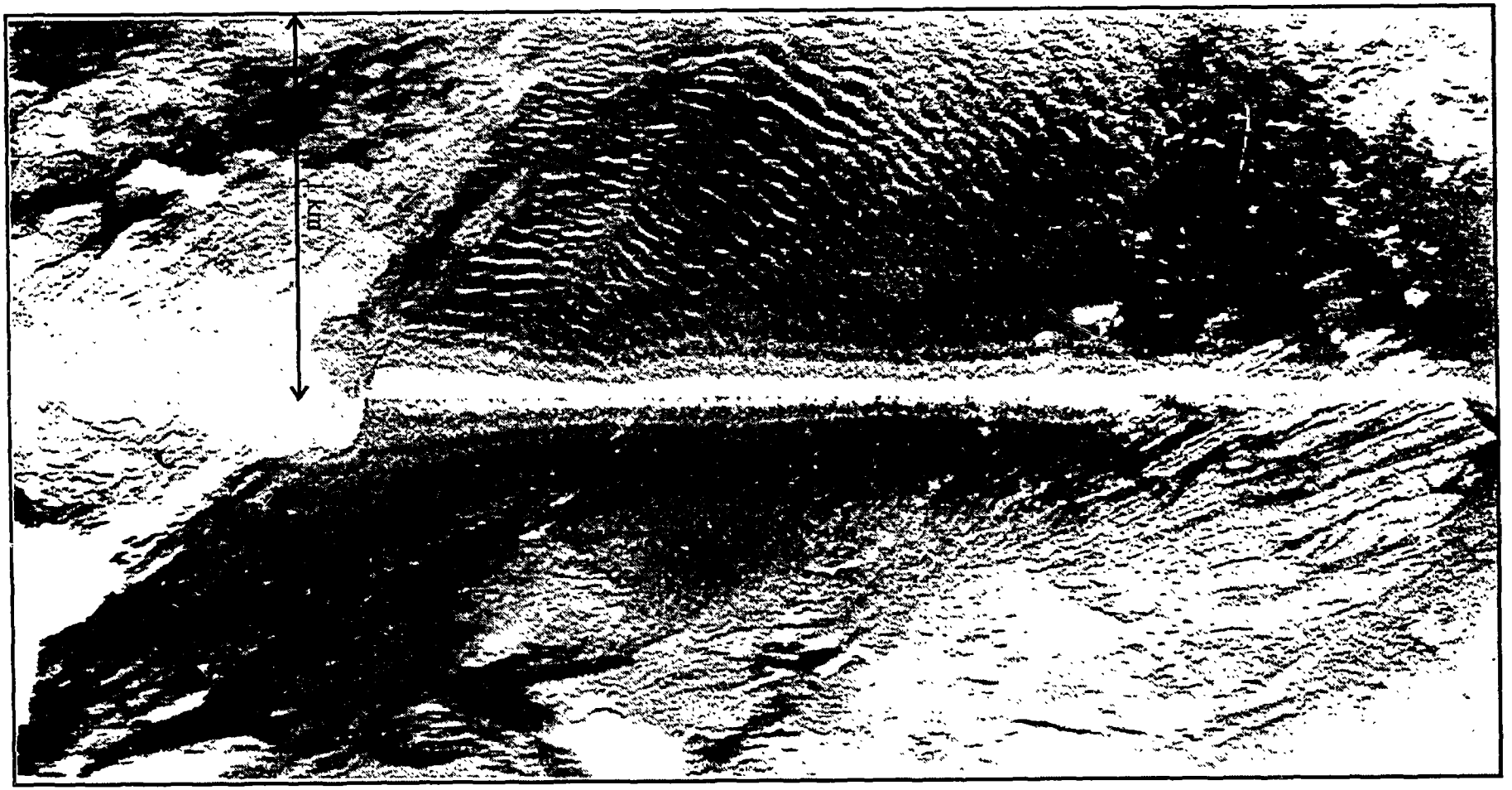

Fig. 60. Sonograph of Acoustic Facies III from the Nurra Escarpment on MAK line 29. These rippled deposits have been interpreted as a sheet of coarse-grained clastics, probably pebbles, fed by minor canyons on the escarpment

block of sediment, and where its northern margin has failed due to sliding, the profile reveals the parallel-bedded nature of the underlying sediments. Downslope from this scarp is an area of irregular small-scale blocks that act as obstacle marks and a cluster of small scarps (see Fig. 59).

Acoustic Facies V is dominated by areas of low to moderate backscatter showing pronounced flow lines, indicating possible sediment pathways. One such area occurs immediately downslope from arcuate scarps (see Fig. 60). On the profile from this region, the sediment flows appear as the transparent facies fill of localized depressions (slide scars).

Acoustic Facies VI is a large area of speckled backscatter, representing groups of sediment blocks and scours. A large part of the apparent flat-lying area is covered by variable low and moderate backscatter, showing numerous flow lineations, minor scours and creep deformation features indicating mass-flow towards the northwest.

Acoustic Facies VII. The profile shows that the erosion is very shallow in this flat-lying area. The profile and sidescan also reveal a localized depression, which appears to have acted as a sediment conduit, trending southwest. Flow lines can be seen on the flanks of this depression, trending into and along its axis. Irregular subbottom reflectors in the base of the depression relate to polyphase fill of this feature.

Acoustic Facies VIII can be seen on the northernmost scarp, marking the base of slope. There are streaks, which represent the scoured surface of the scarp. Irregular high backscatter patches, which may be rafted blocks or emergent high backscatter material and which are exposed due to surface sediment removal can be seen within this area. At the base of slope, an area of mottled low backscatter occurs in an irregular deposit (Acoustic Facies IX), which is interpreted as a debrite, derived locally from the Nurra Escarpment. Beyond this facies, on the basin plain, widespread flat-lying deposits occur, which are believed to be sourced from the north.

It is clear from the MAK-1 record that sediment removal and erosive processes have been active on the steep slopes of the Nurra Escarpment, while sediment transport and flow processes have been active on the gentler slopes. This part of the Sardinia margin is highly dynamic, with a diversity of sediment erosion and transport activity, however, the two cores contain Holocene hemipelagic sediments, indicating that there is not much activity at present.

b. DISTAL RHONE CONE AND VALENCIA CHANNEL

N.H. Kenyon, J. Clark, H. de Haas, J. Millington, and F. Perez

The TTR-2 Cruise to the Western Mediterranean in 1992 made an OKEAN and seismic survey on the western side of the Rhone Cone and down to the north of the Valencia Channel (Limonov et al., 1993). Acoustic facies were distinguished and mapped with the OKEAN sidescan sonar but were not fully understood. However, they showed that there were transport paths for turbidity

currents and other types of gravity-driven flows down the broad basin floor that lies between the foot of the canyoned Spanish slope and the foot of the western Rhone Cone. There was evidence that some of the activity was very recent. Sands dated to the last century had been cored on the new fan lobe that is located high up on the Rhone Cone. The transport paths must feed into the very broad, shallow channel that lies beyond the mouth of the Valencia Channel. Beyond this again, one finds the relatively flat Balearic Basin plain. A MAK profile taken in 1992 (MAK line 2) crosses this channel mouth and shows it to be erosional and cut about 30 m into well-bedded sediments. Its profile is asymmetrical, the steeper wall being on the south side. There are medium-scale bedforms in this channel mouth that indicate that it has been active relatively recently. Among the aims of this investigation are:

1. Finding out what types of bedforms are present, mapping them and determining the transport paths. There have been few studies of bedforms in this type of environment.
2. Finding the locus of sandy deposits that ought to lie distal to the broad, shallow channel. Determining the geometry of the sand bodies.
3. Determining the history of sedimentation in this region and whether there are any relationships to controls such as sea-level. Palanques et al. (1994) have shown from seismic lines that there is an updip migration of depocentres of the sandy deposits, called the Valencia Fan, during sea-level rise. The area that we are in is on the lower part of this fan, and the indications of relatively young sand transport further out into the basin would appear to be in contradiction with this pattern.
4. Studying the causes of backscatter variations on the sidescan sonar.

A grid of OKEAN and seismic lines (PS-148 to PS-153, Fig. 53) was made, which extended existing coverage down the expected transport path. The coverage runs southeastwards from the position of the old MAK line 2, that crossed the shallow channel, to the floor of the Balearic Basin plain. MAK line 30 was run with the sonar at 30 kHz across the distal part of the region and another (line 31) with the sonar at 100 kHz across some intriguing bedforms, seen two years ago on a 30 kHz record, with the intention of seeing them in more detail.

OKEAN data

The area was divided into acoustic facies.

Facies 1. Uniform. Uniform low-backscattering ground. It has good penetration on profiles and is continuously bedded. It is found south of the area and outside the influence of flows coming through the broad channel. It is also found beyond the other facies, where there appears to be a thin bed overlying the relatively opaque echoes seen on the MAK profile 30. Here there are stronger backscattering patches, believed to overly salt domes.

Facies 2. Streaks. Narrow, parallel streaks, prominent on the southern (right hand), deepest part of the broad channel and on the floor beyond the channel. They are longitudinal to the flow direction and regularly spaced.

Facies 3. Long V's. Longitudinal higher backscattering, narrow V-shaped features. They are longitudinal to the flow direction and regularly spaced.

Facies 4. Chevrons. A closely and regularly spaced pattern that appears as a mottled pattern on OKEAN but corresponds to chevron-shaped bedforms when seen on MAK line 30.

Facies 5. Sheets. (Corresponding to Facies 5a of Figs. 4 and 9 in Limonov et al., 1993). This has patches of low backscatter that are fairly large and have irregular outlines. They are found downslope from the Rhone neofan and onto the Valencia Channel mouth. One such patch is crossed on MAK line 31 and seen to be an area of uniform low backscatter. A core into it (core 158G) produced 76 cm of Holocene ooze and a handful of fine well-sorted grey sand.

A number of these facies are regular bedforms, being evenly spaced and oriented either transverse or longitudinal to the flows that are thought to have formed them. The arrangement of the facies zones and the orientation of the bedforms are believed to present a compelling picture for the expansion of flow beyond the shallow channel. The sequence of zones could indicate some weakening of peak current speed with the more erosional and elongate bedforms being in proximal positions. The chevrons and the uniform ground beyond would represent areas of lower peak speed. To what extent these bedforms are a reworking and winnowing of nearby materials is not known.

MAK-1 data

MAK line 30 was designed to investigate acoustic facies changes at the distal end of the OKEAN survey. Three types of facies were crossed.

At the western end of the line there are a few long trains of sediment waves that have a higher backscatter than the surroundings. It is presumed that this is what acoustic Facies 3, the long V's, look like in higher resolution. They are isolated waves, concave down the expected flow direction to the southeast and have a wavelength of about 10 m.

The trains of waves grade into chevrons (Fig. 61). The chevrons are a remarkable regular bedform that have not been described before from the deep sea. The arms are at a fairly constant angle that appears to be 50 to 80°, without taking into account possible distortion in the paper record. They are about 50 m across and the wing tips come to a point. It is not clear whether they represent two prevalent flow directions or whether the flow direction bisects the angle made by the arms. From the narrow shadow-like borders it seems that they are a positive feature, standing proud of the surrounding seabed. In many places their relief of about 1 m can be seen on the profile. Interpretation of the unprocessed profiles is difficult. The bedforms either acoustically mask the immediately underlying layers or they are bodies that are 3-4 m high with a partial later sediment fill of the area between the bedforms.

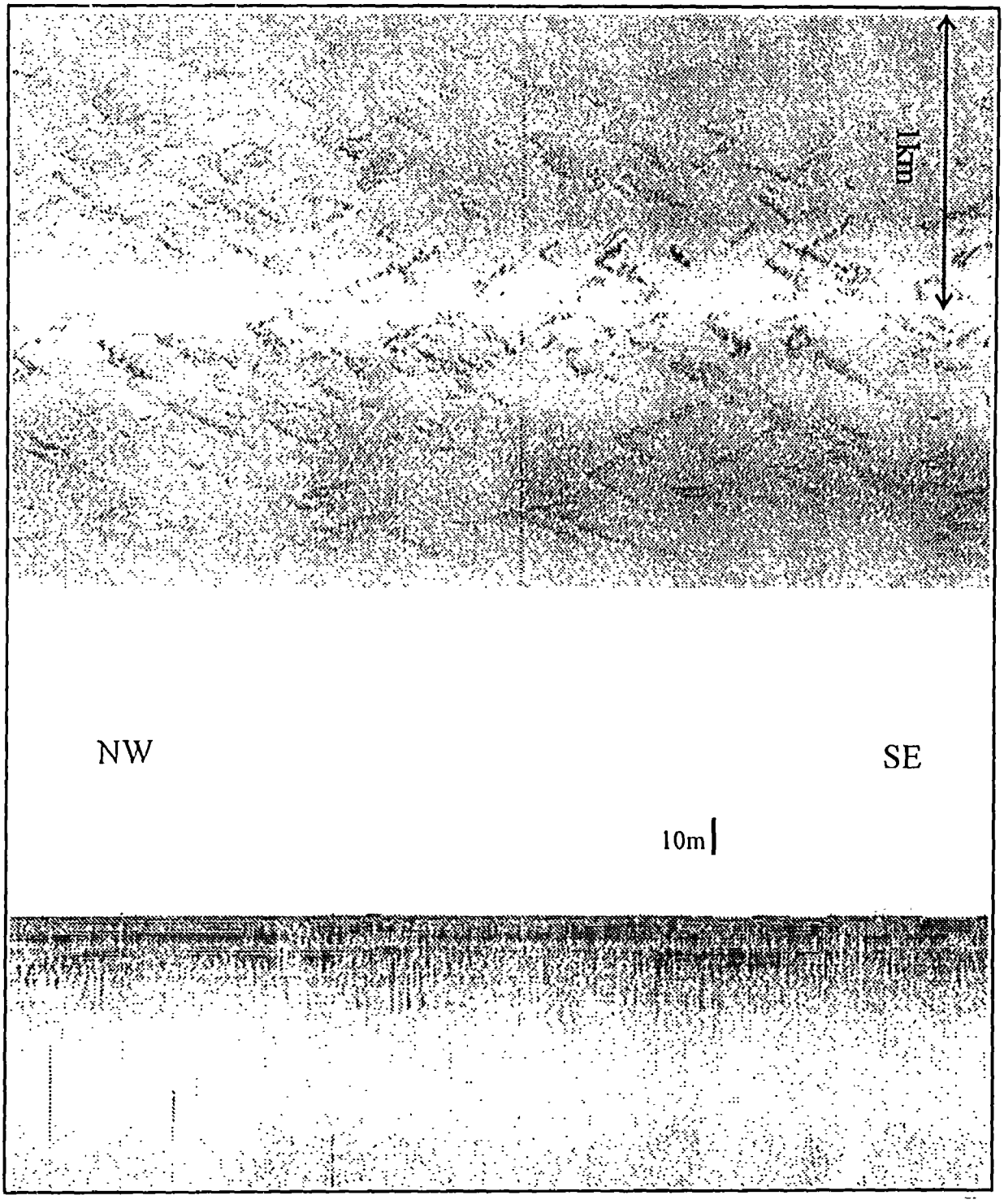

Fig. 61. Chevrons, a regular bedform on the distal Valencia area. The wing tips are about 50 m apart and they point down the flow direction. MAK line 30

At the distal end of the line there is a uniform zone (Facies 1). There are faults associated with underlying salt diapirs and some increase in thickness of the surface layers, the latter being due to some infilling of the depressions made by the salt tectonics. The thickness change may be the cause of broad interference fringes seen near a possible salt diapir.

The profile shows that, apart from where onlapped by a surface layer in the distal area, there is an 8 m thick sequence with stronger reflectors in its upper part. These reflectors are seen as either prolonged echoes or very thinly layered. At the base, there is a transparent layer, that thickens distally and whose upper surface appears to grade into the overlying thin beds. This may be the same thick transparent layer seen on 3.5 kHz profiles off Sardinia (Le Suroit Cruise, 1983; N.H. Kenyon, pers. comm.).

MAK line 31 was run with the sidescan at a frequency of 100 kHz. It starts to the west of the shallow channel and crosses the deep channel floor near to the site of core 158. The OKEAN facies crossed are (from west to east): uniform ground (Facies 1), streaks (Facies 2), and sheets (Facies 5). The sheets are elongated longitudinally in this area.

To the south of the channel there is uniform ground with a monotonous series of closely spaced, continuous reflectors. Penetration is high, up to 100 m, and there is little development of repeated sequences. At the foot of the gently sloping channel wall there is the deepest erosion into the well-layered sediments. The surface of the deepest part is uniform and weakly backscattering. The uppermost sediments are structureless and penetration is limited. This is in keeping with this part of the channel being floored with a massive sand deposit.

Beyond is a zone of bedforms (Fig. 62). They are regularly spaced, elongate and arranged in trains a[illegible]he axis of the channel. They are from 50 to 200 m long, and their length to wi[illegible]tio is fairly constant at about 2 to 1. They appear to be cut into the upper structureless layer. However, there is a rounded profile, which is taken to imply some modification of shape by currents, as they do not have the sharp outline of scours seen elsewhere. In outline they are asymmetrical, with a narrow upslope end and a wider downslope end. Often there is a spot of stronger backscatter near the downslope end of the bedforms. The bedforms are thought to be fields of erosional scours with possible modification by later current or currents, as some have no relief and are only faintly imaged. They are similar in shape and size to megaflutes described from ancient rocks (Vicente Bravo and Robles, 1995). The longitudinal sheet-like bodies, which extend over the remainder of the line, are slightly upstanding features in largely acoustically structureless deposits which may be sheets of sand.

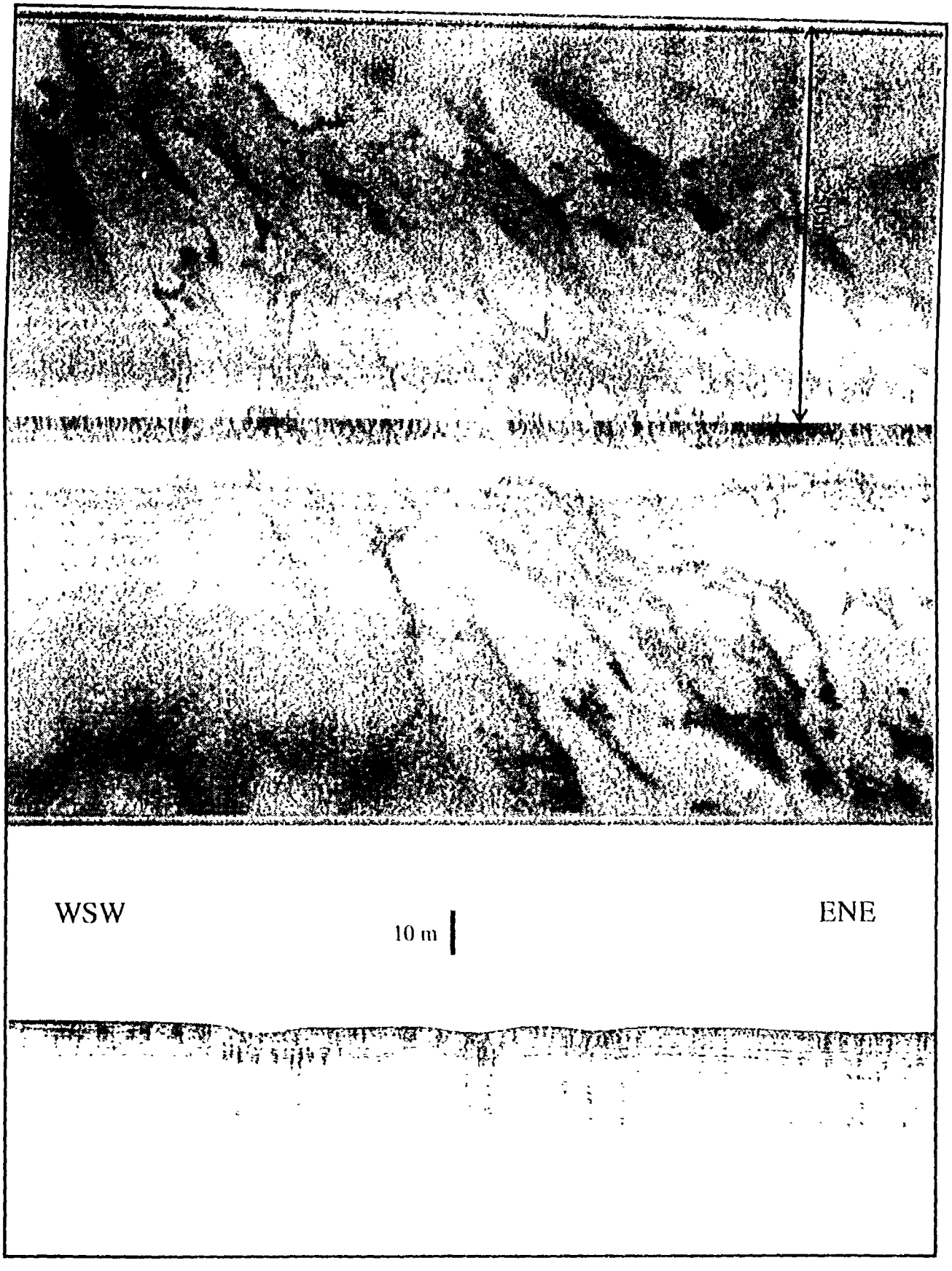

Fig. 62. Sonograph and profile of fields of rounded erosional scours. They are possibly in sands as evidenced by a 6 m thick structureless uppermost layer. MAK line 31

4. BOTTOM SAMPLING

J. van Hinte, B. T. Cronin, R. G. Lucchi, G.G. Akhmanov, E.M. Ivanova, A.A. Lototskaya, A.M. Akhmetzhanov, J. Millington, H. de Haas, J. de Koning, J. Clark, E.V. Kozlova, J. Rey, F. Perez, S. Morris, A. Oosting, J. van der Hoef, and E. Felser

a. INTRODUCTION

Leg 3 of cruise TTR-4 took 23 gravity cores (located on Figs. 50 and 53), recovering a total of 56 m of sediment, the oldest being of Late Pleistocene age (~140 ka). Core data are listed in Table 4, and shipboard analytical results are summarized in Figs. 64 and 66 to 82.

The main objectives of seafloor sampling were:
(i) to sedimentologically calibrate the acoustic facies of OKEAN and MAK-1 sonographs from the distal parts of two turbidity current pathways.
(ii) to document lithofacies distribution and to determine sediment transport processes;
(iii) to collect a sedimentary record for "high resolution stratigraphic" analysis, aimed at helping to reconstruct the oceanographic history of the Western Mediterranean in the Late Quaternary.

The wide core barrel used by MSU on the R/V *Gelendzhik* is well suited for these sampling purposes: recovered core is little deformed, can retain pebbles, shows larger-scale sedimentary structures, and has ample material for intensive sub-sampling. However, when there is low recovery of non-cohesive material, the sediments can get mixed up, since they move freely through the water-filled liner in the large core barrel during hauling and desk handling. During the core extraction process the mixed sediments will be pushed together, producing a seemingly good, short core. Most cores were taken with the "long" gravity corer (6.5 m, 1500 kg), but where it failed to penetrate in the Balearic Basin (sites 149 and 150), attempts were made with a "short" version (2.0 m, 1500 kg) (sites 151 to 153), but without success.

Macroscopic core descriptions were made in the sunlight on deck. Shipboard sample analysis was limited to spot samples, taken in order to roughly "know where we are" with respect to sediment age and depositional environment. This knowledge was essential for the interpretation of the acoustic signals and for setting further coring policy. Of 56-m recovered section, we took 165 microfauna/microfacies samples for shipboard analysis, 161 lithologic smear-slides and 160 nannofossil smear-slides.

The "sedimentology/palaeontology team" produced two voluminous binders containing for each core or sample:
- lithology logs (scale 1: 5.6) per 60-cm section;

Table 4

Summary of coring operations on Leg 3 of TTR-4 Cruise

Core No	Latitude Longitude	Date GMT bottom deck	Depth (corr.)	Cable length	recovery in cm.	TD age uR	Setting
138 G	40°09.17 10°06.79	25.06 21:48 21:59	1370 (1407)	1400	516.0	*E. huxleyi* Z ~ 140 ka 3.9	E. of Sardinia on a small plateau at northern and deeper end of a ridge ("hill A") S. of Orosei Canyon.
139 G	41°30.41 08°15.74	28.06 19:37 19:51	2284 (2332)	2370	516.5	*E. huxleyi* Z ~ 125 ka 4.1	On the lower slope S.W. of Corsica, between Moines and Castelsardo canyons; low backscatter (light on MAK image).
140 G	41°30.16 08°15.64	28.06 20:42 20:57	2284 (2336)	2380	493.0	*E. huxleyi* Z	As above, S.W. of 139 G; high backscatter (dark on MAK image).
141 G	41°04.06 07°40.20	29.06 13:50 14:13	2773 (2834)	2970	347.5	*E. huxleyi* Z ~ 140 ka 2.5	N.W. of Sardinia in "high backscatter stringers" on MAK-28 line perpendicular to Nurra Escarpment. Proximal part of sandy turbidite lobe (?) on basin floor.
142 G	41°02.90 07°43.37	29.06 15:03 15:19	2774 (2835)	2900	440.5	*E. huxleyi* acme Z > 44	S.E. of 141 G also in "high backscatter stringers" on MAK-28 line.
143 G	41°02.40 07°44.03	29.06 16:05 16:24	2780 (2841)	3000	500.5	*E. huxleyi* acme Z > 50	S.E.of 142 G and also in "dark stringers" on MAK-28 line.
144 G	41°01.58 07°46.15	30.06 10:50 11:07	2772 (2833)	2900	149.0	*E. huxleyi* Z ~ 120 ka 1.2	N.W. of Sardinia, S.E. of 143 G slightly off MAK-28 in low backscatter area. On basin floor near "stringers".
145 G	40°56.12 07°41.33	30.06 12:29 12:45	2776 (2837)	2904	577.5	*E. huxleyi* Z	N.W. of Sardinia in a low backscatter area on MAK-29 on basin floor near foot of slope.
146 G	40°54.10 07°42.44	30.06 13:53 14:12	2780 (2841)	Not regist.	416.5	*E. huxleyi* Z	S.E of 145 G in mottled backscatter area on MAK-29 on basin floor nearer to the base of the slope.
147 G	40°47.82 07°45.85	30.06 15:32 15:57	2638 (2696)	2700	492.0	*E. huxleyi* Z ~ 125 ka 3.9	S.E. of 146 G in a low backscatter area on MAK-29 on the lower slope.
148 G	40°44.23 07°47.74	30.06 16:42 16:54	2496 (2552)	Not regist.	18.0	*E. huxleyi* acme Z > 1.8	S.E. of 146 G in a high backscatter area on MAK-29 at the mouth of a gully on a steep part of the slope of Nurra Escarpment.
149 G	39°38.92 06°01.07	02.07 12:37 12:55	2811 (2873)	Not regist.	49.0	*E. huxleyi* acme Z > 4.9	Basin floor. At distal end of area with fishbone acoustic pattern on OKEAN as well as on MAK-1 sonographs
150 G	39°41.01 05°53.15	02.07 14:11 14:26	2796 (2858)	Not regist.	41.0	*E. huxleyi* acme Z > 4.1	As site 149

depth and cable length in meters

Table 4. Continuation

Core No	Latitude Longitude	Date GMT bottom deck	Depth (corr.)	Cable length	recovery in cm.	TD age uR	Setting
151 G	39°41.00 05°53.14	02.07 15:03 15:19	2793 (2854)	Not regist.	33.0	*E. huxleyi* acme Z > .3	As site 149 G
152 G	39°44.74 05°50.88	02.07 16:24 16:40	2793 (2855)	Not regist.	140.0	*E. huxleyi* acme Z > 14	Basin floor, in fishbone pattern with V's pointing upstream
153 G	39°38.04 06°02.63	03.07 12:39 12:54	2800 (2861)	Not regist.	60.0	*E. huxleyi* acme Z > 6.0	As site 149 G
154 G	40°38.48 04°58.86	04.07 12:04 12:23	2691 (2751)	2810	4.0	no sample	Distal end of Rhône lower fan.
155 G	40°37.80 04°59.82	04.07 13:20 13:37	2643 (2702)	2789	498.5	*E. huxleyi* Z ~90 ka 5.5	On top of seafloor high (Millington Dome = saltdome on seismics) to recover hemipelagic section.
156 G	40°35.96 04°57.49	04.07 14:40 14:55	2701 (2762)	2920	4.0	no sample	Valencia Channel floor in acoustic facies of fine dark/light stringer pattern (downslope stream pattern)
157 G	40°30.00 04°55.76	04.07 16:14 16:33	2718 (2778)	2849.5	196.0	*E. huxleyi* acme Z > 20	As site 156
158 G	40°26.13 04°53.98	04.07 17:28 17:46	2726 (2786)	2850	96.0	*E. huxleyi* acme Z > 9.6	As site 156
159 G	40°27.29 05°09.36	05.07 11:20 11:40	2729 (2789)	2824	10.0	*E. huxleyi* acme Z > 1.0	As site 156
23 cores			max. (2873)		total 5599 cm		Average recovery =243 cm per core

depth and cable length in meters

- standard sample description form 1, recording the microfauna and microfacies that was found in washed residues (>63 μm);
- standard sample description form 2, recording the nannoflora and mineral composition of smear slides;
- standard completed Sample Registration Forms, listing all samples (including core length subsamples in plastic trunking) taken for shore-based analysis.

Scientists and students discussed their analytical results to produce the mutually agreed core summary logs like the one of core, 138G (Fig. 64). Summary logs of cores 139G to 158G are included in Section III.4.c "Ground-truthing" MAK-1 profiles.

Leg 3 coring sites are located in three areas:
(1) east of Sardinia in the peri-Tyrrhenian Sardinia Basin (site 138); this core, although located in Study Area 2, is described in this chapter because it was taken on Leg 3, during the transit to Study Area 3;
(2) west of north Sardinia and the Bonifacio Strait (sill depth ~50 m) in the Corso-Ligurian Basin (sites 139 to 148) = Study Area 3a;
(3) east of Menorca in the Balearic Basin, in the lower reaches of the Valencia Channel (sites 149 to 159) = Study Area 3b.

b. CORING RESULTS

Most of the 23 cores largely consist of upper Pleistocene and lower Holocene gravitites - showing a rich and significant variety of turbidites, mass flows, grain flows, etc. - and are topped by upper Holocene hemipelagic mud. Average (uncorrected) accumulation rates can surpass 50 cm/ka. Cores 138G, 139G, and 155G recovered "continuous" hemipelagic mud sections with an (uncorrected) average accumulation rate of ~4 cm/ka, probably recording Termination II (~125 ka).

Area east of Sardinia (core TTR4-138G)

No coring had been planned for this part of the leg. However, on our way to Area 3 we had to pass the Bonifacio Strait by daylight, which allowed time to take one gravity core in the western Tyrrhenian Sea.

We used this opportunity for two reasons:
- to obtain a Late Quaternary record in the western Tyrrhenian Sea for high resolution stratigraphic analysis;
- to recover a core for the "sedimentology - palaeontology team" to get to work and learn shipboard procedures.

The core was taken on a high to stay away from turbidites and scouring, but as deep as we possibly could find a seafloor elevation en route to the Bonifacio Strait in order to sample a record of changing bottom water conditions, such as the periods of sluggish circulation, which produced the sapropels of the Eastern Mediterranean.

To avoid coring on the crest of a high, where the sediment might be winnowed, the chosen site was the low, northern end of the elevated ridge referred to as "Hill A" by Fabbri and Nanni (1980), just after passing its crest, where the echosounder showed a small plateau (Fig. 63a, b, and c). We recovered 5.16 m of hemipelagic mud ranging back to the "isotope stage" 6/5 boundary, or Termination II (Fig. 64). With its ~4 cm/ka accumulation rate the core will be ideally suited for high resolution stratigraphic analysis.

Corso-Ligurian Basin (cores TTR4 139G to 148G)

Coring objectives in this area were to sedimentologically calibrate the acoustic facies seen on the GLORIA sonographs and further mapped during Leg 3 with OKEAN (lines PS-146 and 147) and MAK-1 (lines 27 to 29). Cores were taken at basin floor, rise and lower slope settings, just south of the Ajaccio Canyon and in and near smaller canyons running down the Nurra Escarpment (Figs. 50 and 65) These canyon-fed continental rise systems in their turn feed the large-scale transport route that runs from the Ligurian Sea (including the Var Fan) down into the Corso-Ligurian Basin.

With the exception of the 18-cm long core 148G, which bottomed in pebbles, we had excellent recovery (average 437 cm for the other nine cores). The cores contained a large variety of gravitites, such as sand turbidites, sand-supported mass flows, and mud-supported mass flows with colourful rip-up clasts. The top of all cores consists of Holocene hemipelagic mud showing that the system is less active, or even inactive since the post-glacial sea-level rise. The slightly higher upslope site 139 seems to have only received the very fine end of gravity flows, as recorded in its "complete" hemipelagic mud section (total age ~125 ka), which provides a good basis for paleoceanographic study.

Distal Valencia Channel (cores TTR4 149G to 159G)

This area lies in the mouth of and beyond the Valencia Channel, which is at the confluence of sediment paths from the slopes of southeast Spain and the western Rhone (Fig. 53). The acoustic facies of the broad, shallow (~30 m deep) channel shows a pattern of narrow stripes, parallel to the current direction, which changes downflow into a large "fishbone" (or "chevron") pattern (with the V's pointed upstream) to a further downstream change into a finer "fishbone" patterns (see Chapter III.3.b).

Upstream (patchy) and downstream (striped) sonograph patterns (cores 154G and 156G to 159G respectively) were cored. Core 154G was taken by accident off the high, missing the intended top of the Millington Dome, a seafloor high caused by a salt diapirism (visible on seismic section). It only recovered some 4 cm of Holocene mud in the core catcher and a bit of fine sand. Apparently, the core barrel could not penetrate the sands lying under a thin veneer of upper Holocene hemipelagic mud. The presence of distal turbidite sands was confirmed in cores 156G to 159G, one of which recovered up to 6 turbidite sand layers.

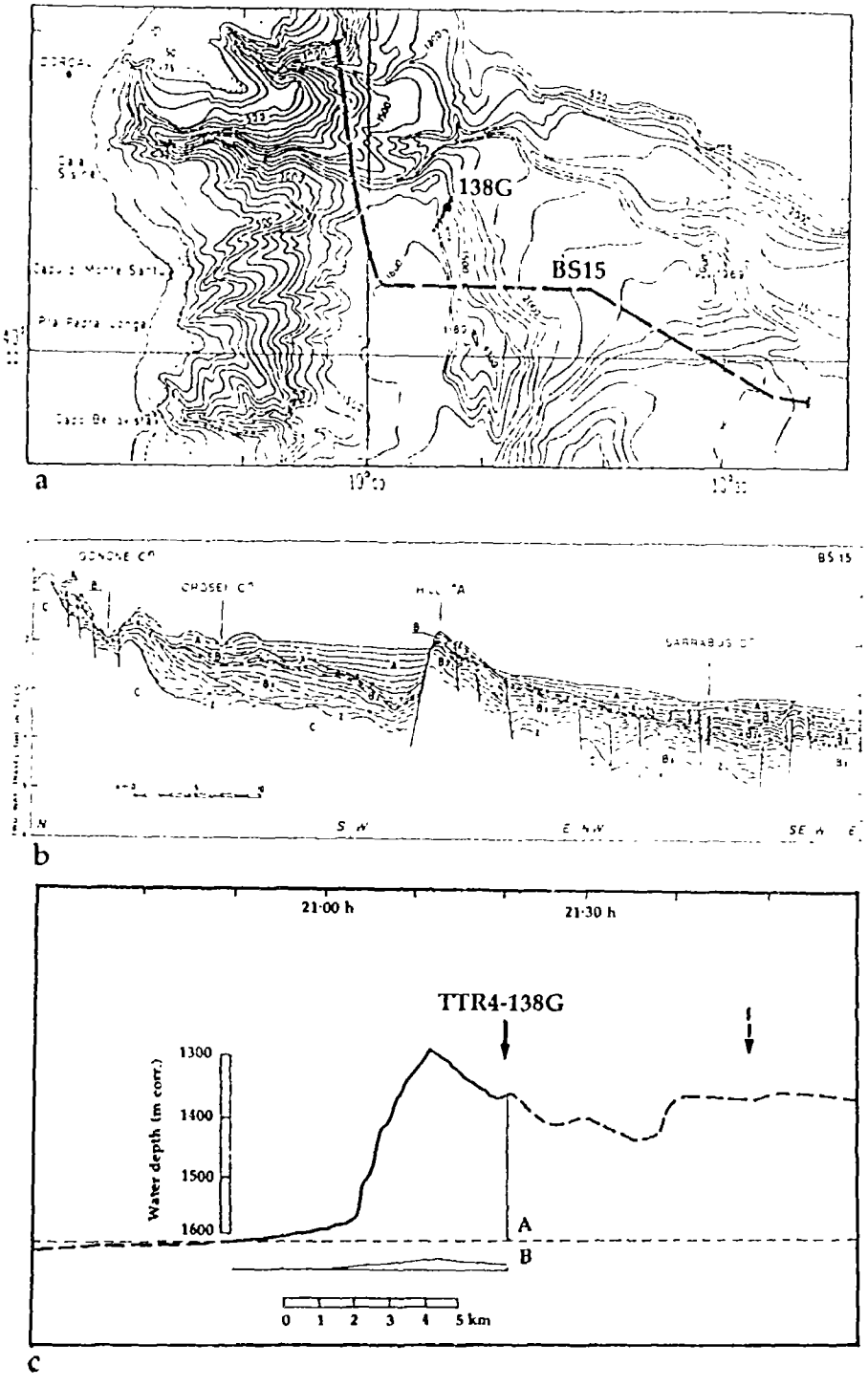

Fig. 63. a: Location of sampling station 138 on the physiographic map of the northern part of peri-Tyrrhenian Sardinia Basin. Also shown are the location of seismic profile BS15 of Fig. 63b (dashed line) and the echosounder profile of R/V *Gelendzhik*'s approach to site 138 (dotted line). Bathymetry in metres. Map and position of BS15 line from L. Casoni (in Fabbri and Nanni, 1980). b: Position of "Hill A" on seismic profile BS15 (after Fabbri and Nanni, 1980). A - Pleistocene-Recent, B - Neogene, C - "basement". X - Plio-Pleistocene unconformity (base glacial), Y - top of the Messinian evapotites, Z - top of "basement". c: Bathymetric profile over the norther tip of "Hill A" on the approach to core site 138. Routine echosounder profile with vertical exaggeration of 1:17 is shown above, and the same but without vertical exaggeration is shown below

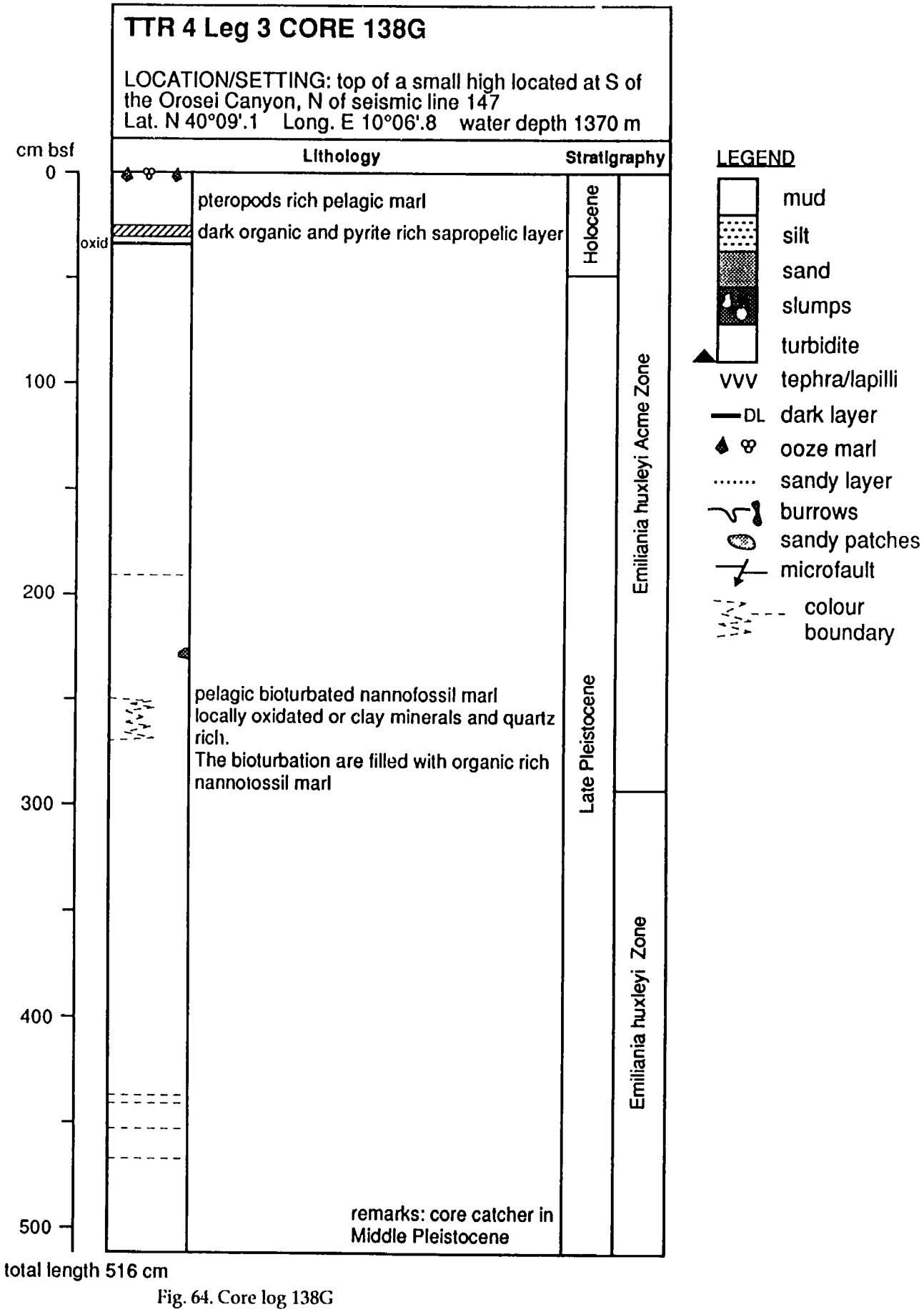

Fig. 64. Core log 138G

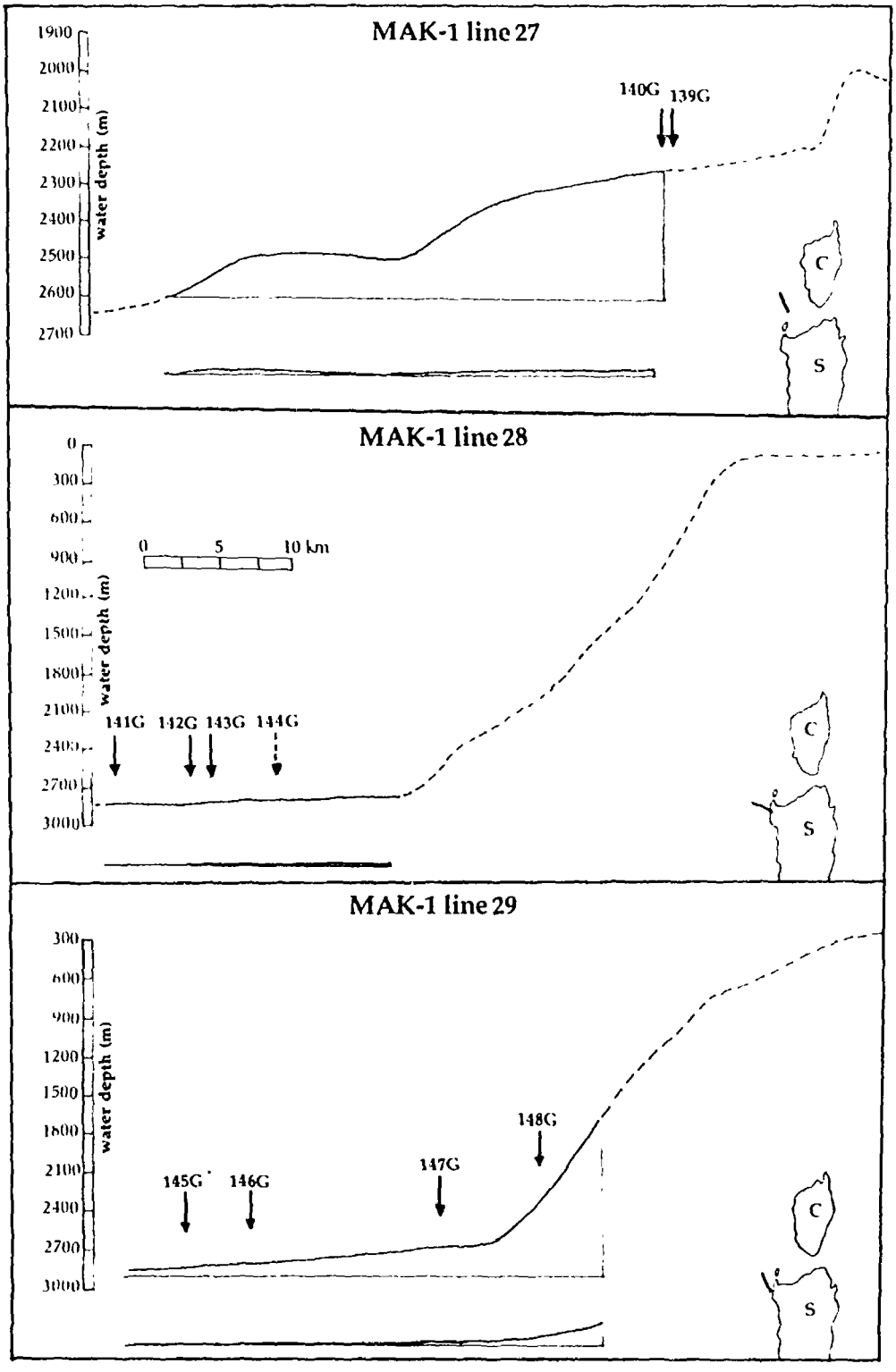

Fig. 65. Bathymetric profiles along MAK-1 lines 27 to 29 in Area 3a showing position of core sites 139 to 148. Also shown are the line locations with respect to Corsica (C) and Sardinia (S), as well as profiles without vertical exaggeration

We expected the sands to have been transported around the high, which then would have only received the tails of turbidites and pelagics. Indeed, core 155G (taken at the correct coordinates by using a pinger attached to the core barrel, so the ship could manoeuvre into position) recovered about 5 m of hemipelagic mud, the bottom of the core being at least 90 ka old. This was our third high resolution record for paleoceanographic study. Cores 149G to 153G were taken to sedimentologically calibrate the fishbone sonograph patterns. Although we had poor core recovery (Table 4), it became apparent that, in contrast to the eastern margin of the Balearic Basin, distal turbidite deposition has remained active in the area well into the Holocene.

Because the "long" gravity corer (6.5 m, 1500 kg) failed to penetrate in the Balearic Basin (sites 149 and 150), attempts were made with a "short" version (2.0 m, 1500 kg) (sites 151 to 153). Sands in the cores or core catchers suggested that the poor penetration and high reflectivity are due to the presence of compact sand layers underneath a thin veneer of upper Holocene hemipelagic muds or without any veneer at all (as had been suspected from the acoustic facies patterns). A high-stand systems track should be deposited after the time of maximum flooding surface of post-glacial sea-level rise. In the western part of this area the distal system appears to have remained active throughout most of the Holocene, while the eastern part died with the sea-level rise.

c. "GROUND-TRUTHING" MAK-1 PROFILES

B.T. Cronin and R.G. Lucchi

Corso-Ligurian Basin

Three MAK-1 deep-towed sidescan profiles, 27, 28 and 29, were run across areas of interest off the Corso-Sardinian margin. Ten gravity cores, 139G-148G, were collected to calibrate the acoustic facies observed on these profiles with the sediment recovered from the cores. The total recovery of sediment was 39.61 m. The cores for each MAK-1 line are described below.

MAK-1 line 27 (Fig. 66)

This line was run along the lower slope off southwestern Corsica. Near the southern end of the line, the light toned areas of relatively low-backscattering were replaced by an area of high-backscattering, and a gravity core was collected from each type to attempt to discover the reason for this difference in acoustic signature (cores 139G and 140G).

Core 139G (516.5 cm), from an area of low acoustic backscatter, consists mainly of pelagic nannofossil marl, with localized dark biogenic layers (Figs. 66 and 67), sandy foram bands and rare oxidized bands. One thin silty turbidite with reworked shallow-water fauna was recorded.

Core 140G (493 cm), from an area of high-backscattering, is again composed of mainly pelagic nannofossil marl (Figs. 66 and 68), but at the top is a unit of slope facies with disturbed and contorted pelagic marl layers and two levels of pebbles. The pebbles were found to be mainly flint and chert in hand specimen. Further analysis (from thin section) of these pebbles will be undertaken in Moscow. We interpreted this acoustic facies to be related to the presence of reworked material and pebbles in a disturbed slope facies, perhaps part of a larger slide.

MAK-1 line 28 (Fig. 69)

Four cores were collected from this area, west of Sardinia. On the OKEAN sonograph, the approaches to the abyssal plain are characterized by a stringer-like pattern of high acoustic backscatter. It is in the flow path of sediments that have come from southern France and from the canyons of western Corsica. The MAK-1 profile 28 showed this pattern in more detail, and four core sites were chosen to traverse the seafloor towards the slope, where the stringer pattern dies out.

Core 141G (347.5 cm) was the most basinward of the four cores (Figs. 69 and 70). It is mainly consists of terrigenous turbiditic sediments. The thickest turbidite sand is 2.5 m thick, comprised of terrigenous sand with shallow-water fauna, and towards the base it has biogenic mud chips. This unit overlies a muddy turbidite with reworked fauna.

Core 142G (440.5 cm) consists of four thin layers of pteropods in terrigenous clay that may be the slopeward continuation of the silty turbidites recorded at the top of core 141G. These turbidites are underlain be three terrigenous sandy turbidites, separated by occasionally thick pelagic intervals (Figs. 69 and 71).

Core 143G (500.5 cm) was taken in a zone of high backscatter. The core comprises a thick sandy turbidite involving large pelagic marl clasts and some smaller mud chips. The sand is medium to coarse and structureless. This overlies a smaller sandy/silty turbidite, which corresponds to a minor or more distal event. The rest of the sequence comprises mainly pelagic and hemipelagic sediment (Figs. 69 and 72).

Core 144G (149 cm) is the shortest of the four cores recovered in the transect, and was taken from the zone of weak backscatter at the base of the slope of the Sardinian margin, corresponding to what has previously been interpreted as a debris flow. It is mainly pelagic with one relatively thin sandy terrigenous turbidite, rich in rock fragments (Figs. 69 and 73).

MAK-1 line 29 (Fig. 74)

Line 29 was run south of line 28, heading to the northwest, obliquely across the abyssal plain and up the slope of the Sardinian margin, as far as the mouth of an incised slope gully. Four cores were recovered.

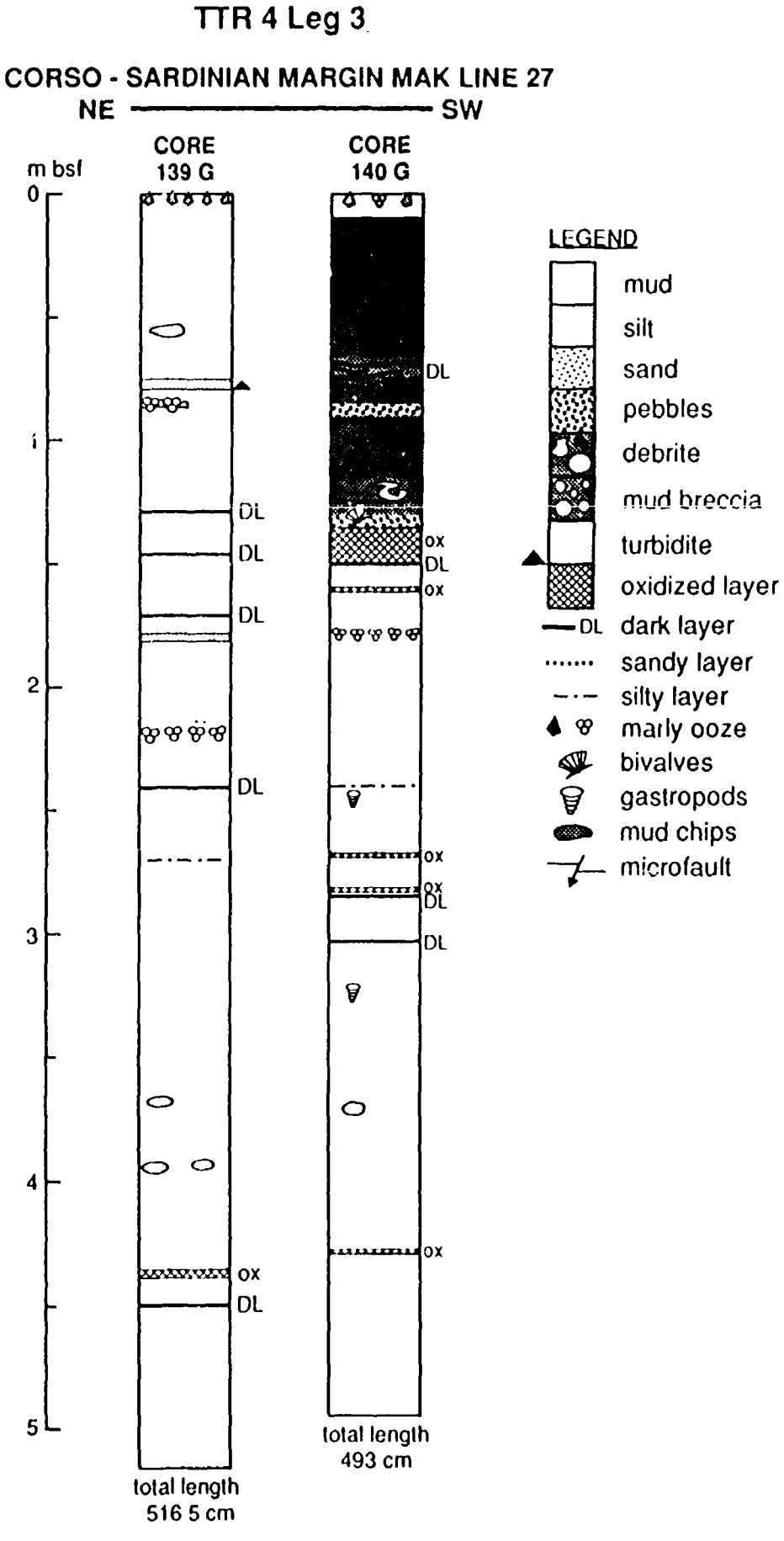

Fig. 66. Cores taken along MAK-1 line 27 in Corso-Ligurian Basin

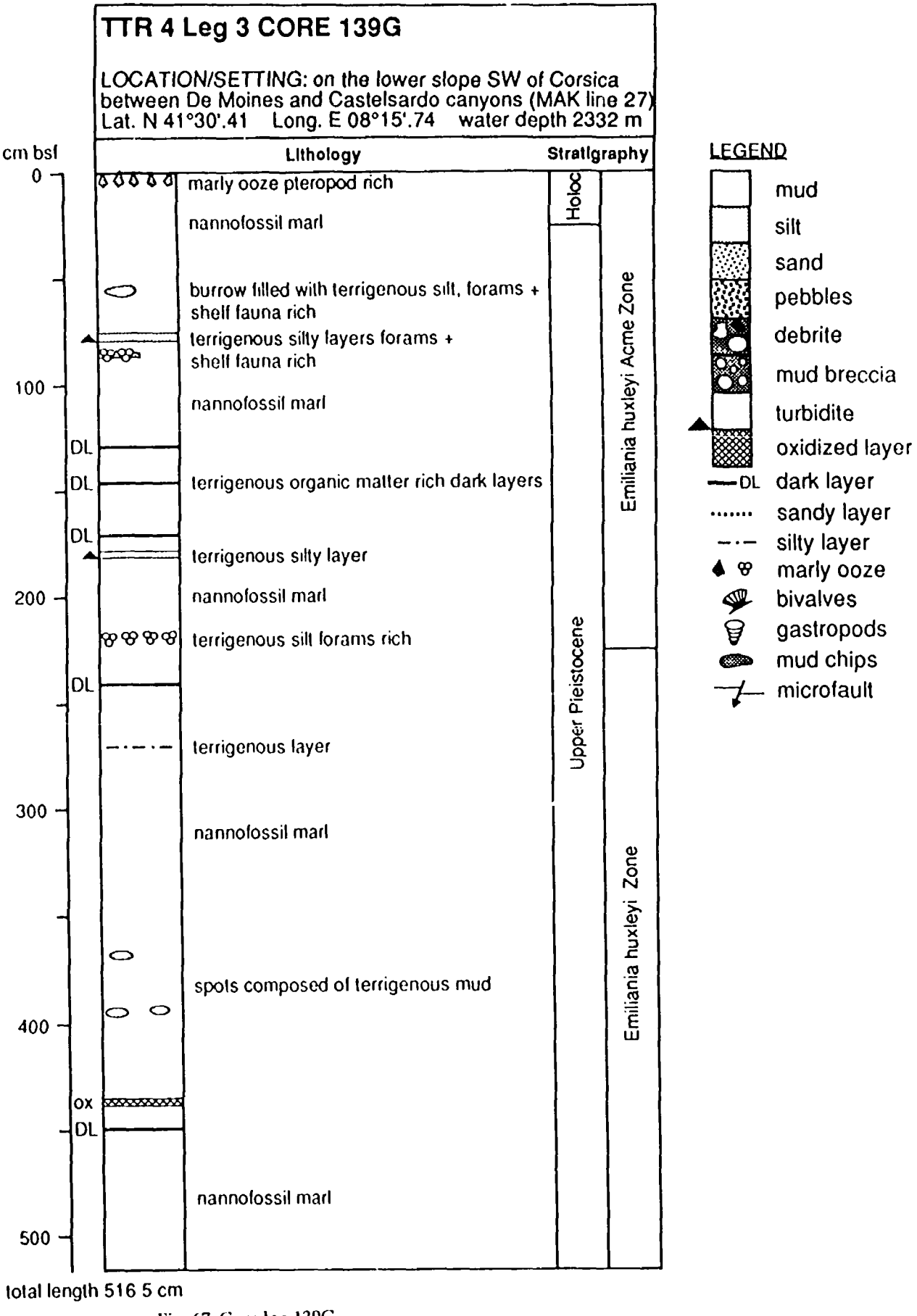

Fig. 67. Core log 139G

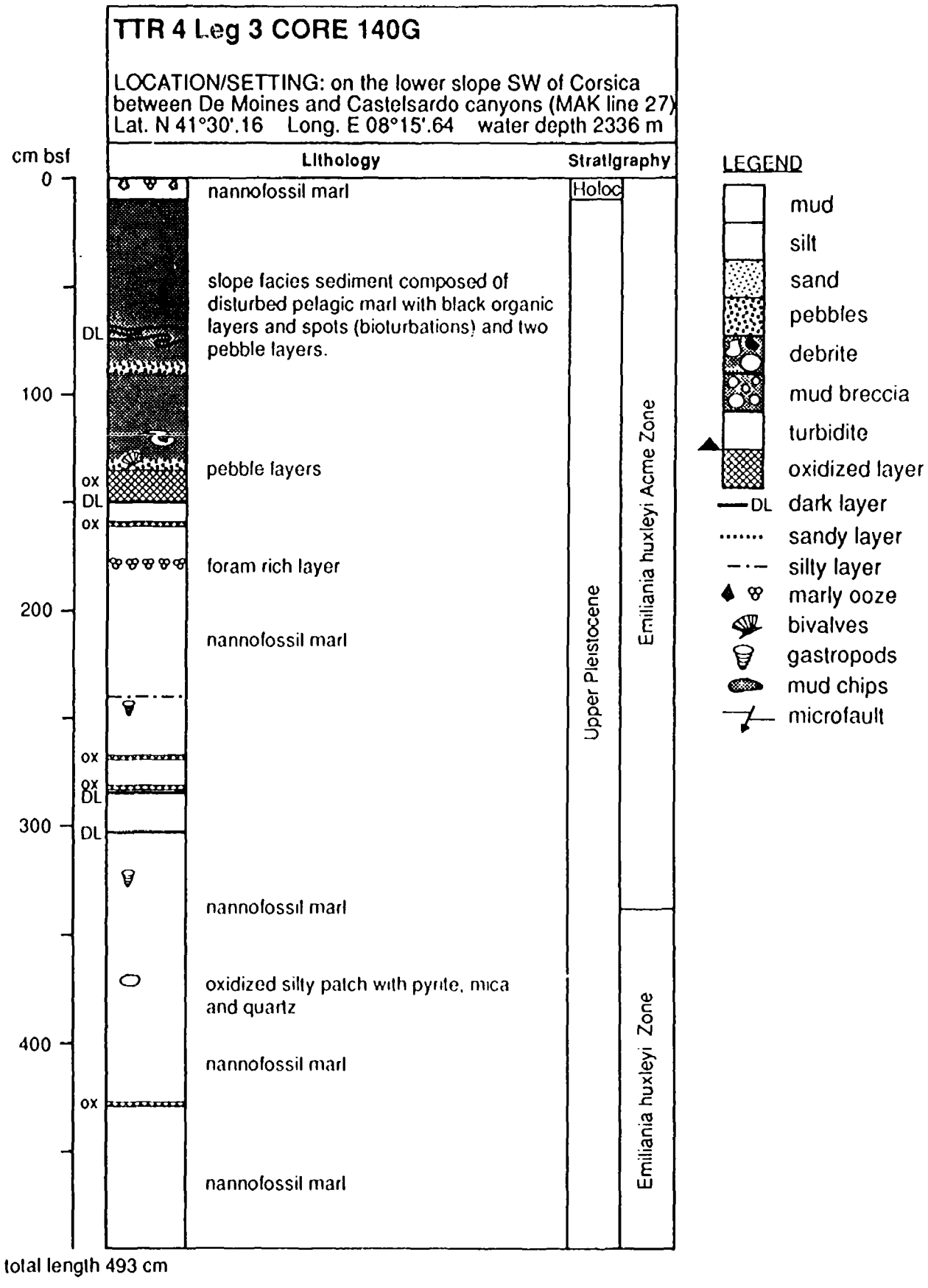

Fig. 68. Core log 140G

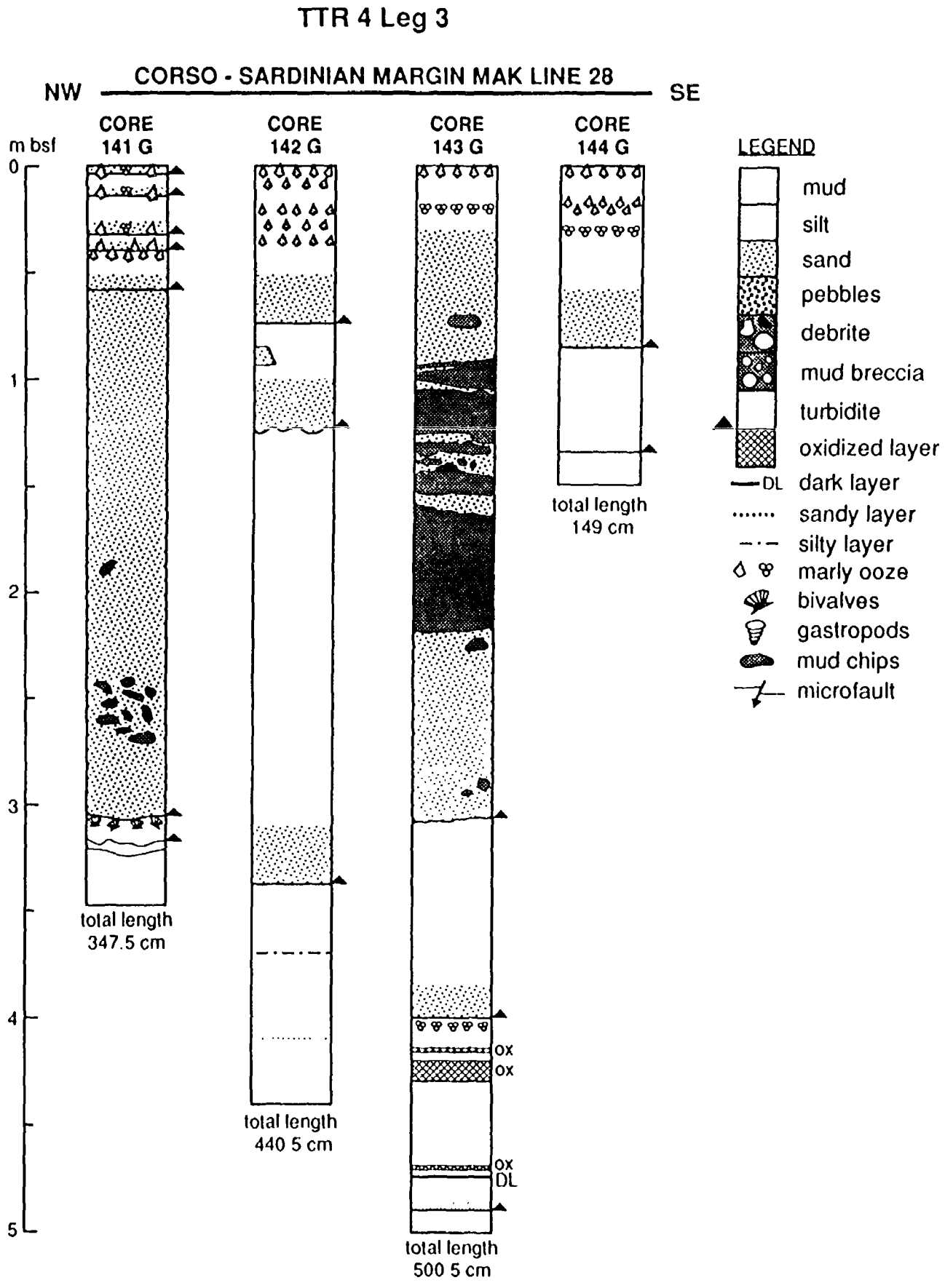

Fig. 69. Cores taken along MAK-1 line 28 in Corso-Ligurian Basin

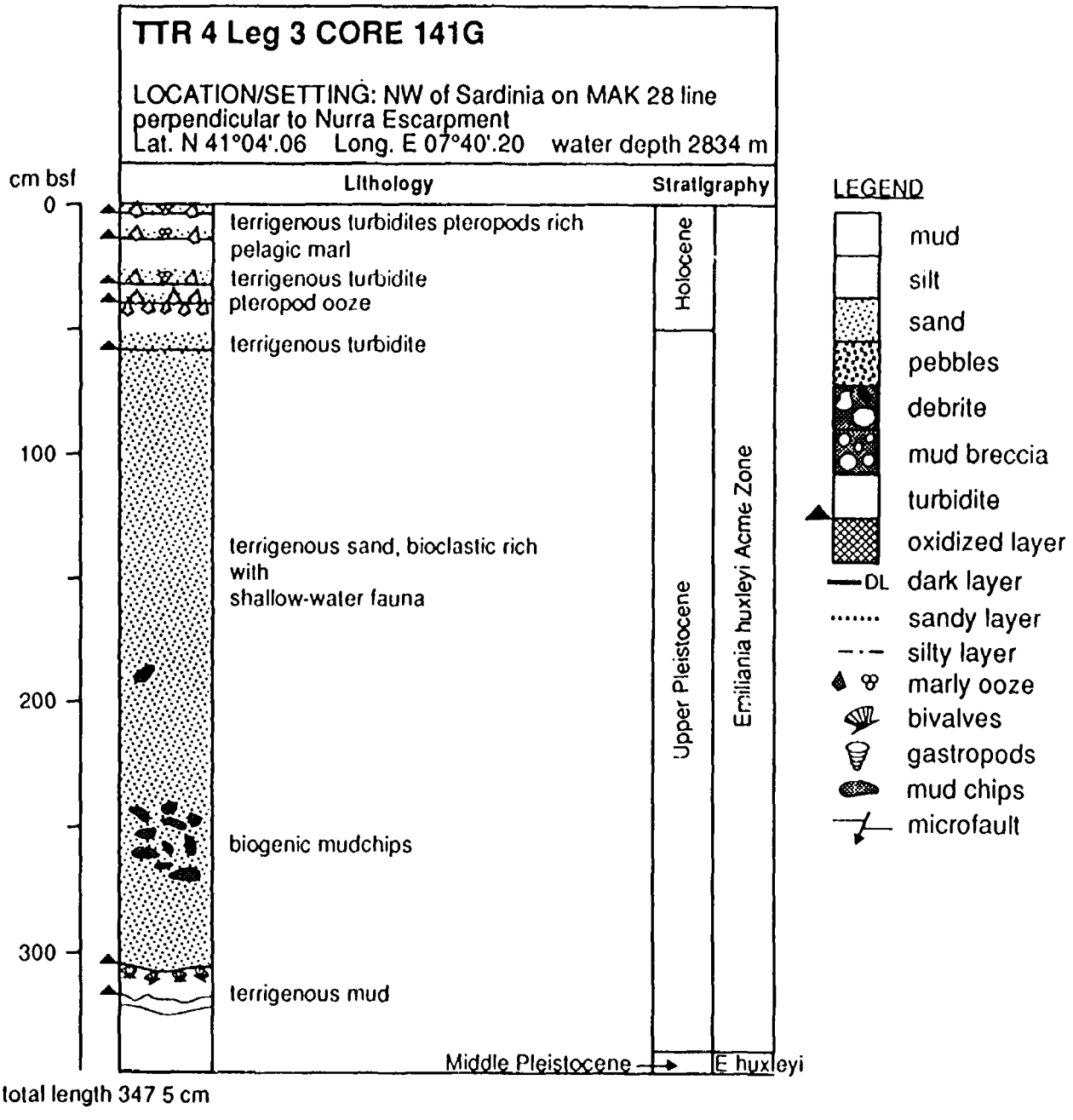

Fig. 70. Core log 141G

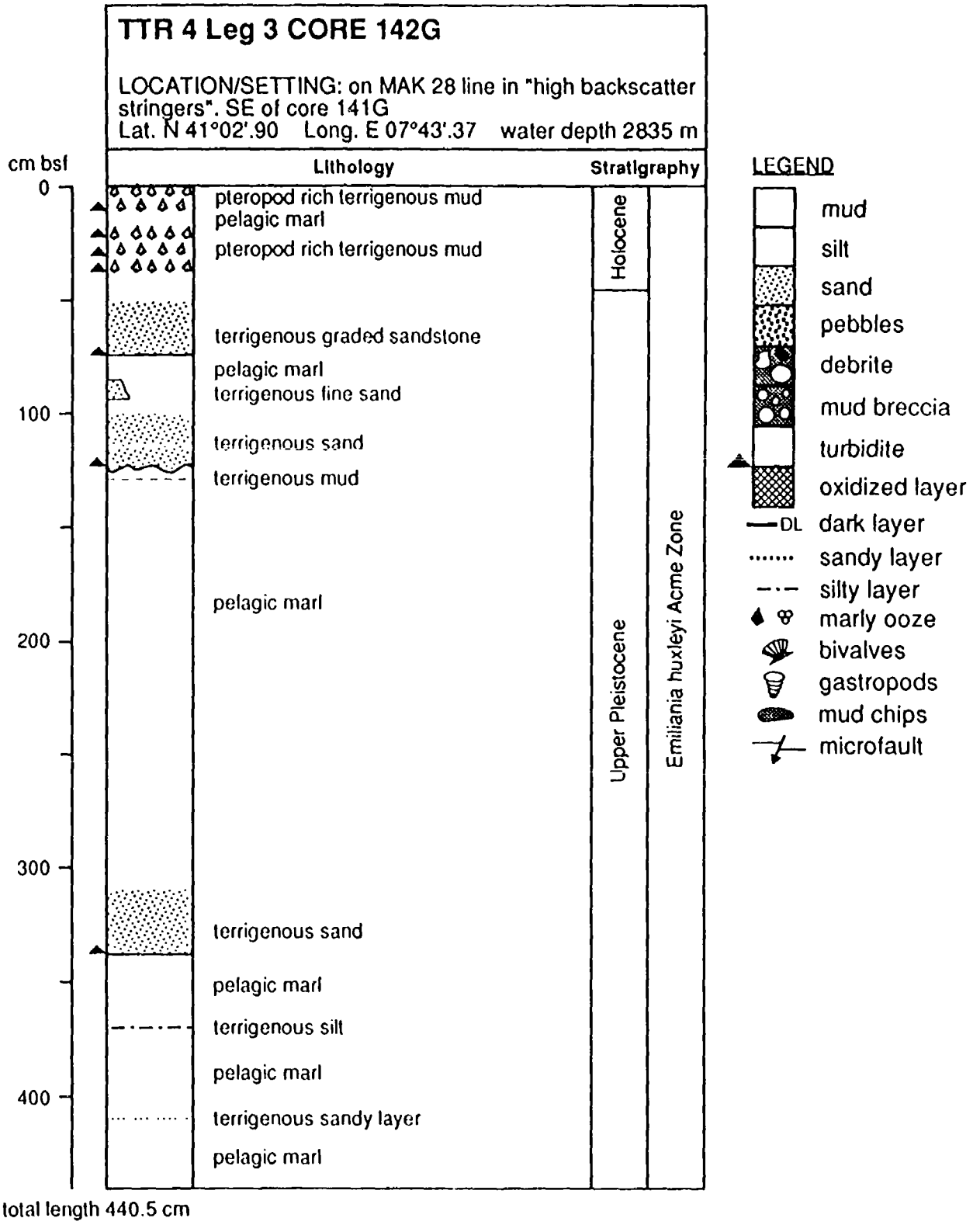

Fig. 71. Core log 142G

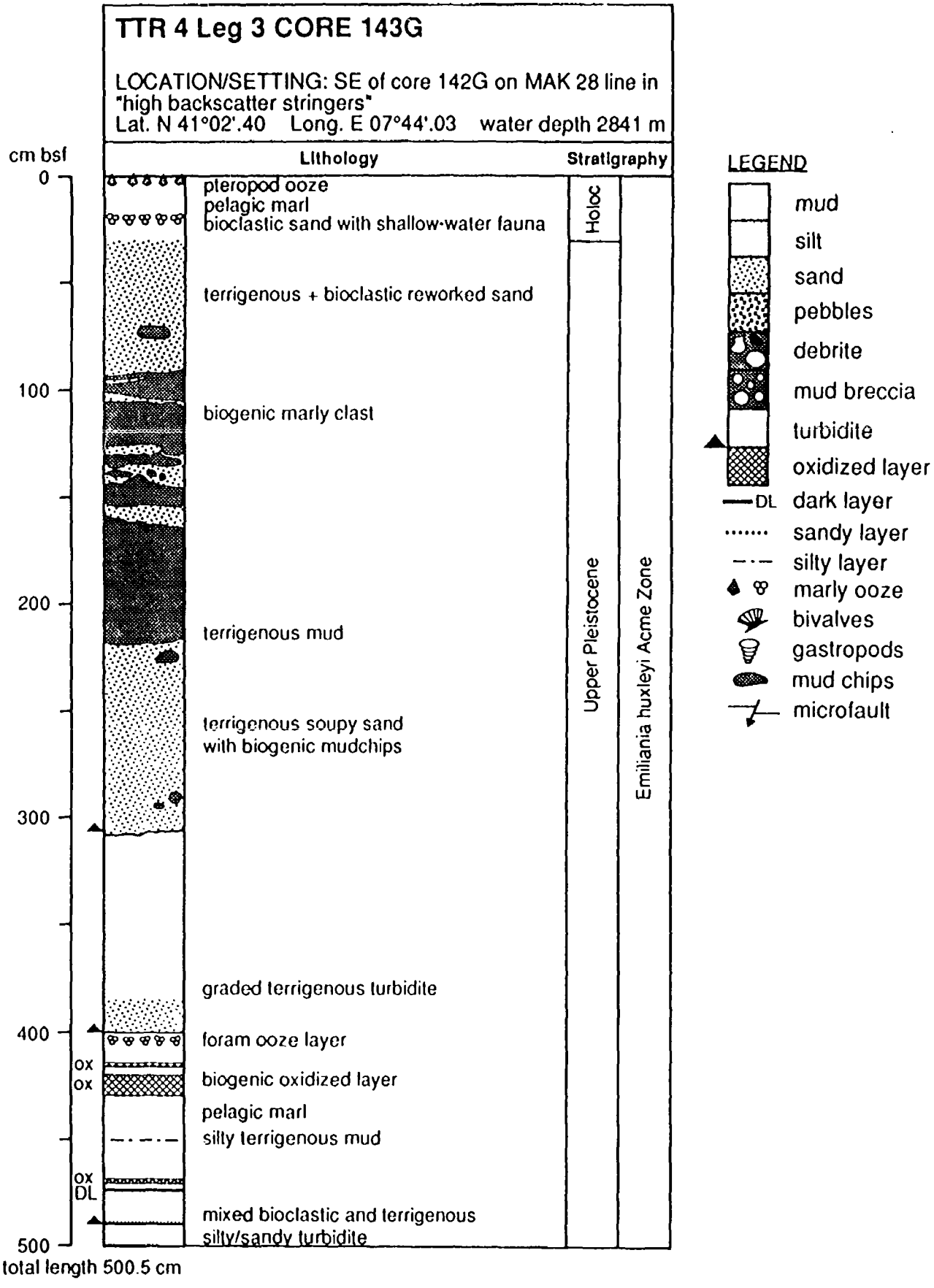

Fig. 72. Core log 143G

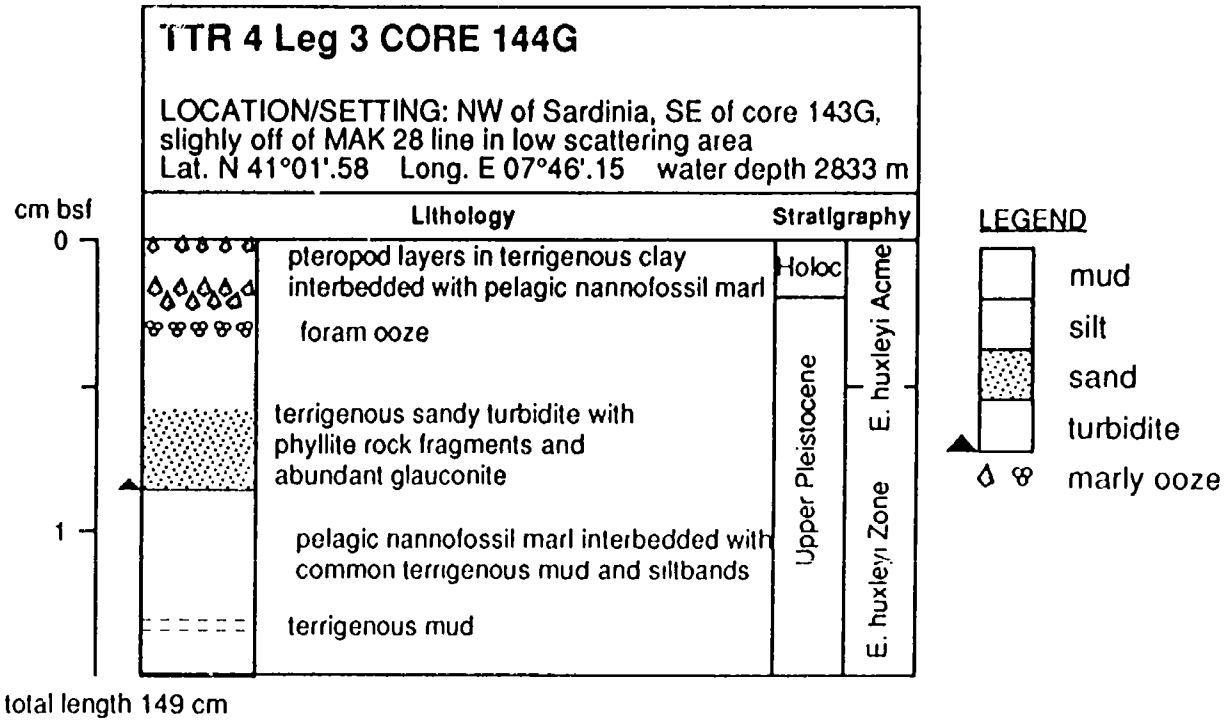

Fig. 73. Core log 144G

Core 145G (577.5 cm) is the longest core recovered in the area, and was taken in a zone of mottled acoustic character out on the abyssal plain. It is composed of a matrix-supported debrite with exotic clasts of broken up pre-lithified biogenic to terrigenous material and occasional pebbles of phyllite, which probably originated on the Sardinian margin. There are two other turbidites. The debrite is overlain by a thin terrigenous sandy turbidite, and underlain by a thick dark grey terrigenous/bioclastic turbidite with reworked shallow-water material (Figs. 74 and 75).

Core 146G (416.5 cm) was taken seaward of the break of slope on the MAK-1 profile, also in a zone of mottled backscatter. The sediment recovered consists of the same units as in core 145G, but the debrite has thickened towards the base of slope, as has the turbidite that overlies it, whereas the underlying turbidite has thinned (Figs. 74 and 76).

Core 147G (492 cm) is located on the lower slope in a zone of low backscatter. It is made up mainly of a very thick (over 3 m) unit comprised of four sub-units: (i) the two thin mud breccias, which are matrix-supported and contain rock fragments (talc, serpentinite, and phyllite); (ii) a debrite with exotic biogenic muddy clasts and terrigenous pebbles: (iii) terrigenous sand with biogenic mud clasts; and (iv) disturbed, faulted and slumped slope facies pelagic marl. The unit overlies a pelagic nannofossil marl with common, intermittent silty layers (Figs. 74 and 77).

Core 148G (18 cm) is the shortest core recovered in the area, and was taken at the mouth of a slope gully on the Nurra Escarpment, in a zone of very strong acoustic backscatter. It comprises pelagic marl but terrigenous pebbles were in the core catcher (1 to 5 cm in diameter) (Figs. 74-78).

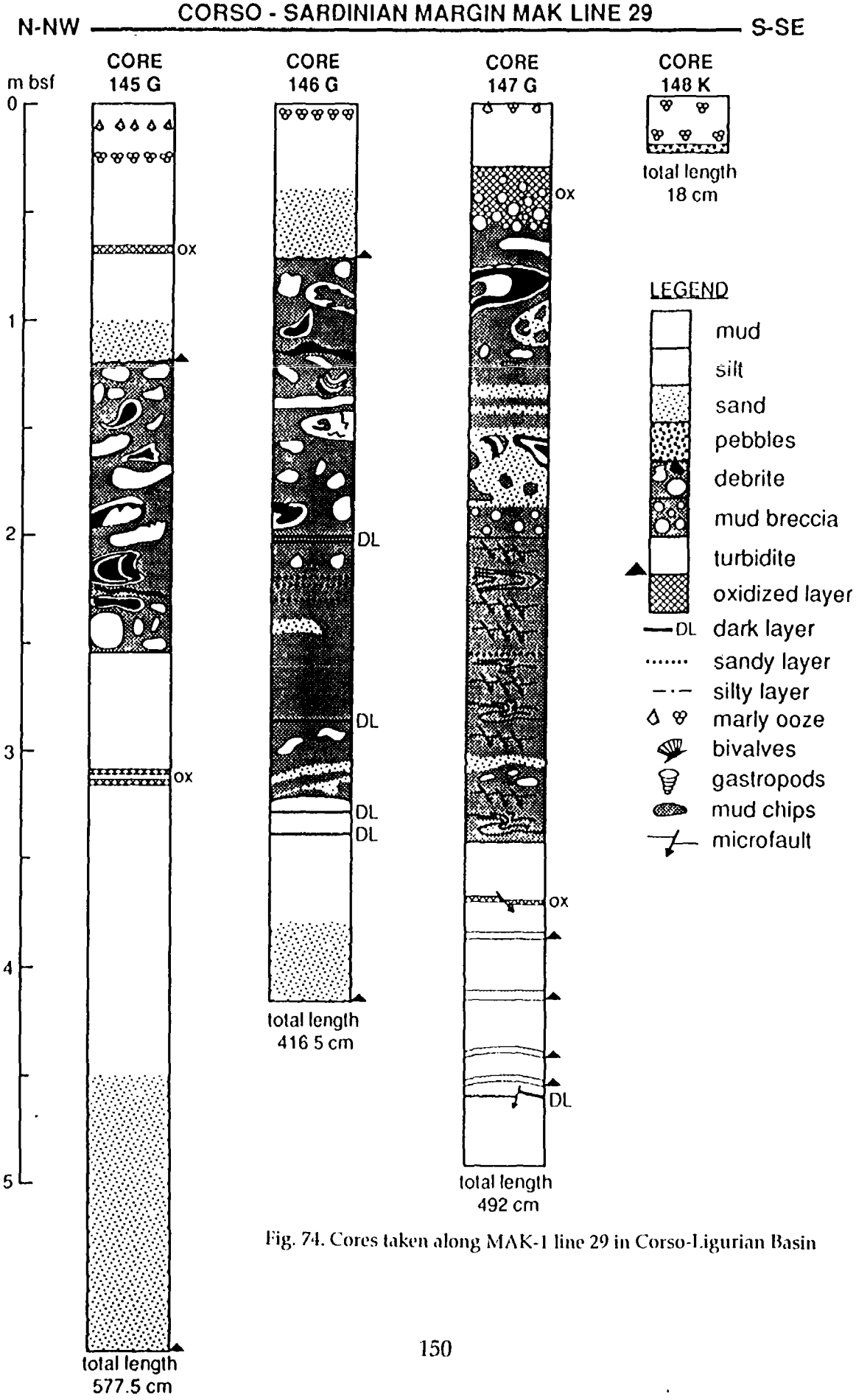

Fig. 74. Cores taken along MAK-1 line 29 in Corso-Ligurian Basin

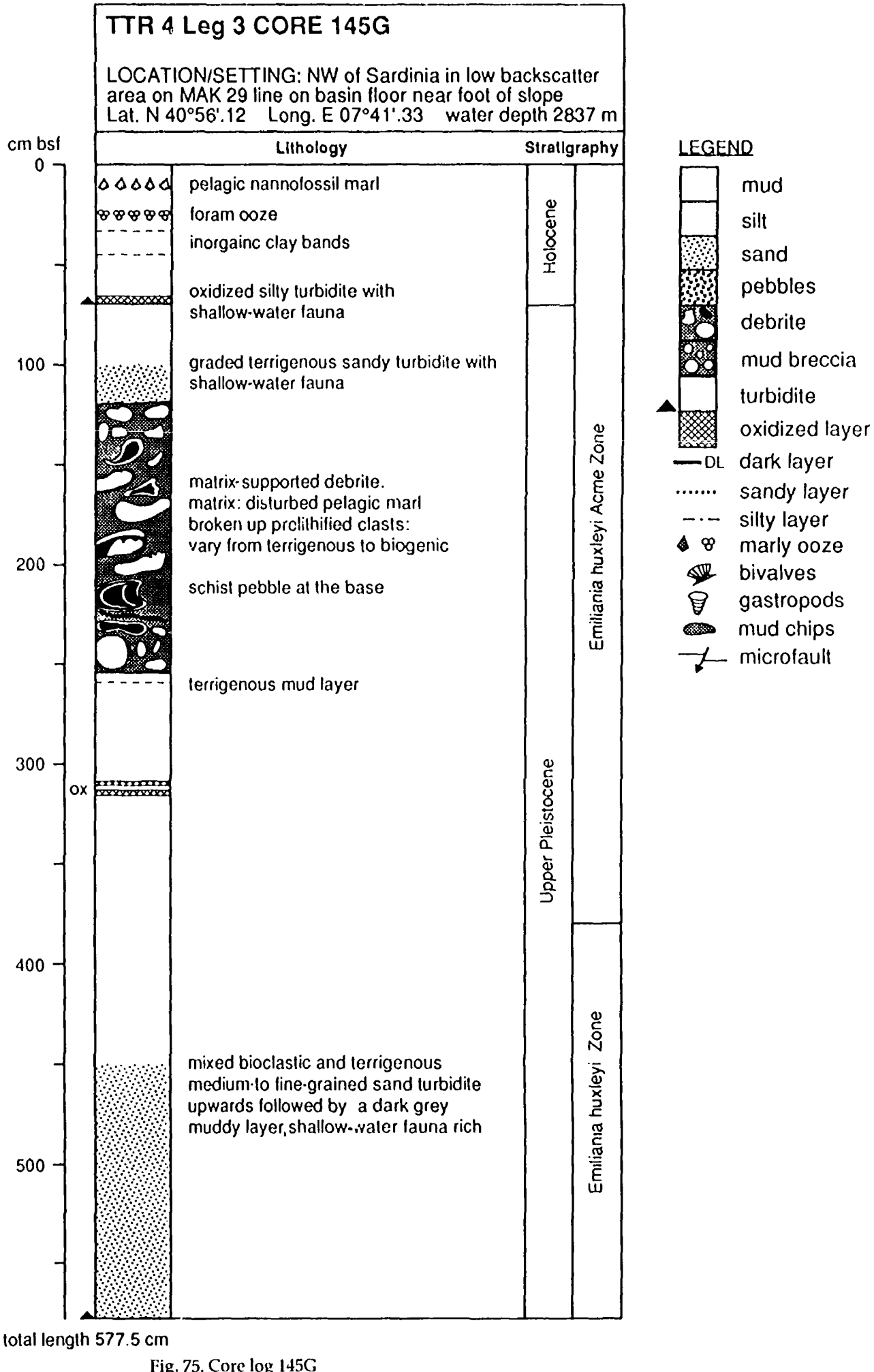

Fig. 75. Core log 145G

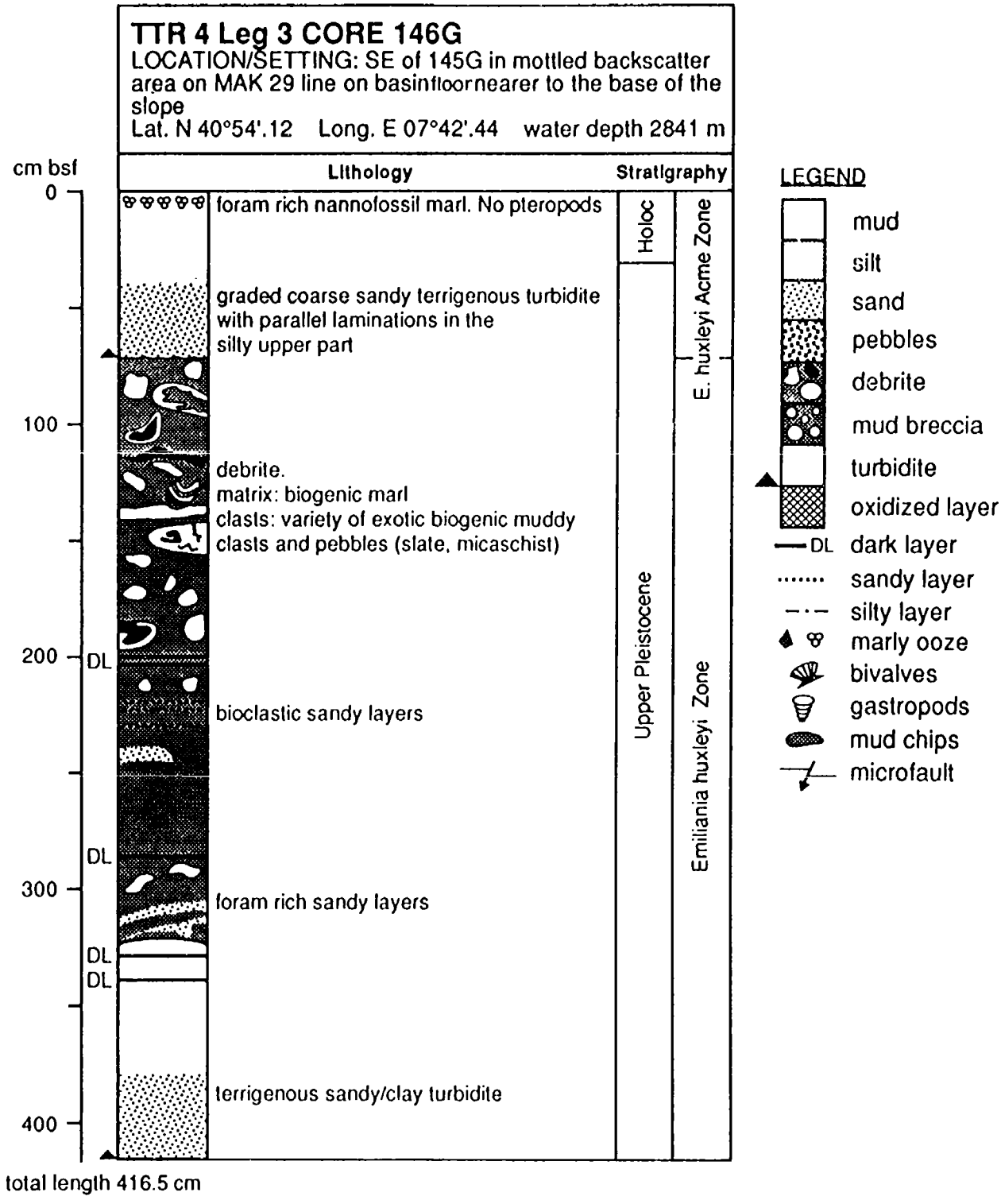

Fig. 76. Core log 146G

Valencia Channel

Cores 149G to 152G (Fig. 79 to 82) were recovered from areas of generally high acoustic backscatter on OKEAN and MAK-1 sonographs, and these areas were found to be sandy. Recovery was poor, mainly comprising pelagic sequences of Holocene - *Emiliania huxleyi* Acme Zone in age, except for cores 155G (Fig. 81) and 157G (Fig. 82), which recovered Upper Pleistocene sediments (in *Emiliania huxleyi* Zone).

A very thick pteropod layer was found in core 152G at 75 cm below the sea floor (Figs. 79 and 80). Core 155G (Figs.79 and 81) was collected at the top of a seafloor high, called the "Millington Dome" (a salt dome on the seismic record). This was the longest core recovered in area 3b, and is mainly composed of oxidized, nannofossil-rich marl interbedded with thin terrigenous silt layers which are locally pyrite-rich. The remaining four cores, 156 to 159G, were collected from the Valencia Channel mouth in zones of bedforms, mapped on sonographs. There was no recovery in core 156G. In core 157G (Figs. 79 and 82), several terrigenous turbidites with quartz, mica, calcite, and gypsum were encountered. In core 158G (Figs.79 and 82), only pelagic sequences were recovered.

d. BIOSTRATIGRAPHY

E.M. Ivanova and A.A. Lototskaya

The Late Quaternary climatic fluctuations determined by changes in foraminifera and coccolith assemblages in 21 cores were interrelated to the standard calcareous nannofossil zonation and used for biostratigraphic subdivision of the cores. For the methods of micropaleontological study see Chapter II.4.

Ten cores (139G to 148G) revealed sediments of Holocene age. Nine cores (139G-147G) extended to the Upper Pleistocene, three of which (139G, 144G, and 147G) almost reached the bottom of the Upper Pleistocene, and one (141G) attributed to the Middle Pleistocene (the base of the core is about 140 ka B.P. in age). The transition from the Middle to the Late Pleistocene is related to the beginning of Termination II (127 ka B.P.), coinciding with the 6/5e isotope stages boundary, and is dated as approximately 125 ka B.P. (Shackleton and Opdyke, 1973) (Figs. 67, 68, 70 to 73, and 75 to 78).

Termination II marks the period of rapid global warming from the peak of the glaciation (132 ka B.P.) to the Riss-Würm interglacial peak at 120 ka B.P. and, in the Western Mediterranean, corresponds to the Sapropel S-5 accumulation in the Eastern Mediterranean. Thus, this part of the Upper Pleistocene in the cores is characterized by warm-water foraminifera and calcareous nannofossil assemblages (see Chapter II.4). In addition to the Holocene, the calcareous nannoplankton assemblage here is rich in "small" Gephyrocapsa's.

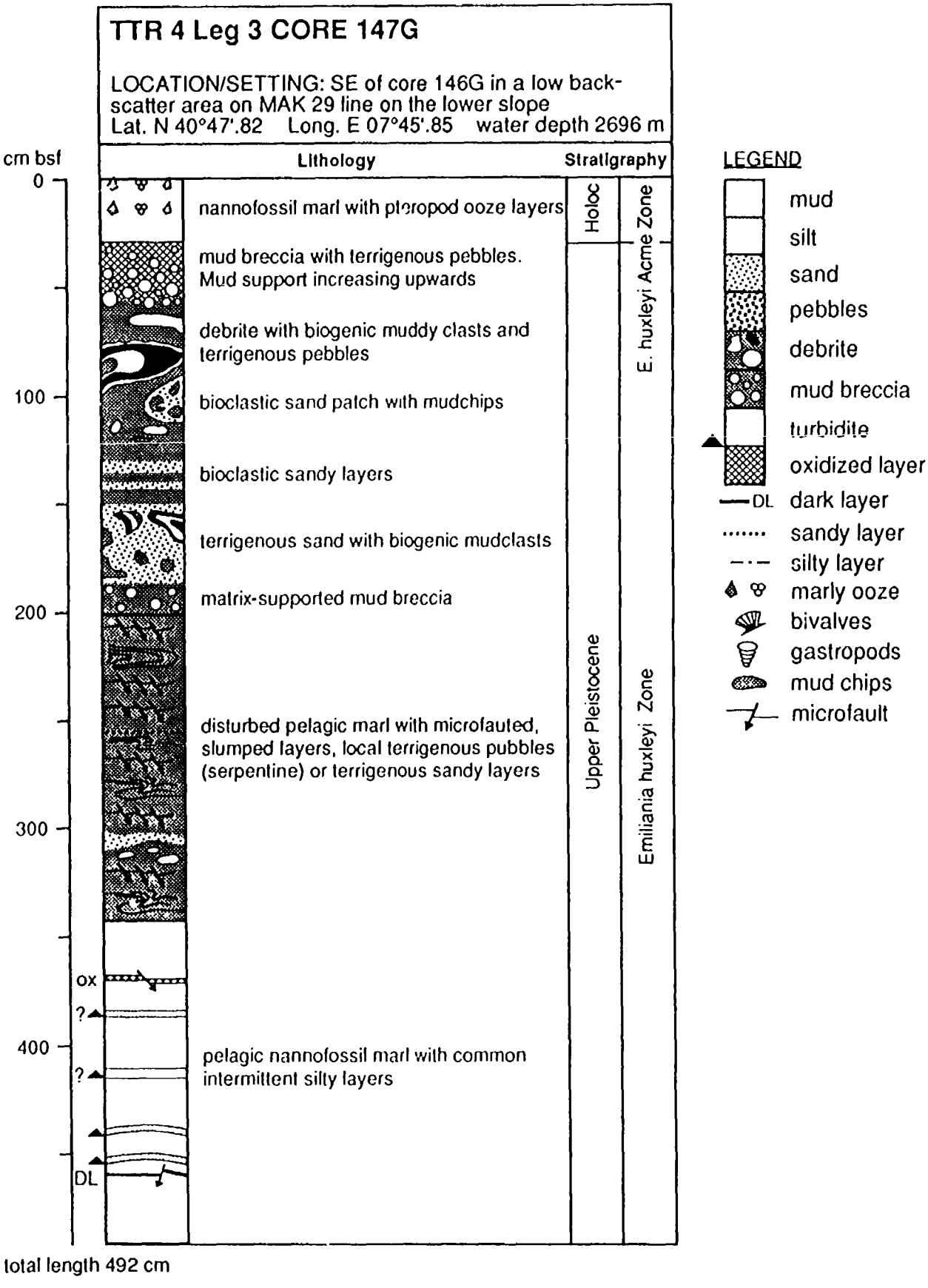

Fig. 77. Core log 147G

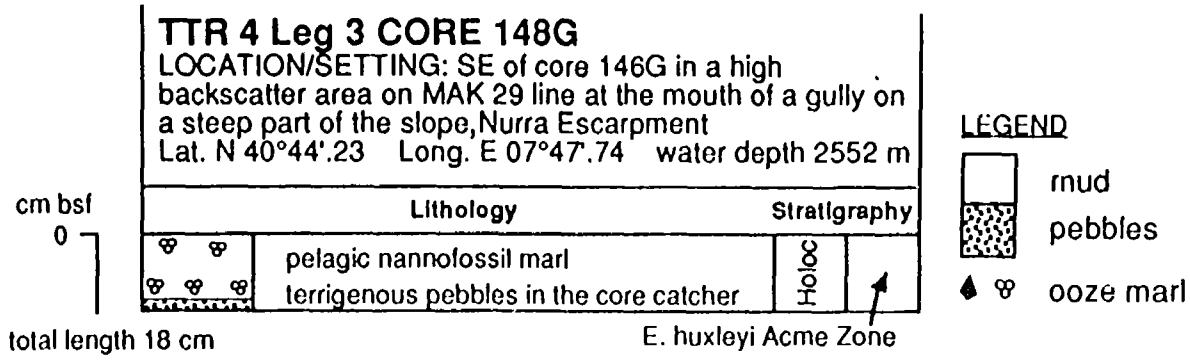

Fig. 78. Core log 148G

Corso-Ligurian Basin

Sediments of the investigated cores from the Corso-Sardinian margin do not extend below the *Emiliania huxleyi* Zone: 3 out of 10 cores bottom within the *Emiliania huxleyi* Acme Zone, the other 7 do not reach it. Clay clasts and pebbles of 3 cores (145G, 146G, and 147G) were studied in detail for calcareous nannofossils and foraminifera when it was possible. They are mostly Late Pleistocene in age. Some of the clasts are represented by Miocene, Pliocene(?), and Middle Pleistocene (*Pseudoemiliania lacunosa* nannoplankton Zone) sediments. Clasts from all other cores are only Upper Pleistocene in age. The normal sediment accumulation rates in this area are supposed to be about 3.5-4 cm/ka (estimated from the hemipelagic core 139G).

The distal Valencia Channel

Ten of the 11 cores studied fall within the *Emiliania huxleyi* Acme Zone, and are Holocene in age except for core 157G, which extends to the Late Pleistocene. The longest core, 155G, bottoms in the *Emiliania huxleyi* Zone. The base of the core was dated by foraminifera and nannoplankton assemblages to about 90 ka B.P. (Figs. 80 to 82). The sediment accumulation rate in this area, which can be estimated from only one hemipelagic core (155G), is 2.7-3 cm/ka.

e. SMEAR-SLIDES

A. Oosting, J. van der Hoef, E. Felser, and J. Rey

As the cores came up and were cut in half, we sampled for smear-slides at places of interest, such as dark spots, oxidized and dark layers, and clay pebbles in sandy turbidites. We did not sample on a regular spacing, so you cannot get a broad idea of the cores based on the smear-slides. They can only be a help in the interpretation of lithologies. This was primarily due to time constraints imposed by the fast turnover of the cores.

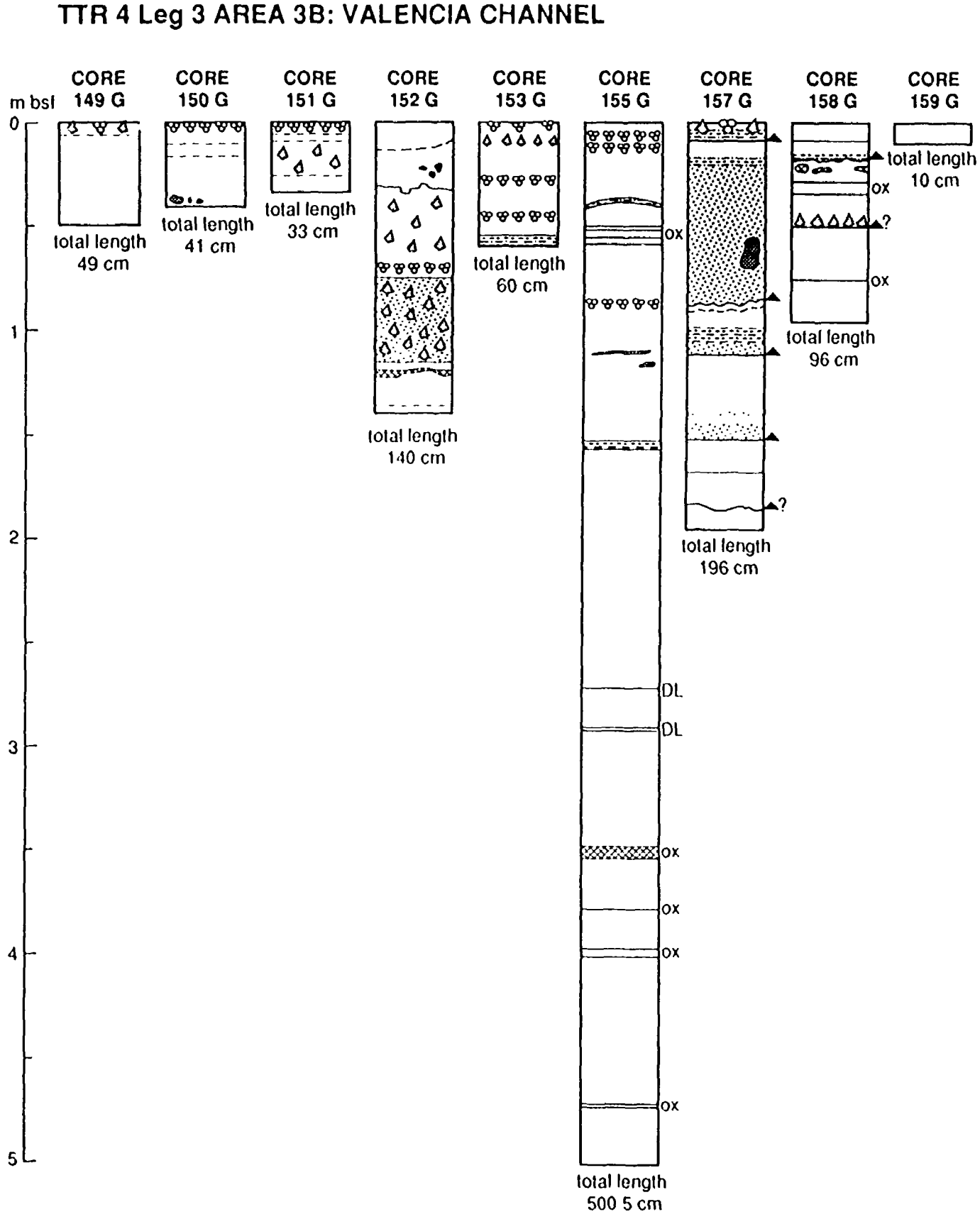

Fig. 79. Cores recovered during TTR-4 Leg 3b in the area of distal Rhone Fan and Valencia Channel (Area 3b)

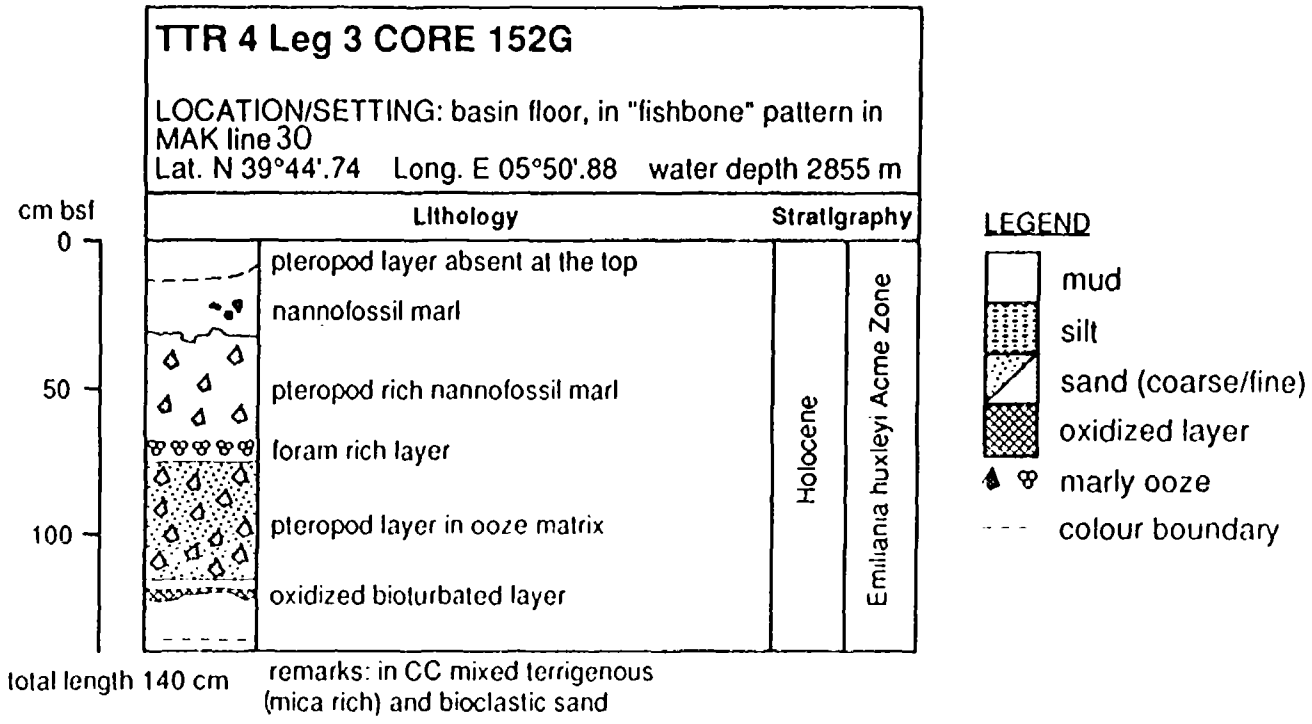

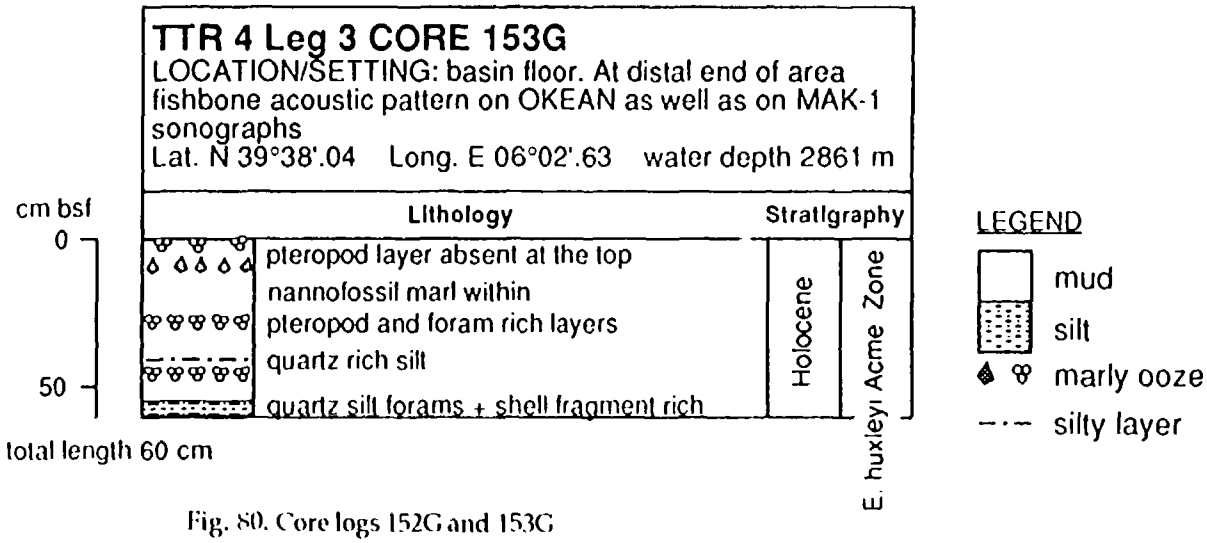

Fig. 80. Core logs 152G and 153G

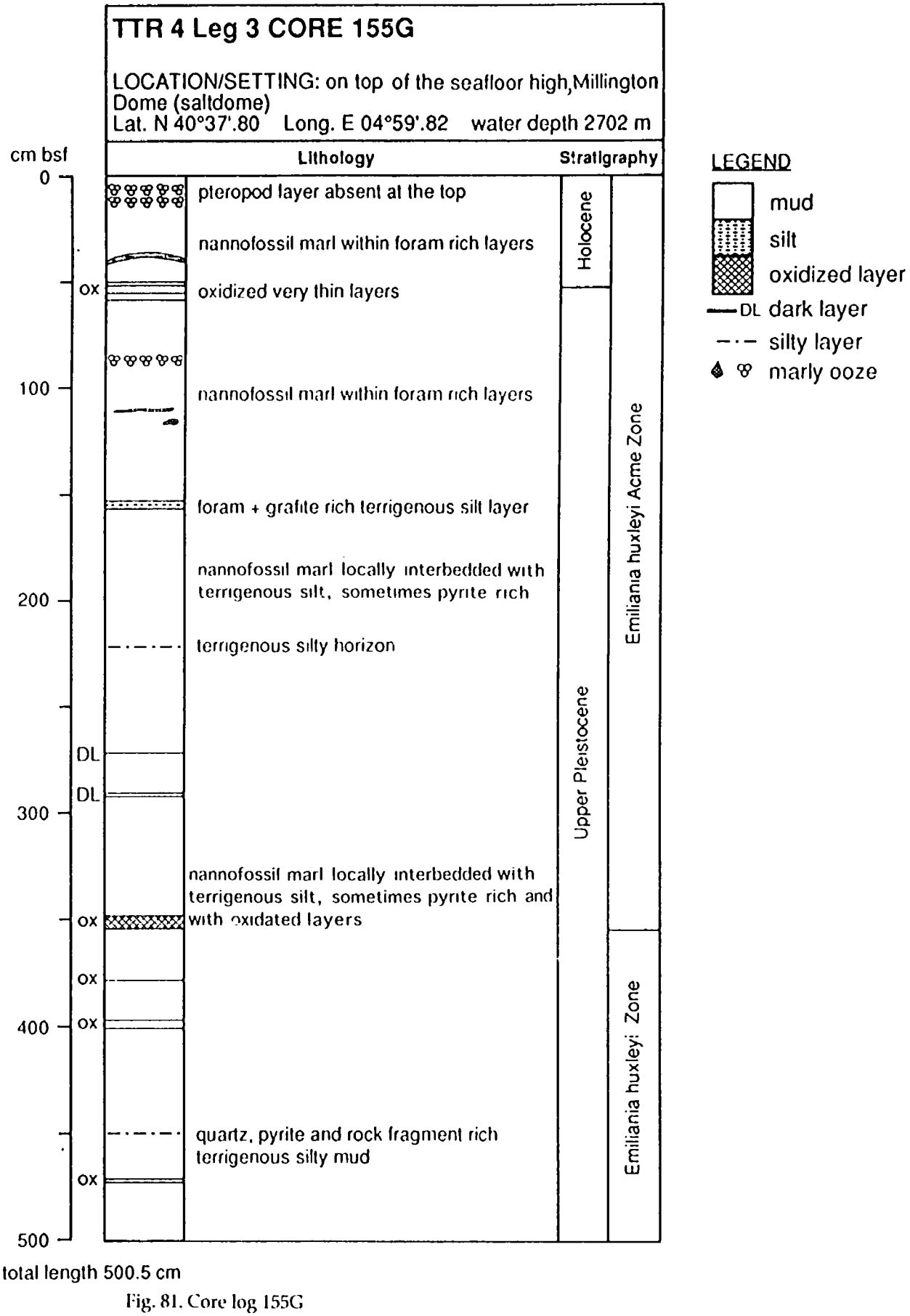

Fig. 81. Core log 155G

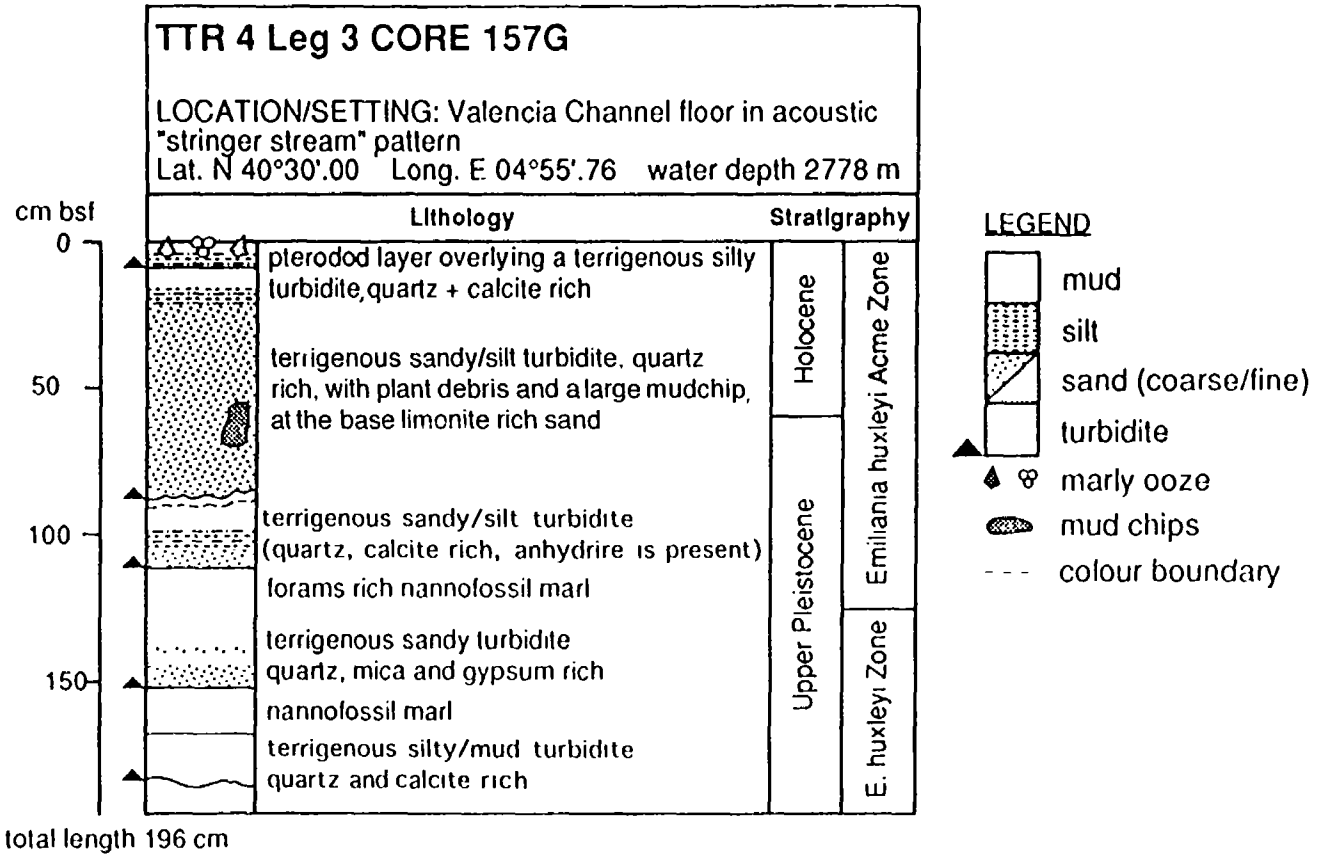

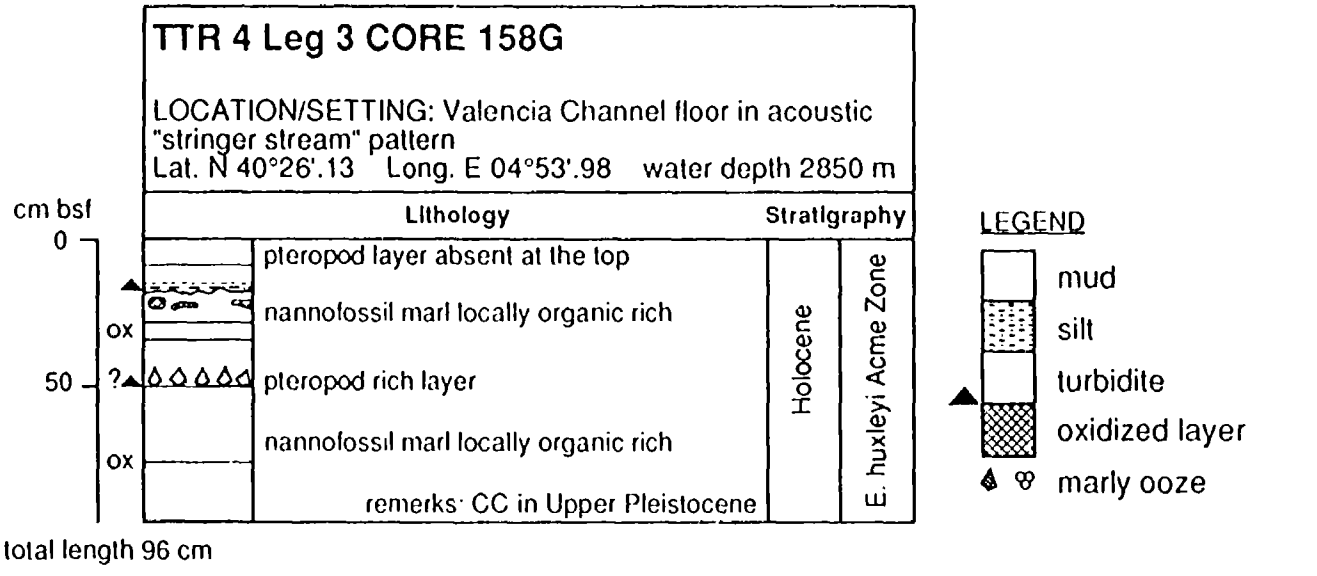

Fig. 82. Core logs 157G and 158G

For the description of the smear slides we used microscopes with 10 and 25 times magnification without gypsum (Rot I), so it was very difficult to determine what minerals and other material was present. We first described whether biogenic ("organic") or the terrigenous ("inorganic") components were predominant in a semi-quantitative manner. After that, we determined the minerals and biogenic material. All our observations were recorded on standard shipboard description forms.

Quartz, calcite, pyrite, amphibole, pyroxene, rutile, mica, and aragonite, in addition to some micronodules and clay minerals were recorded from the slides. The biogenic material consisted of plant debris, coccoliths, shell fragments, planktonic and benthic foraminifera, and sponge spicules.

Although this was a rapid means of summarizing the core composition, it proved a very useful method for distinguishing transported material from particles settled directly from the water column and from the bioclastic material. One could also distinguish shallow-water fauna (forams, bryozoans, echinoid spines) from mixed and deeper water fauna.

f. PRELIMINARY STUDY OF PEBBLES FROM DEBRIS FLOWS IN THE CORSO-LIGURIAN BASIN

G.G. Akhmanov and A.M. Akhmetzhanov

Some pebbles from debris flow deposits were studied from the cores taken in this area. Their composition and provenance were defined for cores 140G, 146G, 147G, and 148G. The pebbles examined from cores 146G-148G have a terrigenous origin and are derived from an area with a prevalence of low-graded metamorphic rocks. The pebbles from core 140G also have a terrigenous origin, but probably came from an area where flints are widespread. Some of these pebbles from cores 146G-148G could be eroded from canyon walls during gravity mass movement.

Core 140G

The debris flow deposits contain many pebbles of different kinds of flint: grey, green, greenish-brown, greyish-yellow, massive and laminated, very indurated, subspherical, and subrounded, as well as granules of milky-white subrounded, spherical quartz and rare clasts of shells.

Core 146G

The debris flow deposits contain 5 large rock pebbles, 3 of which are similar.

1. Three clasts (1.5 to 4 x 1 to 2 cm) of talc-pyrophyllite shale; tabular, with rounded edges. They have patches of grey, greenish-grey and greyish-green colours; with shaly structure.

The rock can be very easily destroyed by an iron pin. A precise study in thin section is needed.

2. A clast (2 x 3 cm) of quartz; tubular, angular, very indurated, white with brown spots. This quartz probably filled in cracks in the talc-pyrophyllite shale sequence, because there are remains of this rock on the clast sides.

3. A clast of marlstone (4 x 6 cm); tabular in shape, with an irregular surface, light grey, probably bioturbated. One side of the clast is softer that the other one.

Core 147G

The debris flow deposits contain a lot of small pebbles (0.5 to 1.5 cm in size) of different composition.

1. Green and greyish-green talc-pirophyllite shale; tabular, subrounded, soft, lepidoblastic, with a shaly structure.

2. Angular and rounded milky-white quartz, very indurated.

3. Chert; subangular, grey, very indurated, massive.

4. Sandstone; sub-isometric, subangular, very coarse-grained, with inclusions of angular quartz grains, feldspar grains, fragments of metamorphic rocks and shell fragments. The cement is calcite.

Core 148G

The debris flow deposits contain 3 large pebbles and many small pebbles and clasts (0.3 to 1 cm) of different compositions. All require further study in thin section:

1. A clast of quartz (2 x 3.5 cm); tabular, sub-isometric, angular, very indurated, transparent, greenish-grey, massive, fractured, monomineral, with rust spots in the surface.

2. A clast of shale rock (3 x 5 cm); tabular, subrounded, very indurated, green and greyish-green, with shaly structure, granolepidoblastic, polymineral.

3. A clast of sandstone (1.5 x 3 cm); foliated, subrounded, indurated, greyish-brown, massive, fine-grained, polymineral, composed of irregular quartz grains, magmatic and metamorphic rock fragments, muscovite, biotite, and feldspar grains coated by crusts of pore-filling limonite.

Granules and small pebbles represent clasts of the same rocks and, additionally, there are:

1. Clasts of talk-pirophyllite shale; tabular, green, subrounded, soft, with shaly structure, lepidoblastic.

2. Clasts of sandstone; subrounded, spherical, composed of irregular quartz grains, mica, and feldspar, cemented by calcite.

3. Clasts of chert; dark grey, massive, indurated, subspherical, granoblastic.

5. CONCLUSIONS

N.H. Kenyon

1. There are marked contrasts between the two areas of sandy turbidites in the path of flows down to the Balearic Abyssal Plain, that we have investigated in the third study area. The pathway through the lower Corso-Ligurian Basin is supplied by steep canyons, that drain the nearby subaerial and submarine slopes west of Corsica and Sardinia, as well as the more distal margin of southern France, including the Var Canyon. The distal Valencia Channel area is much further from its sources on the Spanish margin and the western Rhone Fan.

2. This proximity of the source may be related to the occurrence of the several metres thick sandy turbidites, with mud clasts, that were so successfully cored in the Corso-Ligurian Basin. The sands here were medium to coarse in grain size. Although there are also sands in the distal Valencia area, the sands are probably finer-grained. The core success rate was so much worse in this fine sand than in the medium to coarse sands that the acoustic facies of the profiles is characterized by a more prolonged echo with less penetration.

3. The processes in the two areas seem to be different. The regular 5 m thick sequences in the Corso-Ligurian Basin may be due to sea-level changes, although at what frequency it is not known. It is noted that the latest sequence is thinner than the previous ones. Perhaps it is incomplete. In the distal Valencia area there is transport, and maybe some reworking, of non-cohesive sediments by gravity flows that hugged the seafloor and passed through the shallow channel before expanding out onto the approaches to the basin plain. The bedforms discovered here are of hitherto undescribed types and, hence, it is too early to discuss what they imply in terms of flow parameters. The sequence of bedforms down path is in keeping with the model for a hydraulic jump beyond a channel mouth, which would predict an erosional zone followed by a zone of mobile bedforms. Whether there are sheet deposits from this transport is not known and should be tested by coring. Consideration should also be given to the possibility of oceanic currents flowing down to the basin floor.

IV. EXPERIMENTAL TURBIDITY CURRENT DEMONSTRATION ON TTR-4 LEG-3

S. Morris and J. Millington

We converted the Kasten corer into a temporary flume tank and placed it on two boxes for support. The lid of the corer was unscrewed and removed, and the open ends were blocked and sealed with plywood, cut to size and taped tightly to make water tight seals. Holes in the sides and base were also sealed with tape and bluetack.

The tank dimensions were: length = 400 cm, width = 15 cm, and depth = 15 cm, with a lock of length = 25 cm. An upturned glass was placed in the centre of the tank at about 200 cm from the lock to act as an obstacle to the flow (similar to a seamount or salt dome). The tank was then filled with sea water. We used clay as the sediment to make the flow, as the only other sediment available was coarse sand, which would not have stayed in suspension long enough to flow more than about 50 cm. Approximately 1 kg of the clay was made into a sludge which was easy to mix in to the water in the lock, using a custom-made stirrer.

The clay and water were mixed in the lock, and when the lock gate was removed, the clay-water mixture collapsed under gravity, due to the increased density (Fig. 83). The density flow rapidly assumed the classical form of a turbidity current, with exceptionally well-developed lobes, clefts and billows over the back of the head. The flow splashed up against the front of the obstacle and then curled around the sides, with the velocity of the flow retarded in the area behind the obstacle. Due to the motion of the ship, the water in the tank sloshed backward and forward and caused the current to flow in surges. The current decreased greatly in velocity after approximately 200-cm distance, caused by dilution (from mixing of ambient water and deposition of sediment) and friction (from the tank floor and overlying ambient fluid). However, the current eventually reached the end of the tank and formed a weak reflection. After about 5 minutes, all the clay had settled and it was possible to observe the sediment deposit. The thickness of deposit decreased gradually away from the lock, and a slightly thinner cover was seen behind the obstacle.

This experiment, even with its crude apparatus and some adverse conditions, demonstrated very clearly the form and motion of a turbidity current and also how it interacted with an obstacle. It may, also, have given an insight into the growing importance of understanding the fluid dynamic processes operating in these type of flows, in particular when they interact with topographic features and how they can be applied to the interpretation and more importantly, the prediction of turbidite geometry.

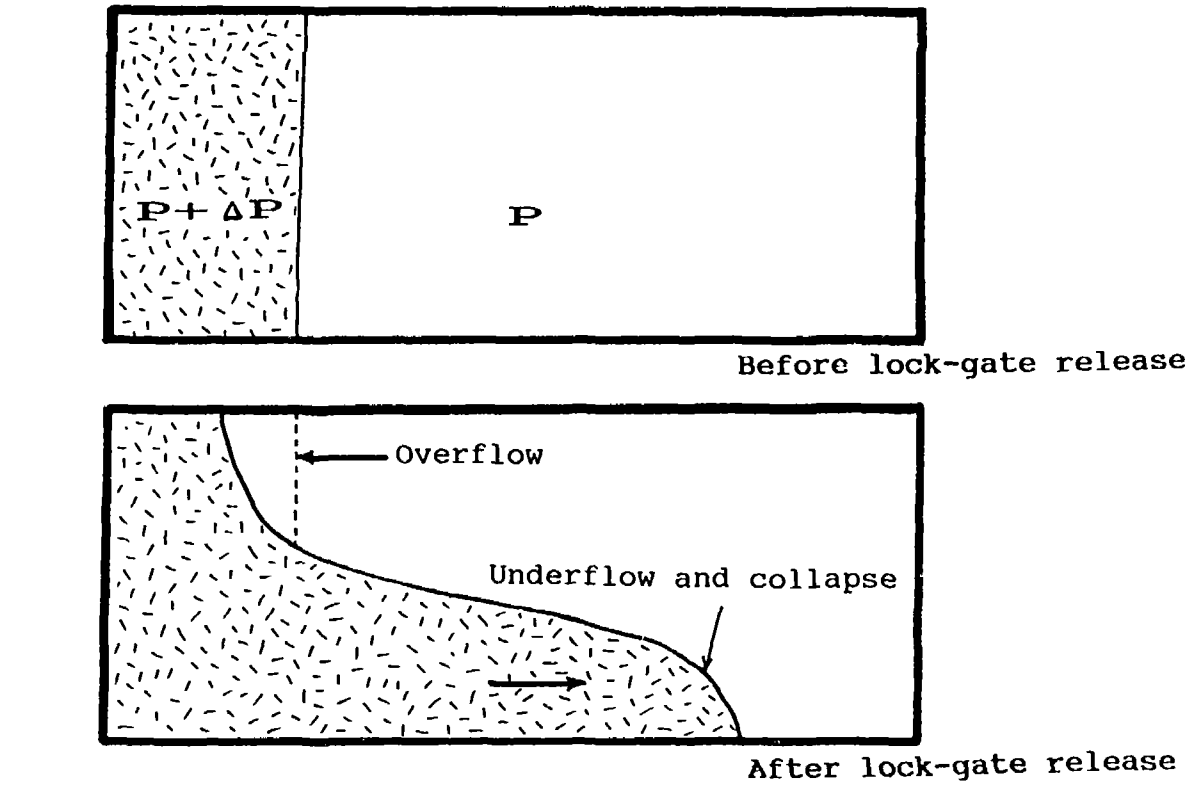

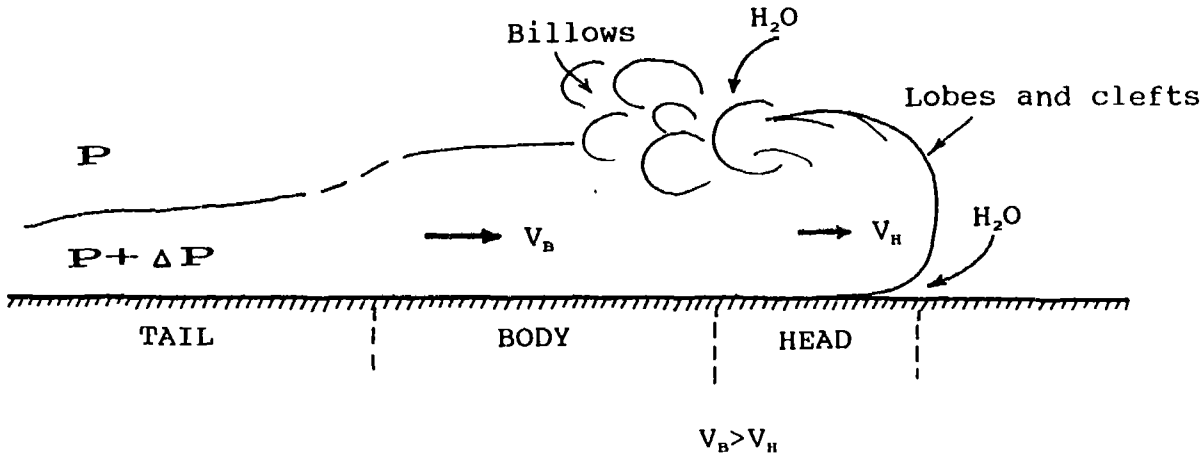

Fig. 83. Experimental turbidity current demonstrated on Leg 3 of TTR-4 Cruise

REFERENCES

Agate, M., Catalano, R., Infuso, S., Lucido, M., Mirabile, L., and Sulli, A., 1993. Structural evolution of the northern Sicily continental margin during the Plio-Pleistocene. In: Max, M.D. and Colantoni, P. (eds.). *Geological Development of the Sicilian-Tunisian Platform.* UNESCO Reports in Marine Science, 58: 25-30.

Alonso, B., Canals, M., Palanques, A., and Rehault, J.P., 1991. The Valencia Valley: origin and evolution of a "mid-ocean channel" sea valley type in the Northwestern Mediterranean. *3ème Congr. Franç. Sedimentol.*: 3-6.

Alonso, B., Field, M.E., Gardner, J.V., and Maldonado, A., 1990. Sedimentary evolution of the Pliocene and Pleistocene Ebro margin, northeastern Spain. *Mar. Geol.*, 95: 313-331.

Alvarez, W., Cocozza, T., and Wezel, F.C., 1974. Fragmentation of the Alpine orogenic belt by microplate dispersal. *Nature*, 248: 309-314.

Argnani, A. and Trincardi, F., 1988. Paola slope basin: evidence of regional contraction on the eastern Tyrrhenian margin. *Mem. Soc. Geol. It.*, 44: 93-105.

Beccaluva, L., Gabbianelli, G., Lucchini, F., Rossi, P.L., and Savelli, C., 1985. Magmatic character and K/Ar ages of volcanics dredged from the Eolian Seamounts: implication for geodynamic evolution of the southern Tyrrhenian Basin. *Earth Planet. Sci. Lett.*, 74: 187-208.

Belderson, R.H., Kenyon, N.H., and Stride, A.H., 1970. 10-km wide views of the Mediterranean deep-sea floor. *Deep Sea Res.*, 17: 267-270.

Belderson, R.H., Kenyon, N.H., and Stride, A.H., 1974. Features of submarine volcanoes seen on long-range sonographs. *Journal of Geol. Soc. London*, 130: 403-410.

Belderson, R.H., Kenyon, N.H., and Stride, A.H., 1978. Local submarine salt-karst formation on the Hellenic Outer Ridge, Eastern Mediterranean, *Geology*, 6: 716-720.

Belderson, R.H., Kenyon, N.H., Stride, A.H., and Pelton, C.D., 1984. A "braided" distributary system on the Orinoco deep-sea fan. *Mar. Geol.*, 56: 195-206.

Bellaiche, G., 1993. Sedimentary mechanisms and underlying tectonic structures of the northwestern Mediterranean margin, as revealed by comprehensive bathymetric and seismic surveys. *Mar. Geol.*, 112: 89-108.

Bellaiche, G., Coutellier, V., and Droz, L., 1990. Seismic evidence of widespread mass transport deposits in the Rhone deep-sea fan: their role in the fan construction. *Mar. Geol.*, 71: 327-340.

Bellaiche, G., Droz, L., Aloisi, J.C., Bouye, Ch., Got, H., Monaco, A., Maldonado, A., Serra-Raventos, J., and Mirabile, L., 1981. The Ebro and the Rhone deep-sea fans: first comparative study. *Mar. Geol.*, 43: 75-85.

Bellaiche, G., Orsolini, P., Petit-Perin, B., Berthon, J., Ravenne, Ch., Coutellier, V., Droz, L., Aloisi, J.C., Got, H., Mear, Y., Monaco, A., Auzende, J.M., Beuzart, P., and Monti, S., 1984. Morphology au "Seabeam" de l'éventail sous-marin profond du Rhône. *Compt. Rend. Acad. Sci.*, Paris, 296: 579-583.

Bigi, G., Cosentino, D., Parotto, M., Sartori, R., and Scandone, P., 1992.

Structural Model of Italy. Sheet no 3. CNR, Progetto Finalizzato Geodynamica.

Bouma, A.H., Normark, W.R., and Barnes, N.E. (eds.), 1985a. *Submarine Fans and Related Turbidite Systems.* Springer Verlag, N.Y., 351 pp.

Bouma, A.H., Stelting, C.E., and Coleman, T.M., 1985b. Mississippi Fan, Gulf of Mexico. In: Bouma, A.H., Normark, W.R., and Barnes, N.E. (eds.). *Submarine Fans and Related Turbidite Systems.* Springer Verlag, N.Y.: 143-150.

Bourcart, J., 1959. Morphologie du precontinent des Pyrenées a la Sardaigne. *Colloq. Intern. Centre Natl. Recherche Sci.* Paris, 83: 33-50.

Burroz, J., 1984. Contribution to a geodynamic synthesis of the Provencal Basin (northwestern Mediterranean). - *Mar. Geol.*, 55: 247-269.

Canu, M. and Trincardi, F., 1989. Controllo eustatico e tettonico sui sistemi deposizionali nel bacino di Paola (Plio-Quaternario), margine Tirrenico orientale. *Giorn. Geol.*, 51, 2: 41-61.

Catalano, R., Di Stefano, P., Nigro, F., and Vitale, F.R., 1993. Sicily mainland and its offshore: a structural comparison. In: Max, M.D. and Colantoni, P. (eds.). *Geological Development of the Sicilian-Tunisian Platform.* UNESCO Reports in Marine Science, 58: 19-24.

Cita, M.B. and Camerlenghi, A., 1992. The Mediterranean Ridge as an accretionary prism in collision context. *Mem. Soc. Geol. It.*, 45: 463-480.

Cita, M.B., Camerlenghi, A., Erba, E., McCoy, F.M., Castradori, D., Cazzani, A., Guasti, G., Giabastiani, M., Lucchi, R., Nolli, V., Pezzi, G., Redaelli, M., Rizzi, E., Toricelli, S., and Violanti, D., 1989. Discovery of mud diapirism on the Mediterranean Ridge. A preliminary report. *Boll. Soc. Geol. It.*, 108: 537-543.

Cita, M.B., Ryan, W.B.F., and Paggi, L., 1981. Prometheus mud breccia: An example of shale diapirism in the western Mediterranean Ridge. *Ann. Geol. Pays Hellen.*, 30: 543-570.

Colantoni, P., Lucchini, F., Rossi, P.L., Sartori, R., and Savelli C., 1981. The Palinuro volcano and magmatism of the southeastern Tyrrhenian Sea (Mediterranean). *Mar. Geol.*, 39: M1-M12.

Damuth, J.E. and Embley, R.W., 1981. Mass-transport processes on Amazon Cone: western equatorial Atlantic. *Amer. Assoc. Petrol. Geol. Bull.*, 65: 629-643.

Damuth, J.E., Flood, R.D., Pirmez, C., and Manley, P.L., 1995. Architectural elements and depositional processes of Amazon Deep Sea Fan imaged by long-range sidescan sonar (GLORIA), bathymetric swath-mapping (Sea Beam), high-resolution seismic and piston-core data. In: Pickering, K.T., Hiscott, R.N., Kenyon, N.H., Ricci Lucchi, F., and Smith, R.D. (eds.) *Atlas of Deep Water Environments.* Chapman and Hall, London: 105-121.

Davis, D., Suppe, J., and Dahlen, F.A., 1983. Mechanics of fold-and-thrust belts and accretionary wedges. *Jour. Geophys. Res.*, 88: 1153-1172.

Della Vedova, B., Pellis, G., Foucher, J.P., and Rehault, J.P., 1984. Geothermal structure of the Tyrrhenian Sea. *Mar. Geol.*, 55: 271-289.

Droz, L., 1991. *Eventails sous-marins profonds: structure et évolution sédimantaire à partit de l'analyse de trois exemples, l'Eventail du*

Rhône, la Ride du Var et le Cône de l'Indus. Diplôme d'Habilitation à Diriger des Recherches. Univ. Paris 6, 279 pp.

Droz, L. and Bellaiche, G., 1985a. Rhone deep-sea fan: morphostructure and growth pattern. *Amer. Assoc. Petrol. Geol. Bull.*, 69, 1: 460-479.

Droz, L. and Bellaiche, G., 1985b. Seismic facies and geological evolution of the central portion of the Indus Fan. In: Bouma, A.H., Normark, W.R., and Barnes, N.E. (eds.), 1985a. *Submarine Fans and Related Turbidite Systems.* Springer Verlag, N.Y.: 383-402.

Fabbri, A., Gallignani, P., and Zitellini, N., 1981. Geologic evolution of the peri-Tyrrhenian sedimentary basins. In: Wezel, F.C. (ed.). *Sedimentary Basins of Mediterranean Margins.* Tecnoprint, Bologna: 101-126

Fabbri, A. and Nanni, T., 1980. Seismic reflection study of the Sardinia Basin (Tyrrhenian Sea). *Geologie Mediterraneenne*, VII: 161-177.

Finetti, I., 1982. Structure, stratigraphy and evolution of Central Mediterranean Sea. *Boll. Geof. Teor. Appl.*, 15: 263-341.

Gabbianelli, G., Romagnoli, C., Rossi, P.L., and Calanchi, N., 1993. Marine geology of the Panarea-Stromboli area (Aeolian Archipelago, southeastern Tyrrhenian Sea). *Acta Vulcanol.*, 3: 11-20.

Gasparini, C., Iannacone, G., Scandone, P., and Scarpa, R., 1982. Seismotectonics of the Calabrian Arc. *Tectonophysics*, 84: 267-286.

Hersey, J.B., 1965 Sedimentary basins of the Mediterranean Sea. *Proc. 17th Symp. of the Colston Res. Soc., Colston Papers*, VII. Univ. Bristol: 75-91.

Hirschleber, H.B., Hartmann, J.M., and Hieke, W., 1994. The Mediterranean Ridge accretionary complex and its forelands - seismic reflection studies in the Ionian Sea, In: Ansorge, R. (ed.). *Universität Hamburg 1994 - Schlaglichter der Forschung zum 75. Jahrestag.* Hamburger Beiträge zur Wissenschaftsgeschichte, 15. Reimer Verlag, Berlin: 491-509.

IOC-UNESCO, 1981. *International Bathymetric Chart of the Mediterranean.* Ministry of Defence, Leningrad.

Kastens, K.A., 1991. Rate of outward growth of the Mediterranean Ridge accretionary complex. *Tectonophysics*, 199: 25-50.

Kastens, K.A. et al., 1988. ODP Leg 107 in the Tyrrhenian Sea. Insight into passive margin and back-arc basin evolution. *Geol. Soc. Amer. Bull.*, 100: 1140-1156.

Kastens, K.A. and Mascle, J., 1990. The geological evolution of the Tyrrhenian Sea: An introduction to the scientific results of ODP Leg 107. *Proc. ODP. Sci. Results*, 107. College Station, TX (Ocean Drilling Program): 3-26.

Kenyon, N.H., Amir, A., and Cramp, A., 1995. Geometry of the younger sediment bodies of the Indus Fan. In: Pickering, K.T., Hiscott, R., Kenyon, N.H., Ricci Lucchi, F., and Smith, R.D.A. (eds.). *An Atlas of Deep Water Depositional Systems.* Chapman and Hall, London: 89-99.

Kenyon, N.H., Belderson, R.H., and Stride, A.H., 1982. Detailed tectonic trends on the central part of the Hellenic Outer Ridge and in the Hellenic Trench System. In: Leggat, J. (ed.). *Trench-Forearc Geology.* Geol. Soc. Spec. Publ., 10: 335-343.

Kenyon, N.H. and Millington, J., 1995. Contrasting deep sea depositional systems in the Bering Sea Basin. In: Pickering, K.T., Hiscott, R., Kenyon,

N.H., Ricci Lucchi, F., and Smith, R.D.A. (eds.). *An Atlas of Deep Water Depositional Systems.* Chapman and Hall, London: 196-202.

Kidd, R.B., Hunter, P.M., and Simm, R.W., 1987. Turbidity-current and debris-flow pathways to the Cape Verde Basin: status of long-range sidescan sonar (GLORIA) surveys. In: Weaver, P.P. and Thomson, J. (eds.). *Geology and Geochemistry of Abyssal Plains.* Geol. Soc. Spec. Publ., London, 31: 33-48.

Kidd, R.B., Simm, R.W., and Searle, R.C., 1985. Sonar acoustic facies and sediment distribution on an area of the deep ocean floor. *Mar. and Petrol. Geol.*, 2: 210-221.

Limonov, A.F., Woodside, J.M., Cita, M.B., and Ivanov, M.K., in press. The Mediterranean Ridge and related mud diapirism: a background. *Mar. Geol.*

Limonov, A.F., Woodside, J.M., and Ivanov, M.K. (eds.), 1993. *Geological and Geophysical Investigations of the Western Mediterranean Deep-Sea Fans. Initial Results of the UNESCO-ESF "Training-through-Research" Cruise of R/V Gelendzhik in the Western Mediterranean (June-July 1992).* UNESCO Reports in Marine Science, 62, 154 pp.

Limonov, A.F., Woodside, J.M., and Ivanov, M.K. (eds.), 1994. *Mud Volcanism in the Mediterranean and Black Seas and Shallow Structure of the Eratosthenes Seamount. Initial Results of the Geological and Geophysical Investigations during the Third UNESCO-ESF "Training-through-Research" Cruise of R/V Gelendzhik (June-July 1993).* UNESCO Reports in Marine Science, 64: 173 pp.

Maldonado, A., Got, H., Monaco, A., O'Connell, S., and Mirabile, L., 1985a. Valencia Fan (Northwestern Mediterranean): distal depositional fan variant. *Mar. Geol.*, 62: 295-319.

Maldonado, A., Palanques, A., Alonso, B., Kastens, K.A., Nelson, C.H., O'Connell, S., and Ryan, W.B.F., 1985b. Physiography and deposition on a distal deep-sea system: the Valencia Fan (Northwestern Mediterranean). *Geo-Marine Letters*, 5: 157-164.

Malinverno, A. and Ryan, W.B.F., 1986. Extension in the Tyrrhenian Sea and shortening in the Apennines as a result of arc migration driven by sinking of the lithosphere. *Tectonics*, 5: 227-245.

Masson, D.G., Kenyon, N.H., Gardner, J.V., and Field, M.E., 1995. Monterey Fan: channel and overbank morphology. In: Pickering, K.T., Hiscott, R., Kenyon, N.H., Ricci Lucchi, F., and Smith, R.D.A. (eds.). *An Atlas of Deep Water Depositional Systems.* Chapman and Hall, London: 74-79.

Masson, D.G., Kidd, R.B., Gardner, J.V., Huggett, Q.J., and Weaver, P.P.E., 1992. Saharan continental rise: facies distribution and sediment slides. In: Poag, C.W. and de Graciansky, P.C. (eds.). *Geologic Evolution of Atlantic Continental Rise.* Van Norstrand Reinhold, N.Y.: 327-343.

McCave, I.N. and Jones, K.P.N., 1988. Deposition of ungraded muds from high-density non-turbulent turbidity currents. *Nature*, 333: 250-252.

Morelli, C., 1970. Physiography, gravity and magnetism of the Tyrrhenian Sea. *Boll. Geof. Teor. Appl.*, 12: 274-309.

Mutti, E., 1977. Distinctive thin-bedded turbidite facies and related depositional environments in the Eocene Hecho Group (South Central

Pyrenees, Spain). *Sedimentology*, 24: 107-131.
Mutti, E. and Normark, W.R., 1991. An integrated approach to the study of turbidite systems. In: Weimer, P. and Link, M.H. (eds.). *Seismic Facies and Sedimentary Processes of Submarine Fans and Turbidite Systems.* Springer Verlag, N.Y.: 75-106.
Nelson, H. and Nilsen, T., 1974. Depositional trends of modern and ancient deep-sea fans. In: Dott, R.H., Jr. and Shaver, R.H. (eds.). *Modern and Ancient Geosynclinal Sedimentation.* Soc. Econ. Paleont. Meneral. Spec. Publ.: 54-76.
Nelson, H., Normark, W.R., Bouma, A.H., and Carlson, P.R., 1978. Thin-bedded turbidites in modern submarine canyons and fans. In: Stanley, D.J. and Kelling, G. (eds.). *Sedimentation in Submarine Canyons, Fans and Trenches.*. Dowden, Hutchinson and Ross, Stroudsburg, Pa.: 177-190.
Normark, W.R., Barnes, N.E., and Coumes, F., 1985. Rhone Fan, Mediterranean. In: Bouma, A.H. et al. (eds.). *Submarine Fans and Related Turbidite Systems.* Springer Verlag, Heidelberg: 151-156.
Palanques, A., Alonso, B., and li Farran, M., 1994. Progradation and retreat of the Valencia fanlobes controlled by sea-level changes during the Plio-Pleistocene (northwestern Mediterranean). *Mar. Geol.*, 117: 195-205.
Palanques, A., and Maldonado, A., 1983. The Messinian erosional surface and evaporites in the northern sector of the Valencia Trough. *Congr. Nac. Sedimentol.*, Menorca: 7.18-7.21.
Palanques, A. and Maldonado, A., 1985. Sedimentology and evolution of the Valencia Valley and Fan (northwestern Mediterranean). *Acta Geol. Hisp.*, 20: 1-19.
Peterschmitt, E., 1956. Quelques données nouvelles sur les seismic profonds de la Mer Tyrrhénienne. *Ann. Geofis.*, 9: 305-334.
Piper, D.J.W., Normark, W.R., and Hiscott, R.N., 1995. Holocene sand body geometry, Hueneme Fan, California Borderland. In: Pickering, K.T., Hiscott, R., Kenyon, N.H., Ricci Lucchi, F., and Smith, R.D.A. (eds.). *An Atlas of Deep Water Depositional Systems.* Chapman and Hall, London: 196-201.
Rehault, J.P., Mascle, J., Fabbri, A., Moussat, E., and Thommeret, M., 1987. The Tyrrhenian Sea before Leg 107. In: Kastens, K.A., Mascle, J., et al. (eds.). *Proc. ODP, Init. Repts.*, 107. College Station, TX (Ocean Drilling Program): 9-35.
Ricci-Lucchi, F. and Valmori, E., 1980. Basin-wide turbidites in a Miocene, over-supplied deep-sea plain; a geometrical analysis. *Sedimentology*, 27: 241-270.
Rio, D., Raffi, I., and Villa, G., 1990. Pliocene-Pleistocene calcareous nannofossils distribution patterns in the Western Mediterranean. In: Kastens, K.A., Mascle, J., et al. (eds.). *Proc. ODP. Sci. Results*, 107. College Station, TX (Ocean Drilling Program): 513-533.
Ronagnoli, C., Kokelaar, P., Rossi, P.L., and Sodi, A., 1993. The submarine extension of Sciara del Fuoco feature (Stromboli Isl.): morphologic characterization. *Acta Vulcanol.*, 3: 91-98.
Rothwell, R.G., Pearce, T.J., and Weaver, P.P.E., 1992. Late Quaternary evolution of the Madeira Abyssal Plain, Canary Basin, NE Atlantic. *Basin Research*, 4:

103-131.

Sartori, R., 1990. The main results of ODP Leg 107 in the frame of Neogene to recent geology of peri-Tyrrhenian areas. In: Kastens, K., Mascle, J., et al. (eds): *Proc. ODP, Sci. Results.*, 107. College Station, TX (Ocean Drilling Program): 715-730.

Savelli, C., in press. Cenozoic migration of arc volcanism in the South Tyrrhenian Sea. *Mem. Soc. Geol. It.*.

Savelli, C., 1992. Il rifting del vulcano Marsili (Mar Tireno): aspetti morfo-tettonici osservati da bordo del sottomarino "MIR 2". *Giorn. Geol.*, 54, 2: 215-227.

Savelli, C. and Gasparotto, G., 1994. Calc-alkaline magmatism and rifting of the deep-water volcano of Marsili (Aeolian back-arc, Tyrrhenian Sea). *Mar. Geol.*, 119: 137-157.

Savelli, D. and Wezel, F.C., 1979. Morfologia e stile tettonico del bacino Tirrenico. *Atti Conv. Sc. Naz. P.F. Oceanografia e Fondi Marini* C.N.R. Roma, 2: 729-738.

Selli, R., 1967. The Pliocene-Pleistocene boundary in Italian marine sections and its relationship to continental stratigraphies. *Progress in Oceanography*, 4: 67-86.

Selli, R. and Fabbri, A., 1971. Tyrrhenian: a Pliocene deep sea. *Rend. Classe Sc. Fis. Mat. Nat.*, Serie 8, 50, 5: 104-116.

Shackleton, N.J. and Opdyke, N.D., 1973. Oxygen isotope and paleomagnetic stratigraphy of equatorial Pacific core V28-238: oxygen isotope temperatures and ice volumes on a 105 and 106 years scale. *Quat. Res.*, 3: 39-55.

Stanley, D.J., 1972. *The Mediterranean Sea: A Natural Sedimentation Laboratory.* Dowden, Hutchinson and Ross, Stroudsburg, Pa., 765 pp.

Steinmetz, L., Ferrucci, F., Hirn, A., Morelli, C., and Nicolich, R., 1983. A 550 km long Moho traverse in the Tyrrhenian Sea from O.B.S. recorded Pn waves. *Geophys. Res. Lett.*, 10, 6: 428-431.

Ulzega, A., 1988. *Geomorphological Map of Marine and Continental Sardinia, 1:500.000.* C.N.R., Dipartimento di Scienze della Terra di Cagliari.

Vail, P.R. and Wornardt, W., 1991. An integrated approach to exploration and development in the 90s: well log seismic stratigraphy analysis. *Trans. in the Gulf Coast Assoc. of Geol. Soc.*, XLI: 630-650.

Vicente Bravo, J.C. and Robles, S., 1995. Large scale mesotopographic bedforms from the Albian Black Flysch, northern Spain: characterization, setting and comparisons with recent analogues. In: Pickering, K.T., Hiscott, R.N., Kenyon, N.H., Ricci Lucchi, F., and Smith, R.D. (eds.). *Atlas of Deep Water Environments.* Chapman and Hall, London: 216-226.

Weaver, P.P.E. and Rothwell, R.G., 1987. Sedimentation on the Madeira Abyssal Plain over the last 300,000 years. In: Weaver, P.P.E. and Thomson, J. (eds.). *Geology and Geochemistry of Abyssal Plains.* Spec. Publ. 31. Geological Society, London: 71-86.

Weaver, P.P.E., Masson, D.G., Gunn, D.E., Kidd, R.B., Rothwell, R.G., and Maddison, D.A., 1995. Sedimentary mass wasting in the Canary Basin. In: Pickering, K.T., Hiscott, R., Kenyon, N.H., Ricci Lucchi, F., and Smith,

R.D.A. (eds.). *An Atlas of Deep Water Depositional Systems*. Chapman and Hall, London: 287-296.

Weaver, P.P.E., Searle, R.C., and Kuijpers, A., 1986. Turbidite deposition and the origin of the Madeira Abyssal Plain. In: Summerhayes, C.P. and Shackleton, N.J. (eds.). *North Atlantic Palaeogeography*. Spec. Publ., 21, Geological Society, London: 131-143.

Weimer, P., 1989. Sequence stratigraphy of the Mississippi Fan (Plio-Pleistocene), Gulf of Mexico. *Geo-Marine Letters*, 9: 185-272.

Zangger, E. and McCave, I.N., 1990. A re-designed Kasten core barrel and sampling technique. *Mar. Geol.*, 94: 165-171.

UNESCO REPORTS IN MARINE SCIENCE

Cont'd from inside of front cover

No		Year
56	Geological and geophysical investigations in the Mediterranean and Black Seas. Initial results of the 'Training-through-Research' Cruise of RV *Gelendzhik* in the Eastern Mediterranean and the Black Sea, June-July 1991 (E)	1992
57	Physical oceanography of the Eastern Mediterranean (POEM). The scientific plan for the second phase of POEM. Fourth POEM Scientific Workshop, Venice, Italy, August-September 1990 (E)	1992
58	Geological development of the Sicilian-Tunisian Platform. Proceedings of the International Scientific Meeting held at the University of Urbino, Italy, 4-6 November 1992 (E)	1993
59	Artificial radioactivity of the Black Sea (E)	1993
60	Inventory of innovative learning materials in marine science and technology (E)	1993
61	Impact of expected climate change on mangroves. UNEP-UNESCO Task Team Report of the First Meeting, Rio de Janeiro, 1-3 June 1992 (E)	1993
62	Geological geophysical investigations of Western Mediterranean deep sea fans. Initial results of the UNESCO ESF 'Training-through-Research' Cruise of RV *Gelendzhik* in the Western Mediterranean (June-July 1992) (E)	1993
63	Sandy coast monitoring: The Dominica example (1987-1992). Prepared for the UNESCO COMAR/COSALC-I Project (E)	1994
64	Mud volcanism in the Mediterranean and Black Seas and shallow structure of the Eratosthenes Seamount. Initial results of the geological and geophysical investigations during the Third UNESCO-ESF 'Training-through-Research' Cruise of RV *Gelendzhik* (June-July 1993) (E)	1994
65	Ichthyoplankton study in Guinean and Senegalese coastal and estuarine waters. Results of surveys 1988-1992. Prepared within the framework of the African Coastal Marine Programme (COMARAF) (E)	1994
66	Coastal systems and sustainable development in Africa. Proceedings of the UNESCO Regional Seminar on Human Impacts on Coastal Ecosystems, their Response and Management Problems, UNESCO-ROSTA, Nairobi, 5-9 April 1993 (E) (in press)	1995

UNESCO REPORTS IN MARINE SCIENCE

Out of stock titles – For availability in microfiche form, please write to: UNESCO (DITAM), 7, place de Fontenoy, 75352 Paris 07 SP, France

No		Year
1	Marine ecosystem modelling in the Eastern Mediterranean. Report of a UNESCO workshop held in Alexandria, Egypt, December 1974 (E)	1977
2	Marine ecosystem modelling in the Mediterranean. Report of the Second UNESCO Workshop on Marine Ecosystem Modelling (E)	1977
3	Benthic ecology and sedimentation of the south Atlantic continental platform. Report of the seminar organized by UNESCO in Montevideo, Uruguay, 9-12 May 1978 (E, S)	1979
7	Coastal ecosystems of the Southern Mediterranean lagoons, deltas and salt marshes. Report of a meeting of experts, Tunis, 25-27 September 1978 (Ar, F, S)	1979
11	Programa de Plancton para el Pacífico Oriental. Informe final del Seminario Taller realizado en el Instituto del Mar del Perú, El Callao, Perú, 8-11 de septiembre de 1980 (S)	1981
12	Geología y geoquímica del margen continental del Atlántico Sudoccidental. Informe final del Taller de Trabajo organizado por la UNESCO en Montevideo, Uruguay, 2-4 de diciembre de 1980 (S)	1981
13	Seminario Latinoamericano sobre Enseñanza de la Oceanografía. Informe final del Seminario organizado por la UNESCO en São Paulo, Brasil, 17-20 de noviembre de 1978 (S)	1981
14	Marine science and technology in Africa: present state and future development. Synthesis of UNESCO/ECA survey missions to African coastal states, 1980 (E, F)	1981
15	Fishery science teaching at the university level. Report of a UNESCO/FAO workshop on university curricula in fishery science, Paris, May 1980. (Ar, E, F, R, S)	1981
16	Marine and coastal processes in the Pacific: ecological aspects of coastal zone management. Report of a UNESCO seminar held at Motupore Island Research Centre, University of Papua New Guinea, 14-17 July 1980 (E)	1981
17	The coastal ecosystems of West Africa: coastal lagoons, estuaries and mangroves. A workshop report, Dakar, 11-15 June 1979 (E, F)	1981
18	Coral reef management in Asia and the Pacific: some research and training priorities. Report of a UNESCO workshop held in Manila, Philippines, 21-22 May 1981 (E)	1982
19	Mareas rojas en el Plancton del Pacífico Oriental. Informe del Segundo Taller del Programe de Plancton del Pacífico Oriental, Instituto del Mar, Callao, Perú, 19-20 de noviembre de 1981. (S)	1982
27	Productivity and processes in island marine ecosystems. Recommendations and scientific papers from the UNESCO/IOC sessions on marine science co-operation in the Pacific, at the XVth Pacific Science Congress, Dunedin, New Zealand, February 1983 (E)	1984
38	Marine Sciences in CMEA countries. Programme and results of co-operation (F, R)	1986
47	Temperate coastal systems of Latin America. Report on meeting on COSALC Pilot Project No. VII, November 1986 (S)	1987